MicroRNA Biogenesis and Cytoophidia in *Drosophila melanogaster*



MOHD GHOWS BIN MOHD AZZAM

Wolfson College

MRC Functional Genomic Unit

Department of Physiology, Anatomy and Genetics

University of Oxford

Submission in fulfilment of the requirements for the degree of
Doctor of Philosophy (D.Phil)

Hilary Term 2012

ABSTRACT

This thesis contains two separate projects. The first project involves the study of Argonaute 1 (Ago1) which is a member of the Argonaute/PIWI protein family involved in small RNA-mediated gene regulation. In *Drosophila,* Ago1 plays a specific role in microRNA (miRNA) function. Previous studies have demonstrated that Ago1 regulates the fate of germline stem cells. However, the function of Ago1 in other aspects of oogenesis is still elusive. Here, the function of Ago1 was analysed in the female germline and follicle cells. The Ago1 protein is enriched in the oocyte and also highly expressed in the cytoplasm of follicle cells. Clonal analysis of multiple *ago1* mutant alleles shows that mutant egg chambers often contain only eight nurse cells and lack an oocyte which is phenocopied in *dicer-1*, *pasha* and *drosha* mutants. This implies a general role of miRNAs in this process. Further analysis of the clones shows that Ago1, Dicer-1, Drosha and miR-124a play a role in maintaining follicle cell integrity. Additionally, it was found that Ago1 protein levels were lowered when miRNAs were not present and that overexpression of miR-124a increased the steady state level of Ago1 proteins. These were believed to be the effect of Ago1 protein stability.

In the meantime, a second project was carried studying a novel filamentous structure called cytoophidia which contains CTP synthase (CTPS) was analysed. Previous studies have shown that the cytoophidia is prominent in the egg chambers but how and why CTPS forms cytoophidia is still unclear. Here, the different CTPS isoforms were analysed and only CTPS isoform C was found to form cytoophidia. This isoform could also induce cytoophidia formation in other tissues that does not have obvious cytoophidia formation. Then, it was identified that the first 56 amino acid of CTPS isoform C is the important region for cytoophidia formation. Furthermore, *ctps* mutants were generated and analysed. CTPS mutations caused lethality during the larval stage and when maternal contribution was removed, lethality was seen during embryogenesis.

ACKNOWLEDGEMENTS

I would like to express my greatest thanks to Allah S.W.T in giving me the strength to finally finish my D.Phil project even though there were a lot of rocky path along this way. All this while, I was surrounded by people who were supportive and helping me with my project. Without HIS consent none of this would be possible.

I am grateful to my supervisor Dr Ji-Long Liu and to my co-supervisor, Prof Chris Ponting for all the guidance and support. Thank you for allowing me to be part of the team throughout these 3 years. My gratitude to the Malaysian Ministry of Higher Education and Universiti Sains Malaysia for funding my D.Phil.

Special thanks to Dr Stuart Grice and Dr Andrew Bassett for all the comments and guidance given for this thesis, Siân Davies for all the laughter and help throughout these years, Zillah Deussen and Mayte Siswick for stock keeping, technical help and fly food preparation. Not forgetting all my friends, especially the past and present members of the Liu lab including; Gabriel Aughey, Dr Rob Young, Dr Jieni Cao, Dr Lin Lee, Dr Ömür Tastan, Dr Charlotte Tibbit, Jenna Schwarz. Also to all Malaysian community in Oxford, thank you for everything.

I would like to wish my sincere thanks to my immediate and extended family members for all their support and understanding throughout this journey. No words can express my thankfulness to them.

My utmost thanks to my wife Nurul Akma, for the endless love, patience and support throughout this work. Thank you for believing in me, giving never ending support and most importantly, being beside me all these while especially during hard times. Not forgetting all the sacrifices that she has made for me to complete this D.Phil. Without her, life would not be the same. Thank you from the bottom of my heart.

It has been a wonderful and exciting experience.

Mohd Ghows Mohd Azzam

Oxford, UK

January 2012

TABLE OF CONTENTS

ABSTRACT ii
ACKNOWLEDGEMENTS iii
TABLE OF CONTENTS iv
LIST OF FIGURES viii
LIST OF TABLES xi
ABBREVIATIONS xii
Chapter 1: Introduction 1
1.1 The world of small RNAs 1
1.2 MicroRNAs (miRNAs) as post-transcriptional regulators 2
1.3 Argonaute proteins are the core components of RISC 4
1.3.1 Argonautes: key players in small RNA mediated silencing 4
1.3.2 *Drosophila* Ago1 5
1.3.3 RISC assembly requires two steps: loading and unwinding. 6
1.3.4 The mechanism of miRNA target recognition and function 7
1.4 CTP synthase and cytoophidia 10
1.4.1 CTP synthase: An essential metabolic enzyme 10
1.4.2 Cytoophidium: a novel organelle containing CTPS 13
1.5 *Drosophila melanogaster* as a model organism 15
1.5.1 Why use *Drosophila melanogaster* 15
1.5.2 Life-Cycle of *Drosophila melanogaster* 16
1.5.3 Genetic techniques in *Drosophila* 18
1.5.3.1 Mitotic clones and germline clones 18
1.5.3.2 Mosaic analysis with a repressible cell marker (MARCM) 21
1.5.3.3 Inducible GAL4 system 21
1.6 Aims and outline 24
Chapter 2: Materials and Methods 25
2.1. *Drosophila* stocks and genetics 25
2.1.1. Fly food and propagation 25
2.1.2. Isolation of new mutant alleles 25
2.1.3. Mitotic clones 29
2.1.4. Germline clones 30

2.1.5. MARCM clones 30
2.1.6. Inducible GAL4 system 30
2.1.7. Scanning electron microscope (SEM) 31
2.1.8. Immunofluorescence 32
2.2. Schneider 2 (S2) cells 32
2.2.7. S2 cell culture 32
2.2.8. S2 cells dsRNA transfection 32
2.3. Protein Biochemistry 35
2.3.7. Western blot 35
2.4. Molecular Biology 36
2.4.7. Genomic DNA extraction 36
2.4.8. Double-stranded RNA(dsRNA) synthesis 36
2.4.9. Total RNA extraction and reverse transcription 37
2.4.10. Quantitative PCR (qPCR) 37
2.5. Transgenic construct generation 40
Chapter 3: Ago1 and its miRNA biogenesis partners are required for oocyte formation and germ cell division 43
3.1. Introduction 43
3.1.1. Oogenesis 43
3.1.2. miRNAs and oogenesis 44
3.1.3. Experiment descriptions 46
3.2. Results 47
3.2.1. Ago1 protein is expressed in egg chambers and enriched in oocytes 47
3.2.2. Ago1 mutations affect germline cell division and oocyte formation 52
3.2.3. The Ago1 phenotype manifests in the germarium 56
3.2.4. *dicer-1*, *pasha* and *drosha* exhibit similar effects on oogenesis as ago1 61
3.2.5. Ago1 co-localizes with P body components in oocytes 67
3.3. Discussion 69
3.3.1. Ago1 in oogenesis 69
3.3.2. Ago1 and senescence 70
3.3.3. Ago1 and the P body 71
3.3.4. The role of miRNAs in oogenesis 72
Chapter 4: The role of miRNAs in follicle cells 75
4.1. Introduction 75

4.1.1. Follicle cells 75
4.1.2. miRNAs in follicle cells 78
4.1.3. Experimental description 79
4.2. Results 80
4.2.1. *ago1* mutant causes non-cell autonomous defect 80
4.2.2. Reduced Dicer-1 and Drosha cause follicle cell defect but not in Pasha 82
4.2.3. Overexpressing Ago1, Dicer-1 and Pasha does not cause any defect 84
4.2.4. Ectopic miR-124 causes follicle cell defects 86
4.3. Discussion 89
4.3.1. The miRNA pathway proteins control follicle cell maintenance 89
4.3.2. miR-124a: a predominantly neuronal miRNA plays a role in follicle cells 90
Chapter 5: Ago1 senses mature miRNA levels 92
5.1. Introduction 92
5.1.1. The stability and posttranslational control of Argonaute proteins 92
5.1.2. Experimental description 93
5.2. Results 94
5.2.1. Ago1 sense mature miRNAs in germline cells 94
5.2.2. Ago1 senses global mature miRNAs levels 96
5.2.3. Ago1 global level is translationally affected in the absence of miRNAs 98
5.2.4. Overexpressing Dicer-1 or Pasha does not increase Ago1 levels 100
5.2.5. Overexpressing miR-124a increases Ago1 expression 102
5.2.6. Ago1 levels are not affected by the levels of siRNAs 104
5.2.7. Ago1 protein stability in S2 cells 106
5.3. Discussion 110
5.3.1. Uncovering a new feature of Ago1 110
5.3.2. Failure of the S2 cell system to test Ago1 stability 112
Chapter 6: Distinct subcellular distributions of CTPS isoforms 114
6.1. Introduction 114
6.1.1. The three isoforms of CTPS 114
6.1.2. Experimental description 117
6.2. Results 118
6.2.1. Generating CTPS isoform specific transgene 118
6.2.2. Characterizing CTP synthase transgene in different tissues 118

6.2.2.1. Egg chambers 118
6.2.2.3. Embryos 125
6.2.2.4. Adult brain and larval CNS 127
6.2.3. Identifying regions in CTPS that are important for cytoophidia formation 131
6.2.4. Analysing the transgenes in the egg chambers 135
6.3. Discussion 141
6.3.1. CTPS isoform C: the cytoophidia forming isoform 141
6.3.2. Regions that are important for cytoophidia formation 142
Chapter 7: Identification of CTPS mutants 145
7.1. Introduction 145
7.1.1. Gene disruption 145
7.1.2. Experimental description 146
7.2. Results 147
7.2.1. Isolating CTPS mutants 147
7.2.2. *ctps* mutants survives until the larval stage 150
7.2.3. CTPS is maternally inherited 152
7.2.4. CTPS isoform C rescues mutant phenotype 154
7.2.5. Characterizing CTP synthase mutant in the egg chamber 155
7.2.6. Reduction of String causes CTPS to be expressed in the nucleus 157
7.2.7. Cytoophidia and miRNAs 159
7.3. Discussion 162
7.3.1. CTPS is important for development 162
7.3.2. CTPS interactions 163
Chapter 8: Discussion and Conclusion 165
8.1. Mature miRNA levels mediate Ago1 driven germ line development 165
8.2. The assembly of cytoophidia is important for development 169
References 172

LIST OF FIGURES

CHAPTER 1

Figure 1.1.	miRNA biogenesis in *Drosophila melanogaster*	3
Figure 1.2.	Schematics of miRNA-mediated regulation	9
Figure 1.3.	Synthesis of CTP from UTP	12
Figure 1.4.	CTPS forms cytoophidia in the egg chambers	14
Figure 1.5.	The life-cycle of *Drosophila melanogaster*	17
Figure 1.6.	Mitotic clones	20
Figure 1.7.	MARCM clones	22
Figure 1.8.	Inducible GAL4 system	23

CHAPTER 3

Figure 3.1.	Schematic of *Drosophila* female germline	45
Figure 3.2.	Ago1 distribution in *Drosophila* egg chambers	48
Figure 3.3.	Ago1 staining is reduced in *ago1* mutants and increases upon overexpression	50
Figure 3.4.	*ago1* mutant allele map and Ago1 staining was reduced in multiple *ago1* mutant alleles	51
Figure 3.5.	Loss of Ago1 disrupts oocyte formation and germ cell division	54
Figure 3.6.	*ago1* phenotype manifests in the germarium	57
Figure 3.7.	*ago1[k08121]* mutant germarium is not undergoing apoptosis and still expressing Cyclin E	58
Figure 3.8.	Orb and Cup staining in the pseudo-oocyte	60
Figure 3.9.	Rough eye phenotype exhibited by *dicer-1* and *pasha* mutants	62

Figure 3.10. *dicer-1*, *pasha* and *drosha* null mutants exhibit phenotypes similar to *ago1* mutants 65

Figure 3.11. Ago1 localizes to P bodies in *Drosophila* oocytes 68

CHAPTER 4

Figure 4.1. Oogenesis showing follicle cell in the germarium and cycles 77

Figure 4.2. Clonal analysis of *ago1[k08121]* in *Drosophila* follicle cells 81

Figure 4.3. Knockdown of Dicer-1, Drosha and Pasha using RNAi with the inducible GAL4 system 83

Figure 4.4. Overexpressing Ago1, Dicer-1 and Pasha in the follicle cells 85

Figure 4.5. Ectopic expression miR-124a causes defects in follicle cells 87

CHAPTER 5

Figure 5.1. Ago1 levels are reduced when miRNAs are not present 95

Figure 5.2. Ago1 sense miRNA levels in somatic cells 97

Figure 5.3. The level of Ago1 RNA was not affected in *pasha* mutant 99

Figure 5.4. Overexpressing Dicer-1 or Pasha does not affect Ago1 levels. 101

Figure 5.5. Ago1 is translationally repressed and overexpressing miR-124a increases the levels of Ago1 103

Figure 5.6. Ago1 levels are not affected by siRNAs 105

Figure 5.7. S2 cells treated with RNAi with about 50-90% knockdown 108

Figure 5.8. Western blot showing Ago1 protein levels of cycloheximide treated S2 cells after RNAi treatment 109

CHAPTER 6

Figure 6.1.	Gene map of *Drosophila* CTP synthase (CG6854)	116
Figure 6.2.	Different CTPS isoforms overexpression in the germline cells using nos-GAL4::VP16 driver	121
Figure 6.3.	CTPS isoform C overexpression in follicle cells	122
Figure 6.4.	CTPS isoform C overexpression in testis	124
Figure 6.5.	CTPS isoform C overexpression in *Drosophila* embryos	126
Figure 6.6.	CTPS in the adult brain and larval CNS	129
Figure 6.7.	BLASTp alignment of CTPS isoform C and CTPS isoform B showing the differences and similarities between the two isoforms	132
Figure 6.8.	The domains of CTPS isoform C in which the transgenes were generated	134
Figure 6.9.	Expression of the different transgenes in the egg chambers using MTD-GAL4	137
Figure 6.10.	N-term and CTG transgenes have nuclear localization expression	140

CHAPTER 7

Figure 7.1.	CTPS mutant lines	149
Figure 7.2.	CTPS mutants survive until larvae stage	151
Figure 7.3.	CTPS mutant failed to complete embryogenesis without maternal contribution	153
Figure 7.4.	*ctps[d06966]* mutant egg chambers	156
Figure 7.5.	String affects CTPS localization	158
Figure 7.6.	Overexpressing miRNA biogenesis proteins and miR-124 does not have any effect on cytoophidia	160
Figure 7.7.	miRNAs and siRNAs biogenesis proteins does not affect cytoophidia	161

LIST OF TABLES

CHAPTER 2

Table 2.1.	Table showing mutant stocks used	26
Table 2.2.	Table showing UAS stocks used	27
Table 2.3.	Primary antibodies used with its concentration and sources.	33
Table 2.4.	Secondary antibodies used with its concentration and sources.	34
Table 2.5.	Primers used to generate dsRNA.	38
Table 2.6.	Primer sequences used for qPCR.	39
Table 2.7	Primer sequences used for generating untagged constructs.	41
Table 2.8	Primer sequences used for generating Venus-tagged constructs.	42

CHAPTER 3

Table 3.1.	Clonal analysis of *ago1* egg chambers	55
Table 3.2.	Clonal analysis of *dicer-1*, *pasha* and *drosha* egg chambers	66

ABBREVIATIONS

Ago1	Argonaute 1
Ago2	Argonaute 2
Aub	Aubergine
ATP	Adenosine triphosphate
bp	Basepair
BSA	Bovine serum albumin
cDNA	Complementary DNA
CNS	Central nervous system
CPO	Clones per ovary
C-terminus	Carboxy-terminus
CTP	Cytidine triphosphate
CTPS	CTP synthase
Dcr-1	Dicer-1
DGRC	*Drosophila* Genomics Resource Center
DNA	Deoxyribonucleic acid
dNTP	Deoxynucleoside triphosphates
DTT	Dithiothreitol
EDTA	Ethylenediaminetetraacetic acid
EGFP	Enhanced GFP
eIF4E	Eukaryotic translation-initiation factor-4E
EMS	Ethane methyl sulfonate
FCS	Fetal calf serum
FISH	Fluorescence *in situ* hybridization
FLP	Flippase
FRT	Flp recombinase target

GFP	Green Fluorescence Protein
GLC	Germline clones
GSC	Germline stem cells
GTP	Guanosine triphosphate
HRP	Horseradish peroxidase
kDA	Kilo Dalton
Loqs	Loquacious
m^7G	5’ monomethyl guanosine
Me31B	Maternal expression at 31B
miRNA	microRNA
mRNA	Messenger RNA
mRNP	Messenger ribonucleoprotein
MTOC	Microtubule organising centre
NCBI	National Center of Biotechnology Information
NP40	Nonyl phenoxypolyethoxylethanol
N-terminus	Amino-terminus
nt	Nucleotide
PAGE	Polyacrylamide gel electrophoresis
P body	Processing body
Pbac	piggyBac
PBS	Phosphate buffered saline
PBT	PBS with 0.4%Triton-X
PCR	Polymerase chain reaction
Pen Strep	Penicillin and streptomycin
PFA	Paraformaldehyde
piRNA	Piwi-interacting RNA
pre-miRNA	Precursor miRNAs

pri-miRNA	Primary miRNAs
qPCR	Quantitative real-time PCR
RISC	RNA induced silencing complex
RNA	Ribonucleic acid
RNAi	RNA interference
SDS	Sodium dodecyl sulphate
siRNA	small interfering RNA
S2	Schneider 2
SEM	Scanning electron microscope
SMN	Survival of motor neurons
UAS	Upstream Activation Sequence
U body	Uridine-rich small nuclear ribonuclear protein body
UTP	Uridine triphosphate
UTR	Untranslated region
XRN	Exoribonuclease

Chapter 1
Introduction

1.1 The world of small RNAs

In 1998, Fire and Mello published the discovery of dsRNA in *Caenorhabditis elegans* (Fire et al., 1998). Although their discovery was unintentional, it opens a whole new field called the small RNA field. Furthermore, the discovery of RNAi also won them the Nobel Prize in 2006, just eight years after the paper was published. The small interfering RNAs (siRNAs) are early examples of RNAi triggered by exogenous dsRNA. In addition, endogenous siRNAs (endo-siRNA) have also been reported (Okamura and Lai, 2008). These siRNAs are cleaved from long exogenous dsRNA into double-stranded siRNAs by a protein called Dicer, a dsRNA-specific RNase III family ribonuclease. Target regulation by the guide strand of the ~21 nucleotide siRNA is mediated by the RNA-induced silencing complex (RISC) which includes the Argonaute protein. siRNA repress target mRNA by binding to its target sequence with perfect complementary. Another widely characterized small RNA is PIWI-interacting RNAs (piRNAs). It is considered the longest small RNAs comprising of ~25-35 nucleotides. Unlike siRNAs that regulate genes, piRNAs are first proposed to ensure germline stability by repressing transposons (Aravin et al., 2004). The piRNAs bind to Piwi proteins and do not require Drosha or Dicer. piRNA biogenesis involves primary and secondary processing mechanisms which involves Aubergine (Aub), Ago3 and Piwi (Ishizu et al., 2011). Now small RNAs have been implicated in many areas including development, cancers, drug therapy and epigenetics (Jones and Newbury, 2010; Rissland and Lai, 2011). The small RNA research has gathered great momentum since its discovery, producing thousands of publication every year.

1.2 MicroRNAs (miRNAs) as post-transcriptional regulators

MicroRNAs (miRNAs) are ~22 nucleotide endogenous short RNAs that have a role in the regulation of gene expression in animals and plants by targeting complimentary mRNAs for degradation or translational repression (Ambros, 2004; Mallory and Vaucheret, 2010). Unlike siRNAs, miRNAs do not bind with perfect complementary to its mRNA target in animals. The first miRNA to be characterized is the *lin-14* which was identified from forward genetics in *C. elegans* (Lee et al., 1993). Two transcripts of *lin-4* were identified with 22 and 61 nt sequence which is now identified as the precursor and mature sequences, were regulating *lin-14* mRNA by sequence complementary. These findings soon led to other miRNAs being identified.

Biogenesis of miRNAs (Figure 1.1) starts with RNA polymerase II transcribing the primary transcript (pri-miRNA) that contains hairpin loop domains, a 7-methyl-guanosine cap, and a poly-A tail (Bartel, 2009). The pri-miRNA is cut by the microprocessor complex, comprising the RNAse III enzyme Drosha and its RNA binding domain-containing partner Pasha (Denli et al., 2004; Gregory et al., 2004; Han et al., 2004), to become a 60-70 nucleotide-long precursor miRNA (pre-miRNA), which is then exported to the cytoplasm by Exportin5, a Ran-GTP-dependent cytoplasmic cargo transporter (Bohnsack et al., 2004; Lund et al., 2004; Yi et al., 2003). In the cytoplasm, Dicer-1, together with its partner, Loquacious, cleaves the hairpin loop of the pre-miRNA to form a miRNA-miRNA* duplex (Forstemann et al., 2005; Saito et al., 2005). This duplex unwinds and one strand is selected as the mature miRNA and preferentially loaded into Ago1 to form the RISC (Forstemann et al., 2007; Tomari et al., 2007). The strand that is not loaded into Ago1, referred to as the miRNA* strand, is presumably degraded most of the time, but in some cases is loaded into the Ago2-containing RISC where it can function as a siRNA (Czech et al., 2009; Okamura et al., 2009).

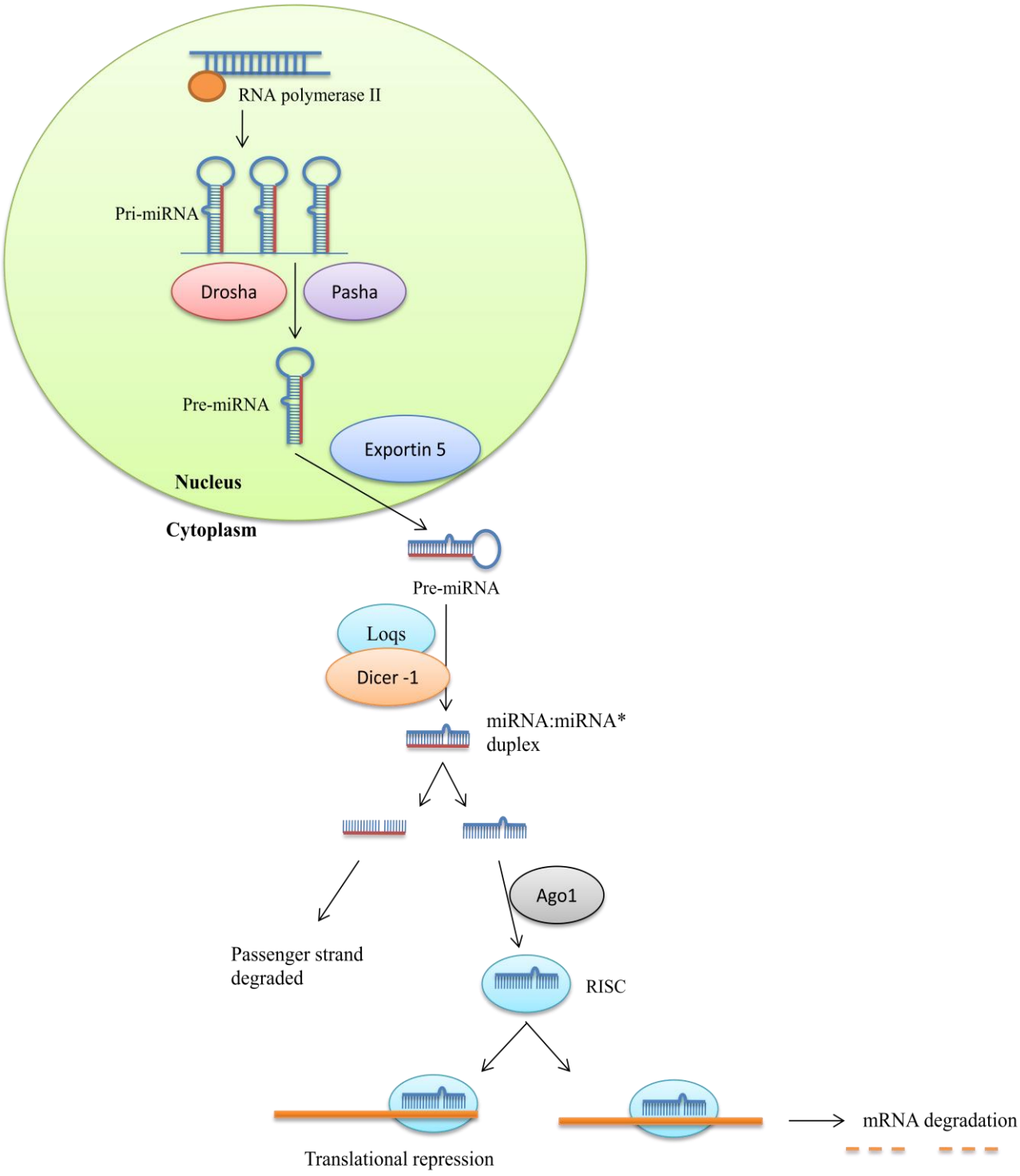


Figure 1.1. miRNA biogenesis in *Drosophila melanogaster*.

Interactions between the miRNA-RISC (miRISC) and mRNA targets involve binding between the 'seed' region of the miRNA (typically nucleotides 2-8) and the complementary target sequence on the mRNA (Bartel, 2009; Lai, 2002). This short recognition sequence means that a single miRNA can target numerous mRNAs and often operates in highly complex regulatory networks in combination with other miRNAs as most UTRs contain potential target sites for several miRNAs (Kim and Nam, 2006). Recent advances from genetic and genomic studies have indicated that miRNAs play important roles in many aspects of cell and animal development such as cell proliferation, differentiation, morphogenesis, and apoptosis (Carrington and Ambros, 2003; Flynt and Lai, 2008; Kim et al., 2006b; Nakahara et al., 2005).

1.3 Argonaute proteins are the core components of RISC

1.3.1 Argonautes: key players in small RNA mediated silencing

Argonaute (Ago) proteins are named after the phenotype of *Arabidopsis thaliana argonaute* mutants which resembles the animal *Argonauta argo* (Bohmert et al., 1998). Ago proteins are conserved throughout species, however, the numbers of Ago proteins between organism varies; humans have eight, *Arabidopsis thaliana* has twenty-seven, *Caenorhabditis elegans* has twenty-seven, *Drosophila melanogaster* has five and *Schizosccharomyces pombe* has only one (Tolia and Joshua-Tor, 2007). The model organism *Saccharomyces cerevisiae* does not have any Ago protein and does not appear to encode small RNAs (Hutvagner and Simard, 2008). When Ago was first characterized, it was referred to as a Slicer protein (Liu et al., 2004; Song et al., 2004). However, this is not true for all Ago proteins because some are capable of slicing while others regulate target RNA by repressing translation or RNA de-stabilization (Bartel, 2009; Mallory and Vaucheret, 2010).

Small RNAs regulate gene expression by guiding Ago proteins to its target RNA. Plants' small RNAs and animal siRNAs generally have precise complementary between the small RNA and its target (Rhoades et al., 2002). However, animal miRNAs have limited complementary with mis-matches in the central region of its seed sequences. Perfect complementary generally promotes endonucleolytic cleavage and mismatches in the central region lead to repression of mRNAs or mRNA de-stabilization (Lewis et al., 2003; Mallory and Vaucheret, 2010). Ago proteins are also thought to function in the nucleus at transcriptional levels. In plants, Ago and Dicer promotes DNA methylation (Moazed, 2009). In mammals, small RNAs mediated DNA and histone modifications have been shown and the Ago2 protein was also detected in the nucleus in HeLa cells (Janowski et al., 2006; Kim et al., 2006a; Weinmann et al., 2009)

1.3.2 *Drosophila* Ago1

The *Drosophila* Ago family has five members: Ago1, Ago2, Ago3, Piwi and Aub. The PIWI subclade of Argonaute proteins, Piwi, Ago3 and Aub, are devoted to the production and function of piRNAs, a class of small RNAs involved in defending the genome from transposable elements (Girard et al., 2006), and are largely confined to the germline and surrounding somatic tissues (Brennecke et al, 2007). The two remaining members of the Argonaute family, Ago1 and Ago2, are predominantly involved in gene regulation mediated by miRNAs and siRNAs, respectively, although there is some degree of overlap between these two pathways (Okamura et al, 2009, Czech et al, 2009). The predicted molecular weight of the Ago1 protein is approximately 106 kDa comprising 950 amino acids (Kataoka et al., 2001). There are three domains in the Ago1 protein: the PAZ domain of 110 amino acids, the well conserved PIWI domain consisting of 300 amino acids and the newly characterized MID domain (Djuranovic et al., 2010). The 3' and 5' ends of the miRNA bind

to the PAZ domain and the MID domain respectively. The PIWI box contains the catalytic centre for cleavage. Yang *et al.,* (2007) showed that Ago1 is required for *Drosophila* germline stem cell (GSC) maintenance. Overexpression of Ago1 leads to GSC over-proliferation while *ago1* mutants lead to GSC loss. Ago1, which is conserved from fruit fly to human, binds to mature microRNAs (miRNAs) to form the RISC. Ago2 forms the RISC by binding to siRNAs instead (Okamura et al., 2004).

1.3.3 RISC assembly requires two steps: loading and unwinding.

Small RNAs cannot work alone; they need the help of RISC assembly to exert their functions. In order to do this, small RNAs need to be loaded to RISC. The loading of small RNAs depends on the small RNA features which are duplex structure, the identity of the 5' end and the thermodynamic asymmetry of the duplex (Seitz et al., 2011). To date, little is known about Ago1 RISC loading. However, by analogy to Ago2, it is thought that a similar occurrence happens in Ago1 as well (Kawamata and Tomari, 2010). In Ago2 loading, siRNA duplex starts with loading to Dicer-2 and R2D2 which form the RISC-loading complex (RLC). Dicer-2 produce siRNAs from long dsRNA precursors but its function in RISC-loading is different from its dicing function. A single amino acid change in the Dicer-2 helicase domain removes its dicing function but still attains its loading function (Lee et al., 2004). The RLC senses the thermodynamic asymmetry of small RNA duplex where R2D2 binds to the more stable end and Dicer-2 binds to less stable end (Tomari et al., 2004). As Ago1 loads miRNAs, it prefers to incorporate the miRNA::miRNA* duplex with central mis-matches at the guide strand position 8-11 but how the central mis-matches are recognized is still unknown (Czech et al., 2009; Ghildiyal et al., 2010; Okamura et al., 2009). The miRNA::miRNA* duplex loading step also requires ATP and the Hsc70/Hsp90 chaperone machinery (Iwasaki et al., 2010; Kawamata et al., 2009; Yoda et al., 2010). Furthermore, the

5’-end nucleotide of the guide stand is another key factor for the sorting of small RNAs. Ago1 prefers U whereas Ago2 prefers C at the 5’ end of the guide stand (Kawamata et al., 2009; Kawamata and Tomari, 2010).

Next is the unwinding of the small RNA duplex. It was thought previously that the unwinding of small RNA duplex requires an “unwindase”. However, to date, no such ‘unwindase’ were found, weakening the model. Recent studies showed that Ago2 unwinds through slicer-dependent manner while Ago1 has a splicer-independent feature that recognizes mis-matches in the seed region and in the middle region of the 3’ end (positions 12-16 on the guide strand) that will unwind the miRNA::miRNA* duplex (Kawamata et al., 2009; Miyoshi et al., 2005; Rand et al., 2005). The guide strand will stay in the RISC but the passenger strand will be discarded and immediately be degraded by nucleases. This unwinding step does not require ATP (Kawamata and Tomari, 2010).

As ATP hydrolysis is required for RISC loading of small RNA duplexes but not for the unwinding, Kawamata and Tomari (2010) has proposed that a ‘rubber band’ model of Argonaute protein in loading of small RNAs. The rubber band model proposed that ATP is consumed to mediate a dynamic conformational opening of Ago proteins so that they can receive the bulky, rigid and small RNA duplexes (Kawamata and Tomari, 2010).

1.3.4 The mechanism of miRNA target recognition and function

miRNA represses its target via translation repression or mRNA degradation (Figure 1.2) although it has been suggested that mRNA degradation is more favoured than translational repression (Guo et al., 2010; Hendrickson et al., 2009; Rissland and Lai, 2011). This act of negative regulation exerts their effect through various mechanisms upon loading to RISC. It was first reported that *lin-4* inhibits the translation on *lin-14* mRNA without reducing

its mRNA levels in *C.elegans* and similar observations were seen in HeLa cells with the inhibition of lin41 by let-7 (Nottrott et al., 2006; Olsen and Ambros, 1999). The target inhibition employed by miRNAs requires both cap and poly-A tail structures (Pillai et al., 2005). miRNAs are thought to inhibit translation by inhibiting eIF4F cap binding-complex (Mathonnet et al., 2007). Also the mammalian Ago2 protein contains a cap-binding domain that competes with eIF4E which binds to the m7GpppG cap and eIF4G (Iwasaki et al., 2009; Kiriakidou et al., 2007).

The miRNA-dependent mRNA degradation is caused by the deadenylation of the target mRNA (Behm-Ansmant et al., 2006; Eulalio et al., 2009; Wakiyama et al., 2007). Deadenyalation which is required for decapping and mRNA decay, requires many interacting factors. The fully transcribed mRNA is thought to be in a circular messenger ribonucleoprotein (mRNP) form which is composed of the cap-binding protein, eIF4E, the scaffold protein eIF4G, poly-A binding protein (PABP), ribosomes and other related proteins. The deadenyation step starts with the interaction of Ago with the CCR4-CAF1 deadenylase complex and the PABP-dependent poly(A) nuclease 2 (Pan2)-Pan3 deadenylase complex (Chen et al., 2009; Fabian et al., 2009). The CCR4-CAF1 deadenylase complex is composed of chromatin assembly factor (CAF1), chemokine receptor (CCR4) and CAF1 deadenylase enzyme. After the deadenylation step has occurred, the mRNA is then degraded by exosomes in the 3'-5' direction or through decapping and subsequent 5'-3' degradation by exonuclease Xrn1 (Garneau et al., 2007).

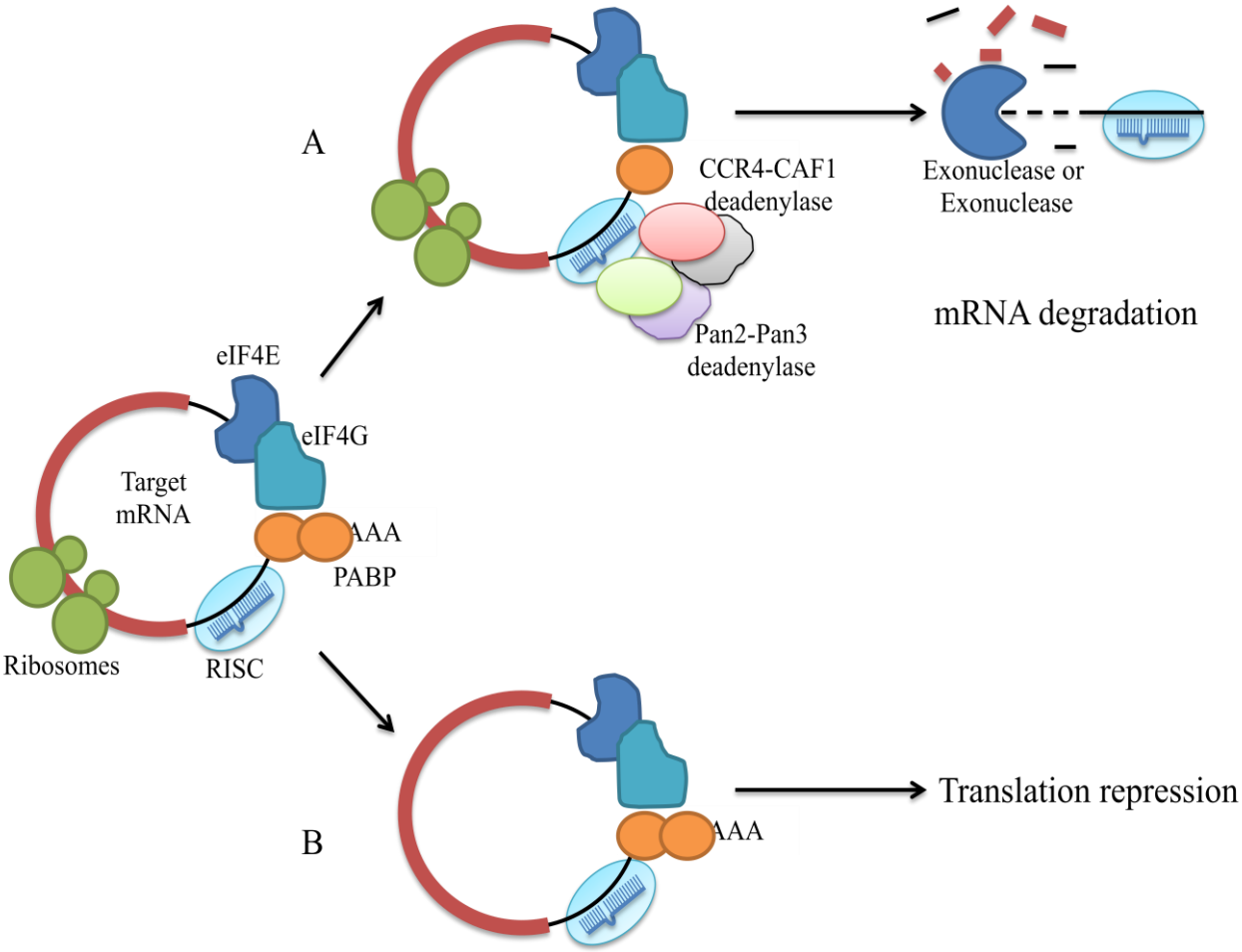


Figure 1.2. Schematics of miRNA-mediated regulation. (A) mRNA degradation process which starts with the deadenylation of the poly(A) tail followed by mRNA decay. (B) Translation repression which inhibits binding of ribosomes by the RISC. Adapted from Rissland and Lai (2011).

1.4 CTP synthase and cytoophidia

1.4.1 CTP synthase: An essential metabolic enzyme

Adenosine (A), thymine (T) for DNA or uridine (U) for RNA, guanosine (G) and cytidine (C) nucleotides are the basic molecules that make up DNA and RNA. These genetic materials in cells are important for a cell to properly develop and function. The four basic nucleotide triphosphates (NTPs) that make up RNAs are adenosine-5'-triphosphate (ATP), uridine-5'-triphosphate (UTP), guanosine-5'-triphosphate (GTP) and cytidine-5'-triphosphate (CTP). Other than generating DNA and RNA, nucleotides are also energy carriers which participate in cellular signalling and as important cofactors of enzymatic reactions make them especially important to tightly regulate their levels (Liu, 2010). CTP is not only important for making DNA and RNA but is also an important for phospholipids and sialoglycoproteins (Yang et al., 1996). Mitochondria and chloroplast are specialized organelles which contain ATP synthase, the enzyme that makes ATP. It serves as the major site for ATP synthase to generate ATP and the mitochondrion has been considered the as the 'power house' of a cell because it is responsible for 90% of the cellular energy. It is not surprising that ATP synthase and the mitochondrion have been extensively studied during the past 100 years. Defects in mitochondria have been linked to a wide range of human diseases such as mitochondria myopathy, Leigh syndrome, Parkinson's disease and diabetes (Raza, 2011).

By contrast, little is known about the subcellular distribution of CTP synthase (CTPS). In many cells, CTP can be synthesized via the salvage pathway or the *de novo* pathway (Chakraborty and Hurlbert, 1961; Kammen and Hurlbert, 1959; Lieberman, 1956; Long and Pardee, 1967). CTPS belongs to the triad family of amidotransferases having a conserved Cys-His-Glu catalytic triad in the glutaminase active site. CTPS produces CTP from UTP and glutamine which regulates intracellular CTP levels though interactions with all four

nucleotides triphosphates (Figure 1.3). CTPS generates CTP from UTP in three reaction steps (kinase reaction, glutaminase reaction and ligase reaction) involving two active sites (Levitzki and Koshland, 1971). In one active site, GTP binds allosterically to activate the rate-limiting glutamine hydrolysis (glutaminase reaction) and generates ammonia. A gated channel that spans between the glutamine hydrolysis and amidoligase active sites provides a path for ammonia diffusion (Bearne et al., 2001; Endrizzi et al., 2004; Goto et al., 2004; Levitzki and Koshland, 1972b; Scheit and Linke, 1982). In a separate active site, the kinase reaction activates Mg-ATP-dependent phosphorylation of the UTP O4 oxygen which follows by ligase reaction where the displacement of UTP uracil O4 phosphate by ammonia generating CTP (Anderson, 1983; Endrizzi et al., 2004; Goto et al., 2004; Levitzki and Koshland, 1972a; Long and Pardee, 1967; Pappas et al., 1998; Robertson, 1995). The CTP product provides a negative feedback by competitively inhibiting the UTP substrate. The uracil O4 phosphatase is displaced by ammonia to yield the CTP product, which provides negative feedback by competitively inhibiting the UTP substrate (Aronow and Ullman, 1987; Endrizzi et al., 2004, 2005; Kizaki et al., 1985; Long and Pardee, 1967; Yang et al., 1994).

CTPS is present in monomeric, dimeric, and tetrameric forms based on its concentration and other factors (Anderson, 1983; Levitzki and Koshland, 1972a). CTPS is known to be upregulated in many forms of cancer such as leukaemia, hepatomas and colon cancer (Kizaki et al., 1980; Liu, 2011). Furthermore, CTPS is an attractive target for cancer therapy and also drug development against viral and parasitic disease (e.g. African sleeping sickness, malaria, and infectious blindness).

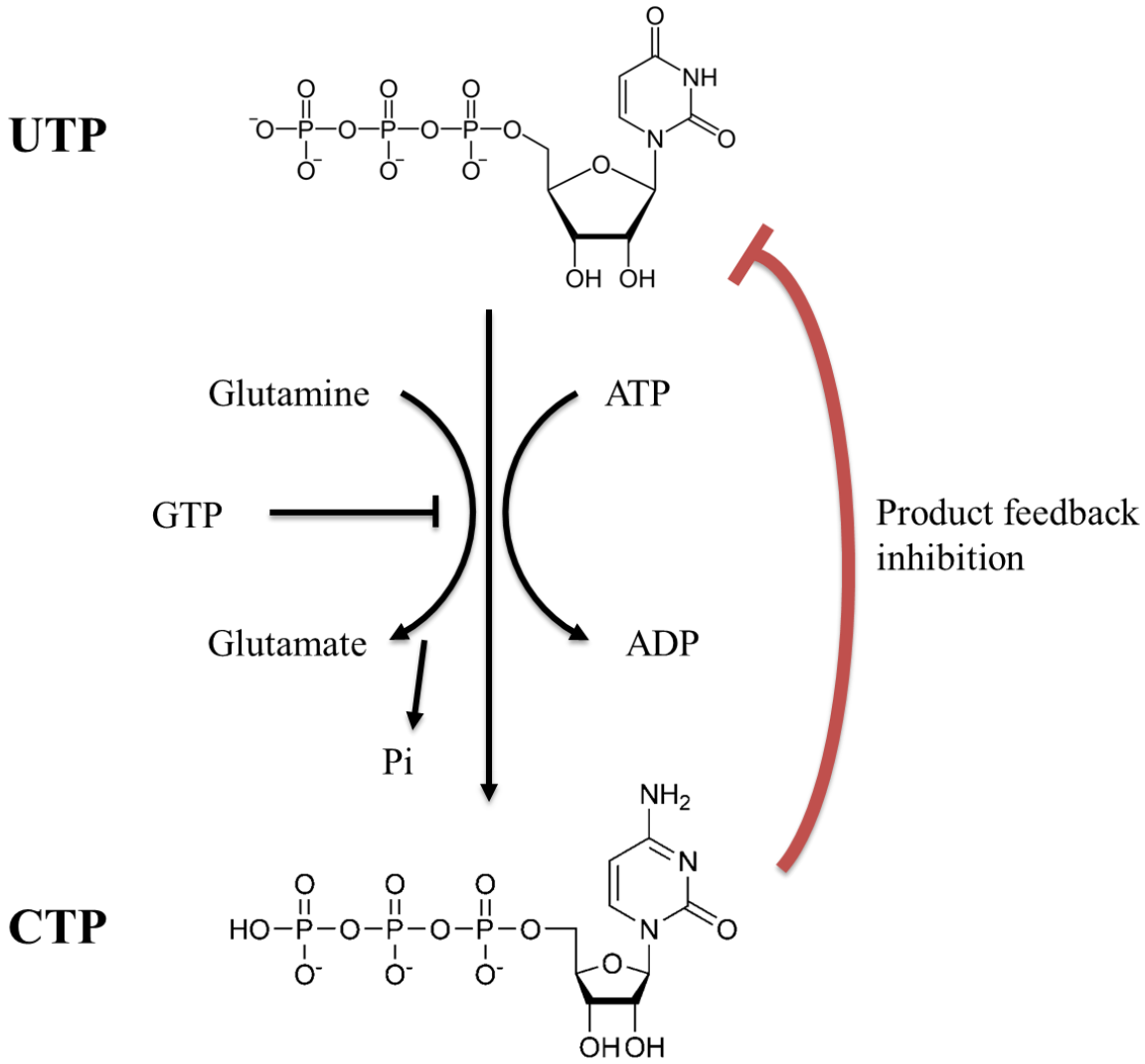


Figure 1.3. Synthesis of CTP from UTP.

1.4.2 Cytoophidium: a novel organelle containing CTPS

Compartmentation is important for the efficiency and biological processes in cells (Alberts et al., 2008). ATP synthases which makes ATP localize to organelles such as mitochondria and chloroplasts have been intensively studied. The compartmentation of ATP synthase into organelles is essential for its efficient function. It was recently discovered that CTPS is enriched in a filamentous structure called the cytoophidium (which means 'cellular serpent' in Greek) (Figure 1.4) (Liu, 2010). Two studies from other groups reported that CTPS forms similar filaments in bacteria (Ingerson-Mahar et al., 2010), budding yeast and rats (Noree et al., 2010). More recently, it was discovered that CTPS also forms cytoophidium in human cells (Chen et al., 2011). Even bacterial and mammalian lineages, which diverged about three billion years ago, localizes their CTPS molecules to cytoophidia. Filament-formation thus appears to be a highly conserved and very ancient property of CTPS. This conservation also means that cytoophidia is indispensable throughout evolution.

Despite a study showing that the CTPS filament (i.e. the cytoophidium) regulates cell shape in a curved bacterium, *Caulobacter crescentus* (Ingerson-Mahar et al., 2010), the exact function of this novel subcellular structure in other organisms is still elusive. Furthermore, organelles have been shown to be very important in disease pathology. For example, cilia were initially thought not to be relevant but ciliopathies are now a well-established and important class of diseases. The high conservation and widespread distribution of the cytoophidium among diverse organisms and cell-types indicates that this novel compartment contributes to fundamental cellular processes. The cytoophidium will be not only of considerable importance in the cell and developmental biology fields, but also relevant to the understanding of the pathological mechanism of human diseases. Further details will be discussed in Chapter 5.

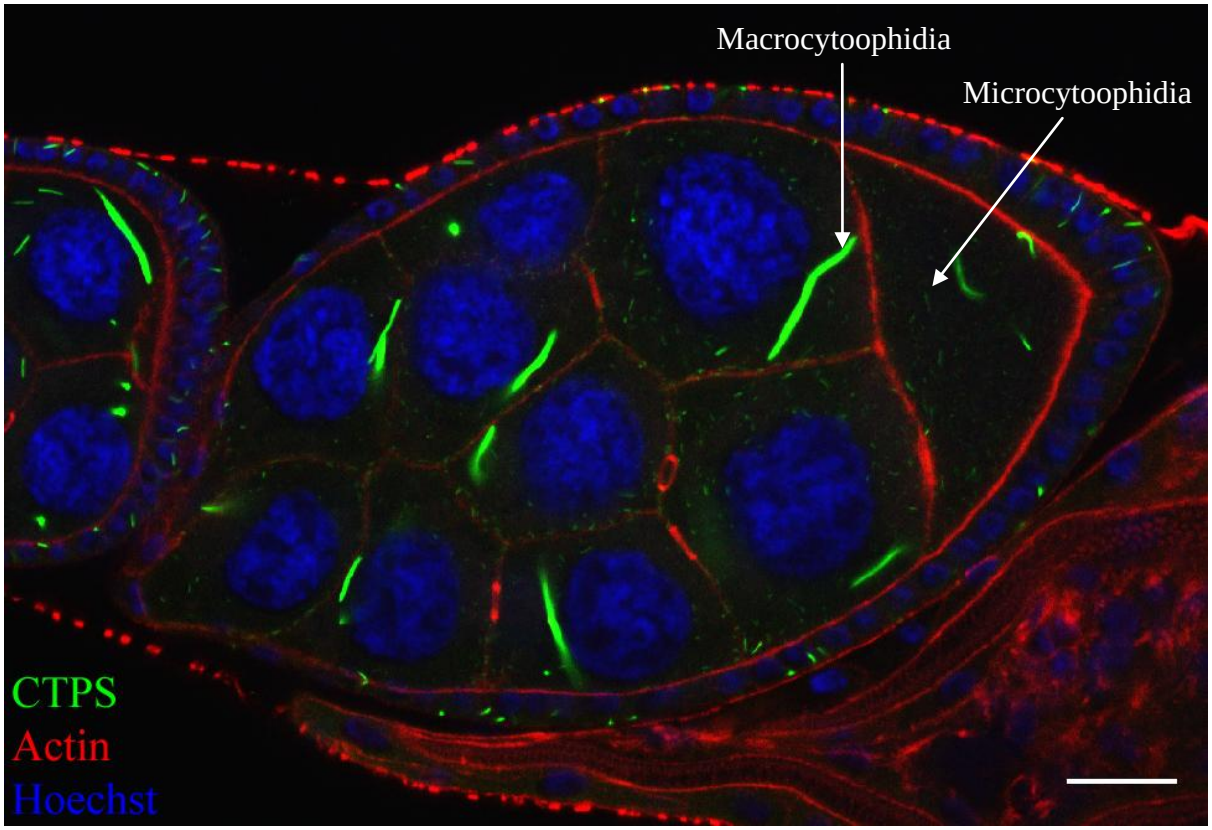


Figure 1.4. CTPS forms cytoophidia in the egg chambers. Two types of cytoophidia are present in the egg chamber, the big filaments are called macrocytoophidia and the small filaments are called microcytoophidia. Scale bars, 20 μm.

1.5 *Drosophila melanogaster* as a model organism

1.5.1 Why use *Drosophila melanogaster*

Ever since Thomas Morgan began using *Drosophila melanogaster* in 1910, this amazing organism has been studied intensively as it can be said that we know more about some aspects of *Drosophila* than humans. The research of *Drosophila* has mainly been focused on genetics but in the past few decades the field of *Drosophila* research has opened up from developmental biology to behavioural studies. The amount of techniques developed for genetic studies on *Drosophila*, together with the combining microsurgical manipulations has made *Drosophila* one of the most understood developmental systems (Wolpert *et al.* 1998). In addition, *Drosophila* have a wide range of genetic tools including balancer chromosomes, huge collection of mutants in stock centres, well-characterized transposon based-method for gene manipulation and the UAS-GAL4 system that allows controlled ectopic gene expression. Furthermore, the male fly's chromosomes do not undergo any recombination during meiosis which is an important feature in fly genetics. *Drosophila* has four pairs of chromosomes which are the sex chromosomes, autosome 2, autosome 3 and autosome 4. Most genes are located in the first three chromosomes while the fourth chromosome contain about 80 genes and does not undergo recombination (Riddle et al., 2008). The size of the genome is about 165 million bases and contains an estimated 15,458 genes (Flybase) from the *Drosophila* Genome Project which include about 5000 genes which can be mutated to lethality. Interestingly, the *Drosophila* genome contains about 177 of 289 human genes that are responsible for inherited human disorder (Snustad and Simmons, 2003). It has also been reported that approximately 75% of the disease-related loci in humans have a *Drosophila* homologue and about 60% of the total *Drosophila* gene are conserved in humans (Adams et al., 2000; Reiter et al., 2001).

One of the most significant contributions to *Drosophila* work was done by C. Nusslein-Volhard and E. Wieschaus, published in 1980, screening for major signalling pathways and cellular processes that are conserved from flies to mammals (Nusslein-Volhard and Wieschaus, 1980). They carried out a forward screen in embryos to identify genes required for normal development in which they have found 139 mutations affecting embryogenesis and 15 loci were described in the paper to disrupt the segmental pattern of the larva. They were awarded the Nobel Prize in Physiology or Medicine in 1995 for this work.

1.5.2 Life-Cycle of *Drosophila melanogaster*

Drosophila melanogaster is an excellent model organism for biological research, partly because of its short life cycle, estimated to be around 10 to 12 days at its optimum temperature of 25°C (Figure 1.5). However the life cycle varies in different conditions. It has four phases in its life cycle which are embryo, larva, pupa and adult. The embryogenesis has 17 stages which last approximately 24 hours then it hatches into a larvae. There are three larval instars; 1st instar, 2nd instar and 3rd instar which last about 24 hours, 48 hours and 48 hours respectively. The larvae eat about three-to-five times their own body weight during normal growth. Before pupation, the 3rd instar larvae will begin its wandering stage to find a suitable place to start pupation. When first formed, the pupa is soft and white before it becomes hard and darkens its colour. The entire metamorphosis of the pupa to adult takes about 4 – 4.5 days.

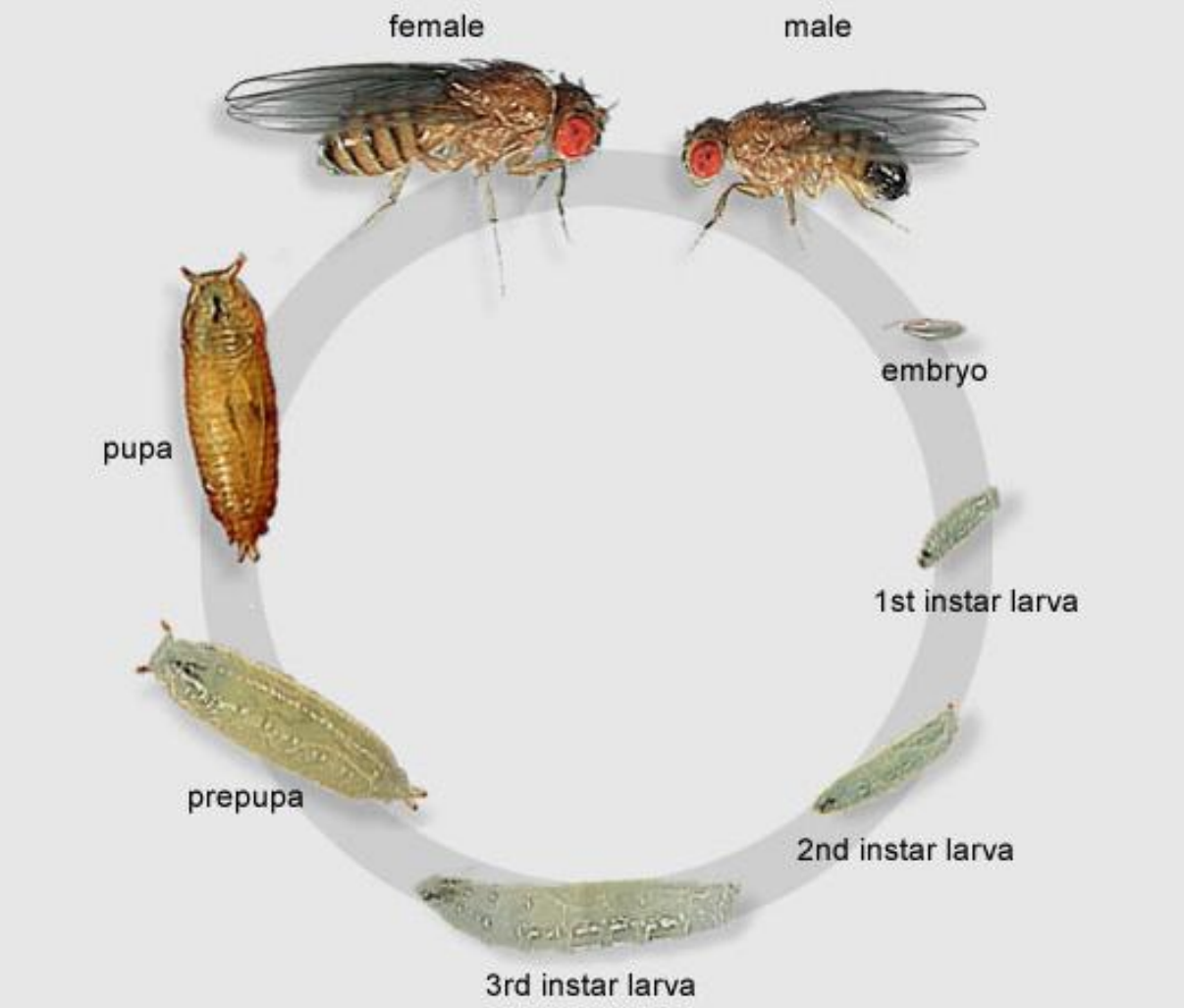


Figure 1.5. The life-cycle of *Drosophila melanogaster*. Adapted from Weigmann et al., (2003)

1.5.3 Genetic techniques in *Drosophila*

The genetic techniques that have been developed using *Drosophila* made it a powerful model system to study. One of the most useful techniques that is used is based on the FLP/FRT (Flippase Recognition Target) system (Golic and Lindquist, 1989). Site specific recombination between two short 34bp FRT sites can be induced by FLP recombinase enzyme (FLP) which derived from *Saccharomyces cerevisiae*. Another powerful technique that is commonly used is the UAS-GAL4 system (Brand and Perrimon, 1993). This technique is very useful for studying gene expression. The system uses the GAL4 gene which will activate gene transcription on the Upstream Activation Sequence (UAS), a short section of the promoter region. Genes that are inserted downstream of the UAS site will be activated with the GAL4 "driver" which can be coupled with different promoter to induce ubiquitous or tissue specific expression. These two techniques, the FLP/FRT and the UAS-GAL4 systems have been utilized and even combined to generate even more powerful techniques which will be discussed further.

1.5.3.1 Mitotic clones and germline clones

Mitotic clones utilize the FLP/FRT system coupled with green fluorescent protein (GFP) tag. This technique is very useful when studying gene mutations that are homozygous lethal. Using mitotic clones, mosaic mutant cells could be generated in the wild-type background which will eliminate its lethality. The FLP gene is coupled with a heat-shock promoter so that it can be induced. On one stock, a ubiquitous-GFP (ubi-GFP) is recombined downstream of a FRT site. On the other stock, a FRT site is recombined to the mutated gene. During mitosis, the chromosome will duplicate before dividing. If heat-shock treatments were given, the FRT site will flip and the resulting cells will not be identical (Figure 1.6). The heat-shock must be timed so that it occurs when the cell of interest is dividing (undergoing

mitosis). This technique is very versatile because it works in most cells as long as the heat-shock timing is correct. Since downstream of the FRT is tagged with GFP, the GFP –ve cells are now homozygous mutant. However, the FRT site on both chromosomes must be identical for this technique to work.

The germline clone employs the same idea as mitotic clone. However, the germline clone can only work in the germline cells. It uses a dominant female sterile mutation, *ovoD1,* instead of ubi-GFP in the mitotic clone. The *ovoD1* causes the germcells to degenerate beyond stage 4 in the oogenesis so after heat-shock treatment, only egg chambers that have lost the *ovoD1* will survive (Chou et al., 1993; Chou and Perrimon, 1996). This technique is also useful to remove maternal contribution when studying embryos. Since many genes are maternally inherited, embryos that are homozygous mutant to a specific gene sometimes still survive embryogenesis with the maternal contribution.

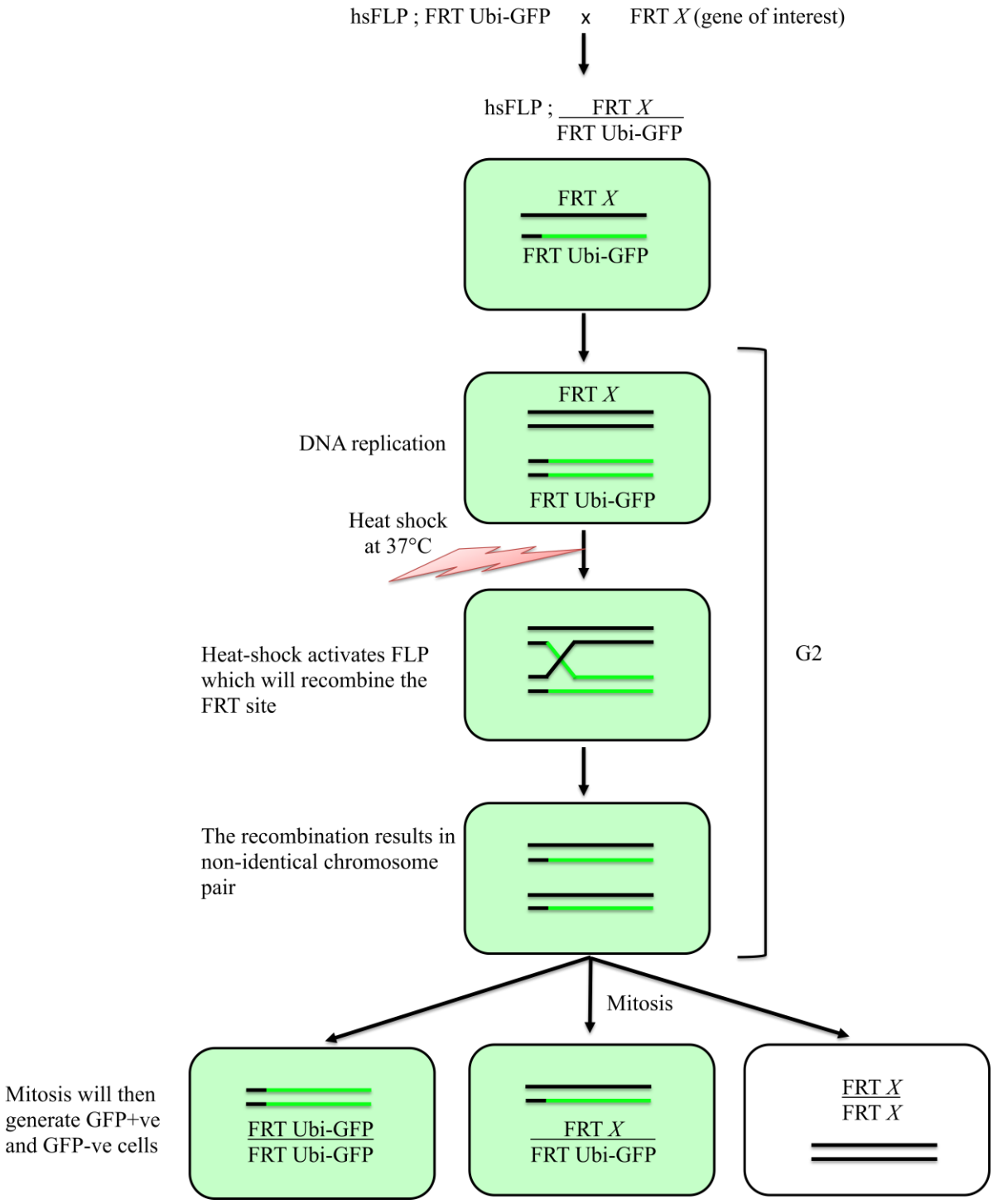


Figure 1.6. Mitotic clones

1.5.3.2 Mosaic analysis with a repressible cell marker (MARCM)

The MARCM technique was developed by Lee and Luo (2001) to study *Drosophila* neural development. However, it can also be adapted to work on other somatic cells (Wu and Luo, 2006). Like mitotic clones, it uses the FLP/FRT system as well. Two FRT sites are required and must be in the same position on homologous chromosomes. Furthermore, it also employs the UAS-GAL4 system with the addition of GAL80. In the UAS-GAL4 system, the expression of GAL4 activates the gene under the control of a UAS promoter. In MARCM system, the GAL4 is repressed by the GAL80 protein resulting in unmarked cells that are heterozygous for both GAL80 and the mutation (Figure 1.7). Upon heat-shock treatment, the FLP recombinase will be activated and catalyses double-stranded DNA breaks and recombines the two FRT sites. After the FLP/FRT-dependent mitotic recombination, the cells lacking GAL80 will activate the GAL4 and drive UAS-GFP to mark the cells (Figure 1.7). These GFP +ve cells are the homozygous mutant cells.

1.5.3.3 Inducible GAL4 system

Like MARCM, the inducible GAL4 system it uses the combination of the FRT/FLP and UAS-GAL4 systems (Zecca and Struhl, 2002). On the third chromosome, the tubulin promoter, GAL80 gene and the GAL4 gene were cloned sequentially and two FRT sites are present on both side of the GAL80 gene (Figure 1.8). Upon heat shock treatment, the two FRT site will be removed and the tubulin promoter will activate the GAL4 transcription. The GAL4 will then induce the UAS-GFP as a marker and the UAS will be coupled with the gene of interest. The UAS could also be coupled with RNAi sequences to generate mosaic knockdown.

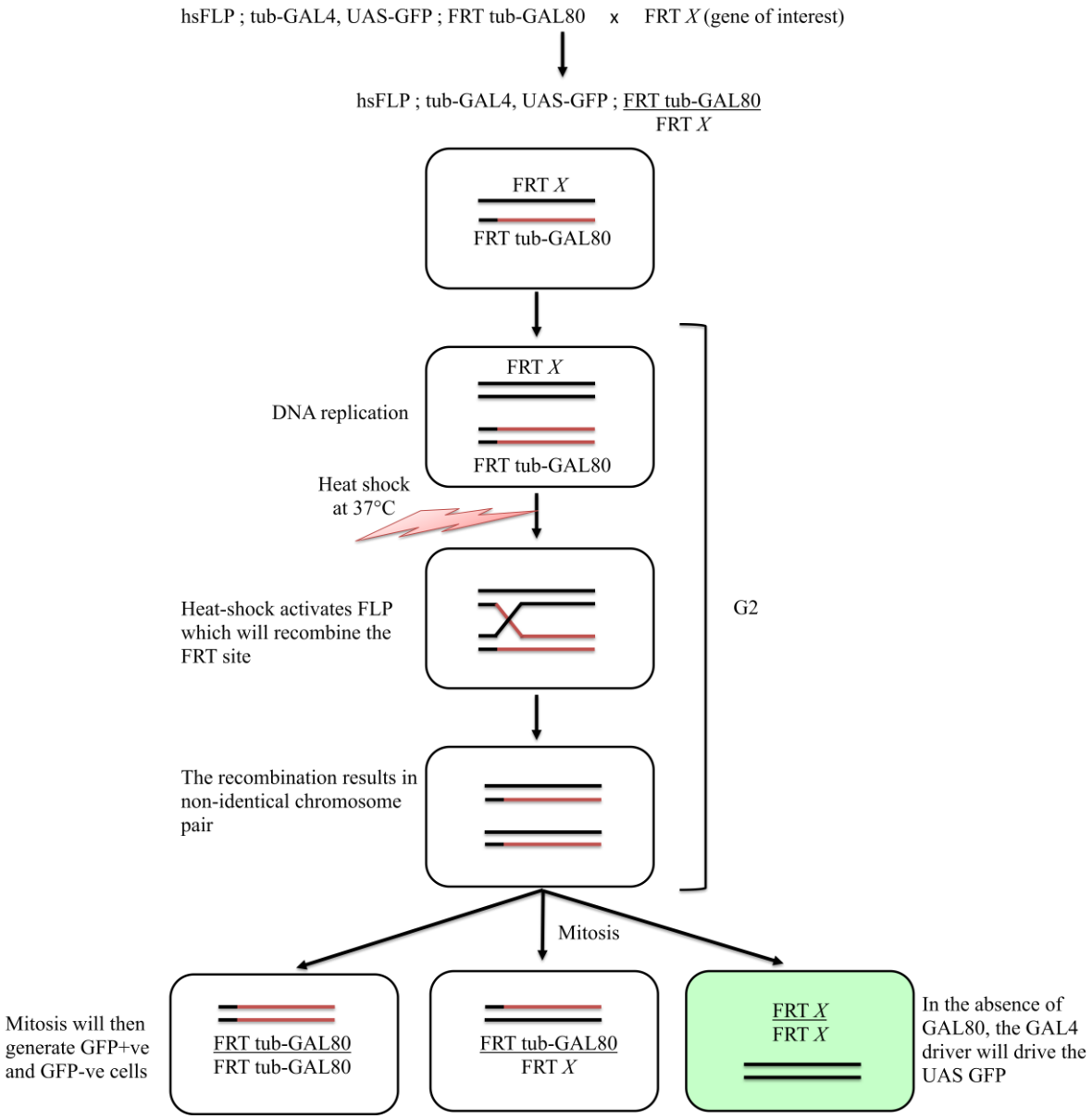


Figure 1.7. MARCM clones.

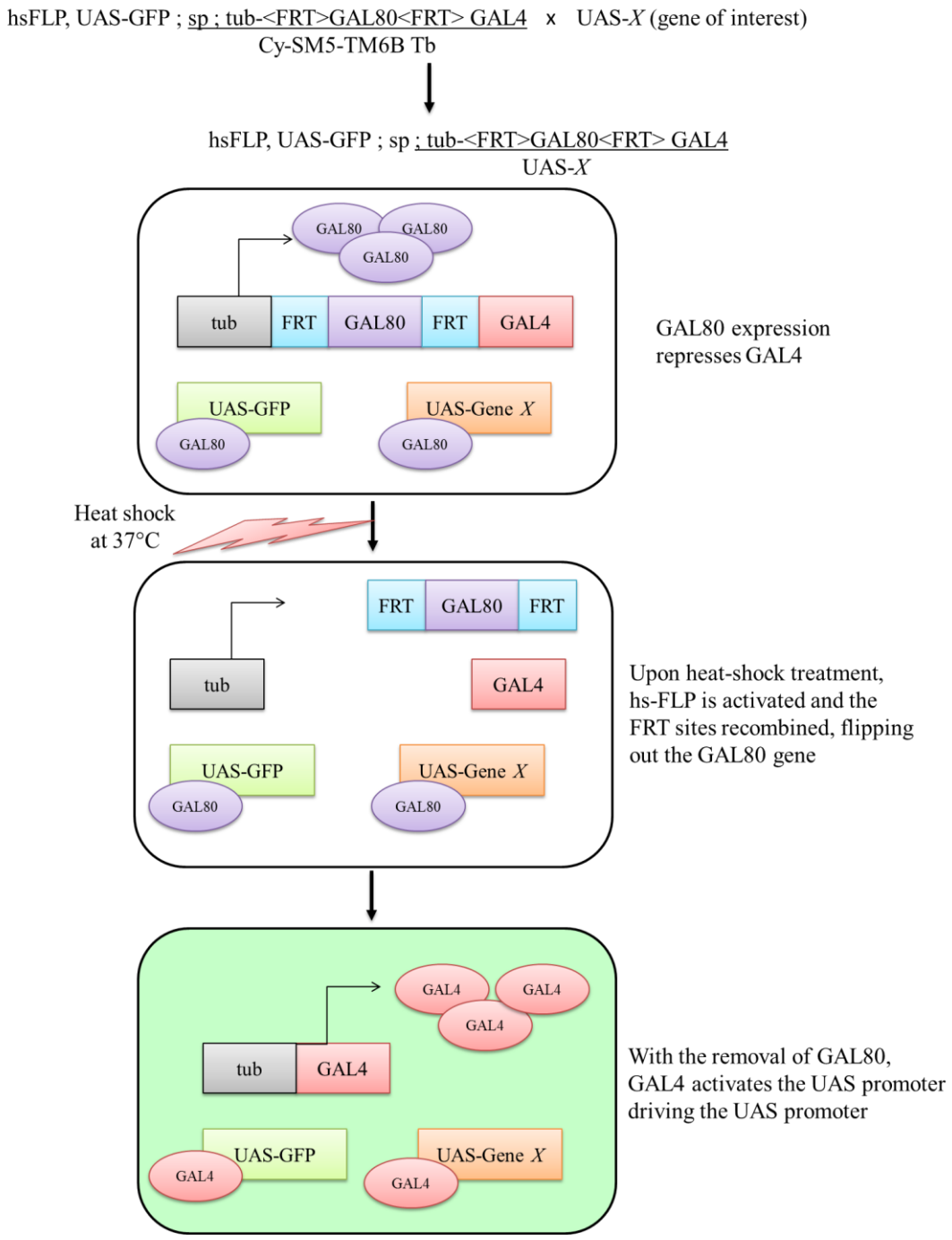


Figure 1.8. Inducible GAL4 system. The inducible GAL4 stocks are balanced using a compound balancer which links chromosome 2 and chromosome 3. The progenies are selected against Cy (for adults) or TM6B Tb (for larvae).

1.6 Aims and outline

The first aim of this thesis is to characterize the spatial and temporal distribution of Ago1 in the developing egg chambers. In Chapter 3, the work was focused on the germline cells. Using the information generated, the role of Ago1 in the egg chamber can then be studied using the genetic techniques. The relationship between Ago1 and P body components were also investigated. Furthermore, since Ago1 is an important protein for miRNA biogenesis, other miRNA biogenesis proteins were also analysed in order to determine if the phenotype is Ago1 specific or due to miRNA regulation. The roles of Ago1 and miRNAs were then analysed in the follicle cells in Chapter 4. With the information gathered from Chapter 3 and Chapter 4, it was then hypothesized that Ago1 protein stability is affected by the presence and absence of miRNAs. In Chapter 5, the stability of Ago1 was analysed using different tissues and S2 cells.

The identification of a novel structure containing CTPS, termed cytoophidia opens new opportunities to characterize the structure using the available genetic techniques in *Drosophila*. In Chapter 6, transgenic flies were generated with specific CTPS protein isoforms to study if all the CTPS isoforms localize to cytoophidia and to analyse CTPS overexpression transgene. With the results, the question was then focused on the regions in CTPS that are required for the formation of cytoophidia. Then in Chapter 7, CTPS mutants were then generated and characterized. Specifically, the mutants were analysed for development defects and lethality. Finally, Chapter 8 summarises the overall findings of the thesis. This chapter unifies the relevant areas and discussing the results as a whole.

Chapter 2
Materials and Methods

2.1. *Drosophila* stocks and genetics

2.1.1. Fly food and propagation

All stocks were raised at 25°C on standard cornmeal. *y w* flies were used as a control in all experiments if not indicated. List of stocks used in this thesis are listed in Table 2.1 and Table 2.2.

2.1.2. Isolation of new mutant alleles

New mutants of *pasha* and *dcr-1* described in this study were identified as part of an on-going genetic screen against a miRNA reporter that affects eye pigmentation (Smibert et al., 2011a). New mutations in *dicer-1*: *w; FRT82B dicer-1[21B2]/TM6B, w; FRT82B dicer-1[30D2]/TM6B, w; FRT82B dicer-1[37A1]/TM6B, w; FRT82B dicer-1[38E3]/TM6B* and *pasha*: *w; FRT82B pasha[36B2]/TM6B* were generated as part of the collaboration with the Lai lab at the Sloan-Kettering Institute, New York, USA. New mutants of *ctps* were generated in this study and described in Chapter 7. The mutants *FRT2A ctps[d06966]/ TM3 Ser, FRT2A ctps[e01207]/TM3 Ser* and *FRT2A ctps[d07411]/ TM3 Ser* were isolated based on the absence of cytoophidia.

Genotype	Nature of mutation	Comments	References
FRT42D ago1[k08121]	P-element	Hypomorphic mutant	Kataoka et al, 2001
FRTG13 ago1[k08121]	P-element	Hypomorphic mutant	Yang et al, 2007
FRTG13 ago1[14]	P-element	Null mutant	Yang et al, 2007
FRTG13 ago1[EMS]	EMS	Null mutant	Yang et al, 2007
Ago1::GFP	P-element	Ago1 GFP protein trap	Carnegie Protein Trap Collection Buszczak et al., 2007
CTPS::GFP	P-element	Ago1 GFP protein trap	Carnegie Protein Trap Collection Buszczak et al., 2007
FRT82B dicer-1[LL06357]	*piggyBac*	Null mutant	Berdnik et al., 2008
FRT82B dicer-1[Q1147X]	EMS	Null mutant	Lee et al., 2004
FRT82B pasha[LL03360]	*piggyBac*	Null mutant	Berdnik et al., 2008
FRT82B pasha[KO]	deletion of approximately 10kb	Null mutant	Martin et al., 2009
FRT42D drosha[21K11]	P-element	Null mutant	Smibert et al., 2011
FRT2A smn73A	Point mutation	Null mutant	Chan et al., 2003
FRT2A ctps[e01207]	*piggyBac*	Disrupts cytoophidia	Generated
FRT2A ctps[d07411]	P-element	Disrupts cytoophidia	Generated
FRT2A ctps[d06966]	P-element	Disrupts cytoophidia	Generated

Table 2.1. Table showing mutant stocks used.

Genotype	Comments	References
hsFLP, UAS-GFPnls; tub-FRT-GAL80-FRT-GAL4 / SM5, Cy-TM6 Tb	Inducible GAL4 system	Zecca and Struhl, 2002
hsFLP, UAS-GFPnls; UAS-Dicer-2; tub-FRT-GAL80-FRT-GAL4 / SM5, Cy-TM6 Tb	Inducible GAL4 system with UAS-Dicer-2	Zecca and Struhl, 2002
UAS-Ago1 T2.1	Ago1 overexpression construct	(Dietzl et al., 2007)
UAS-Dicer-1	Dicer-1 overexpression construct	Dietzl et al., 2007
UAS-Pasha	Pasha overexpression construct	Berdnik et al., 2008
UAS-miR-124a	miR-124a overexpression construct	Xu et al., 2008
UAS-miR124a-mutant	miR-124a mutant overexpression construct	Xu et al., 2008
UASp-String	String overexpression construct	Mata et al., 2000
UASp-Tribbles	Tribbles overexpression construct	Mata et al., 2000
UASp-CTPS isoC	CTPS isoC overexpression construct	Generated
UASp-CTPS isoB	CTPS isoB overexpression construct	Generated
UASp-CTPS isoA	CTPS isoA overexpression construct	Generated
UASp-CTPS isoC-Venus	C-terminal tagged CTPS isoC overexpression construct	Generated
UASp-CTPS isoB-Venus	C-terminal tagged CTPS isoB overexpression construct	Generated
UASp-CTPS isoA-Venus	C-terminal tagged CTPS isoA overexpression construct	Generated
UASp-Venus-CTPS isoC	N-terminal tagged CTPS isoC overexpression construct	Generated
UASp-Venus-CTPS isoB	N-terminal tagged CTPS isoC overexpression construct	Generated
UASp-Venus-CTPS isoA	N-terminal tagged CTPS isoC overexpression construct	Generated

UASp-Venus-N-term	N-terminal tagged N-term region overexpression construct	Generated
UASp-Trun isoC-Venus	C-terminal tagged Trun isoC overexpression construct	Generated
UASp-Venus-Trun isoC	N-terminal tagged Trun isoC overexpression construct	Generated
UASp-CTG-Venus	C-terminal tagged CTG domain overexpression construct	Generated
UASp-Venus-CTG	N-terminal tagged CTG domain overexpression construct	Generated
UASp-GATase1-Venus	C-terminal tagged GATase1 domain overexpression construct	Generated
UASp-Venus-GATase1	N-terminal tagged GATase1 domain overexpression construct	Generated
UAS-Dicer-1 RNAi	Dicer-1 RNAi construct	Bloomington #28598 & TRiP #HMS00064
UAS-Pasha RNAi	Pasha RNAi construct	Bloomington #26293 & TRiP #HMS00929
UAS- Dicer-2 RNAi	Dicer-2 RNAi construct	Bloomington #33656 & #27486
UAS-R2D2 RNAi	R2D2 RNAi construct	Bloomington #34784
UAS-CTPS RNAi	CTPS RNAi construct	Bloomington #31924

Table 2.2. Table showing UAS stocks used.

2.1.3. Mitotic clones

To generate Ago1 mitotic clones, *hsFLP; FRTG13 Ubi-GFP/CyO* flies were crossed to *y w; FRTG13 ago1[k08121]/CyO, y w; FRTG13 ago1[14]/CyO* or *y w; FRTG13 ago1[EMS]/CyO* flies. *y w; FRTG13* was used as positive control. To generate Pasha or Dicer-1 clones, *hsFLP; FRT82B Ubi-GFP/TM3 Ser* were crossed with *y w; FRT82B dicer-1[LL06357]/TM3Ser, y w; FRT82B dicer-1[Q1147X]/TM3 Ser, w; FRT82B dicer-1[21B2]/TM6B, w; FRT82B dicer-1[30D2]/TM6B, w; FRT82B dicer-1[37A1]/TM6B, w; FRT82B dicer-1[38E3]/TM6B, w; FRT82B pasha[LL03360]/TM3 Ser, w ; FRT82B pasha[KO]/TM6B* or *w ; FRT82B pasha[36B2]/TM6B. y w; FRT82B* was used as a positive control. To generate Drosha clones, *hsFLP; FRT42D Ubi-GFP/CyO* flies were crossed with *w; FRT42D drosha[21K11]/CyO* and *y w; FRT42D* was used as a positive control. To generate CTPS and SMN clones, *hsFLP; FRT2A Ubi-GFP/TM3 Ser* were crossed with *w; FRT2A ctps[d06966]/TM3 Ser, w; FRT2A ctps[d07411] /TM3 Ser, w; FRT2A ctps[e01207] /TM3 Ser* or *FRT2A smn73A/TM3 Ser*. *y w; FRT2A* was used as a positive control.

Eggs were collected in vials for 24 hours and heat-shocked after 4 days (3rd instar larvae) in a 37 °C water bath for 1 hour, once per day for 3 days. The larvae were left to pupate and newly eclosed flies were collected. The flies were then aged in fresh vials with wet yeast and transferred to new vials every day or every two days. Mutant cells are marked by the absence of GFP.

2.1.4. Germline clones

To generate CTPS germline clones, *w*; *FRT2A ovoD1/ DM3/ TM3 Sb* flies were crossed to *hsFLP ; FRT2A ctps[d06966]/TM3 Ser, hsFLP ; FRT2A ctps[d07411] /TM3 Ser, hsFLP ; FRT2A ctps[e01207] /TM3 Ser. y w; FRT2A* was used as a positive control.Eggs were left to grow at 25°C. Adult flies were collected and heat-shocked after 2 days in a 37 °C water bath for 1 hour, once per day for 3 days. The flies were then aged in laying cage with wet yeast and eggs were collected using apple juice plates with wet yeast.

2.1.5. MARCM clones

To generate Dicer-1 and Pasha MARCM clones in the larval central nervous system (CNS), *w, tub-GAL4 hsFLP122, UASnGFPmyc; FRT82B, tub-GAL80 / TM6B* flies were crossed with *y w; FRT82B dicer-1[LL06357]/TM3Ser, y w; FRT82B dicer-1[Q1147X]/TM3 Ser, w; FRT82B dicer-1[21B2]/TM6B, w; FRT82B dicer-1[30D2]/TM6B, w; FRT82B dicer-1[37A1]/TM6B, w; FRT82B dicer-1[38E3]/TM6B, w; FRT82B pasha[LL03360]/TM3 Ser, w ; FRT82B or w ; FRT82B pasha[36B2]/TM6B. y w; FRT82B* was used as a positive control. Eggs were collected in vials and heat-shocked at 24 and 48 hours in a 37 °C water bath for 1 hour. Larvae were dissected at wandering 3rd instar larvae stage. Mutant cells are marked by the presence of GFP.

2.1.6. Inducible GAL4 system

To generate clones overexpressing Ago1, Dicer-1, Pasha, miR-124a, miR-124a-mutant, String and Tribbles; *hsFLP, UAS-GFPnls; sp; tub FRT-GAL80-FRT-GAL4 / SM5, Cy-TM6 Tb* flies were crossed with *UASp-Ago1, UAS-Dicer-1, UAS-Pasha, UAS-miR-124a, UAS-miR124a-mutant, UASp-String* and *UASp-Tribbles*. To generate CNS clones, eggs were

collected in vials and heat-shocked at 24 hours in a 37 °C water bath for 1 hour. To generate follicle cell clones, eggs were collected in vials for 24 hours and heat-shocked after 4 days in a 37 °C water bath for 1 hour. The cells expressing the construct are marked by the presence of GFP.

To generate RNAi knockdown clones of Drosha, Dicer-1, Pasha, Dicer-2, R2D2, CTPS and String, *hsFLP, UAS-GFPnls; UAS-Dcr2 ; tub-FRT-GAL80-FRT-GAL4 / SM5, Cy-TM6 Tb* was crossed to *UAS-Drosha RNAi* (Bloomington #22704), *UAS-Dicer-1 RNAi* (Bloomington #28598 & TRiP #HMS00064), *UAS-Pasha RNAi* (Bloomington #26293 & TRiP #HMS00929), *UAS- Dicer-2* RNAi (Bloomington #33656 & #27486), *UAS-R2D2 RNAi* (Bloomington #34784), and *UAS-CTPS RNAi* (Bloomington #31924). To generate CNS knockdown clones, eggs were collected in vials and heat-shocked at 24 hours in a 37 °C water bath for 1 hour. To generate follicle cell knockdown clones, eggs were collected in vials for 24 hours and heat-shocked after 4 days in a 37 °C water bath for 1 hour. The cells expressing the RNAi construct are marked by the presence of GFP.

2.1.7. Scanning electron microscope (SEM)

To prepare for SEM, flies were incubated in absolute ethanol, dried using a critical point dryer, Autosamdri-815 (Tousimis) and coated with gold. Silver coating was added to improve conductivity. The eye is then photographed using a JOEL JSM-6390.

2.1.8. Immunofluorescence

Tissues were dissected in Grace's insect medium (Invitrogen Cat. #11605045) and fixed with 4% paraformaldehyde for 10 minutes, washed with PBT (PBS + 0.4% Triton X-100), blocked with 5% horse serum for one hour and incubated in primary antibodies (Table 2.3) at room temperature overnight. Samples were washed with PBT and then incubated overnight with the DNA dye Hoechst 33342 and secondary antibodies (Table 2.4). All samples were examined and captured using a laser-scanning confocal microscope (Zeiss LSM 510 META, Oberkochen, Germany).

2.2. Schneider 2 (S2) cells

2.2.7. S2 cell culture

The S2 cell line derived from late embryonic stage Oregon R line (Schneider, 1972). The S2 cells used here were acquired from *Drosophila* Genomics Resource Center (DGRC) stock labeled S2-DRSC (stock number 181). This S2-DRSC line has been extensively analysed by the modENCODE project for the RNAi screening. S2 cells were cultured in Schneider's medium (Sigma, S0146) with 10% foetal calf serum (FCS) (Invitrogen Cat. #10082) and Penicillin – Streptomycin (Invitrogen Cat. #15070-063) at 25°C incubator.

2.2.8. S2 cells dsRNA transfection

The S2 cells were counted and 1-5 x 10^6 cells/ml were re-suspended in serum-free media. 470ul of water and 30ug (30ul of 1ug/ml) of dsRNA were added in to each well of a 6 well plate. Then, 500ul of cells are added into each well and incubated for 30 minutes at room temperature. After the incubation, 3ml of complete media (Schneider+10%FCS) was added to each well. The cells were then incubated at 25°C for at least four days.

Primary antibody	Concentration	Source
Rabbit anti-dAgo1	1:500	Abcam ab5070
Rabbit anti-alpha tubulin	1:3000	Abcam ab15246
Rabbit anti-Oskar	1:3000	Paul Lasko
Rabbit anti-CTPS y-88	1:1000	Santa Cruz sc-134457
Rabbit anti-Me31B	1:2000	Kobayashi
Rabbit anti-cyclin-E	1:500	Santa Cruz sc-33748
Rabbit anti-Vasa	1:50	Santa Cruz sc-30210
Rabbit anti-Caspase 3	1:100	Cell Signaling - Cat # 9661S
Rabbit anti-Cup	1:1000	A. Nakamura
Rabbit anti-Coilin	1:1000	Joseph Gall
Rabbit anti-SMN	1:2000	Jianhua Zhou
Rabbit anti-ABP2	1:5000	Paul Lasko
Rabbit anti-Syntaxin 16	1:1000	Abcam ab32340
Goat anti-GFP	1:3000	Abcam ab6673
Goat anti-CTPS yD-18	1:1000	Santa Cruz sc-33304
Guinea pig anti-Gawky	1:1000	Andrew Simmonds
Mouse anti-Orb (6H4)	1:1000	DSHB 6H4
Mouse anti- dAgo1 (1B8)	1:1000	Haruhiko Siomi
Mouse anti-HTS (1B1)	1:20	DSHB 7H9 1B1
Mouse anti-Cup	1:5000	A. Nakamura
Mouse anti-Armadillo (N2 7A1)	1:100	DSHB N2 7A1
Mouse anti-Engrailed (4D9)	1:1000	DSHB 4D9
Mouse anti-Miranda	1:200	Fumio Matsuzaki
Mouse anti-MPM2	1:100	Joseph Gall

Table 2.3. Primary antibodies used with its concentration and sources.

Secondary antibody	Concentration	Source
Goat anti-mouse Alexa 488	1:1000	Molecular probes A11029
Goat anti-mouse Alexa 546	1:1000	Molecular probes A21123
Goat anti-mouse Alexa 633	1:1000	Molecular probes A21126
Donkey anti-mouse Cy5	1:500	Jackson 715-175-150
Donkey anti-mouse Cy3	1:500	Jackson 711-165-152
Goat anti-rabbit Alexa 488	1:1000	Molecular probes A11034
Goat anti-rabbit Alexa 546	1:1000	Molecular probes A21123
Goat anti-rabbit Alexa 532	1:1000	Molecular probes A11009
Goat anti-rabbit Alexa 633	1:1000	Molecular probes A21070
Donkey anti-rabbit Dylight 549	1:500	Jackson 711-505-152
Donkey anti-rabbit Cy5	1:500	Jackson 715-175-150
Donkey anti-guinea pig Dylight 649	1:1000	Jackson 706-495-148
Donkey anti-goat Alexa488	1:1000	Molecular probes A11055
Donkey anti-goat Cy5	1:500	Jackson 715-165-150
Rhodamine-conjugated Phalloidin	1:500	Invitrogen R415
Hoechst 33342	1:1000	Invitrogen H1399

Table 2.4. Secondary antibodies used with its concentration and sources.

2.3. Protein Biochemistry

2.3.7. Western blot

Tissues were dissected in Graces medium and transferred into radio immunoprecipitation assay (RIPA) lysis buffer (150mM NaCl, 0.5% sodium deoxycholate, 0.1% SDS, 50mM Tris pH 8 and 1% NP40) and homogenised on ice. For cell cultures, approximately 100µl containing $1x10^6$ cells are taken and spun down at 13 000 RPM at 4°C for 10 minutes. The supernatant was then removed and washed with cold PBS. The cell pellet is then resuspended with RIPA lysis buffer and left for 5 minutes on ice. The lysates (from tissues or cells) were then centrifuged at 13 000 RPM for 10 minutes at 4°C. Then, the supernatant was taken out and mixed with LDS (Invitrogen NP0008) and a sample reducing agent (Invitrogen NP0009). The mixture was then heated at 70°C for 10 minutes. Samples now are either loaded straight after or stored at -20°C.

Samples are run on NuPAGE NOVEX 10% Bis-Tris pre-cast gel (Invitrogen NP0315BOX) on an XCell SureLock™ Mini-Cell (Invitrogen EI0001) with NuPAGE MOPS SDS running buffer (Invitrogen NP0001) supplemented with NuPAGE Antioxidant (Invtrogen NP0004) for 1 hour at 200V. The gel was transferred onto a nitrocellulose membrane (Hybond ECL, RPN68D) using the XCell II™ Blot Module CE Mark (Invitrogen EI9051) using the NuPAGE transfer buffer (Invitrogen NP0006). The nitrocellulose membrane was then blocked using 5% non-fat milk in TBST for 1 hour. Primary antibodies; rabbit anti-Ago1 (1:1000) (Abcam ab5070) and rabbit anti-alpha-tubulin (1:5000) (Abcam ab15246) were added and incubated overnight at 4°C. The nitrocellulose membranes were washed in TBST and incubated with donkey anti-rabbit HRP (1:5000) (Jackson 711-035-152) for 1 hour at room temperature. The HRP signals were detected using chemiluminescent and exposed to film (Amersham Hyperfilm ECL) which was later developed.

2.4. Molecular Biology

2.4.7. Genomic DNA extraction

Genomic DNA extraction were carried out by grinding flies in squishing buffer (10mM Tris-HCl pH8, 1mM EDTA, 25mM NaCl and 200g/ml Proteinase K). The samples were then incubated at 37°C for 30 minutes, and then Proteinase K was inactivated by incubating samples at 95°C for 3 minutes. Samples were then used immediately or stored at -20°C.

2.4.8. Double-stranded RNA(dsRNA) synthesis

The dsRNA primers for knocking down Ago1, Dicer-1, Pasha, Dicer-2, Ago2, CTPS and eGFP in S2 cells were designed using the SnapDragon software (http://www.flyrnai.org/cgi-bin/RNAi_find_primers.pl) and a T7 promoter sequences (TAATACGACTCACTATAGGG) were added to the 5' end of both primers. The purified dsRNA were tested in S2 cells and the sequence that gave the best knockdown and was used in further studies is shown in Table 2.5 as with the sequence of miR-124, miR-124-mutant (Xu et al., 2008), Bantam and miR-14.

A standard PCR was carried out using *y w* genomic DNA, *w, FRT42D Ubi-eGFP* genomic DNA for eGFP dsRNA and *w; miR-124-mutant* for miR-124 mutant dsRNA. In vitro RNA transcription (Ambion MEGAscript T7 kit Cat. No 1334) was then carried out using the PCR product and incubated O/N at 42°C. The dsRNA product is then run on a 1% agarose gel to check the integrity and size.

Ethanol purification was then carried out. The product was then diluted with sterile water into 100µl. 1/10 volume of 3M sodium acetate (NaOAc) (pH5.2) was added with 1µl of Glycoblue (Ambion Cat. No AM9515). The mixture is vortex to mix and 2½ volume of 100%

ethanol was added. After mixing by inverting, the mixture is then incubated at 4°C for 30 minutes. It is then centrifuged for 30 minutes at 4°C. 70% ethanol is then added to the mixture and spun at 4°C. The pellet is then washed with 70% ethanol and spun again at 4°C for 5 minutes. Repeat this wash twice. Remove as much ethanol as posiblee and leave it to dry for 10 minutes at room temperature. The pellet is then resuspended with 50µl of sterile water and the concentration was quantified using Nanodrop 1000. Then the dsRNA concentration was adjusted with sterile water to 1 µg/µl and stored at -20°C.

2.4.9. Total RNA extraction and reverse transcription

RNA extraction was performed by homogenizing sample using Qiagen QIAshredder (Cat no. 79654) and RNA was extracted using Qiagen RNeasy Plus Mini Kit (Cat.no 74134) as per manufacturer's instructions. Samples were kept at -80°C. Reverse transcription was carried out using Qiagen QuantiTect Rev. Transcription Kit (Cat no. 205311) with the gDNA removal step following the manufacturer's instruction. The cDNA were then further diluted 1:10 with nuclease free water (Ambion, AM9938) and kept at -20°C.

2.4.10. Quantitative PCR (qPCR)

About 1µl of diluted cDNA from the reverse transcription were mixed with Fast SYBR Green Master Mix (Applied Biosystem Cat. No 4385612) and 1uM of primers (Table 2.6) for each 10µl qPCR reactions. The reactions were carried out using 7500 Fast Real-Time PCR System (Applied Biosystems) using the Fast setting; initial denaturation at 95°C for 20seconds, denaturation at 95°C for 3 seconds, primer annealing and elongation at 60°C for 30 seconds, repeated for 40 cycles then final denaturation at 95°C for 15 seconds and final primer annealing and elongation at 60°C for 1 minute. Expression values were normalized using reference gene *RP49*. Melting curve was carried out on all sets of primers.

Primer Name	Sequence	Product Size
Ago1 RNAi T7 Forward	TAATACGACTCACTATAGGGAAGCAGTTCTTCACTGGCGT	519
Ago1 RNAi T7 Reverse	TAATACGACTCACTATAGGGGGCAATCGATGGTTTCTTGT	
Dicer-1 RNAi T7 Forward	TAATACGACTCACTATAGGGGTGGATCAAATGGACCAACC	405
Dicer-1 RNAi T7 Reverse	TAATACGACTCACTATAGGGCTCCAACTCAGCCTCTTTGG	
Pasha RNAi T7 Forward	TAATACGACTCACTATAGGGACTTGAATTGCGCAGCTTTT	491
Pasha RNAi T7 Reverse	TAATACGACTCACTATAGGGACTTCGTCGAGAACCTGGAA	
Dicer-2 RNAi T7 Forward	TAATACGACTCACTATAGGGATTCCCAAAACGCTCAACAC	321
Dicer-2 RNAi T7 Reverse	TAATACGACTCACTATAGGGATCGGCTATCACCTTGTTGG	
Ago2 RNAi T7 Forward	TAATACGACTCACTATAGGGGGTCGGTCTGTATCAGGCAT	318
Ago2 RNAi T7 Reverse	TAATACGACTCACTATAGGGGACGCAATGGTGACCTTCTT	
CTPS RNAi T7 Forward	TAATACGACTCACTATAGGGTAGCCATGGCATCCTAGTCC	585
CTPS RNAi T7 Reverse	TAATACGACTCACTATAGGGCCGCGCTGAATATATTGGTT	
eGFP RNAi T7 Forward	TAATACGACTCACTATAGGGACGTAAACGGCCACAAGTTC	495
eGFP RNAi T7 Reverse	TAATACGACTCACTATAGGGTGTTCTGCTGGTAGTGGTCG	
miR-124 T7 Forward	TAATACGACTCACTATAGGGTCATTTGGTACGTTTTTCTC	100
miR-124 T7 Reverse	TAATACGACTCACTATAGGGATTTGTAGAACTGCGTTCGC	
miR-124 mutant T7 Forward	TAATACGACTCACTATAGGGGGTACGTTTTTCTCCTGGTA	94
miR-124 mutant T7 Reverse	TAATACGACTCACTATAGGGATTTGTAGAACTGCGTTCG	
Bantam T7 Forward	TAATACGACTCACTATAGGGATTTGACTACGAAACCGGTT	81
Bantam T7 Reverse	TAATACGACTCACTATAGGGTTGACAAAATCAGCTTTCAA	
miR-14 T7 Forward	TAATACGACTCACTATAGGGTGTGGGAGCGAGACGGGGAC	63
miR-14 T7 Reverse	TAATACGACTCACTATAGGGTATAGGAGAGAGAAAAAGAC TGA	

Table 2.5. Primers used to generate dsRNA.

Primer Name	Sequences	Product Size
Ago1 Forward	GTTCTGTGGGACGACAATCAC	150
Ago1 Reverse	ATGATATCTGGCACGGAAGG	
Dicer-1 Forward	GCTGATCACAGAACTTAACG	150
Dicer-1 Reverse	AGCTGCAAGAGGCTGATGAC	
Pasha Forward	CTGCGACAGTTCCAGGTTCT	150
Pasha Reverse	ATCGTATTCTTCGCCGTCAC	
Drosha Forward	CCAACAATGCCCTTAAGAAGTAAC	160
Drosha Reverse	GCATACGCAAAGCTGTTCATC	
Dicer-2 Forward	TGCCAACAAGAACTTGGTTTT	149
Dicer-2 Reverse	AGGCGGTGCACCAACTTTA	
Ago2 Forward	GGAAGTGACTGTGACAGATCGTA	101
Ago2 Reverse	AAGTAGTTAACGATTTAAGGTCAATGG	
CTPS Forward	AGAGGACCAAATGCTTGCAG	174
CTPS Reverse	GCGTACGAATCCGTGAACTT	
RP49 Forward	CCGCTTCAAGGGACAGTATCTG	156
RP49 Reverse	ATCTCGCCGCAGTAAACGC	

Table 2.6. Primer sequences used for qPCR.

2.5. Transgenic construct generation

To make the untagged constructs, the gene sequence was amplified by PCR from cDNA using Pfx polymerase (Invitrogen 11708-021) and specific primers with additional restriction site sequences (Table 2.7). Both PCR products and the pUASp-K10-attB vector were then digested using specific restriction enzyme individually and ligated using T4 DNA ligase (NEB M202). The product is then sequenced before being injected into embryos.

To make the Venus tagged construct, the gene sequence was amplified by PCR from specific cDNA using Pfx polymerase (Invitrogen 11708-021) and isoform specific primers (Table 2.8) that have additional sequences as described by the *Drosophila* Gateway Vector Collection protocol. The PCR products were then cloned into a pENTR using the pENTR/D-TOPO cloning kit (Invitrogen K240020). Then, to make the destination construct, the sequences cloned into the pENTR vector were recombined into the UASp-Venus (N-terminal tagged or C-terminal tagged) vector using LR clonase II (Invitrogen 11791020). The final constructs were then sequenced before being sent to be injected.

Embryo injections were carried out by GenetiVision Inc. (Texas, USA) or Department of Genetics, University of Cambridge, UK. Constructs that have the attB sequence were injected using the PhiC31 integrase-mediated site specific injection with specific landing site (Bischof et al., 2007). P-element construct were injected and the progenies were scored using eye marker.

Primer Name	Sequence	Product Size
UASp-Ago1 Forward Reverse	GTGGTACCATGTCCACGGAGCGTGAGCT GTGGATCCTTAGGCAAAGTACATGACCT	4316
UASp-CTPS isoA Forward Reverse	GTGGTACCATGGCGCCAAAAAAGTCCAC GTTCTAGACTACTTGGACTCCTCAAGAT	1596
UASp-CTPS isoB Forward Reverse	GTGGTACCATGGCGCCAAAAAAGTCCAC GTGGATCCTTACTTATGGCCATTGGTAG	2423
UASp-CTPS isoC Forward Reverse	GTGGTACCATGAAATACATCCTGGTAAC GTGGATCCTTACTTATGGCCATTGGTAG	2397

Table 2.7. Primer sequences used for generating untagged constructs.

Primer Name	Sequence	Product Size
UASp-CTPS isoA-Venus Forward Reverse	CACCATGGCGCCAAAAAAGTCCAC CTTGGACTCCTCAAGATCTTCTTTGTAG	1596
UASp-Venus-CTPS isoA Forward Reverse	CACCGCGCCAAAAAAGTCCACCAT CTACTTGGACTCCTCAAGATCTTCTTTGT	1596
UASp-CTPS isoB-Venus Forward Reverse	CACCATGGCGCCAAAAAAGTCCAC CTTATGGCCATTGGTAGGAT	2423
UASp-Venus-CTPS isoB Forward Reverse	CACCGCGCCAAAAAAGTCCACCAT TTACTTATGGCCATTGGTAG	2423
UASp-CTPS isoC-Venus Forward Reverse	CACCATGAAATACATCCTGGTAAC CTTATGGCCATTGGTAGGAT	2397
UASp-Venus-CTPS isoC Forward Reverse	CACCAAATACATCCTGGTAACTGGTGGCG TTACTTATGGCCATTGGTAG	2397
UASp-N term-Venus Forward Reverse	CACCATGAAATACATCCTGGTAAC CATGCTCATAAGGCGA	166
UASp-Venus-N term Forward Reverse	CACCAAATACATCCTGGTAACTGGTGGCG TTACATGCTCATAAGGCGA	169
UASp-Trunc isoC-Venus Forward Reverse	CACCATGGAGGTTTACGTTTTGGACG CTTATGGCCATTGGTAGGAT	1879
UASp-Venus-Trunc isoC Forward Reverse	CACCGAGGTTTACGTTTTGGACG TTACTTATGGCCATTGGTAG	1886
UASp-CTG-Venus Forward Reverse	CACCATGAAATACATCCTGGTAAC TTCACGGCGAACGGTCT	895
UASp-Venus-CTG Forward Reverse	CACCAAATACATCCTGGTAACTGGTGGCG TTATTCACGGCGAACGG	898
UASp-GATase1-Venus Forward Reverse	CACCATGATTGAATACCTAAATGA CTTATGGCCATTGGTAGGAT	1169
UASp-Venus-GATase1 Forward Reverse	CACCATTGAATACCTAAATGA CATGCTCATAAGGCGA	1166

Table 2.8. Primer sequences used for generating Venus-tagged constructs.

Chapter 3
Ago1 and its miRNA biogenesis partners are required for oocyte formation and germ cell division

3.1. Introduction

3.1.1. Oogenesis

Drosophila oogenesis has been extensively studied and provides an excellent system for studying genetics, cellular and developmental biology. Each adult female has two ovaries (Figure 3.1A). Each ovary contains about 14-20 strings of egg chambers called ovarioles (Figure 3.1B) (Spradling, 1993a). The egg chamber also contains two types of cells; the germline cell and the somatic follicle cells. Germline cells are formed in the germarium, at the most anterior part of the ovariole, which contains two to three germline stem cells (GSC) (Figure 1.5C). The GSC divides into two daughter cells along the anterior-posterior axis. The anterior daughter cell remains as a stem cell, contacting cap cells in the niche and maintaining its identity, while the posterior daughter cell differentiates into a cystoblast (Xie and Spradling, 2000). The cystoblast undergoes four mitotic divisions with incomplete cytokinesis to form 16 cyst cells. These cyst cells are connected to each other via stable intercellular bridges named ring canals. One cyst cell will become the oocyte while the other 15 will become the nurse cells (Spradling, 1993a).

Oocyte determination starts in the germarium at region 2a after the 16 cell cyst has formed. Two pro-oocytes are determined in region 2a before the mature oocyte forms in region 2b (Figure 1.5C). How the oocyte is chosen remains unclear. The oocyte will continue to grow and receive all its nutrients from the nurse cells via the microtubule network. The

large and active cells in the egg chamber make it a very attractive tissue to work with. The somatic stem cell (SSC) resides on the border of region 2a and region 2b. It divides to produce follicle cells which will encapsulate the germline cell in region 2b to form an egg chamber.

3.1.2. miRNAs and oogenesis

Oogenesis in *Drosophila* is rich in post-transcriptional control of gene expression hence it is not surprising that miRNA regulation is active in this setting (Lipshitz and Smibert, 2000; Reich et al., 2009). At least 43 miRNAs are expressed in the *Drosophila* germline (Neumuller et al., 2008). Furthermore, miRNAs are also maternally deposited into the egg (Liu et al., 2007). However, most miRNA studies in oogenesis focus on the GSCs. Dicer-1, Loquacious (Loqs) and Ago1 are miRNA biogenesis proteins that have been implicated to be important for GSCs' differentiation and maintenance (Hatfield et al., 2005; Jin and Xie, 2007; Park et al., 2007; Yang et al., 2007). Individual miRNAs have also been implicated on their role in GSCs. Elimination of Bantam phenocopies the *dicer-1* mutation and results in GSC loss after 14 days (Shcherbata et al., 2007). Another miRNA, miR-7, has a distinct role in the differentiation of GSCs (Pek et al., 2009).

Ionive et al., (2009) characterized miR-184 and reported multiple roles of miR-184 during germline development. Although the mutant of miR-184 survives untill adulthood, the adult female flies lay significantly less eggs compared to the wild-type. Furthermore, the eggs laid also show phenotypic defects in dorsoventral patterning. In their studies on the egg chamber, they found that the dorsoventral patterning defects manifested during oogenesis through the misregulation of K10, which is a transport factor for Gurken. The GSCs are also maintained by miR-184 where the loss of miR-184 leads to the loss of GSCs.

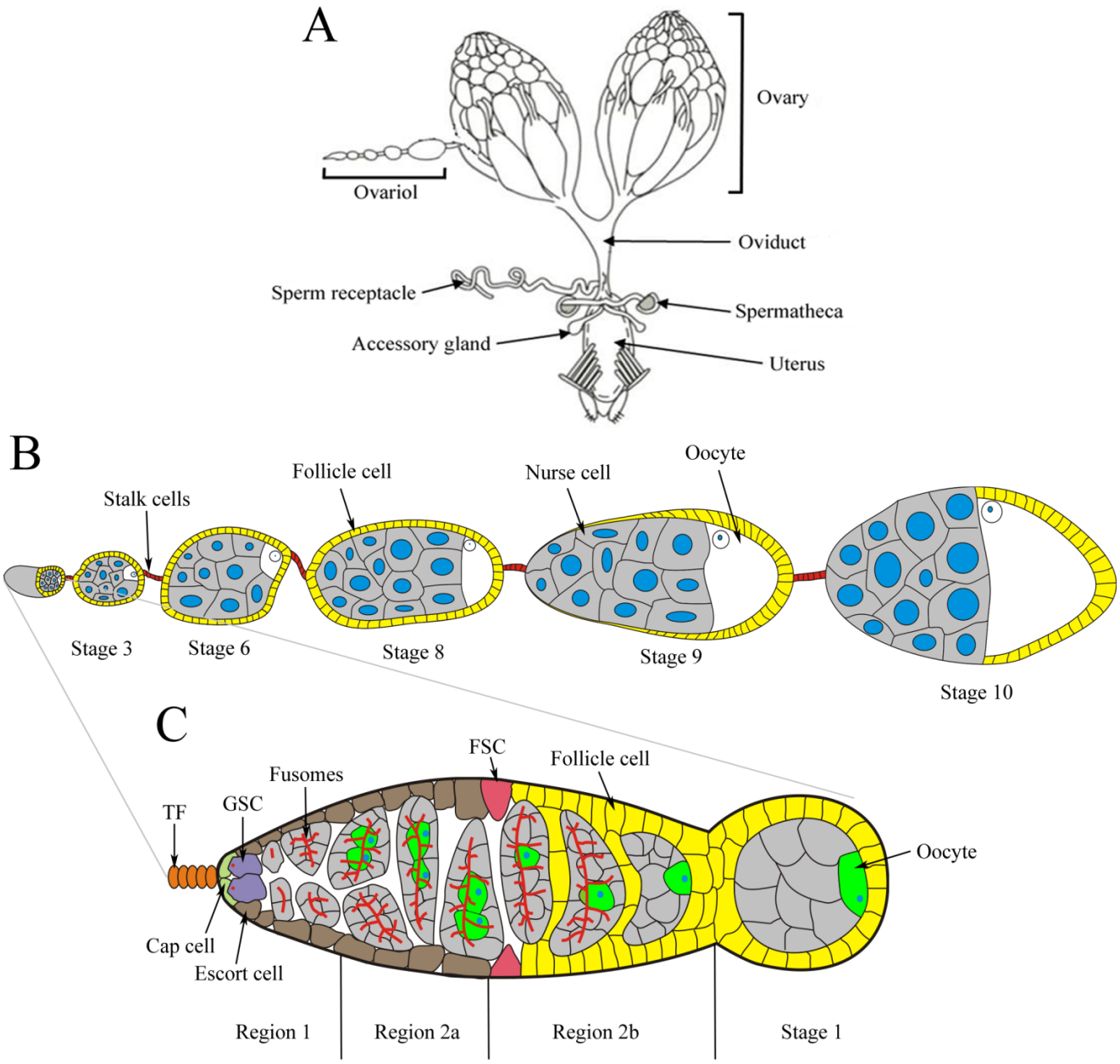


Figure 3.1. Schematic of *Drosophila* female germline. (A) Each female fruit fly has two ovaries which contain about 14-20 strings of ovarioles. (B) *Drosophila* oogenesis. Ovarioles contain stings of egg chambers. Each egg chamber consists of follicle cells (yellow), nurse cells (grey) and one oocyte (green). They are separated by stalk cells. (C) The germarium contains two sets of stem cells, the GSCs (purple) and follicle stem cells (FSCs) (red). Both germline cells and follicle cells work in tandem to continuously generate egg chambers.

3.1.3. Experiment descriptions

Many studies on miRNAs focus on the GSCs but the role of miRNAs in the later stages is still elusive. The main purpose of this study is to investigate the role of Ago1 during oogenesis. With the tools available, the spatial and temporal expression of Ago1 is going to be investigated. The expression of Ago1 will give early indication of the level of miRNA activity. The role of Ago1 during oogenesis will be determined using clonal analysis on three different *ago1* mutants. Ago1 has been shown to localize with P bodies in S2 cells. However, it is yet to be established whether this localization is also happening *in vivo*. Several P body markers are going to be used to answer this question. Then, the results found will be repeated with *dicer-1, pasha* and *drosha* mutants to see if it is due to miRNA depletion phenotype or an independent role of Ago1.

3.2. Results

3.2.1. Ago1 protein is expressed in egg chambers and enriched in oocytes

In order to characterize the expression of Ago1 in the *Drosophila* ovary, a protein trap line, *CA06914* was analysed (Buszczak et al., 2007). In this line, a *P-element* was inserted in an intron of the *ago1* gene such that a fusion protein (Ago1::GFP) was produced and expressed under the endogenous promoter. In *CA06914* flies, Ago1::GFP tagged fusion was expressed in the cytoplasm of nurse cells, oocytes and follicle cells. Follicle cells showed a much higher expression of GFP than nurse cells. In addition, GFP expression was found to be highly enriched in oocytes at all developmental stages (Figure 3.2A and A'). The enriched GFP signals were more or less evenly distributed in the ooplasm at the early- and middle-stages but preferentially localized to the posterior cortex of oocytes at stages 9 and 10.

To confirm that Ago1::GFP expression in *CA06914* is indicative of Ago1 localization, endogenous Ago1 protein was stained using both anti-rabbit and anti-mouse antibodies against *Drosophila* Ago1 (Table 2.3) (Figure 3.2B and C). The expression pattern of Ago1 labelled by two Ago1 antibodies in wild-type ovaries resembled the Ago1::GFP pattern observed in *CA06914* flies (Figure 3.2A, B and C). The staining of Ago1 in the oocyte is clear until the egg chamber reaches stage 7, double staining of Ago1 and Oskar revealed that they co-localized at the posterior cortex in stage 10 oocytes (Figure 3.2D). This shows that Ago1 protein localized to the posterior end of the egg chamber after stage 7.

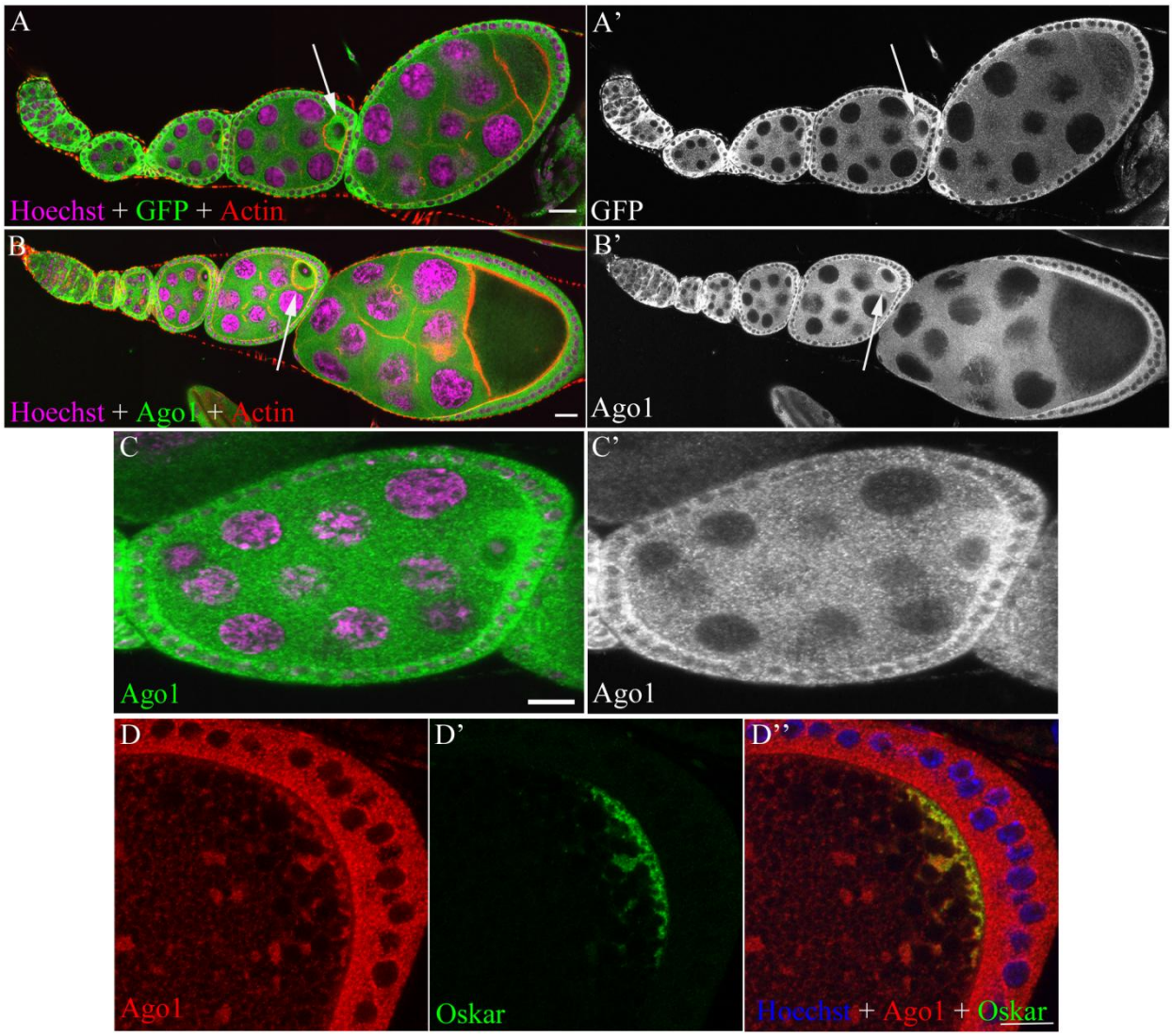


Figure 3.2. Ago1 distribution in *Drosophila* egg chambers. (A & A') Ago1::GFP protein trap line and (B & B') Ago1 antibody staining in the *Drosophila* egg chambers showing the distribution of Ago1 protein. Ago1 is distributed in the cytoplasm but it is enriched in the developing oocyte (arrow) and clearly seen in egg chamber stage 7. GFP / Ago1 are shown in green, DNA in magenta and F-actin in red (C-E) Ago1 colocalizes with Oskar at the posterior cortex of a stage-10 oocyte. Ago1 is shown red, Oskar in green, and DNA in blue. Scale bars, 20 µm.

The expression pattern of Ago1 protein was further confirmed by clonal analysis of *ago1* mutants (Chapter 2.1.3). Larvae were heat-shocked at 2nd instar to induce follicle cell clones or 3rd instar to induce germline clones. The Ago1 antibodies were markedly reduced in *ago1* mutant follicle cells and germline cells (Figure 3.3A-B'' and 3.4B-C''). Within the germline, the reduction in Ago1 is most obvious in the oocyte, where the relative enrichment of Ago1 protein compared to the nurse cells (Figure 3.2B) was greatly decreased (Figure 3.3B). Similar observations were seen when analysing clones of all three *ago1* mutant alleles; *ago1[k08121]*, *ago1[14]*, and *ago1[EMS]* (Figure 3.3 and 3.4).

In addition, an inducible GAL4 driver (Chapter 1) was used to overexpress Ago1 in 'flip out' clones, where the co-expression of a UAS-GFP transgene marks the cells that are overexpressing Ago1 (Zecca and Struhl, 2002). Staining of follicle cells for Ago1 revealed that Ago1 expression in GFP positive cells was clearly higher than that in GFP negative cells (Figure 3.3C). Together, these data demonstrate that the expression pattern detected by the Ago1 protein trap is representative of endogenous Ago1 and that the antibodies used are specific to Ago1.

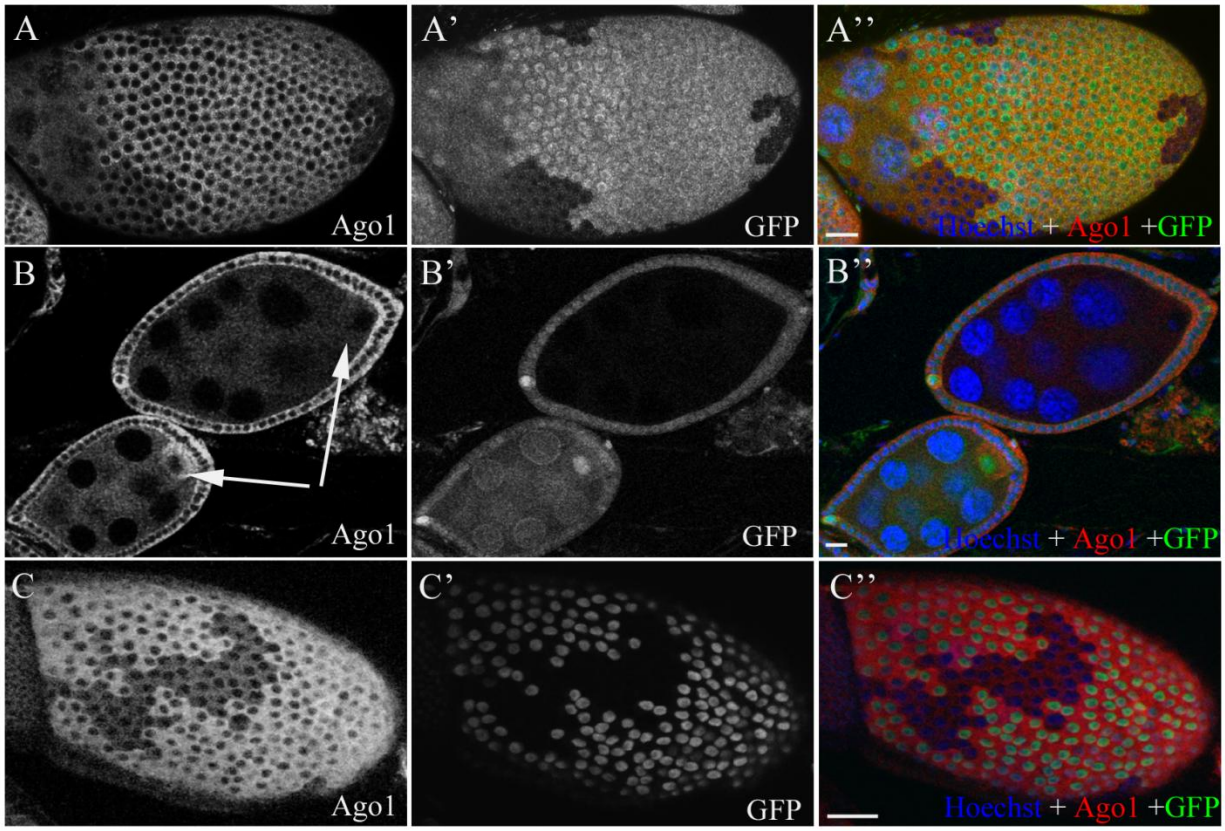


Figure 3.3. Ago1 staining is reduced in *ago1* mutants and increases upon overexpression. (A-C'') Different timing of heat-shock generates clones on either follicle cells (A) or germline cells (B). (A-B'') Mutant clones (GFP –ve) show lower expression of Ago1 compared to wild-type (GFP +ve) cells. (A-A'') Ago1 expression in follicle cell clones of the *ago1[k08121]* mutant. (B-B'') Ago1 expression in germline clones. Ago1 enrichment in the oocyte was also dramatically reduced in the *ago1[k08121]* mutant clones compared to positive control (arrow). (C-C'') Overexpression using an inducible GAL4 driving UAS-Ago1 shows overexpressing clones (GFP +ve) have brighter Ago1 staining compared to wild-type (GFP –ve) cells. Scale bars, 20 µm.

A

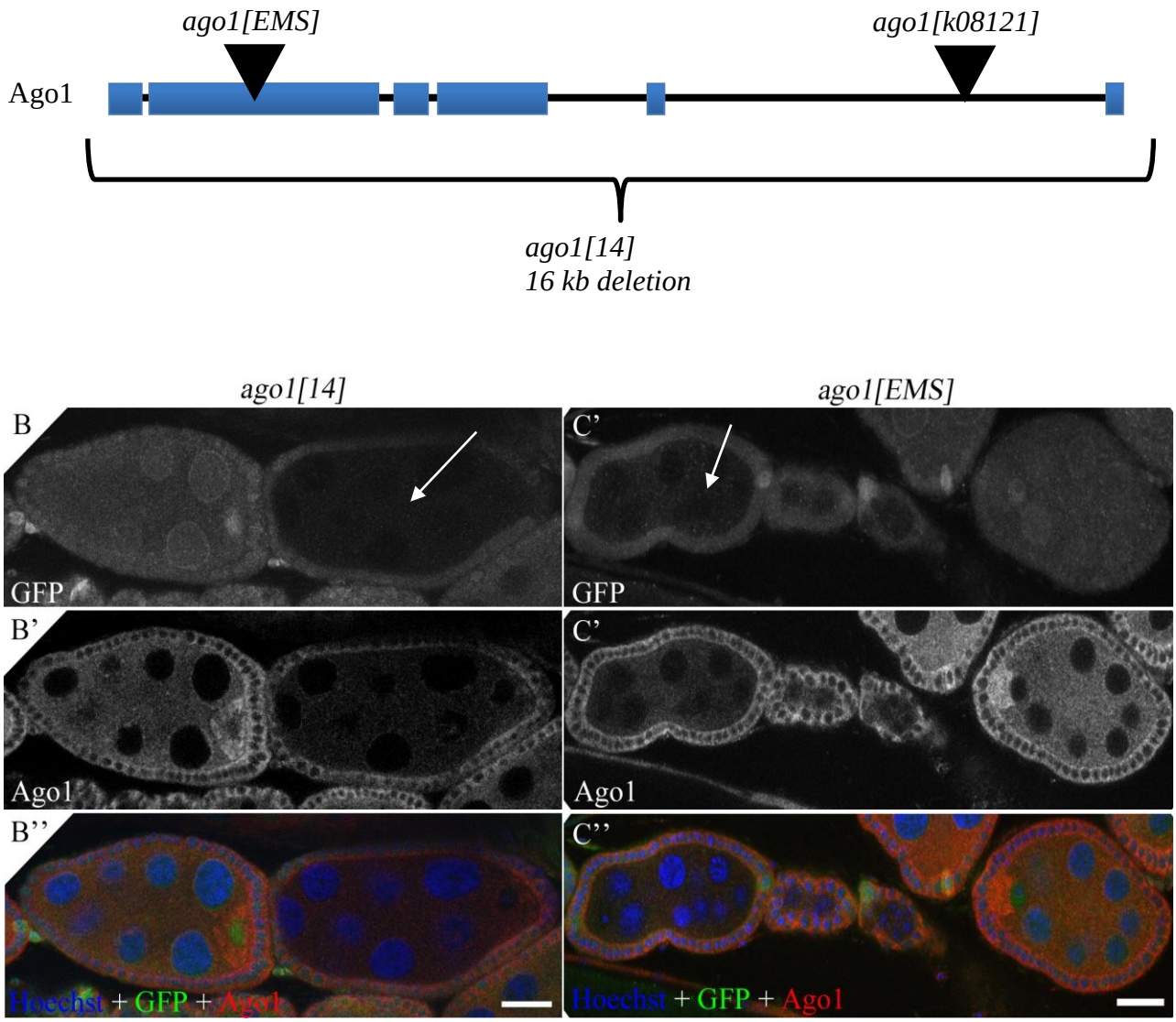


Figure 3.4. *ago1* mutant allele map and Ago1 staining in multiple *ago1* mutant alleles. (A) Schematic map of Ago1 gene with the corresponding mutations. (B-B'') Mutant clones (GFP –ve) from *ago1[14]* show lower expression of Ago1 staining compared to wild-type (GFP +ve) egg chambers. (C-C'') Mutant clones (GFP –ve) from *ago1[EMS]* show a lower expression of Ago1 staining compared to wild-type (GFP +ve) egg chambers. Scale bars, 20 µm.

3.2.2. Ago1 mutations affect germline cell division and oocyte formation

To further investigate the role of Ago1 in the egg chambers, clonal analysis of *ago1[k08121]* mutant germline was carried out. These clones have a variable phenotype of oocyte loss (Figure 3.5 and Table 3.1). One third of egg chambers in which the oocyte failed to form still survived and continued to grow in size (Figure 3.5B). In wild-type egg chambers, follicle cells begin migrating to the posterior side, where the oocyte resides, at stage 9. However, in those egg chambers without an oocyte, follicle cells did not migrate but degraded at stage 9, resulting in nurse cell-only egg chambers (Figure 3.5B). Using an antibody against the oocyte marker Orb, the failure of some egg chambers to develop an oocyte suggests that oocyte determination or maintenance might be affected in the absence of Ago1 (Figure 3.5D'' and Table 3.1). Despite approximately 2/3 of egg chambers producing oocytes, and in some cases embryos that were successfully laid, but in no cases did the Ago1 mutant embryos survive embryogenesis (data not shown). Nurse cells in the nurse cell-only egg chambers continued to grow.

At 7 days after eclosion (DAE), *ago1[k08121]* and *ago1[14]* clones had a low rate of oocyte-less egg chambers (5% and 1.25%, respectively). Fewer clones were present for all three *ago1* alleles than in control groups. Both *ago1[k08121]* and *ago1[14]* had similar phenotypes with approximately 3 clones per ovary at seven DAE, while *ago1[EMS]* had a more severe phenotype with only 0.74 clones per ovary. All alleles had fewer clones than the control groups, which had an average of 9.17 clones per ovary. The effects of three *ago1* alleles during *Drosophila* oogenesis were analysed by clonal analysis and the investigations were extended from 7 DAE to 14 DAE so that transient clones (non-stem cell derived clones), even the ones growing slower, would in theory, not be present in the ovaries (Table 1). The frequency of oocyte-less egg chambers increased dramatically at 14 DAE (38% in

ago1[k08121] and 27% in *ago1[14]*, Table 3.1). The most commonly observed developmental arrest amongst the oocyte-less egg chambers was at 8 nurse cells. In the most severe allele, *ago1[EMS]*, 66% (33/50) of egg chambers exhibited an oocyte-less phenotype, even at 7 DAE. Among the oocyte-less egg chambers, half of them (16/33) contained 8 nurse cells, and about 20% have only two or four nurse cells. This indicates that Ago1 is involved in controlling germ cell division. These results might also suggest that *ago1[k08121]* and *ago1[14]* mutants are not completely null.

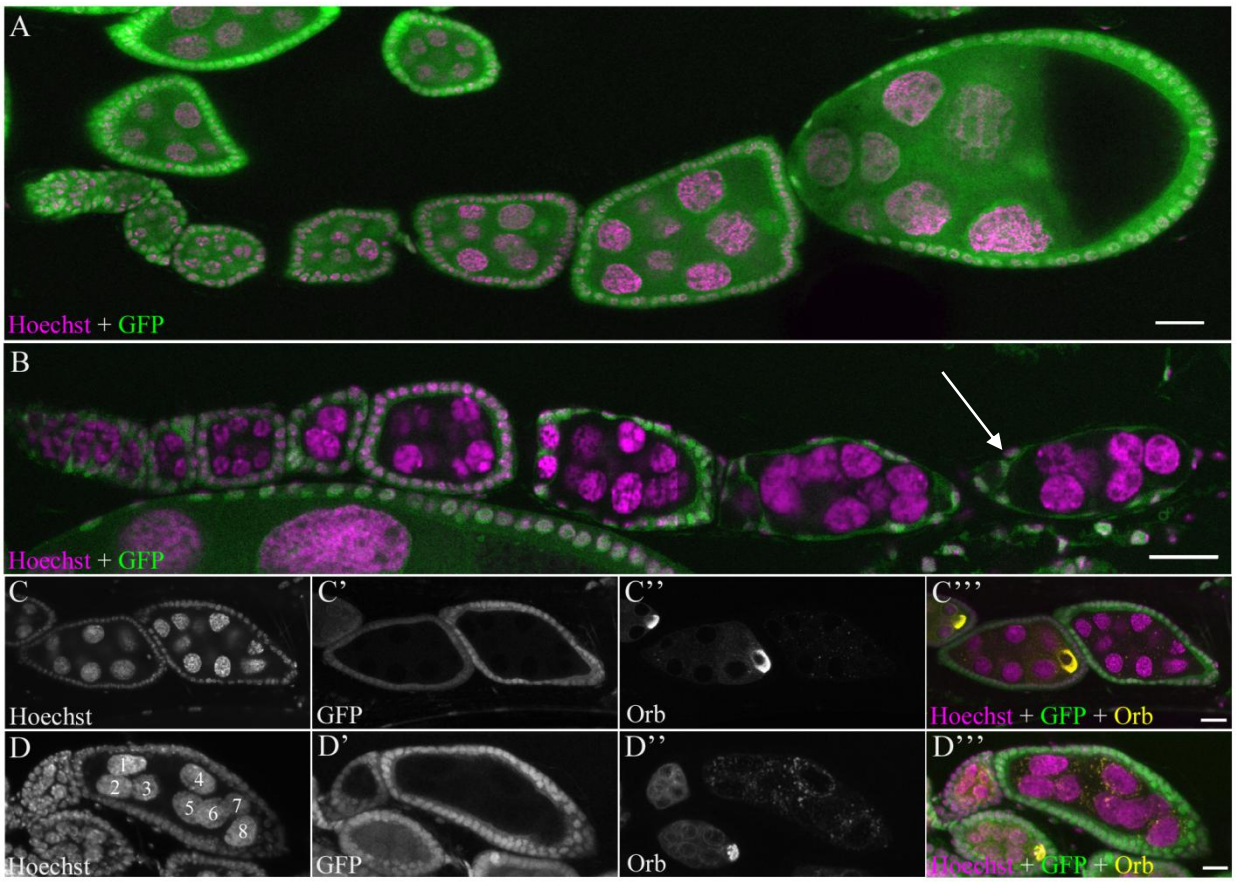


Figure 3.5. Loss of Ago1 disrupts oocyte formation and germ cell division. (A) A heterozygous GFP +ve ovariole. (B) Ovariole comprised of germline cell clones of *ago1[k08121]*. Follicle cells in late stage egg chambers seem to be degrading (arrow). (C-C''') Two neighbouring *ago1* mutant egg chambers, one with an oocyte and one without (orb staining marks the oocyte). (D-D''') Z-stack of *ago1[k08121]* clone with only 8 nurse cells and no oocyte formation. Scale bars, 20 µm.

Table 3.1. Clonal analysis of *ago1* egg chambers. DAE = Days after eclosion and NCs = Nurse cells.

7 DAE

	Total ovaries counted	Ovaries with clones	Clones	Clones per total ovaries	Normal clones	Clones with no oocyte					
						2 NCs	4 NCs	8 NCs	16 NCs	32 NCs	Total clones
Control	58	48	532	9.17	532	0 (0%)	0 (0%)	0 (0%)	0 (0%)	0 (0%)	0
ago1[k08121]	47	29	142	3.02	135	0 (0%)	0 (0%)	2 (1.4%)	4 (2.8%)	1 (0.7%)	7
ago1[14]	52	39	160	3.08	158	0 (0%)	0 (0%)	2 (1.3%)	0 (0%)	0 (0%)	2
ago1[EMS]	68	14	50	0.74	17	1 (2%)	5 (10%)	16 (32%)	11 (22%)	0 (0%)	33

14 DAE

	Total ovaries counted	Ovaries with clones	Clones	Clones per total ovaries	Normal clones	Clones with no oocyte					
						2 NCs	4 NCs	8 NCs	16 NCs	32 NCs	Total clones
Control	81	63	758	9.36	758	0 (0%)	0 (0%)	0 (0%)	0 (0%)	0 (0%)	0
ago1[k08121]	84	43	172	2.05	106	2 (3%)	0 (0%)	55 (32%)	8 (4.6%)	1 (0.6%)	66
ago1[14]	94	56	261	2.78	191	0 (0%)	1 (0.4%)	65 (25%)	3 (1.1%)	1 (0.4%)	70
ago1[EMS]	106	31	117	1.10	69	3 (2.6%)	3 (2.6%)	35 (30%)	7 (6%)	0 (0%)	48

3.2.3. The Ago1 phenotype manifests in the germarium

To assess these phenotypes further, germarium of *ago1[k08121]* clones at 14 DAE were analysed to determine whether this phenotype was due to apoptosis or cell division. Firstly, the germarium were stained against Vasa, a DEAD-box RNA-binding protein and Hu-li Tai Shao (HTS), the *Drosophila* homologue of Adducin which labels the fusomes (Figure 3.6A-H). In wild-type germarium (Figure 3.6A-D), the cystoblasts divide four times to produce 16-cell cysts by the time they reach region 2A. However, in *ago1* mutant germarium, 8-cell cysts with smaller and less branched fusomes were observed in region 2 (Figure 3.6E-H). Furthermore, *ago1* mutant germarium are also smaller, with a noticeably smaller region 2 as shown with an antibody against Orb (Figure 3.6L-M, compare to wild-type, Figure 3.6I-K). However, cleaved-caspase 3 was not detected in *ago1[k08121]* (n=26), *ago1[14]* (n=40), *ago1[EMS]* (n=37) and FRT control (n=67) germarium. Therefore they do not appear to be undergoing apoptosis (Figure 3.7A-D). Cyclin E staining was still detected in the germarium with 60% (9/15) of *ago1[k08121]*, 56% (17/30) of *ago1[14]* and 72% (8/11) of *ago1[EMS]* region 1 cell clones have Cyclin E staining compared to 69% (38/55) in the FRT control region 1 clones (Figure 3.6E-H).

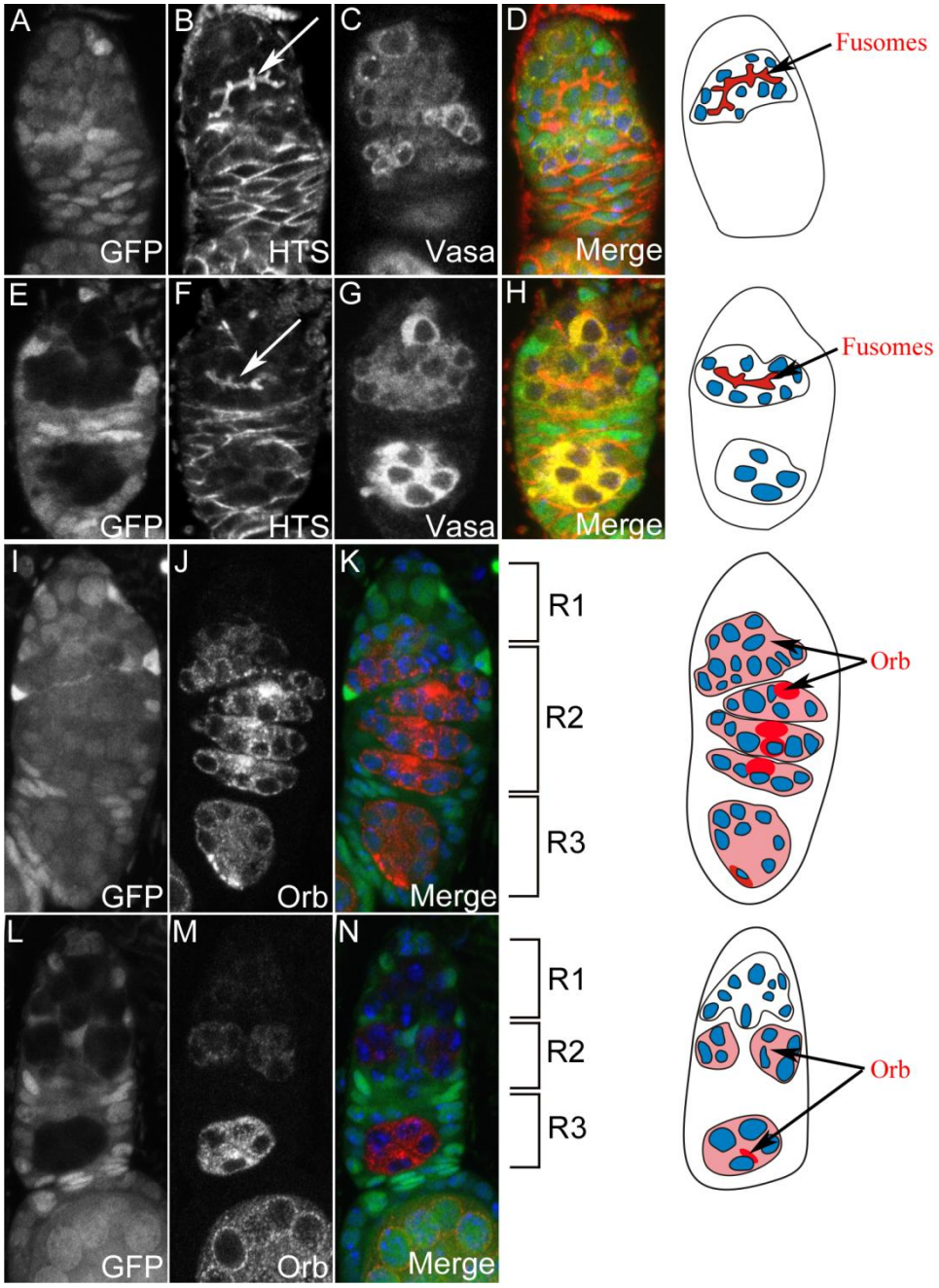


Figure 3.6. *ago1* phenotype manifests in the germarium. (A-H) Germarium with GFP +ve wild-type clones (A-D) showing normal branching of the fusomes (arrow) compared to GFP –ve *ago1[k08121]* mutant clones (E-H) showing less branching of the fusomes (arrow). In merge pictures, GFP - green, HTS - red and Vasa - yellow. (I-N) Germarium with GFP +ve wild type clones (I-K) showing normal size germarium compared to the smaller GFP –ve *ago1* mutant clones (L-N) germarium. In merge pictures, GFP is green and Orb is red. R1, R2 and R3 denotes to region 1, region 2 and region 3 in the germarium.

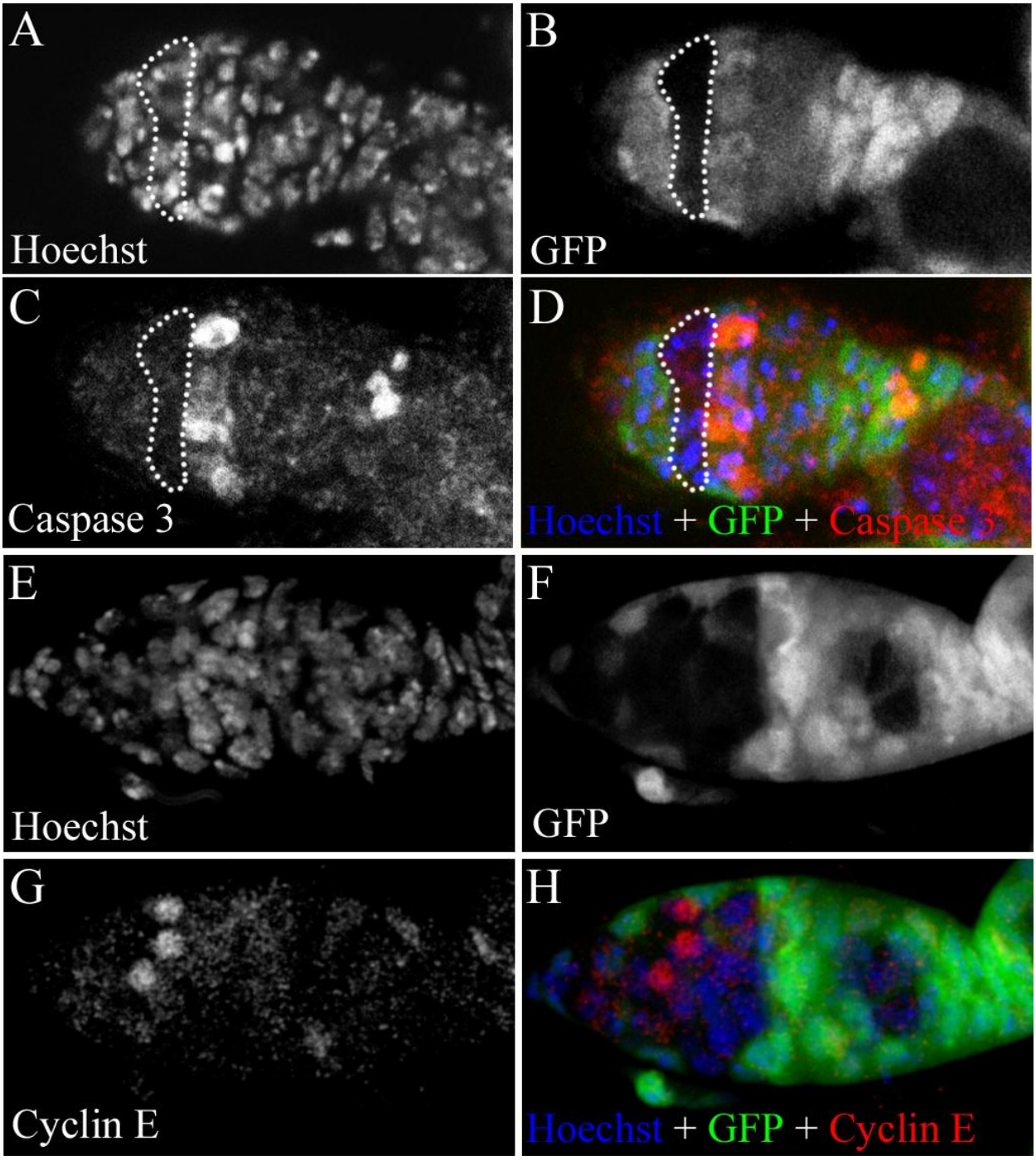


Figure 3.7. *ago1[k08121]* mutant germarium is not undergoing apoptosis and still expressing Cyclin E. (A-D) Mutant *ago1[k08121]* (GFP –ve, dotted lines) clone cells in the germarium do not have Caspase 3 staining showing the mutant germarium is not undergoing apoptosis. (E-H) Cyclin E staining can still be detected in the mutant germarium.

To further study the oocyte determination defect, Orb and Cup expression were examined in the germarium. Orb is very dynamically expressed in the germarium and its expression starts in region 2A (Figure 3.8A') in a relatively ubiquitous pattern (Christerson and Mckearin, 1994; Lantz et al., 1994). As it reaches region 2B, the Orb protein starts to localize to the pro-oocytes and finally to the determined oocyte. Cup protein however, starts accumulating in region 2B of the oocyte (Figure 3.8A'') (Piccioni et al., 2005; Zappavigna et al., 2004). Intriguingly, both Orb and Cup seemed to be expressed in the egg chambers with 8 nurse cells even though the oocyte is not properly formed (Figure 3.8B-B'''). Orb protein accumulated in region 2A (Figure 3.8B) but Cup was not detected until stage 1 egg chamber (Figure 3.8B''). Furthermore, analysis of stage 1 egg chamber mutant clones showing the 8 nurse cell phenotype indicated that although the egg chamber failed to form a proper oocyte, it produced a pseudo-oocyte without a condensed karyosome (Figure 3.8C). However, the accumulation of Orb protein in the pseudo-oocyte seemed to be unaffected (Figure 3.8C''). These results are indications that the oocyte was successfully determined but was unable to maintain itself and reverted back to a nurse cell.

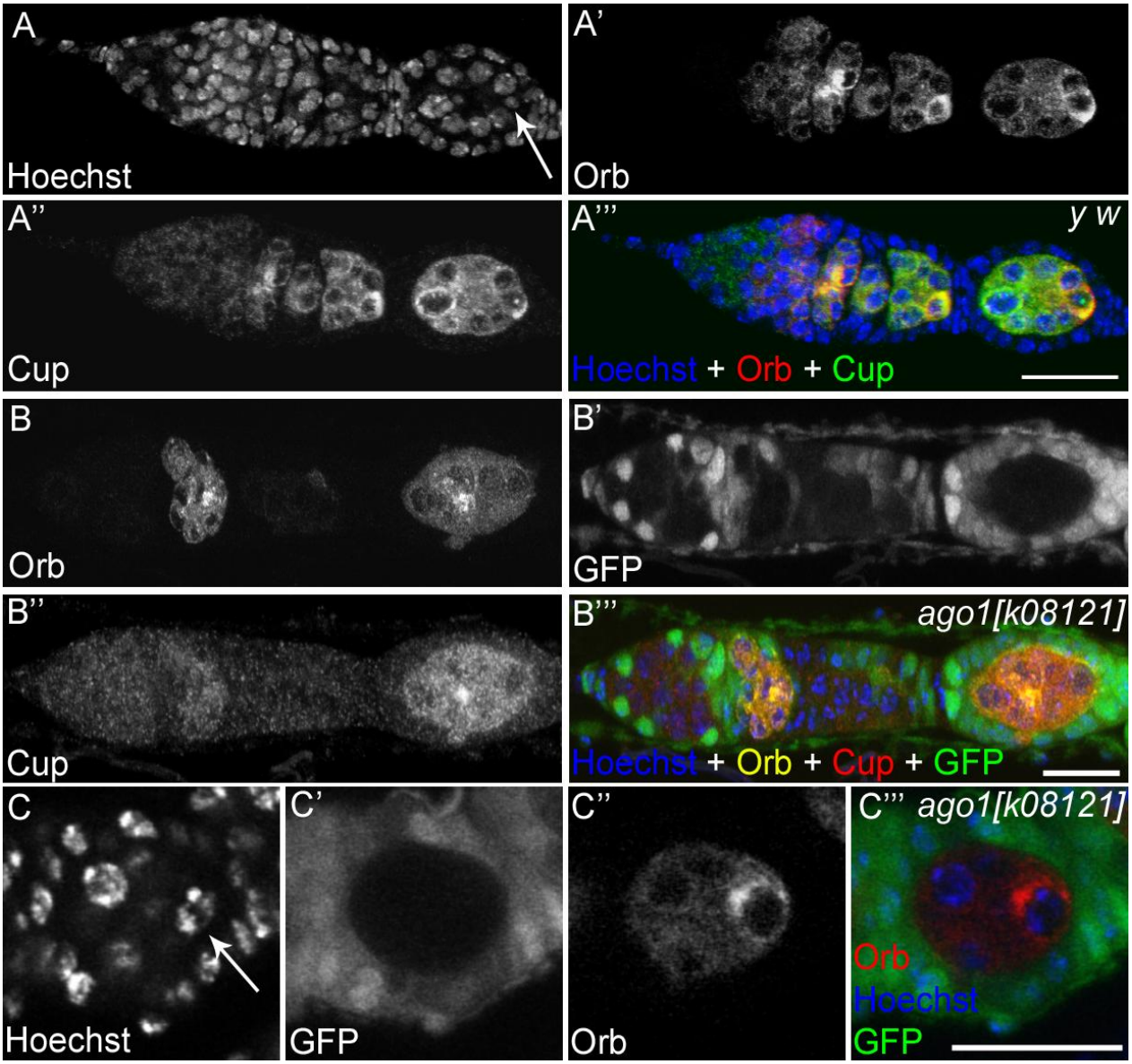


Figure 3.8. Orb and Cup staining in the pseudo-oocyte. (A-A’’’) *y w* germarium showing normal staining of Orb and Cup. Orb expression starts at region 2A and Cup expression starts at region 2B. (B-B’’’) Germarium with GFP –ve *ago1* mutant clones stained with anti-Orb and anti-Cup. Orb protein is present in region 2B while Cup can only be seen in stage 1 egg chamber. (C-C’’’) Stage 1 egg chamber with 8 nurse cells stained with anti-Orb showing the Orb protein accumulates at the pseudo-oocyte. Scale bars, 20 µm.

3.2.4. *dicer-1*, *pasha* and *drosha* exhibit similar effects on oogenesis as ago1

Since Ago1 is a critical effector of miRNA biogenesis and function, it would be important to see if mutation of other genes in this pathway have similar developmental defects to Ago1. Previously characterized mutant alleles of genes involved in miRNA biogenesis which are used include *dicer-1[Q1147X]*, *dicer-1[LL06357]*, *pasha[LL03360]* and *drosha[21K11]* stocks (Table 2.1) (Berdnik et al., 2008; Lee et al., 2004; Smibert et al., 2011a). Additionally, to rule out the effects of genetic background in the assay, analyses were also carried out on newly generated alleles of *dicer-1* and *pasha* that were provided by our collaborator (Eric Lai, Sloan-Kettering Institute, NY), which were isolated from an on-going genetic screen (Smibert et al, 2011). These mutants, *dicer-1[21B2]*, *dicer-1[30D2]*, *dicer-1[37A1]*, *dicer-1[38E3]* and *pasha[36B2]* all contain premature stop codons and are expected to be null for protein function (Azzam et al., 2012)

These newly generated mutants also exhibited a rough eye phenotype (Figure 3.9) when clones were generated using eyFLP. The rough eye phenotype was previously described for *dicer-1* and *pasha* mutants (Lee et al., 2004; Martin et al., 2009). Analysis of scanning electron microscope (SEM) eye pictures shows the eye bristles were missing in the rough eye area and the ommatidia do not form properly. The *Drosophila* eye is composed of 750 ommatidia which were built up from a fixed number of cells. The ommatidia are separated by interommatidial cells which differentiate into secondary and tertiary pigment cells and interommatidial bristles (Wolff and Ready, 1991). Missing bristles and the failure to form proper ommatidia could result from by cell differentiation defects. However, more experiments are needed, for example sectioning to look at whether any of the photoreceptor and other cells are forming properly to fully understand the mechanism of this eye phenotype.

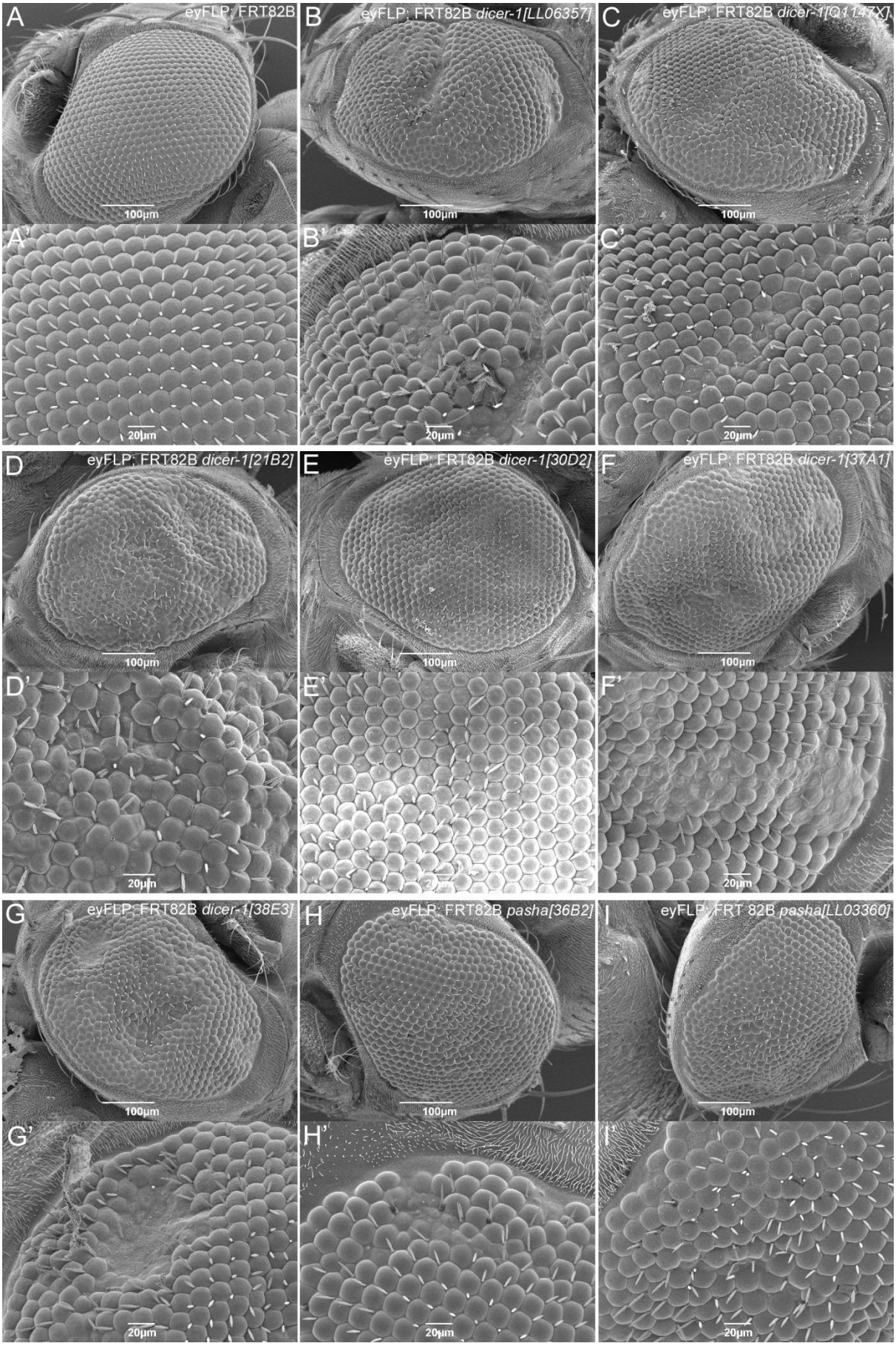

A
eyFLP; FRT82B
100µm
A'
20µm
B
eyFLP; FRT82B dicer-1[LL06357]
100µm
B'
20µm
C
eyFLP; FRT82B dicer-1[Q1147X]
100µm
C'
20µm
D
eyFLP; FRT82B dicer-1[21B2]
100µm
D'
20µm
E
eyFLP; FRT82B dicer-1[30D2]
100µm
E'
F
eyFLP; FRT82B dicer-1[37A1]
100µm
F'
20µm
G
eyFLP; FRT82B dicer-1[38E3]
100µm
G'
20µm
H
eyFLP; FRT82B pasha[36B2]
100µm
H'
20µm
I
eyFLP; FRT 82B pasha[LL03360]
100µm
I'
20µm

Figure 3.9. Rough eye phenotype exhibited by *dicer-1* and *pasha* mutants. (A-I) Eye pictures with scale 100µm scale bar. (A'-I') Zoomed in pictures of the rough eye phenotype patch with 20µm scale. (A) FRT positive control showing normal eye. (B-C) Previously characterized *dicer-1* mutant alleles *dicer-1[LL06357]* and *dicer-1[Q1147X]* showing the rough eye phenotype. (D-G) Four newly generated dicer-1 mutant alleles, *dicer-1[21B2]*, *dicer-1[30D2]*, *dicer-1[37A1]* and *dicer-1[38E3]* also showing the rough eye phenotype. (H-I) Two *pasha* mutants of newly generated *pasha[36B2]* and previously characterized *pasha[LL03360]* showing the rough eye phenotype as well.

To investigate the role of other miRNA biogenesis genes in the germline, mitotic clones were generated on all six *dicer-1*, two *pasha* and one *drosha* mutants. All the *dicer-1* alleles examined exhibit the same phenotype of egg chambers with 8 nurse cells and lacking an oocyte with 30-53% penetrance, phenocopying the *ago1[EMS]* mutant at 7 DAE (Figure 3.10 and Table 2). One *pasha* mutant allele, *pasha[LL03360]*, behaved like the wild-type in this assay even after 14 DAE (n=128, Figure 3.2H). However, the newly generated *pasha* mutant allele, *pasha[36B2]* phenocopied *ago1[EMS]* and *dicer-1* mutant alleles with 50% penetrance at 7 DAE (Figure 3.10I and Table 2). The *drosha[21K11]* mutant also shows a similar penetrance of 48% at 7 DAE (Figure 3.10J and Table 2). Together, these results suggest a role for the miRNA pathway in oogenesis.

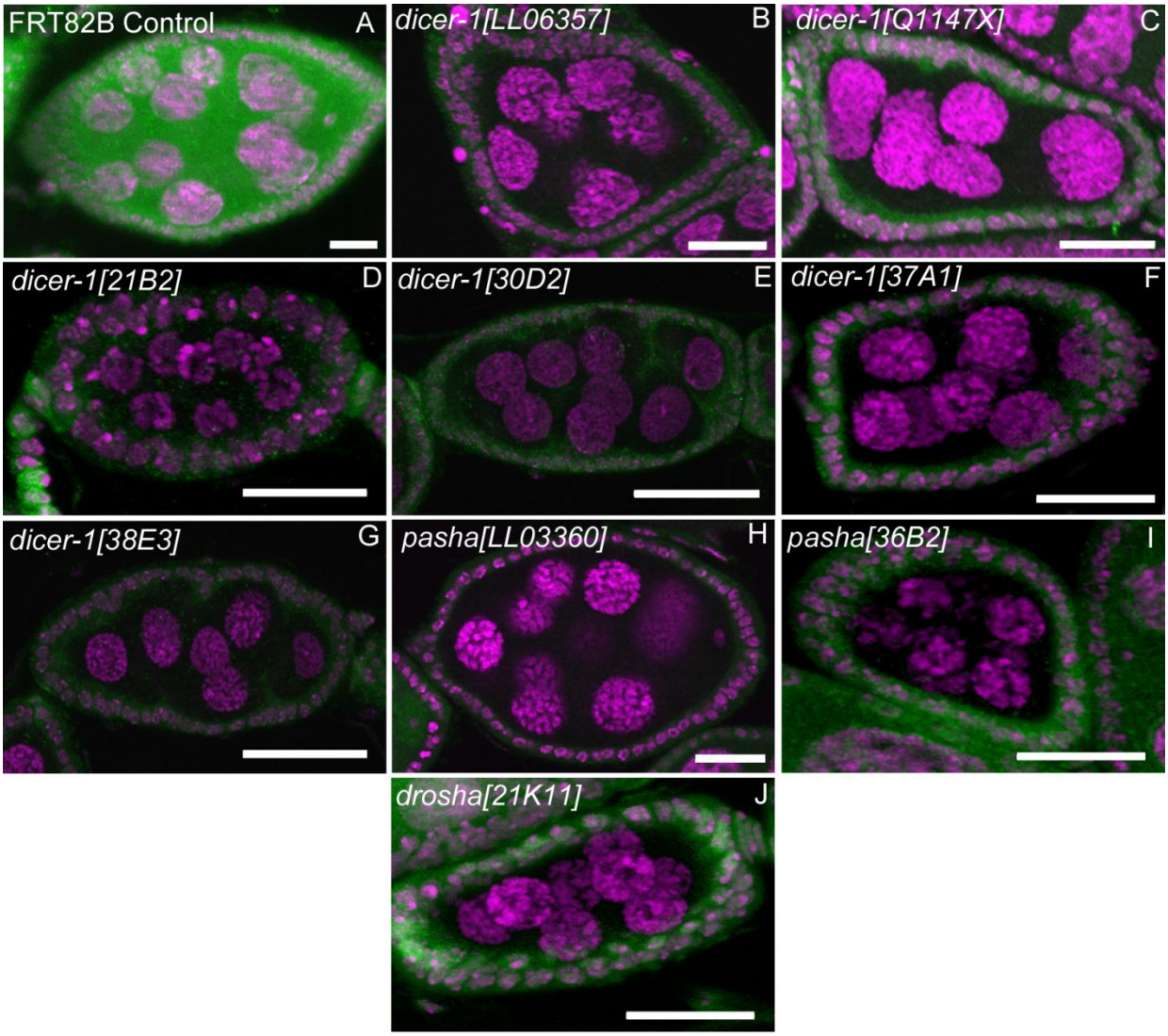


Figure 3.10. *dicer-1, pasha* and *drosha* null mutants exhibit phenotypes similar to *ago1* mutants. (A) Positive control (GFP +ve) showing a normal egg chamber. (B-G) Selected examples demonstrating the ~30-60% of germline clones for the indicated genotypes that exhibit the oocyte-less 8 nurse cell egg chamber phenotype. Six independent *dicer-1* mutant alleles showing selected egg chamber exhibiting the same germ cell division and oocyte formation defect as in an *ago1* mutant. (H-I) Germline clones of two independent *pasha* alleles. *pasha[LL03360]* does not show the same germ cell division or oocyte formation defects as in *ago1*, while *pasha[36B2]* phenocopies the *ago1* and *dicer-1* mutant phenotype. (J) *drosha* mutant showing the 8 nurse cells phenotype. GFP is green and DNA is shown in magenta. Scale bars, 20 µm.

Table 3.2. Clonal analysis of *dicer-1*, *pasha* and *drosha* egg chambers.

DAE = Days after eclosion and NCs = Nurse cells.

7 DAE

			Clones with no oocyte					
	Clones	Normal clones	2 NCs	4 NCs	8 NCs	16 NCs	32 NCs	Total clones
Control FRT82B	187	187	0	0	0	0	0	0
dicer-1[LL06357]	104	70	0	0	31	3	0	34
dicer-1[Q1147X]	70	41	0	0	26	3	0	29
dicer-1[21B2]	42	19	0	0	19	4	0	23
dicer-1[30D2]	55	31	0	0	23	1	0	24
dicer-1[37A1]	43	18	0	0	25	0	0	25
dicer-1[38E3]	56	20	0	0	35	1	0	36
pasha[LL03360]	128	128	0	0	0	0	0	0
pasha[36B2]	121	54	0	0	59	8	0	67
drosha[21K11]	159	72	1	3	77	6	0	87

3.2.5. Ago1 co-localizes with P body components in oocytes

Ago1 has been previously described to localize in the processing bodies (P bodies) of mammalian cells (Liu et al., 2005). P-bodies are cytoplasmic foci that have emerged as important subcellular structures that are involved in mRNA metabolism. In *Drosophila*, most P body components are enriched in the oocytes and localize at the posterior cortex of late stage oocytes. To study the relationship between Ago1 and other P body components, double staining for Ago1 and P body components such as Me31B, Cup and Gawky were carried out. Ago1 was observed to co-localized with these P body components in the oocyte, confirming that Ago1 is a component of P bodies in *Drosophila* oocytes (Figure 3.11A-I). However, Me31B, Cup and Gawky were correctly localized in *ago1[k08121]* oocytes, suggesting that the normal distribution of P bodies in oocytes are not dependent on Ago1 (Figure 3.11J-L).

Gawky, the GW182 homologue in *Drosophila*, associates with Ago1 in the RISC, and was previously described to colocalize with Ago1 in S2 cells (Behm-Ansmant et al., 2006). This study is the first to report the observation of Gawky co-localizing with Ago1 *in vivo*. This observation in *Drosophila* ovaries provides further support that Ago1 interacts with Gawky. Similarly to Ago1, Gawky protein was also enriched in the oocyte (Figure 3.11I). In the clonal analysis, the absence of Ago1 does not dramatically affect the expression of Gawky in the germ cells as the enrichment of Gawky in the *ago1[k08121]* oocytes remains similar to that of wild-type oocytes (Figure 3.11L). However, Gawky expression was clearly reduced in *ago1* follicle cell clones (Figure 3.11M-O).

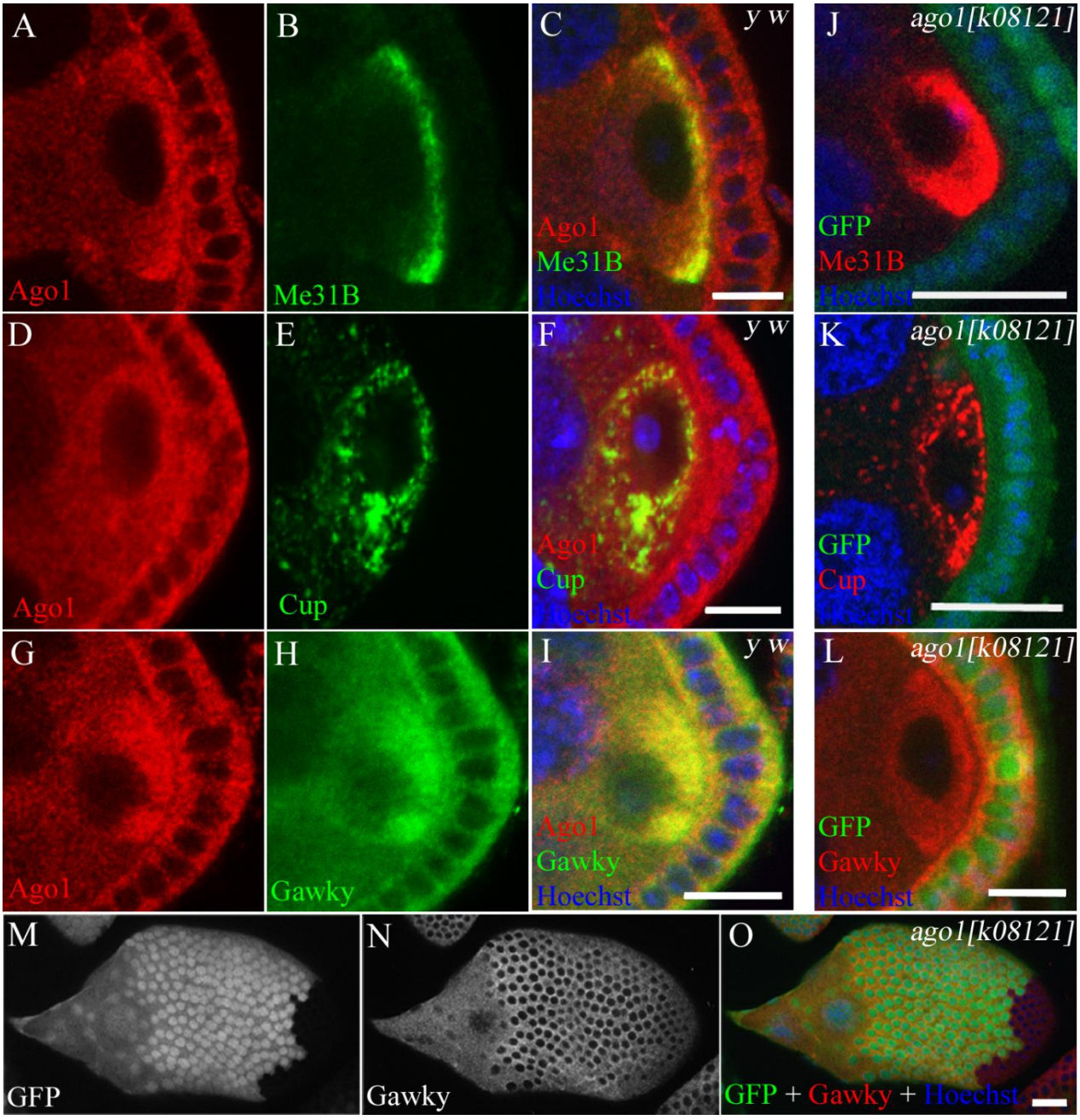


Figure 3.11. Ago1 localizes to P bodies in *Drosophila* oocytes. (A-I) Colocalization of Ago1 and P-body components Me31B, Cup and Gawky in the oocyte. (J-L) Ago1 homozygous clone in the germline showing the P-body localization was not affected. (G-I) Ago1 and Gawky antibody staining in wild-type egg chamber. Gawky is also enriched in the oocyte and co-localizes with Ago1 in all cells. (M-O) Gawky protein levels were reduced in *ago1* follicle cell mutant clones. Scale bars, 20 µm.

3.3. Discussion

3.3.1. Ago1 in oogenesis

Drosophila Ago1 forms a complex with mature miRNAs and acts to repress mRNAs. However, the spatial distribution of Ago1 during development has not been well characterized. The protein trap lines from Carnegie Protein Trap library provide a powerful way to characterize the spatial and temporal distribution of a particular gene (Buszczak et al., 2007). The distribution of Ago1 in the cytoplasm has been described and shown to be localized in small puncta in the egg chamber (Reich et al., 2009). The findings in this chapter using two independent assays for Ago1 localization have shown that Ago1 is enriched in the oocyte, and mutant analysis has revealed a role in oocyte formation and germ cell division.

Nurse cells supply nutrition for oocyte growth. The germ cell division defect described here has been previously observed in a *cyclin-E* mutant where 30% of the egg chambers have 8 cells, but the egg chamber still manages to develop an oocyte (Lilly and Spradling, 1996). Mata et al., (2000) have also described 8 cell egg chambers when String is over expressed as well as in a *tribbles* mutant. Both String overexpression and the *tribbles* mutant have 8 cells per egg chamber, but only a proportion fail to develop an oocyte. This defect occurs in the germarium while the cyst cells are undergoing mitosis. In the wild-type situation, the cystoblast divides four times to produce 16 cyst-cells. In the absence of *ago1*, some of the cystoblasts undergo only three divisions, producing 8-cell cysts. However, the *ago1* mutant ovarioles with this phenotype still express Cyclin E, suggesting that mitosis is still occurring although perhaps at a slower rate. Combined with the oocyte formation defect, the resulting egg chambers only have 8 nurse cells and lack an oocyte. The cyst cell division in the germarium is not well understood. One potential explanation for the observed phenotype is that when Ago1, and presumably miRNA mediated gene regulation, are lost, the

signal to stop dividing occurs early. Another possibility is because the egg chamber grows more slowly, the oocyte reaches region 2A before it manages to divide four times, thus receiving a premature signal to stop dividing, or being prematurely enclosed by the migrating follicle cells. The smaller germarium of *ago1* mutant might also be an effect of cyst-cells dividing slower. The defective egg chamber however still manages to grow. Furthermore, the observation of Orb protein in region 2 and the stage 1 egg chamber could mean that the oocyte is trying to enter meiosis (Senger et al., 2011), or has entered meiosis but is unable to maintain the meiotic state because the Orb accumulation is lost in later stage egg chambers and no oocyte is formed. The oocyte differentiation and maintenance in the meiotic cycle are reliant on the microtubule based transport of mRNAs and proteins from the nurse cells to the oocyte (Huynh and St Johnston, 2004). Orb, the germline specific RNA-binding protein that is microtubule-dependent starts accumulating in the in the oocyte at region 2a.Mutation of Orb causes the egg chamber to produce 8 nurse cells and no oocyte (Huynh and St Johnston, 2000), similarly to the *ago1*, *dicer-1*, *drosha* and *pasha* mutant phenotype seen in this study. However, since Orb is still expressed, it could be ruled out that the phenotype is caused by loss of Orb. The inability to maintain the accumulation of Orb in the oocyte in later stages of oogenesis could relate to a defect in maintaining the meiotic cycle (Cox et al., 2001; Hong et al., 2003; Huynh and St Johnston, 2004).

3.3.2. Ago1 and senescence

The results on the *ago1* mutant have shown that a greater proportion of older *ago1* flies (14 DAE) exhibit the 8-nurse cell phenotype than younger mutant flies (7 DAE). This could be due to the level of Ago1 in older flies decreasing to a certain threshold level to show an obvious phenotype. There is also the possibility that the remaining or leaky (due to hypomorphic allele) Ago1 is diluted through GSC division and maintenance such that GSCs

from flies at 14 DAE have less Ago1 than GSCs from flies at 7 DAE. Previous studies suggest that GSC loss in *ago1* mutants are age-dependent (Yang et al., 2007). This could also potentially explain the age-dependent 8-nurse cell phenotype that was observed in *ago1* mutants. Self-renewal of GSC in the absence of Ago1 could be defective, so cystoblasts produced by defective GSC might not be able to divide normally. Although *ago1[k08121]* and *ago1[14]* showed a more severe phenotype in older flies, *ago1[EMS]*, as the strongest allele, showed a very severe phenotype even in young flies. This is consistent with a previous study (Yang et al., 2007).

3.3.3. Ago1 and the P body

Most of the P-body components are localized in the oocyte in a similar pattern to Ago1. Me31B, Cup and Gawky are some of the P-body components that co-localize with Ago1 in the oocyte. Me31B, the *Drosophila* orthologue of yeast or human DEAD/H-box RNA helicase 1 (Dhh1), is a protein which is very important in oocyte formation (Nakamura et al., 2001). Oocytes in Me31B mutants fail to grow normally after stage 6, and undergo apoptosis (Nakamura et al., 2001). Cup is required for proper egg chamber development. Cup mutants show a strong chromosome morphology defect and the egg chambers fail to develop (Keyes and Spradling, 1997). The important function of Gawky in miRNA biogenesis was uncovered recently in a series of studies (Chekulaeva et al., 2009; Eulalio et al., 2008; Schneider et al., 2006). Gawky is an important factor in Ago1 miRNA-mediated silencing and Ago1 alone cannot silence mRNAs (Eulalio et al., 2008). In this chapter, it was shown that Gawky colocalizes with Ago1 in the egg chamber by antibody staining. The level of Gawky was also reduced in the absence of Ago1 in the follicle cells. However, the reduction of Gawky was not as severe in the germline. This suggests that Gawky stability is affected in the absence of Ago1. Localization of some P body components was not affected upon depletion

of Ago1, suggesting Ago1 is not the scaffold for the integrity of P bodies. However, Ago1 doesn't always localize to P bodies in the nurse cells. The co-localization with P body components in the oocytes are very consistent but Ago1 localization in the P bodies are not as consistent. This could be due to the antibody staining protocol or maybe Ago1 only localizes to P bodies in certain conditions for example during stress.

3.3.4. The role of miRNAs in oogenesis

Ago1, Dicer-1, Loquacious and Piwi have roles in small RNA biogenesis and all of them have been shown to be important for germline stem cell maintenance (Forstemann et al., 2005; Hatfield et al., 2005; Jin and Xie, 2007; Megosh et al., 2006; Yang et al., 2007). The role of miRNAs regulating in GSC division was first reported by Hatfield et al., (2005) by studying null mutants of *dicer-1*. A similar study looking at *ago1* mutants revealed that Ago1 also regulates the fate of the GSC (Yang et al., 2007). Both of these studies showed a similar phenotypic defect in the germline. Furthermore, there are some cases where mutations in individual miRNA genes show phenotypes in the germline cells. The miRNA bantam has been previously found to be important for GSC maintenance (Shcherbata et al., 2007). Both miR-278 and miR-7 have been shown to regulate GSC division (Yu et al., 2009). Also, miR-184 controls GSC differentiation, dorsoventral patterning of the egg shell and anteroposterior patterning (Iovino et al., 2009). Although the effect in the GSC is quite reproducible from previous studies, it is not uncommon to see this in knockouts of miRNA biogenesis factors. Bejarno *et al.*,(2010) showed this quite well in the developing wing primordium where clones lacking *mir-9a* upregulate dLMO and induce wing notching. This phenotype is however not fully reproducible in *dicer-1* and *pasha* mutant clones. The effect of removing all miRNA could mask the effect of a single miRNA mutation.

Experiments carried out in this chapter have showed that the *dicer-1*, *pasha* and *drosha* mutants phenocopy the *ago1* mutant during oogenesis. However, one of the two Pasha mutant alleles, *pasha[LL03360]*, did not phenocopy *ago1* and *dicer-1*. This mutant is a piggyBac insertion into the 5'UTR of *pasha* and despite showing a convincing loss of *pasha* protein in adult neurons (Berdnik et al., 2008) it is possible that the allele may only be hypomorphic in the ovary. Pasha has not been studied in the *Drosophila* germline but it has been shown to play a role in olfactory neuron morphogenesis in the *Drosophila* adult brain (Berdnik et al., 2008). In that study, they found that Pasha and Dicer-1, but not Ago1, are required for arborization of projection neurons. This argues for Ago1-independent roles of Dicer-1 and Pasha. Alternatively, the mutant allele a*go1[k08121]* used in Berdnik et al., (2008) and this study, might not be completely null or the protein from the parental cell could be compensating for the loss of Ago1. *pasha* homozygous mutants also have smaller larval CNS and their discs failed to developed properly (Martin et al., 2009). Recent studies have suggested that neural processes are exquisitely sensitive to miRNA pathway activity (Smibert et al., 2011a), so perhaps a more complete loss of Pasha function is required to produce phenotypic consequences in the ovary compared to neurons. Indeed, the relative phenotypic strength of *ago1[k08121]* versus *ago1[EMS]* and the null mutants of miRNA biogenesis enzymes argues for the hypomorphic nature of *ago1[k08121]*. Mirtrons are another class of small RNAs which bypass Pasha/Drosha processing by utilizing the splicing machinery, but are still processed by Dicer-1 and loaded into Ago1 (Okamura et al., 2008; Ruby et al., 2007). However, *drosha[21K11]* and the newly generated *pasha[36B2]* mutant show the same phenotype, qualitatively and quantitatively, as *ago1* and *dicer-1* mutants. There are also the possibility of a redundant function between Pasha and Drosha. Also Drosha might be able to process some function independent of Pasha in the miRNA biogenesis. This suggests that the majority of the phenotypes observed are due to loss of canonical miRNAs and that mirtrons

have a comparably insignificant role (if any) in the phenotypes analysed. Altogether, the study in this chapter confirms that an integrate miRNA biogenesis is critical for germ cell development.

Chapter 4
The role of miRNAs in follicle cells

4.1. Introduction

4.1.1. Follicle cells

The follicle cells contribute significantly to egg chamber formation, maturation and survival which includes establishment of oocyte polarity, nutrient uptake and egg shell production during *Drosophila* oogenesis (Figure 4.1) (Deng and Bownes, 1998; Klusza and Deng, 2011). It also responds to cues from the environment and monitors the health of the egg chambers (Grewal, 2009). Follicle cell formation starts at region 2b in the germarium where the follicle cell stem cells (FSCs) resides (Bolivar et al., 2006; Margolis and Spradling, 1995). Then, after division, about 16 precursor follicle cells enclose the cyst cells creating an egg chamber (Wu et al., 2008). These cells cease division and some become pre-polar cells which will eventually become the polar cell and stalk cells (Dobens and Raftery, 2000; Ruohola et al., 1991; Wu et al., 2008) (Figure 4.1A). The differentiation of the five-to-eight stalk cells separates the newly formed egg chambers which detach themselves from the germarium.

Elegant developmental and genetics studies have revealed that the follicle cells co-ordinately develop with the oocyte and establish the body axes of the resulting embryo. The follicle cells remain in a cuboidal epithelium shape until the egg chamber reaches stage 8. At stage 9, the follicle cells start migrating to the posterior side of the egg chamber. In the meantime, the six-to-ten of the most anterior follicle cells will form the border cells which migrate through the nurse cells to the anterior side of the egg chamber. At this stage, most follicle cells will change shape and become a columnar epithelium. Furthermore, the follicle

cells will synthesize yolk protein which will be taken up by the oocyte and make it grow substantially, occupying half of the egg chamber by stage 10a and continuing to grow until it becomes a mature egg (Spradling, 1993b). During stage 10b to stage 14, the nurse cells undergo a dumping process where the nurse cells rapidly expel their cytoplasm into the oocyte and at this stage the follicle cells will also deposit the vitelline membrane and egg shell over the oocyte.

The follicle cells undergo three different cell cycles; mitotic cell cycle, endocycle and gene amplification cycle (Figure 4.1B). First, in the mitotic cell cycle, the follicle cells undergo mitosis which occurs from the germarium until the stage 6 egg chamber (Shcherbata et al., 2004). Then the follicle cell will enter the endocycle stage in which the cell replicates its genomic DNA but without undergoing mitosis. The endocycle stage starts at stage 6 and lasts until the egg chamber reaches around stage 10b (Deng et al., 2001). The gene amplification stage begins at stage 10b where specific sets of genes such as those giving rise to the chorion are selectively replicated to produce the large amount of eggshell proteins necessary to protect the mature egg from the environment (Klusza and Deng, 2011).

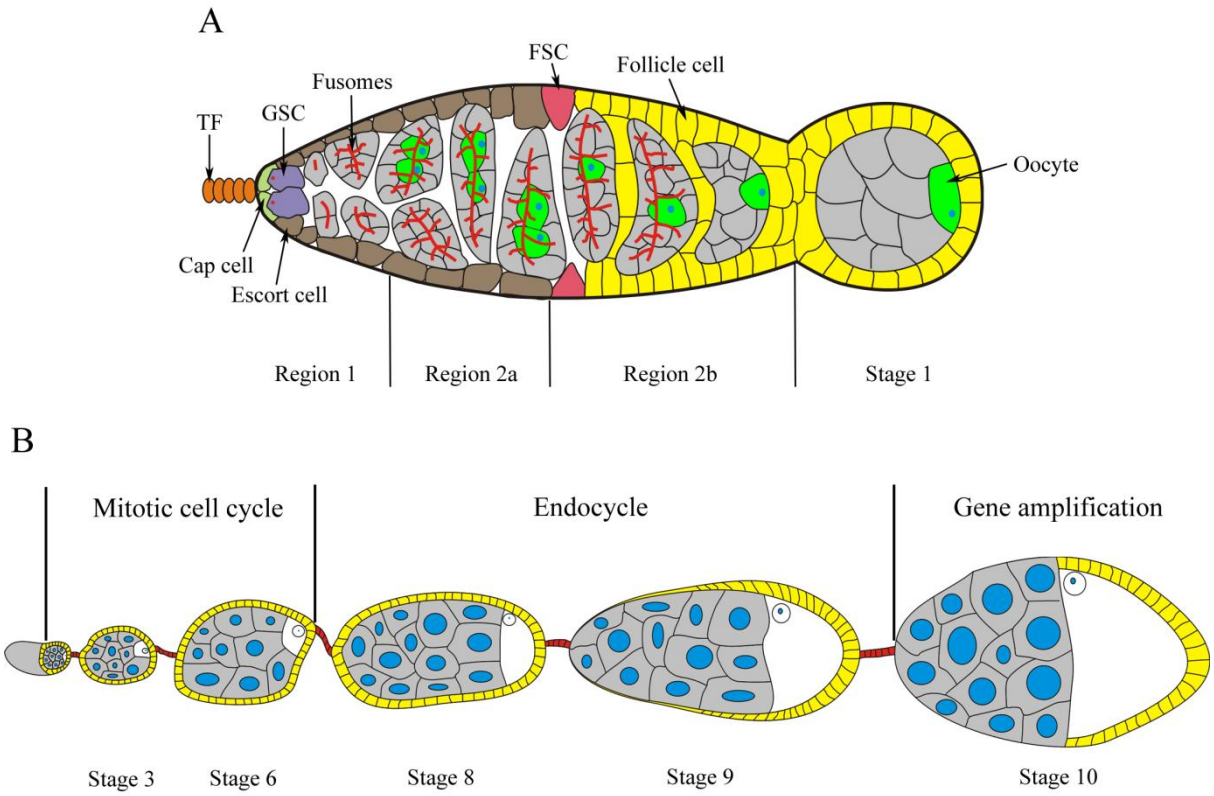


Figure 4.1. Oogenesis showing follicle cell in the germarium and cycles. (A) FSCs (red) are located in region 2b. (B) Follicle cell (yellow) cycles comprises of mitotic cell cycle from egg chamber stage 1 till stage 6, endocycle from egg chamber stage 6 to 9 and the gene amplification stage from stage 10 and above. Germline cells are grey, nucleus are blue and oocytes are green.

4.1.2. miRNAs in follicle cells

Several studies have implicated the role of miRNAs in follicle cells. Kalidas et al., (2008) found that Dicer-1 heterozygotes in a R2D2 homozygous mutant background showed stronger defects in the follicle cell than in only R2D2 homozygous cells. The females were totally sterile when the *dicer-1* heterozygous mutant was introduced to the *r2d2* homozygous mutant.

The ovarian somatic sheet line (OSS) (Niki et al., 2006) which is thought to have derived from ovarian follicle cells has been shown to contain high level of miRNAs, endo-siRNAs and primary piRNAs (Lau et al., 2009). They have shown about 121 out of the 140 miRNAs characterized at that point and were expressed in the OSS cells.

A recent study has also shown that the core components of miRNA biogenesis, Dicer-1 and Pasha are required for the proper switch from the mitotic cell cycle to the endocycle in follicle cells (Poulton et al., 2011). Both Dicer-1 and Pasha regulate Notch signalling by controlling the timing of Notch activity. Disruption of miRNAs delay Notch activation and inactivation in follicle cells by targeting Delta, a Notch binding ligand.

In Chapter 3, the high expression of Ago1 in the follicle cells shows an early indication of high miRNA activity (Figure 3.2). This was strengthened by previous studies of the follicle cells (Kalidas et al., 2008; Lau et al., 2009). The purpose of this study is to investigate the role of miRNAs in follicle cells using *ago1, dicer-1, pasha* and *drosha* mutants and RNAi lines then look for specific miRNAs that are involved in follicle cell division and maintenance. However, while the experiment was carried out, a manuscript by Poulton et al., (2011) was published showing that *dicer-1* and *pasha* mutant regulates Notch signalling in the follicle cells.

4.1.3. Experimental description

In Chapter 3, the high expression of Ago1 in the follicle cells shows an early indication of high miRNA activity. This was strengthened by previous studies in the follicle cells (Kalidas et al., 2008; Lau et al., 2009). The purpose of this study is to investigate the role of miRNAs in follicle cells using *ago1, dicer-1, pasha* and *drosha* mutants and RNAi lines then using the available tools, looking for specific miRNAs that are involved in follicle cell division and maintenance. However, while the experiment was carried out, a manuscript by Poulton et al., (2011) was published showing that *dicer-1* and *pasha* mutants regulate Notch signalling in the follicle cells.

4.2. Results

4.2.1. *ago1* mutant causes non-cell autonomous defect

As seen in Chapter 3, the levels of Ago1 in the follicle cells are higher than the germline cells. This enrichment may indicate high miRNA activity in the follicle cells. To study the effect of knocking down Ago1, mitotic clones were generated in the follicle cells (Chapter 2.1.3). From the mosaic expression, most of the time the follicle cells do not show any obvious phenotype (Figure 4.2A-D). However, occasionally there are some *ago1* mutant follicle cell clones that exhibit condensed nuclei (Figure 4.2B-D’’’). Furthermore, the condensed nucleus phenotype seemed to spread out to its neighbouring GFP +ve wild type cells non-autonomously (Figure 4.2E). This can be seen in the wild-type GFP +ve cells at the boundaries of the clone whose nuclei are also condensed (Figure 4.2B-D’’’). Furthermore, alpha-tubulin staining of the microtubule shows decondensation and lower expression level in certain *ago1* mutant GFP –ve cells. This effect is also observed in wild type GFP +ve cells that have condensed nuclei due to non-cell autonomous effect of the clones. (Figure 4.2B-D’’’).

The condensed nuclei phenotype could be the cause of cells undergoing apoptosis and dying. To test this, the cells were stained against Caspase 3 which is an apoptotic marker, to see if they are undergoing apoptosis. If the cells are undergoing apoptosis, Caspase 3 protein will be activated. As expected, Caspase 3 protein was detected in the clonal cells (Figure 4.2D’’). In addition, HTS was used to stained the cell boundaries and saw that the follicle cell clone boundaries were badly affected (Figure 4.2D’’’).

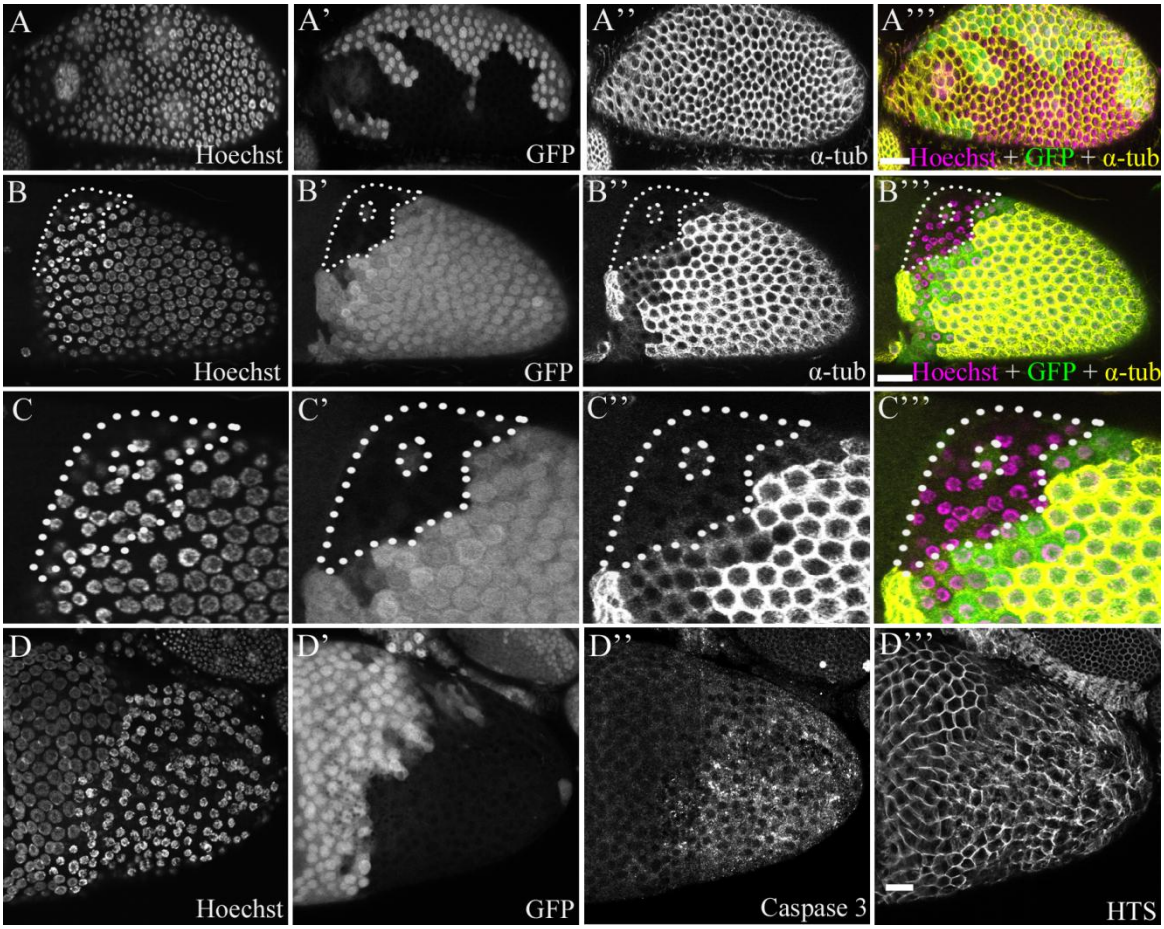


Figure 4.2. Clonal analysis of *ago1[k08121]* in *Drosophila* follicle cells. (A) *ago1[k08121]* clones (GFP –ve) showing no clear phenotypic defects. (B-D) Condensed follicle cell nuclei spread non-cell autonomously from *ago1* clone cells (in dotted lines) to neighbouring cells. (B'') Microtubules are not present in the *ago1* mutant cells (GFP –ve) with the condensed nucleus (dotted) and reduced in the neighbouring cells with condensed nuclei. (C'') Zoomed in picture showing close up view of the region with the non-cell autonomous effect (D-D''') Caspase 3 is expressed in the condensed nucleus cells (D'') and the follicle cell boundaries are badly affected as marked by HTS (D'''). Scale bars, 20 μm.

4.2.2. Reduced Dicer-1 and Drosha cause follicle cell defect but not in Pasha

To investigate if the condensed nucleus phenotype in *ago1* mutant is due to the removal of miRNAs, Dicer-1, Drosha and Pasha RNAi were induced using the inducible GAL4 system co-expressed with UAS-Dicer-2 to increase the efficiency of the knockdown. This is first done because *dicer-1* mutant cells are outcompeted in the follicle cells resulting in very few follicle cell clones (Poulton et al., 2011). Interestingly, Dicer-1 and Drosha knockdown caused quite a severe phenotype in the follicle cells depending on the number of clones present (Figure 4.3A-D). There seemed to be a cell division defect in the follicle cells because there were a lot of gaps in the egg chambers that would normally be occupied by follicle cells (Figure 4.3). There were also no cell membranes in the gaps meaning that there were no intact follicle cells present, although there were some signs of dying/apoptotic cells (Figure 4.3C-D). Furthermore, there is also a cell migration defect seen in the follicle cells. In both Dicer-1 and Drosha RNAi lines, the follicle cells did not migrate to the posterior end of the egg chamber as they should in wild type stage 9 egg chambers (Figure 4.3A, C & D). Although the frequency of the condensed nuclei phenotype seen in Ago1 is relatively low, the phenotype seen in Dicer-1 RNAi and Drosha RNAi is more frequent depending on the number of clones present. Surprisingly, there was no phenotype in the Pasha RNAi lines even with a high frequency of clones, although Ago1 expression was decreased suggesting that Pasha knockdown were successful (further discussed in Chapter 5).

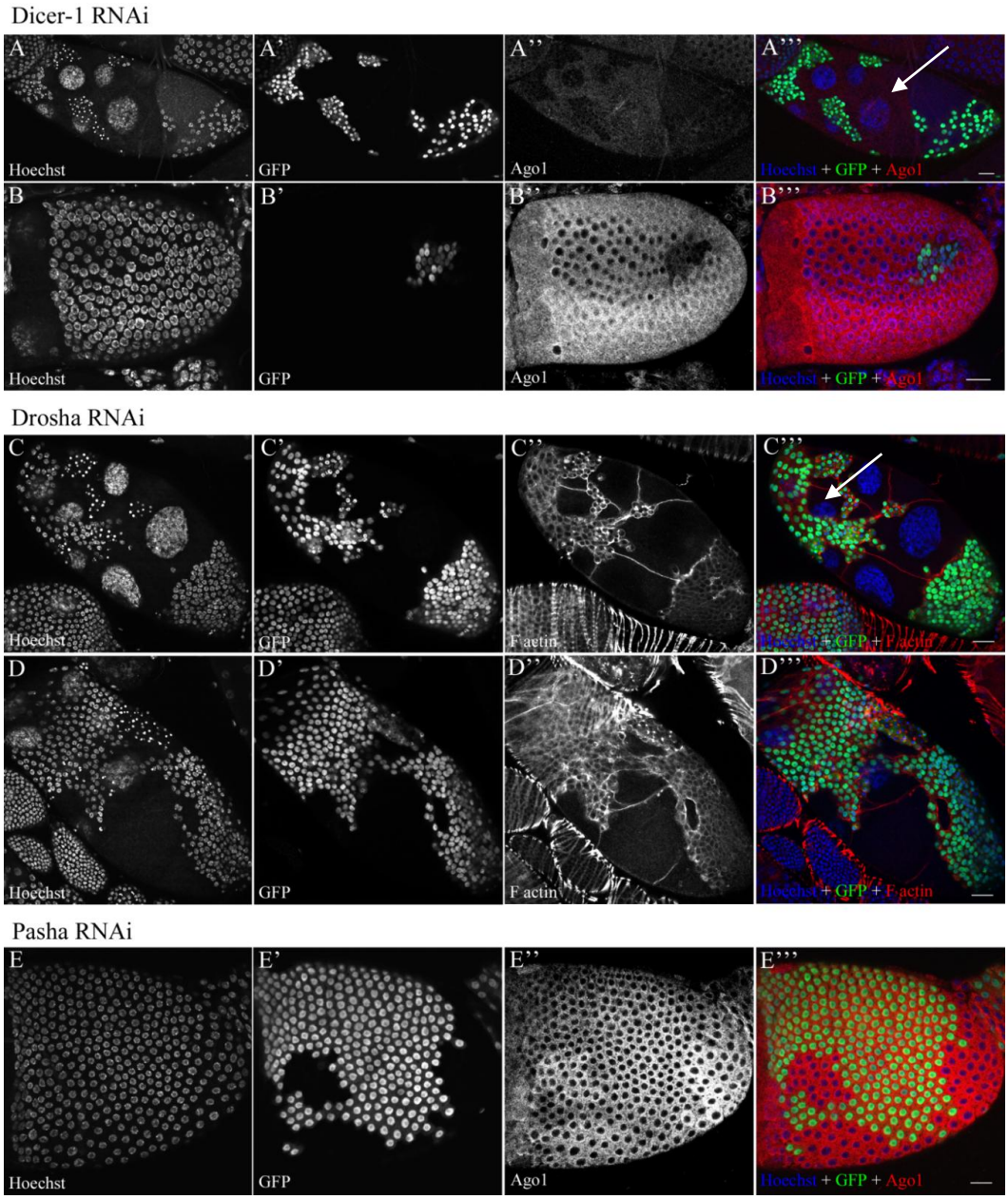


Figure 4.3. Knockdown of Dicer-1, Drosha and Pasha using RNAi with the inducible GAL4 system. (A-B’’’) Dicer-1 RNAi (GFP +ve cells) caused severe follicle cell defects when expressed in most cells (A-A’’’) with apoptotic cells detected (by the condensed nucleus) and ‘gaps’ were seen in the follicle cells (arrow). (B-B’’’) Dicer-1 RNAi cells were outcompeted when expressed in few cells. (C-D’’’) Drosha knockdown also caused the severe follicle cells phenotype with ‘gaps’ (arrow). (E-E’’’) Pasha knockdown (GFP +ve cells) did not cause the follicle cell defects although it caused the reduction of Ago1 (E’’). In all images, anterior is on the left. Scale bars, 20 µm.

4.2.3. Overexpressing Ago1, Dicer-1 and Pasha does not cause any defect

After seeing the phenotypes in *ago1* mutants, Dicer-1 and Drosha knockdowns, it was hypothesized that the overexpression of these miRNA biogenesis proteins may trigger over-proliferation of follicle cells. To test this hypothesis, UASp-Ago1, UAS-Dicer-1 and UAS-Pasha were expressed using the inducible GAL4 system. However, the overexpression of Ago1, Dicer-1 and Pasha did not show any clear phenotype even when most of the follicle cells expressed the transgenes (GFP +ve) (Figure 4.3). The follicle cells looked normal even when the cross were done at 29°C to maximize the overexpression. There were no follicle cell migration defects, no over-proliferation, no size defects and no apoptotic cells detected in both 25°C and 29°C overexpressing flies.

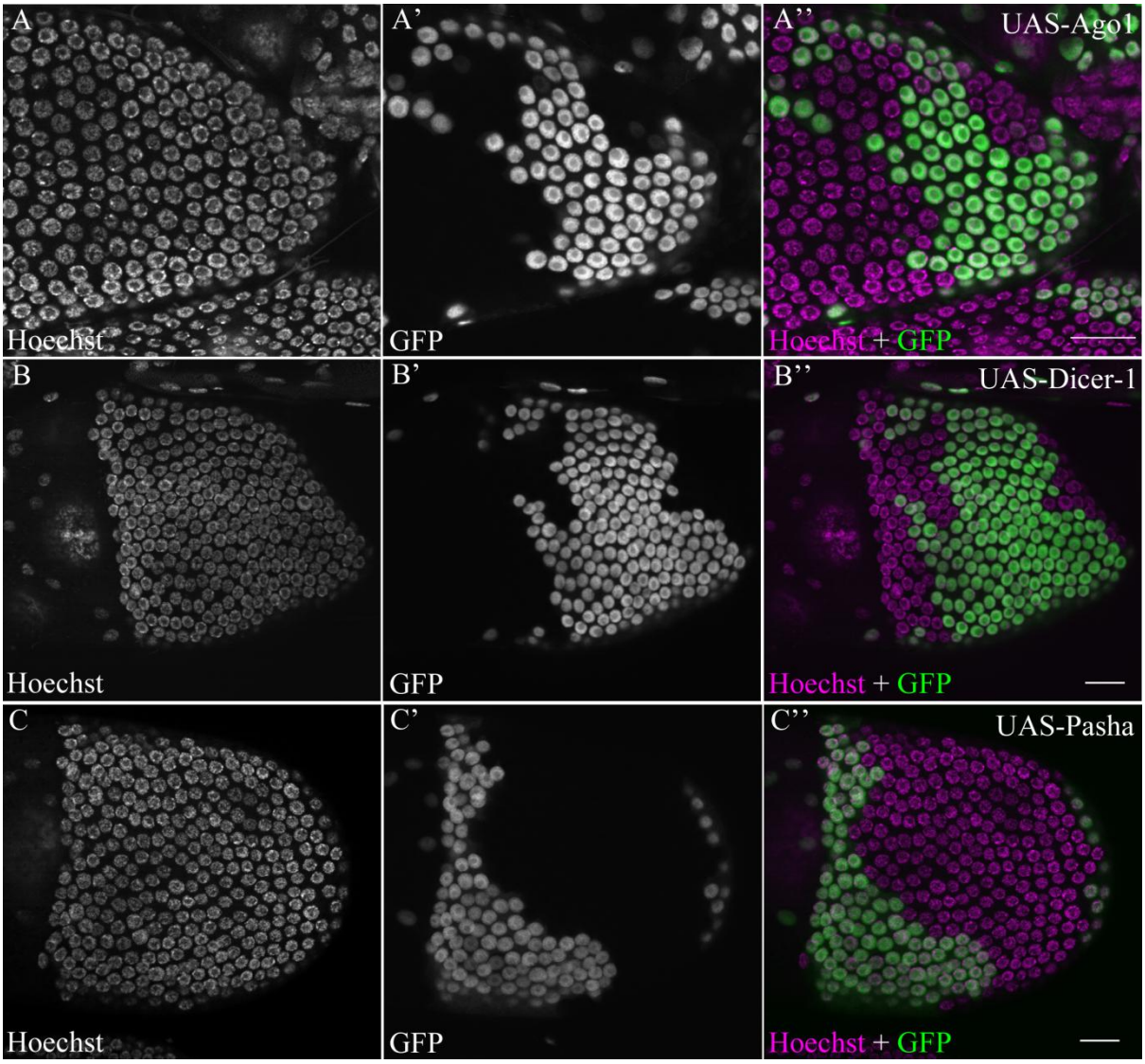


Figure 4.4. Overexpressing Ago1, Dicer-1 and Pasha in the follicle cells. (A-A'') UAS-Ago1, (B-B'') UAS-Dicer-1 and (C-C'') UAS-Pasha overexpression using the inducible GAL4 system did not show any cell migration, over-proliferation or size defects in the follicle cells. Overexpression cells are GFP +ve and wild-type cells are GFP -ve. Scale bar, 20µm.

4.2.4. Ectopic miR-124 causes follicle cell defects

Ectopic expression of miR-124 is known to suppress the expression of non-neuronal transcripts (Conaco et al., 2006; Lim et al., 2005; Makeyev et al., 2007). This raises the hypothesis that miR-124 might also have other functions besides affecting the neurons. To test this hypothesis, UAS-miR-124a (Table 2.2) was overexpressed using the inducible GAL4 system in the follicle cells. Surprisingly, given its neuronal-specific expression pattern (Xu et al., 2008), overexpressing miR-124a caused defects in the follicle cells. Overexpressing miR-124a using the inducible GAL4 system causes severe defects in the follicle cells and its severity depends on the number of clones generated. A very severe follicle cells defect could result in fused egg chambers especially if heat-shock treatments were given during the larvae stage for three consecutive days (Figure 4.5A-A'). The fused egg chambers could be due to the failure of the follicle cells to encapsulate the egg chambers in the germarium and this makes the female sterile. A milder heat-shock treatment, given to adult flies, does not cause the severe fused follicle cells but showed missing follicle cells which result in the gap phenotype just like the Dicer-1 and Drosha knockdowns but not as severe (Figure 4.5B-C'''). To exclude the possibility that ectopic expression of any small RNA was responsible for this phenotype, a mutant version of miR-124a with a 6nt deletion on its mature sequence was expressed and did not show any phenotype (Figure 4.5D-D''').

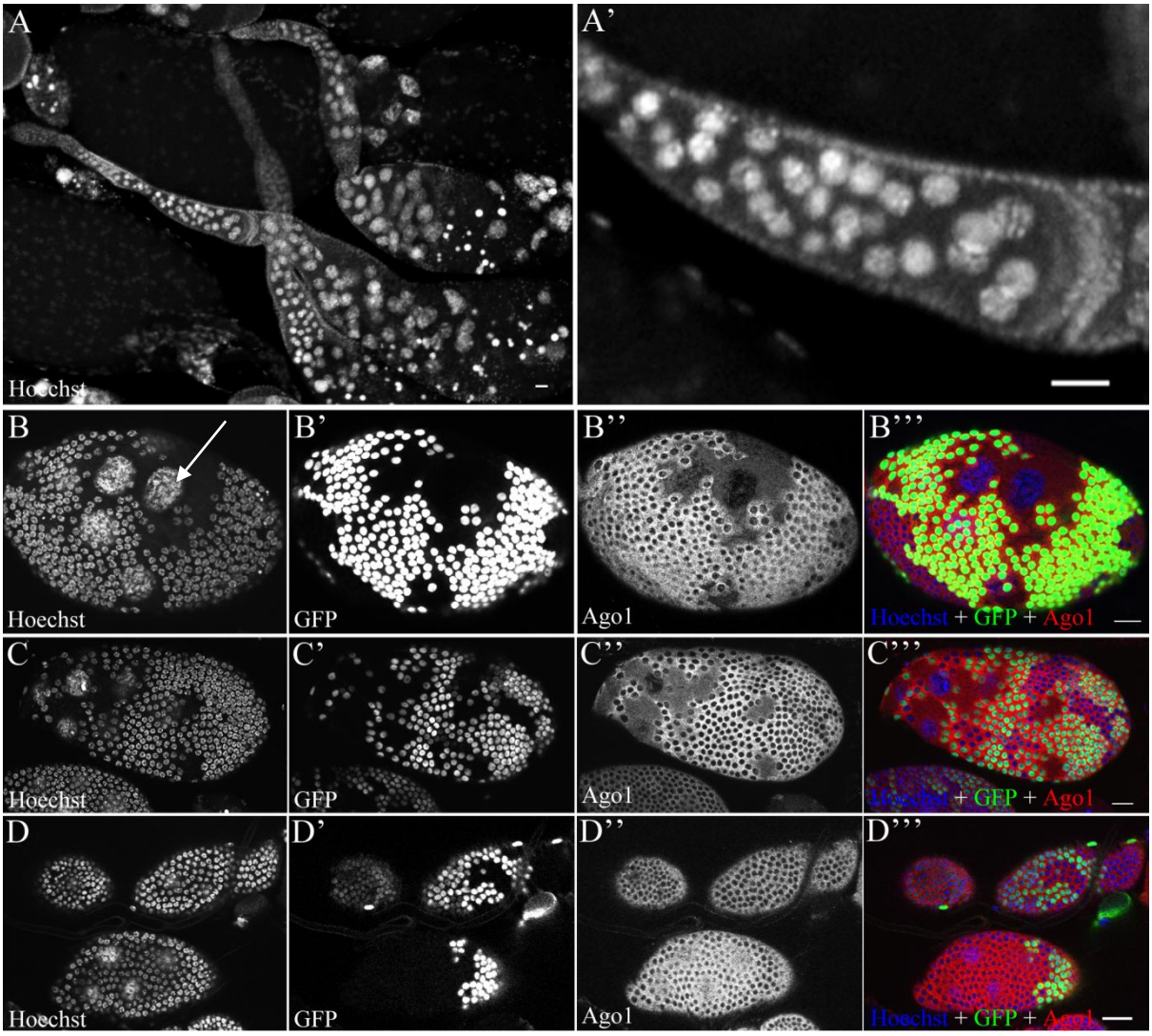


Figure 4.5. Ectopic expression miR-124a causes defects in follicle cells. (A-A') Low magnification images showing the defects in the ovariole when overexpressing miR-124. The flies were heat-shocked at 3rd instar larvae for three days resulting fused egg chambers and a lot of apoptotic egg chambers are seen in later stages. (B-C''') Milder heat-shock were given to adult flies showing gaps (arrow) in the follicle cells are seen in individual egg chambers when miR-124 is overexpressed (GFP +ve) in most cells. (D-D''') UAS-miR-124a-mutant control clones induced during larval stage showing no phenotypic defect. Scale bar 20 µm.

To further test the role of miR-124a in fertility, UAS-miR-124a and UAS-miR124a-mutants were crossed with follicle cell drivers T155-GAL4 (Zhang et al., 2006), Slbo-GAL4 (Bortolamiol et al., 2007) and 55B-GAL4 (Bortolamiol et al., 2007). The T155-GAL4 driver is expressed mostly in the 3rd instar larvae but also has expression in the follicle cell in egg chambers after stage 9. When T155-GAL4 was crossed with UAS-miR124a, the embryos failed to hatch. Next, the Slbo-GAL4 driver which is expressed in centripetally migrating follicle cells and border cells were crossed with UAS-miR-124a. The progenies survive but the females were sterile. There were few eggs laid but none of them hatched. Finally, the 55B-GAL4 driver which is expressed in the adult brain, embryos and follicle cells from egg chambers stage 8 until stage 14 were crossed with UAS-miR-124a. Similar to Slbo-GAL4, the progenies survives but are also sterile. As a negative control, all three GAL4 drivers were also crossed with UAS-miR-124a-mutant. All the progenies were viable and the females were not sterile showing it is not due to background effect.

4.3. Discussion

4.3.1. The miRNA pathway proteins control follicle cell maintenance

Mutants of *ago1* and knockdown of Dicer-1 or Drosha all resulted in follicle cell defects both in nuclear structure and microtubule localisation. Interestingly, *ago1* mutants also show a non-cell autonomous effect whereupon neighbouring cells show a condensed nuclear phenotype and look like they are dying because the GFP is fading and the microtubules are less dense (Figure 4.2). Staining with Caspase 3 showed that those cells are undergoing apoptosis and the cell borders are also affected. The degeneration of microtubules appears to precede other effects because there are cells that still have normal GFP signal but where the microtubule staining is already less dense. Microtubules are very stable especially in follicle cells (Doerflinger et al., 2003; Gutzeit, 1986) and runs parallel to the apicobasal axis with their minus ends at the apical membrane and their plus ends at the basal membrane (Baum et al., 2000; Bre et al., 1990; Clark et al., 1997). The stability of microtubules has been implicated with the PAR-1 where the removal of PAR-1 causes microtubules to disassociate easily (Doerflinger et al., 2003). Ago1 could also cause the microtubules to be unstable, by acting upstream of PAR-1 or other microtubule stabilizing genes. It will also be interesting to test if the microtubules in *ago1* mutants are not as stable as in wild type using colchicine or cold treatments. This is because the disassociation of microtubules in *ago1* mutants is not ubiquitous; it was only seen in some egg chambers. If it is true that the microtubules in ago1 mutants are unstable, then colchicine or cold treatment would cause the microtubule defects in ago1 mutants to be more severe or occur in higher frequency.

The Dicer-1 and Drosha knockdown shows a more severe phenotype where the follicle cells have cell migration defects. At stage 9, the follicle cells are supposed to migrate to the posterior end of the egg chamber and by stage 10 there are usually no follicle cells

present at the anterior end. In the knockdowns, there are still follicle cells at the anterior end of the egg chamber but most of the time the middle part of the egg chamber is empty or has very few follicle cells (Figure 4.3). However, some cells seem to have successfully migrated to the posterior end. A second possibility would be when the follicle cell migration signal is lost, so while the egg chamber is rapidly expanding, the follicle cells are pulled by the anterior and posterior end of the egg chamber resulting in follicle cells present at the anterior and posterior end while the middle section is empty. Furthermore, Pasha knockdown did not show any clear phenotype in the follicle cells. It is surprising that the Pasha knockdown did not show the same phenotype as Drosha because Pasha is required for Drosha stability thus knocking down Pasha should also result in the reduction of Drosha (Han et al., 2009). This might suggest that the miRNA biogenesis could be more complex than previously thought. Overexpressing Ago1, Dicer-1 and Pasha also did not show any clear phenotypic defect in the follicle cells. This could be due to the miRNA processing 'bottleneck' of the other miRNA biogenesis proteins that were not overexpress. For example, overexpressing Ago1 would in theory increase miRNA activity, however, because Dicer-1, Pasha and Drosha are still at normal levels, the amount of miRNAs processed by those proteins would still be the same hence the 'bottleneck' term and the failure to see any defects in the follicle cells.

4.3.2. miR-124a: a predominantly neuronal miRNA plays a role in follicle cells

One of the major finding here is that ectopic expression of miR-124a caused defects in the follicle cells. If the ectopic expression of miR-124 suppressed the expression of other non-neuronal transcripts, there must be some important transcripts in the follicle cells that are suppressed leading to the phenotype. Although miR-124 is one of the most abundant brain-specific miRNA and plays a unique function during neurogenesis (Conaco et al., 2006; Krichevsky et al., 2003; Sempere et al., 2004), this is one of the few studies to show that miR-

124 has a role at other points in the animals development. Overexpressing miR-124 (Table 2.2) in the follicle cells is enough to make the female sterile. The sterility is due to the fact that the egg chamber failed to develop properly resulting in extensive apoptosis in the later stage as seen in Figure 4.5A. Gaps in the egg chamber follicle cells are quite common upon miR-124a overexpression, similarly to Dicer-1 and Drosha knockdown. It is unknown how knocking down all miRNAs and overexpressing just miR-124a alone could have similar defects. The miR-124a is highly conserved between human and *Drosophila* (Lagos-Quintana et al., 2002) and its expression is regulated by dFMR1 which is the *Drosophila* homolog of human fragile X mental retardation protein 1 (hFMR1) (Xu et al., 2008) which has been shown to be expressed during the ovarian folliculogenesis (Schuettler et al., 2011).This may suggest an analogous mechanism of action of miR-124a in ovarian tissues between *Drosophila* and humans. The dFMR1 has also been linked with both Ago1 and Ago2 which shows its close relationship with small RNAs (Pepper et al., 2009; Xu et al., 2008). The relationship between miR-124a, dFMR1 and the follicle cells is a complex regulatory network that needs further experiments to uncover. The available data from modENCODE project showed that miR-124a is expressed at very low levels in the follicle cells. The repression of miR-124a in the follicle cells might be a safe-guard employed by the system as its targets might be highly expressed in the follicle cells. However, extensive expression data plus the creation of a miR-124a null mutant or knocking down miR-124a using miRNA sponges (Loya et al., 2009) are required to properly understand the function of miR-124a in the follicle cells.

Chapter 5
Ago1 senses mature miRNA levels

5.1. Introduction

5.1.1. The stability and posttranslational control of Argonaute proteins

Diverse biological functions can be regulated by miRNAs as they repress translation or degrade their target mRNAs. Recently, an increasing number of studies have started to reveal mechanisms for the turnover of miRNAs (Ameres et al., 2011; Chatterjee and Grosshans, 2009). However, the mechanism and factors that regulate the stability of the core component, Argonaute proteins are less understood.

The heat-shock protein 90 (Hsp90) has been shown to be required for human Ago2 (hAgo2) protein stability (Johnston et al., 2010; Suzuki et al., 2009). Geldanamycin or 17AAG are Hsp90 inhibitors and decrease the level of hAgo2 protein in HeLa cells (Johnston et al., 2010). It has also been shown that increasing the amount of siRNA prevents geldanamycin from having an effect on hAgo2. Furthermore, it has also been shown in flies that Hsp70/Hsp90 are required for Ago1 and Ago2 RISC loading, so a similar situation might operate in flies (Iwasaki et al., 2010).

Argonaute proteins also have a negative feedback loop mediated by miRNAs in *Arabidopsis* (Vaucheret, 2009; Vaucheret et al., 2006). Here, miR-168 is able to target AGO1 mRNA when there is a high level of AGO1 protein. When AGO1 level is decreased, less miR-168 is loaded to RISC, thus maintaining a constant AGO1 level in the cell. However, to date, analogous mechanisms in other organisms have remained elusive. Studies on human Argonautes might shed light on this phenomenon. *In vitro* studies shows that Ago2 and Ago4 were more susceptible to hydroxylation than Ago1 and Ago3 (Qi et al., 2008). Ago2 requires

prolyl-4 hydroxylation of proline 700 (P700) for stability and without it would reduce RNAi efficiency but it is dispensable for miRNA-mediated translation repression.

Since miRNAs are key regulators of many different cellular processes, it is not surprising that the pathway is controlled by multitude of mechanisms. Previous studies have demonstrated that Argonaute expression can be the rate-limiting step for miRNA maturation and repression. Similarly, the stability of unloaded Argonaute has been previously demonstrated to be lower than loaded Argonaute. Also, the inhibition of Hsp90 that stabilises unloaded Argonautes leads to the proteasome-mediated degradation (Johnston et al., 2010). It has also been suggested that ubiquitination and even SUMOylation are good candidates for regulation of miRNA homeostasis by influencing Argonaute stability (Johnston and Hutvagner, 2011).

5.1.2. Experimental description

The expression of Ago1 in the female germ line cells was previously described in Chapter 3. In this chapter, the distribution of Ago1 protein in the absence of miRNAs was studied by examining *pasha* and *dicer-1* mutants as well as Drosha RNAi stocks in both germ line cells and somatic cells. These experiments were carried out to study the relationship between miRNAs and Ago1 *in vivo*. Ago1 expression correlates with the level of miRNA in the cells leading to the hypothesis that Ago1 stability is affected by miRNAs *in vivo*. To test this hypothesis, S2 cells in which miRNA levels were manipulated and analysed.

5.2. Results

5.2.1. Ago1 sense mature miRNAs in germline cells

It has already known that Pasha is required for Drosha stability (Han et al., 2009). Smibert et al., (2011) also showed that in the absence of Drosha, the level of Pasha increased and in the absence of Pasha, the level of Drosha decreased. However, the relationship between Ago1 and its miRNA biogenesis partners has never been analysed. First, *pasha* mutant mitotic clones were generated in the egg chambers and stained against Ago1 antibody. Interestingly, the staining of Ago1 in egg chamber clones of the two Pasha mutant alleles, *pasha[LL03360]* and *pasha[36B2]*, marked by the lack of GFP, were significantly lowered compared to the GFP +ve wild-type clones (Figure 5.1). To further confirm that the relationship is between the levels of miRNAs and Ago1, mitotic clones for *dicer-1[Q1147X]*, *dicer-1[LL06357]*, *dicer-1[21B2]* and *dicer-1[37A1]* were generated. All of the different *dicer-1* mutant clones exhibited strongly reduced Ago1 staining equivalent to *pasha* mutant clones. The Ago1 levels in the *pasha* and *dicer-1* mutants are similar to those of *ago1* mutants where even the enrichment of Ago1 in the developing oocyte was lost. The *smn73A* mutant (Figure 5.1H), a housekeeping gene which is not involved in the miRNA biogenesis and a FRT82B chromosome lacking any mutation were used as negative controls to confirm that this is not a general effect. The two different Pasha mutant alleles and four different Dicer-1 mutant alleles were used to test different genetic backgrounds to remove the possibility that the reduction of Ago1 is caused by background mutation. These results clearly show a correlation between the levels of miRNAs and Ago1 in the germ line cells.

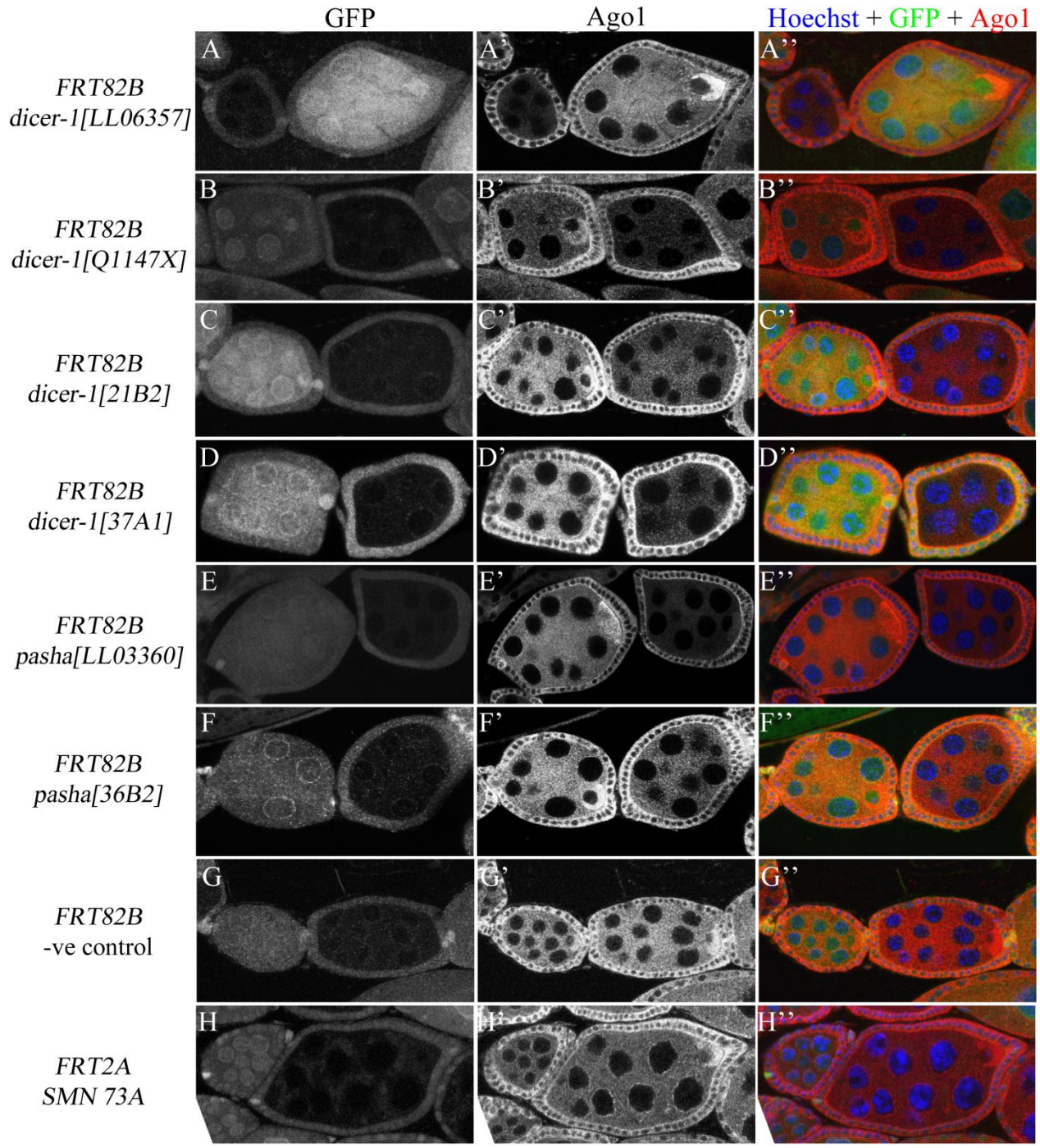


Figure 5.1. Ago1 levels are reduced when miRNAs are not present. (A-F'') All four *dicer-1* and two *pasha* mutant clones in the germline (GFP -ve) show lower Ago1 staining compared to heterozygous control (GFP +ve). FRT82B and *SMN73A* control were used as negative controls. Scale bar 20 µm.

5.2.2. Ago1 senses global mature miRNAs levels

Seeing the reduction of Ago1 protein levels in the germline cells is an interesting observation. However, it is still unknown whether this phenomenon occurs generally. To understand whether this is a tissue-specific or germline cell-specific phenomenon, the MARCM technique was used to analyse loss of Dicer-1 and Pasha function in 3rd instar larval brain (Chapter 2.1.5). The MARCM technique uses the same principle as mitotic clones however in MARCM, the mutant clones are marked with GFP and the wild-type cells have no GFP, which is the opposite of mitotic clones.

Here, the reduction of Ago1 protein levels in the mutant (GFP +ve) clones of *pasha[LL03360]*, *pasha[36B2]*, *dicer-1[LL06357]*, *dicer-1[Q1147X]*, *dicer-1[21B2]*, *dicer-1^{30D2}*, *dicer-1[37A1]* and *dicer-1^{38E3}* were apparent when compared to the GFP –ve control cells (Figure 4.2A-H). This is similar to the effect seen in the germline cells. In addition, a completely independent approach was taken to further verify this phenomenon. UAS-Drosha RNAi, UAS-Dicer-1 RNAi and UAS-Pasha RNAi were induced using the inducible GAL4 system in the larval CNS and the results were reproducible (Figure 5.2I-K). These results in different systems and tissues clearly show that loss of function of any proteins upstream of Ago1 in the miRNA biogenesis pathway caused a global reduction in the level of Ago1.

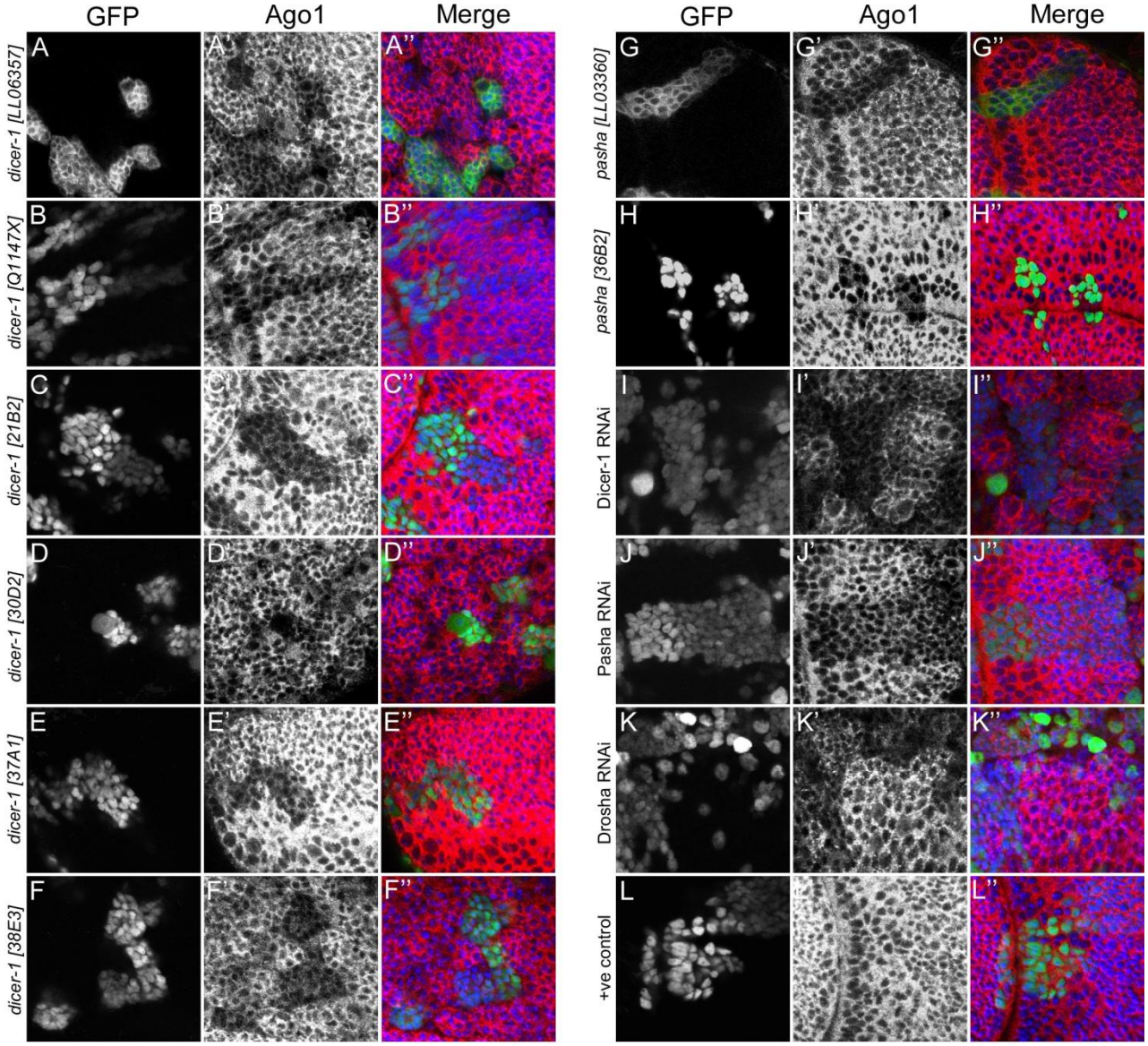


Figure 5.2. Ago1 sense miRNA levels in somatic cells. (A-H'') Six *dicer-1* and two *pasha* mutant clones (GFP +ve) showing lower Ago1 staining compared to heterozygous control (GFP -ve) cells in the larval CNS. (I-K) Dicer-1, Pasha and Drosha RNAi knockdown cells (GFP +ve) also showed lower Ago1 staining in the larval CNS. (L-L'') FRT82B negative control showing no differences in Ago1 staining. In merge image, Hoechst is blue, GFP is green and Ago1 is red.

5.2.3. Ago1 global level is translationally affected in the absence of miRNAs

Previous results in this chapter show that the Ago1 protein level is reduced in the absence of miRNAs but whether it is affected at the level of transcription, translation or protein stability is of interest. Larvae from *pasha[LL03360]* homozygous mutants were collected. The level of Ago1, Dicer-1, Drosha and Pasha mRNA were analysed using quantitative RT-PCR (qPCR) (Chapter 2.4.10). Pasha mutant was used because the homozygous mutant survives until 3rd instar larvae stage while the Dicer-1 homozygous mutant dies during embryogenesis. Also, preliminary data shows that Ago1 levels were reduced in the discs as well. This makes using the whole larvae a viable choice. The qPCR results show that the level of Pasha RNA was reduced dramatically but the result also shows that the Ago1 RNA level did not change significantly (Figure 5.3). This shows that Ago1 transcription or mRNA stability is not affected in the absence of miRNAs.

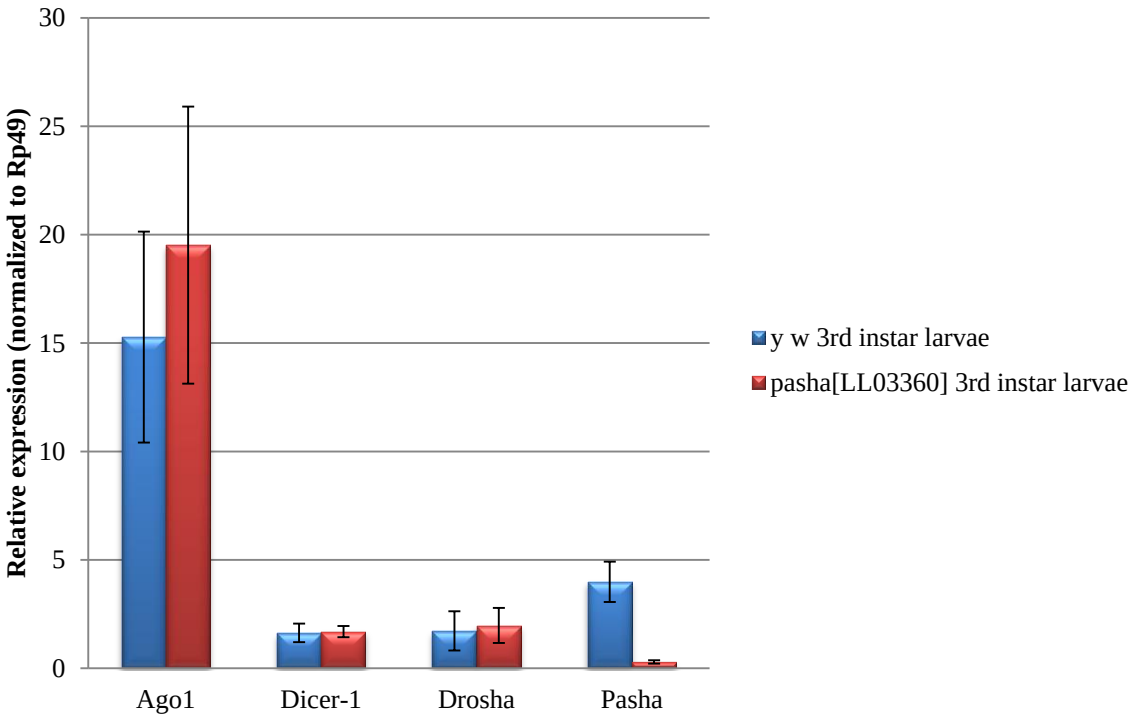


Figure 5.3. The levels of Ago1 RNA were not affected in *pasha* mutant. QPCR were carried out on *pasha* homozygous mutant 3rd instar larvae. The relative quantification was normalized to *rp49*. Negative controls are S2 cells that do not receive the RNAi but still undergoes the same treatments.

5.2.4. Overexpressing Dicer-1 or Pasha does not increase Ago1 levels

Data from previous studies shows that the reduction of Dicer-1, Pasha and Drosha levels will reduce the total level of mature miRNAs dramatically in *Drosophila* (Denli et al., 2004; Lee et al., 2004; Okamura et al., 2004). The previous results in this chapter show that Ago1 levels are affected by the reduction of miRNA present in the cells. However, it is unknown whether overexpressing miRNAs will have the opposite effect on Ago1. First UAS-Ago1 (+ve control), UAS-Dicer-1 and UAS-Pasha-HA were overexpressed using the inducible GAL4 system in the follicle cells. Overexpression of Ago1 resulted in dramatically increased staining intensity, however, overexpressing Dicer-1 or Pasha did not increase the levels of Ago1. Both UAS-Dicer-1 and UAS-Pasha-HA lines have been previously tested (Berdnik et al., 2008) but overexpression of UAS-Pasha-HA was also verified by antibody detection against its HA tag (data not shown).

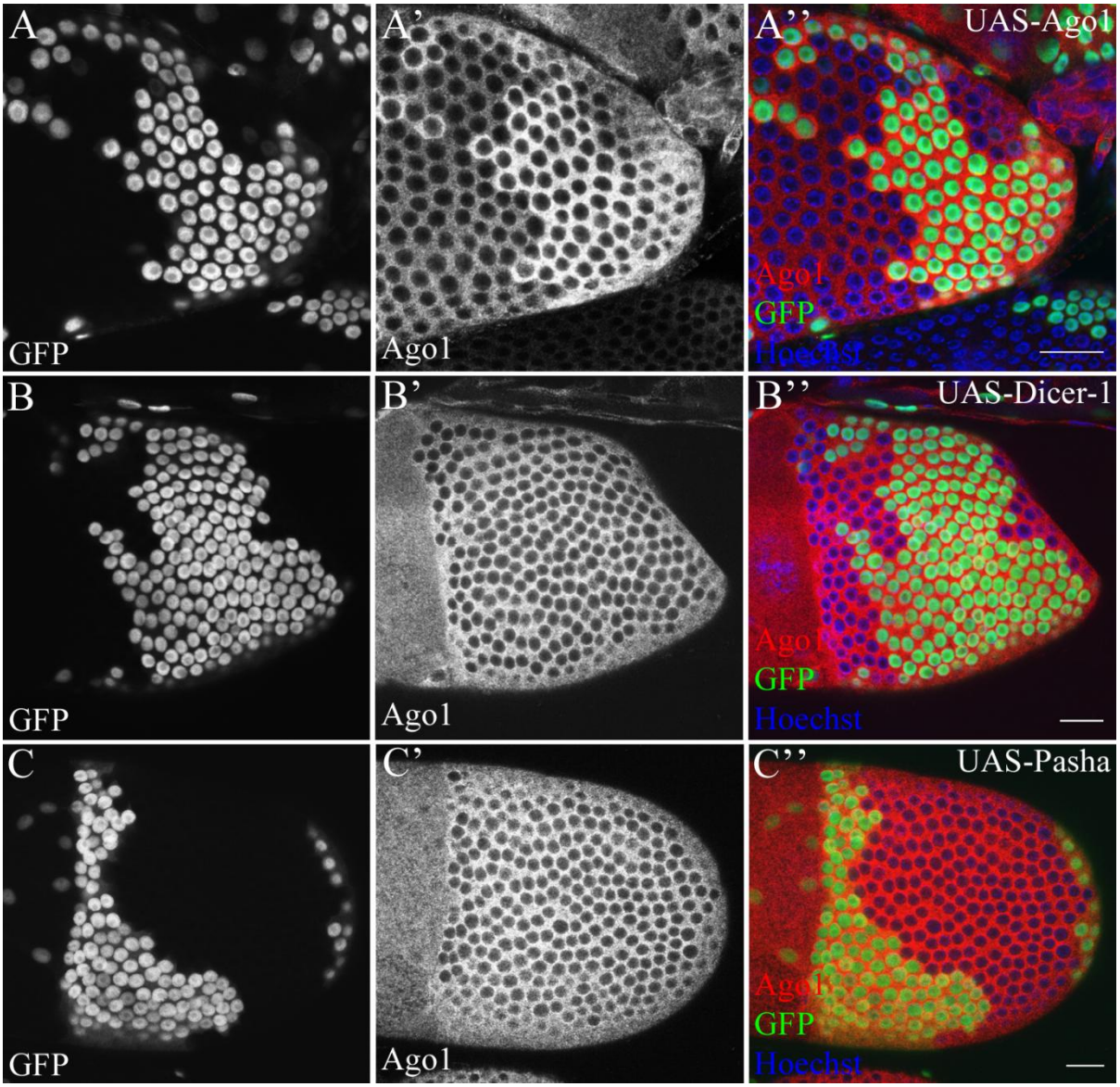


Figure 5.4. Overexpressing Dicer-1 or Pasha does not affect Ago1 levels. (A-A'') UASp-Ago1 was used as a positive control. Overexpressing UAS-Ago1 using the inducible GAL4 system increased the staining of Ago1 (A'). (B-C'') UAS-Dicer-1 and UAS-Pasha-HA were overexpressed using the inducible GAL4 system but did not increase the level of Ago1. Scale bar 20 µm.

5.2.5. Overexpressing miR-124a increases Ago1 expression

Even though overexpressing Dicer-1 or Pasha did not increase the level of Ago1, this could be because of many reasons which will be discussed. However, overexpressing a single miRNA could show a different result. To test whether overexpression of a single miRNA had an effect on Ago1 levels, UAS-miR-124a line was used to overexpress miR-124 in the follicle cells using the inducible GAL4 system (Chapter 1.5.3.3). UAS-miR-124a mutant which has a six base pair deletion on its mature sequence, results in a non-functional miRNA as a control (Xu et al., 2008). The results show that the level of Ago1 protein is higher in the follicle cells where miR-124a is overexpressed compared to the basal levels in wild-type follicle cells in the same egg chamber (Figure 5.3B). Furthermore, the level of Ago1 is unchanged upon overexpression of UAS-miR124a-mutant suggesting that only mature miRNAs would affect the level of Ago1 protein (Figure 5.3C). These results are consistent with the idea that Ago1 level is controlled by global miRNA expression.

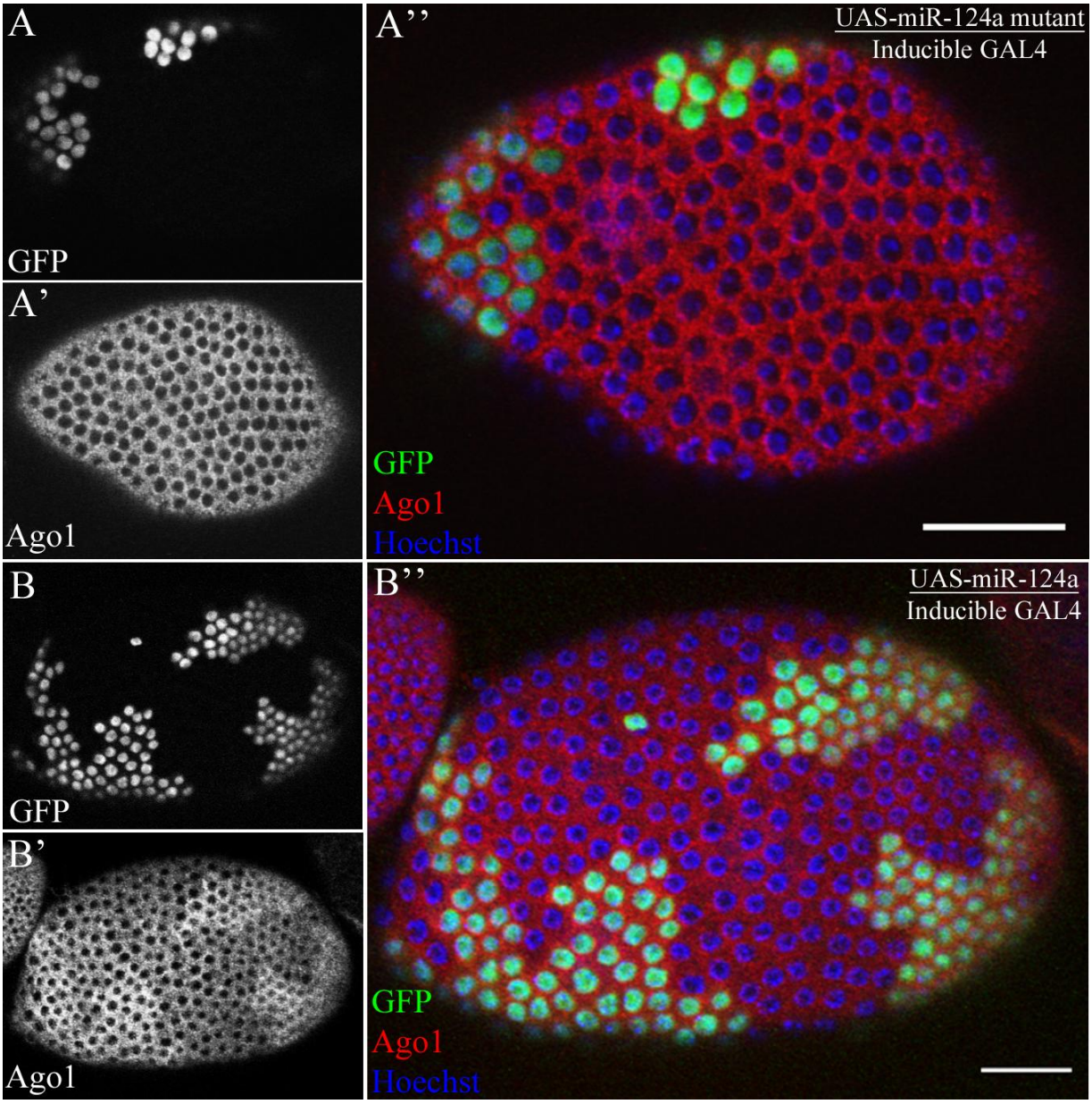


Figure 5.5. Overexpressing miR-124a increases the levels of Ago1. (A-A'') Overexpressing UAS-miR-124a-mutant (GFP +ve) using the inducible GAL4 system does not affect the level of Ago1. (B-B'') Overexpressing UAS-miR-124a (GFP +ve) using the inducible GAL4 system increase the level of Ago1 (B') in the follicle cells. Scale bar 20 µm.

5.2.6. Ago1 levels are not affected by the levels of siRNAs

In general, siRNAs in *Drosophila* are processed by a different small RNA pathway where they are loaded into Ago2 instead of Ago1. However, there are some circumstances where siRNAs are loaded to Ago1 although this does not happen very frequently (Okamura et al., 2011). If Ago1 is sensing the level of miRNAs in the cell, altering siRNA levels should not alter Ago1 levels.

To knock-down the siRNA components, flies carrying the RNAi construct from TRiP were used. TRiP has made two types of construct that have been shown to succesfully knockdown genes in both somatic and germline cells. The first generation constructs (Valium 1 and Valium 10) utilizes long double-stranded RNA which utilizes the siRNA machinery to knockdown genes (Ni et al., 2008). The second generation constructs (Valium 20 and Valium 22) utilizes short hairpin RNA which uses the miRNA machinery (Ni et al., 2011).

Mosaic expressions of two different UAS-Dicer-2 RNAi (Valium 10 and Valium 20) stocks were induced using the inducible GAL4 stock and Ago1 levels were monitored by immunofluorescence. Both Valium 10 and Valium 20 stocks were used to eliminate potential side effect of using only Valium 10 constructs which depends on Dicer-2 activity. As hypothesised, since *Drosophila* siRNA and miRNA biogenesis are separated, there is no change in Ago1 levels when Dicer-2 is knocked down.

To further confirm this, UAS-R2D2 RNAi clones were induced using the inducible GAL4 system to knockdown R2D2 in the follicle cells (Figure 5.6C). R2D2 binds to Dicer-2 in the siRNA biogenesis and it is also required for organizing small RNA network in *Drosophila* (Okamura et al., 2011). The level of Ago1 also did not decrease in the R2D2 knockdown cells. Taken together, these results suggest that the levels of Ago1 proteins are only affected by the level of mature miRNAs and independent of the levels of siRNAs.

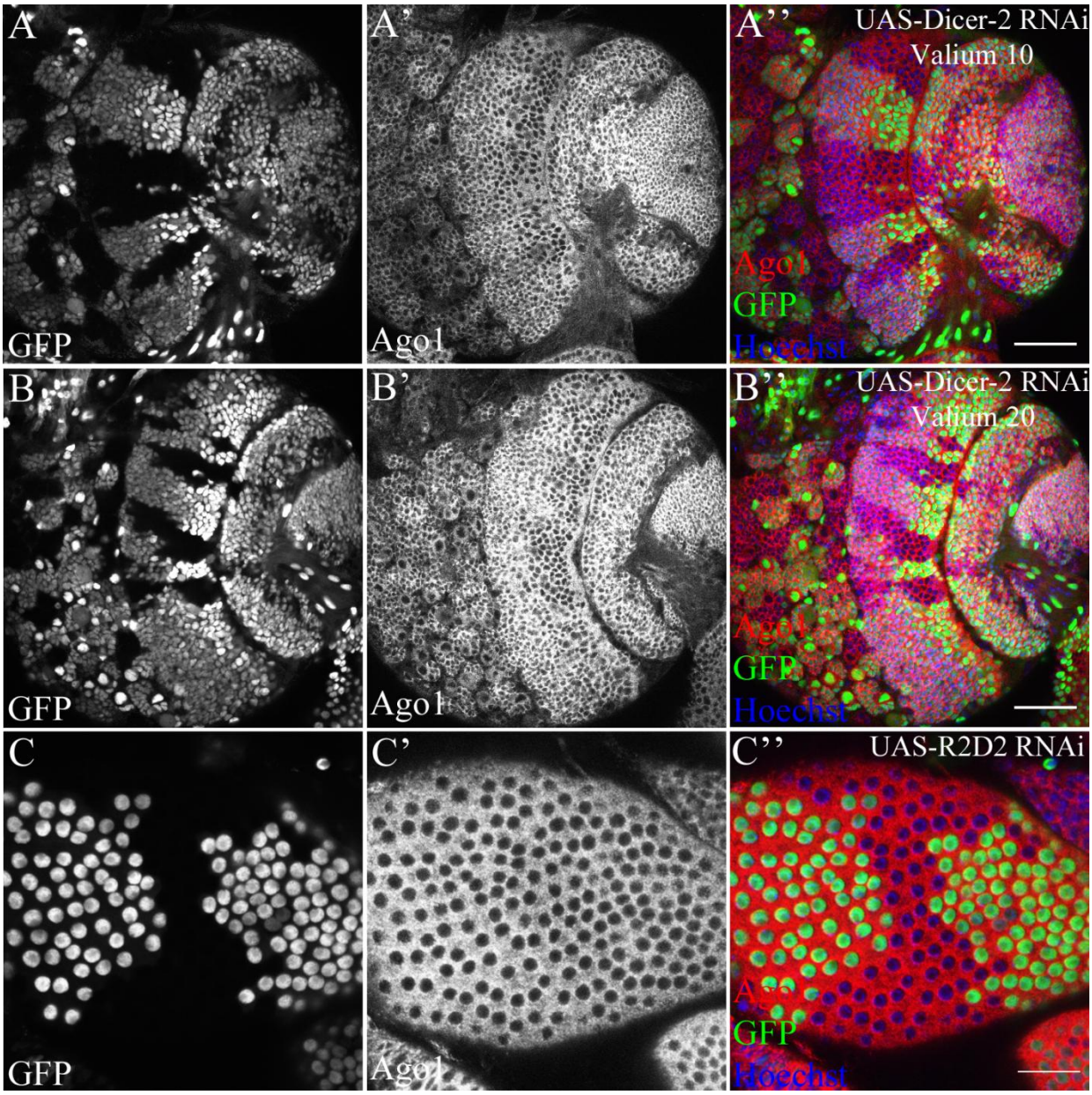


Figure 5.6. Ago1 levels are not affected by siRNAs. (A-B'') Two UAS-Dicer-2 RNAi constructs were induced using the inducible GAL4 system and knocked down cells (GFP +ve) showed no difference in Ago1 levels in the larval CNS. (C-C'') UAS-R2D2 RNAi was used with the inducible GAL4 system in the follicle cells and showed no difference in Ago1 staining (GFP +ve). Scale bar 20 µm.

5.2.7. Ago1 protein stability in S2 cells

The results presented in this chapter point to the hypothesis that Ago1 protein stability is affected by mature miRNA levels. Previous studies have shown that the Argonaute complex undergoes conformation changes when it binds to mature miRNA and their target mRNAs (Wang et al., 2008). It is possible that unloaded Ago1 is unstable and loaded Ago1 is more stable due to these conformational changes. This idea has been raised previously in conjunction with Hsp90 (Johnston et al., 2010). To address this issue, Ago1 stability test were carried out using S2 cells, a cell line derived from late stage embryos (Schneider, 1972). The S2 cells used were acquired from *Drosophila* Genomics Resource Center (DGRC) which has the capability to transport dsRNA across the cell membrane and cause knockdown of gene without any transfection reagent. This method of 'soaking' has been widely used (Armknecht et al., 2005).

First of all, Ago1, Dicer-1, Pasha and Drosha needed to be knocked-down in S2 cells using dsRNA (RNAi) transfection. The SnapDragon tool (http://www.flyrnai.org/cgi-bin/RNAi_find_primers.pl) was used to design dsRNAs against Ago1, Dicer-1, Pasha and Drosha (Chapter 2.4.8). Two non-overlapping sequences were chosen and tested for each gene. The efficiency of the knockdown for all the genes were tested using qPCR and about 50 to 90% knockdown of mRNA levels were obtained (Figure 5.7). The dsRNA that produced better knockdown was then chosen for subsequent experiments. Dicer-2 and Ago2 RNAi were designed to confirm that the siRNA pathway does not affect Ago1 levels. dsRNAs targeting two unrelated genes, CTPS and eGFP were used as a negative control. All the miRNA sequences are mature sequences taken from miRBase. Another negative control is 'no transfection' in which S2 cells were not given any dsRNA/RNAi but still underwent all the other steps.

To carry out the stability test, the S2 cells were incubated with the dsRNA for 3 days (Chapter 2.2.8) then treated with 100μM cycloheximide to stop protein translation followed by Western blotting to quantify protein levels. Cycloheximide is an inhibitor that blocks the translocation step in protein synthesis hence blocking translational elongation. The idea of blocking protein synthesis is to see the turnover or stability of Ago1 protein when there is no translation occurring. After treating the S2 cells with RNAi for 3 days, the level of Ago1 protein in Ago1 RNAi treated cells were reduced dramatically (Figure 5.8). Surprisingly, the levels of Ago1 in S2 cells treated by Dicer-1, Pasha and Drosha RNAi did not change even after six hours of cycloheximide treatment. A band corresponding to Ago1 protein can still be seen clearly in the knockdowns. After 6 hours of cycloheximide treatment, the cells began to die, so it is not feasible to prolong the treatment.

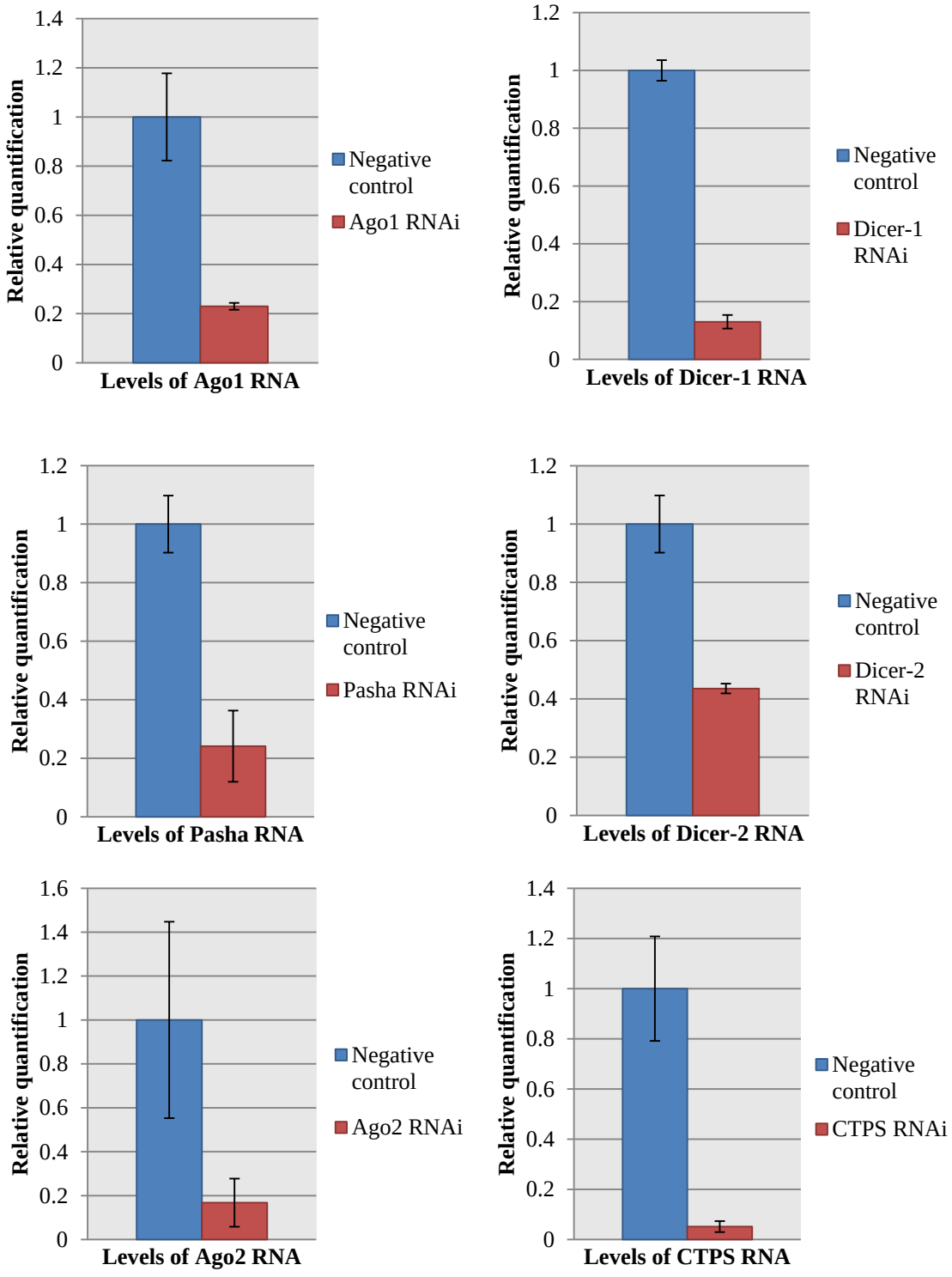


Figure 5.7. S2 cells treated with RNAi with about 50-90% knockdown. QPCR were carried out on S2 cells after 4 days of RNAi treatment. The relative quantification was normalized to *rp49*. Negative controls are S2 cells that do not receive the RNAi but still undergoes the same treatments.

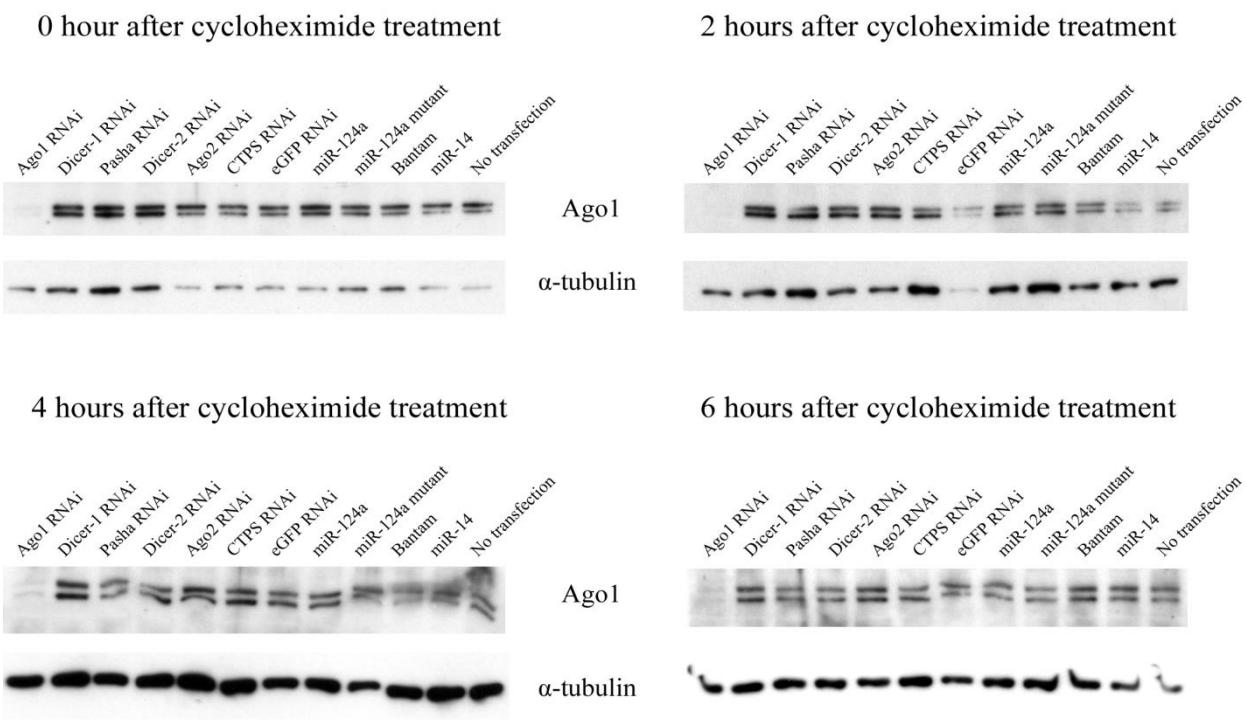


Figure 5.8. Western blot showing Ago1 protein levels of cycloheximide treated S2 cells after RNAi treatment. Ago1 western blot showed two bands corresponding to the isoforms of Ago1 with predicted molecular weight of 106.2 kDa and 109.9 kDa. The levels of Ago1 were reduced dramatically in Ago1 RNAi treated cells, but the levels of Ago1 did not change on other RNAi-treated cells and even after six hours of cycloheximide treatment.

5.3. Discussion

5.3.1. Uncovering a new feature of Ago1

Although Ago1 has been intensively studied over the years, there have been no reports to show that Ago1 protein level is affected by any of its upstream miRNA biogenesis proteins partners or the global miRNA levels. The results presented in this chapter shows that the level of Ago1 is affected by the level of mature miRNAs. The loss of Ago1 expression is consistent across multiple mutant alleles with different genetic backgrounds as well as RNAi knock downs, and the converse can be observed upon overexpression of miR-124a. This discovery could show that the main component of RISC is affected by the miRNAs that it binds to. These results provide a mechanism for regulation of Ago1 levels, but also complicate the study of Dicer-1, Pasha and Drosha because these mutants also reduce the level of Ago1, thus resulting in potential for a secondary effect.

Overexpressing Dicer-1 or Pasha did not increase the levels of Ago1 and this could be due to the bottleneck created by the other miRNA biogenesis proteins if they are expressed at a normal level. For example, overexpressing Dicer-1 could make the process of removing the hairpin of pre-miRNAs more efficient, but the amount of pre-miRNAs present is determined by the activity of Pasha and Drosha. This is also true for Pasha overexpression where the amount of Drosha protein available to bind to could be the bottleneck in the efficiency of producing pre-miRNAs from pri-miRNAs. Also, both Pasha and Dicer-1 activity could be limited by the level of pri-miRNA transcript available in the cell. This seems plausible because when miR-124a was produced ectopically, an increased level of Ago1 was observed. By producing massive amounts of pri-miRNA transcript, the increased level of Ago1 suggests that the level of mature miRNAs was also elevated. It seems likely that endogenous levels of Pasha and Dicer-1 are enough to process the huge amount of pri-miRNAs present. However,

since only miR-124 was tested, there is also the possibility that this effect could be due to overexpressing miR-124 only. Since trying to obtain other miRNA overexpression did not bear any fruit, this could not be confirmed. Testing other miRNA overexpression is vital to ensure that the amount of mature miRNA is causing Ago1 levels to elevate.

How the abundance of miRNAs affects the level of Ago1 is still remains unknown. Pasha is required for Drosha stability (Han et al., 2009) and absence of Drosha increases the level of Pasha protein (Smibert et al., 2011b). This reciprocal stability could be due to the binding of those proteins to each other to form the microcomplex, stabilising both proteins. In the case of Ago1, removing the miRNAs which it binds to might be an evolutionary feature that was placed when its 'substrate' miRNA is not present. This could be intended to improve responsiveness to changes in miRNA levels or to prevent non-specific effects. Ago1 protein may be unstable by itself, until it forms the RISC, whereupon the protein is stabilised. How Ago1 is degraded in the absence of miRNAs is still unknown, although there is a suggestion that Argonaute proteins are degraded by the ubiquitin-proteosome system (Johnston and Hutvagner, 2011). Plant studies on the degradation of Ago1 also show that it is ubiquinated and degraded (Bortolamiol et al., 2007; Bortolamiol et al., 2008; Csorba et al., 2010). It is also proteolytically cleaved into two halves in a regulated manner (Zhang et al., 2006).

The focus of this study is on Ago1, but there are still areas which have not been covered due to time and other limitations. Further experiments that have not been performed include analysis of protein levels between Pasha or Drosha mutants and Dicer-1 mutants that would uncover the difference between the level of Ago1 in the presence and absence of mirtrons. Mirtrons arise from spliced out introns that bypass the microprocessor complex of Drosha and Pasha by splicing and debranching itself to generate pre-miRNA hairpin in which these pre-miRNAs will then be loaded into Dicer-1 and continue the miRNA biogenesis

(Martin et al., 2009; Okamura et al., 2007). Pasha and Drosha mutants would reduce the levels of miRNAs but not mirtrons.

5.3.2. Failure of the S2 cell system to test Ago1 stability

The results from the *in vivo* studies described the hypothesis that miRNAs act to alter the stability of Ago1. When there are reduced levels of miRNAs, the level of Ago1 is reduced and when miRNA was overexpressed, the level of Ago1 increased. Surprisingly, the level of Ago1 did not change in the RNAi transfected S2 cells even though decreased level of Dicer-1 and Pasha transcripts were detected. However, there are several reasons why this stability test failed which will be discussed here. Firstly, the high level of endogenous siRNA in S2 cells plus the abundance of exogenous dsRNA added to the cells could be masking the effect of Ago1 stability. Ago1 in S2 cells have the potential to load siRNAs in certain conditions (Okamura et al., 2011), so Ago1 could be forced to load other small RNAs when they present in massive amounts. This effect however, was not seen *in vivo* when UAS-RNAi constructs were driven in the somatic cells so it may be limited to S2 cells only. There is also the possibility that transient RNAi treatment in S2 cells with 50-90% knockdown is insufficient to de-stabilize Ago1. The remaining RNA is enough to produce proteins that will process miRNAs which will be loaded and stabilize Ago1. Furthermore, previous study has also shown that treating S2 cells with Dicer-1 dsRNA did not reduce the level of Ago1 (Jiang et al., 2005). Although this system failed to show the reduction of Ago1 in the absence of mature miRNAs as seen *in vivo*, the hypothesis of Ago1 stability is affected by mature miRNA could not be ruled out. Further experiments are needed to confirm this discrepancy between the experiments *in vivo* and those in S2 cells. S2 cells were chosen in this study because of its ease to treat with double stranded RNA and the shorter time required compared to *in vivo*.

The stability of Argonaute proteins has also been tested in human cells with conflicting results. Johnston et al., (2010) reported that Argonaute proteins loaded with small RNAs are more stable than unloaded Argonaute proteins. However, Pare et al., (2009) showed in HeLa cells that the stability of hAgo2 mutants that are unable to bind small RNA are not much different from the wild-type loaded hAgo2. This may be due to the similarity to some effect of the cell culture system used.

To more directly test the hypothesis that miRNA binding alters Ago1 levels *in vivo,* a tagged mutant Ago1 construct which prevents it from loading miRNA could be injected into flies and compared to the wild type protein. This will provide early indication if this hypothesis is true. The level of transgenic Ago1 could be detected with a tag (GFP for example) to distinguish it from the endogenous Ago1. It would be expected that the mutated Ago1 would be present at lower levels than the wild type Ago1, and be independent of mutations in the other miRNA pathway components such as Dicer-1 and Pasha. *Drosophila* might be the best model organism to further pursue this as the biogenesis of miRNAs is separated from the siRNA pathway.

A series of systematic studies are necessary to identify the mechanism of Ago1 homeostasis, but nevertheless these results highlight an important and novel regulatory mechanism controlling Ago1 protein levels that appears to be evolutionarily conserved throughout animals and possibly also plants.

Chapter 6
Distinct subcellular distributions of CTPS isoforms

6.1. Introduction

6.1.1. The three isoforms of CTPS

The *Drosophila* CTPS gene produces three different isoforms. The first transcript, CTPS isoform A, encodes 1872bp transcript mRNA from the CTPS gene which then produces a 429 amino acid protein. The CTPS isoform A protein consists of two different domains, the N-terminal myb/SANT-like domain in Adf-1 (MADF) and the C-terminal BEAF, Suvar(3)7 and Stonewall (BESS) motif (Figure 6.1B). This architecture is conserved in at least 14 *Drosophila* proteins (Bhaskar and Courey, 2002). The MADF domain is also an alcohol dehydrogenase transcription factor myb/SANT-like and consists of 93 amino acids (Figure 6.1B). It is thought to direct the sequence specific DNA binding to a site consisting of multiple tri-nucleotide repeats. Furthermore, the MADF domain is found in 46 genes in *Drosophila* is also often associated with the BESS domain (Bhaskar and Courey, 2002). The BESS domain consists of about 40 amino acids and has two predicted alpha helices. The BESS domain appears to be specific to *Drosophila* and is predicted to be a DNA binding domain. This domain is found in 19 proteins which are all encoded in *Drosophila* and 14 proteins have both MADF and BESS domains (Bhaskar and Courey, 2002).

Next, the CTPS isoform B encodes 2397bp transcript mRNA which produces a 623 amino acid protein. The CTPS isoform B has two predicted incomplete domains; MADF and P-loop containing Nucleoside Triphosphate Hydrolases (NTPase) domain and type 1 glutamine amidotransferase (GATase 1) domain (Figure 6.1). The incomplete MADF domain

present in this isoform is only 41 amino acids long and the incomplete P-loop NTPase domain consists of 205 amino acids. The P-loop NTPase have been implicated in many biochemical and mechanical processes in the cell which includes transcription, replication, trafficking, membrane transport and activation of various metabolites. (Aravind et al., 2004; Saraste et al., 1990; Vetter and Wittinghofer, 1999). Also, the P-loop NTPase consists of Walker A and B motifs which bind to the beta-gamma phosphate moiety of typically ATP or GTP and the Mg2+ ion (Walker et al., 1982). Further down of the P-loop NTPase domain is the GATase1 domain. One role of the GATase1 domain is to utilize bind glutamine, form a glutaminyl intermediate and hydrolyses it to produces ammonia (Weng and Zalkin, 1987). The ammonia is used at a separate site to activate UTP O4 oxygen by Mg-ATP-dependent phosphorylation. The amidotransferase also contains a conserved Cys-His-Glu catalytic triad in the active site. A channel is present between the glutamine hydrolysis and the active site which provides a path for ammonia diffusion.

Finally, CTPS isoform C encodes 2380bp transcript mRNA and produces a 627 amino acid protein. CTPS isoform C has two domains; the CTG domain and the previously discussed GATase1 domain (Figure 6.1). The CTG domain is the synthetase domain which has an active site, catalytic site and a UTP binding site. Isoform C has five UTP binding site and five catalytic site which is required to make CTP from UTP hence giving the idea that this could be the most important isoform. However, isoform B has four UTP binding site and three active site which means that isoform B could still produce CTP but might not be as efficient as isoform C.

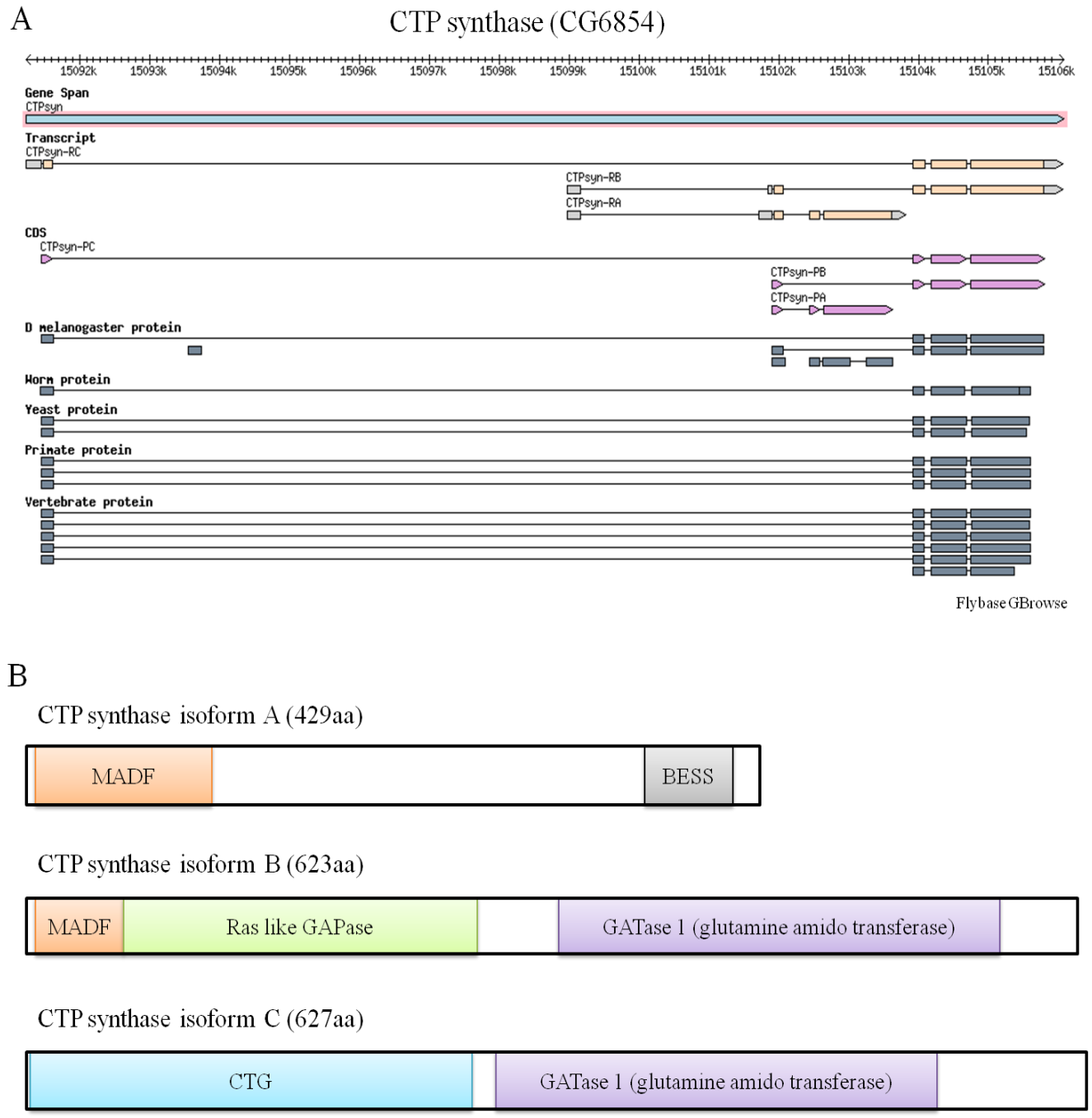


Figure 6.1. Gene map of *Drosophila* CTP synthase (CG6854). (A) Flybase Genome Browser (GBrowse) view of CTPS gene showing the three different isoform transcripts and the similarities between fly, worm, yeast, primate and vertebrate CTPS protein (B) The protein map of all three different *Drosophila* CTPS isoforms with their different domains.

6.1.2. Experimental description

In this chapter, transgenic flies were generated using CTPS isoform specific UASp Venus tagged construct to study their distribution and localization. Tissues with or without obviously detectable cytoophidia were analysed to characterize the effect of overexpressing CTPS. Then after identifying the filament forming isoform, the domains in the isoform were identified and more transgenic flies were generated with the domain specific construct. Furthermore, with these constructs, the filament forming region is narrowed down. The primary antibody that is used in these experiments is CTPS (y-88) from Santa Cruz Biotechnology, Inc. (sc-134457) which recognizes amino acids 31-118 mapping near the N-terminus of CTPS of *Saccharomyces cerevisiae*. This antibody sequence also matches 87% of *Drosophila* CTPS isoform C amino acids 31-119 near the N-terminus.

6.2. Results

6.2.1. Generating CTPS isoform specific transgene

Antibody staining against CTPS (Table 2.3) and the study using CTPS::GFP protein trap line (Table 2.1) shows that CTPS localizes to cytoophidium in many tissues. However, *Drosophila* CTPS has three different isoforms and whether all three isoforms localize to cytoophidia is still unknown. To study their distribution, both tagged and untagged constructs of each isoform were made. All tagged constructs were made using a Venus (Nagai et al., 2002) tagged UASp vector from the Gateway clones (Terrance Murphy collection) and the untagged constructs were made using the modified pUASp vector (Thomsen et al., 2010) which contain attB sites for PhiC31 integrase-mediated site specific injection (Chapter 2.5). To make the constructs, these cDNA clones were used; LD27370 (isoform A), LD27537 (isoform B) and LP25005 (isoform C) which was acquired from the *Drosophila* Genomics Resource Center (DGRC) gold collections.

6.2.2. Characterizing CTP synthase transgene in different tissues

6.2.2.1. Egg chambers

All the UAS-Venus tagged transgenic flies were first crossed with nos-GAL4::VP16 driver and analysed by staining against CTPS antibody to see if there is any change in the cytoophidia shape or length. To our surprise, these three isoforms exhibit distinct intracellular localizations. The egg chambers of CTPS isoform A overexpression flies were first analysed. Surprisingly the CTPS isoform A forms distinct punctate structures in the nucleus (Figure 6.2B-B''). Both N-terminal and C-terminal tagged transgene showed the same expression. However, staining against CTPS antibody shows that the cytoophidia morphology did not change when CTPS isoform A was overexpressed. Furthermore, ubiquitously using Act-GAL4 to overexpress CTPS isoform A is lethal while overexpressing only in the female

germline using nos-GAL4::VP16 makes the female sterile. Analysing the egg chambers further showed that many egg chambers were undergoing apoptosis, leading to smaller ovaries.

Next, egg chambers of CTPS isoform B overexpression flies were analysed. CTPS isoform B overexpression, detected by Venus tag, also did not localize to cytoophidia. Instead, the CTPS isoform B was dispersed in the cytoplasm on both N-terminal (Figure 6.2C-C'') and C-terminal tag transgene. The morphology of cytoophidia, analysed by antibody staining against CTPS, remained unchanged compared to wild-type (Figure 6.2A-A''), even with the untagged transgene (data not shown). However, compared to flies overexpressing isoform A, overexpressing isoform B does not cause lethality or sterility. Flies overexpressing CTPS isoform B using Actin-GAL4 are also viable and showed no clear phenotypic defect.

Finally, the egg chambers of flies overexpressing CTPS isoform C, which is the longest isoform of CTPS, were analysed. Interestingly, the C-terminal Venus-tagged CTPS isoform C transgene localized to cytoophidia (Figure 6.2D). Antibody staining against CTPS confirms this localization even though not all cytoophidia seen in the tagged isoform were stained; this could be due to penetration of the antibody (Figure 6.2D'). The egg chambers of flies overexpressing CTPS isoform C have more cytoophidia and the cytoophidia are clearly longer than the wild-type cytoophidia (Figure 6.2A'). The cytoophidia in the CTPS isoform C overexpression are also more flexible and tangled up compared to the wild-type cytoophidia. However, overexpressing the N-terminal Venus tagged CTPS isoform C cause defects on the cytoophidia formation (Figure 6.2E-E''). The cytoophidia lost its flexibility, making straight cytoophidia which clumped together forming a 'spider web'. In addition, this disruption also affects the endogenous cytoophidia as seen by antibody staining against CTPS (Figure 6.2E'). The untagged transgene also leads to longer and more flexible cytoophidia as seen in the C-

terminal tagged CTPS isoform C (data not shown). Flies overexpressing CTPS isoform C are also viable and fertile. However, there are signs that the overexpression flies grow slower and live longer but more detailed studies are required.

In wild-type follicle cells, approximately one cytoophidia is present in each cell (Figure 6.3A-A'). So looking at the overexpression of CTPS isoform C could result in two things; there are more cytoophidia per cell or bigger and longer cytoophidia. Looking at the follicle cells of CTPS isoform C overexpression line using the Act-GAL4 driver, the number of cytoophidia per cell does not seem to change, however, the length of the cytoophidia is clearly longer compared to the wild-type cytoophidia in the follicle cells (Figure 6.3B-B').

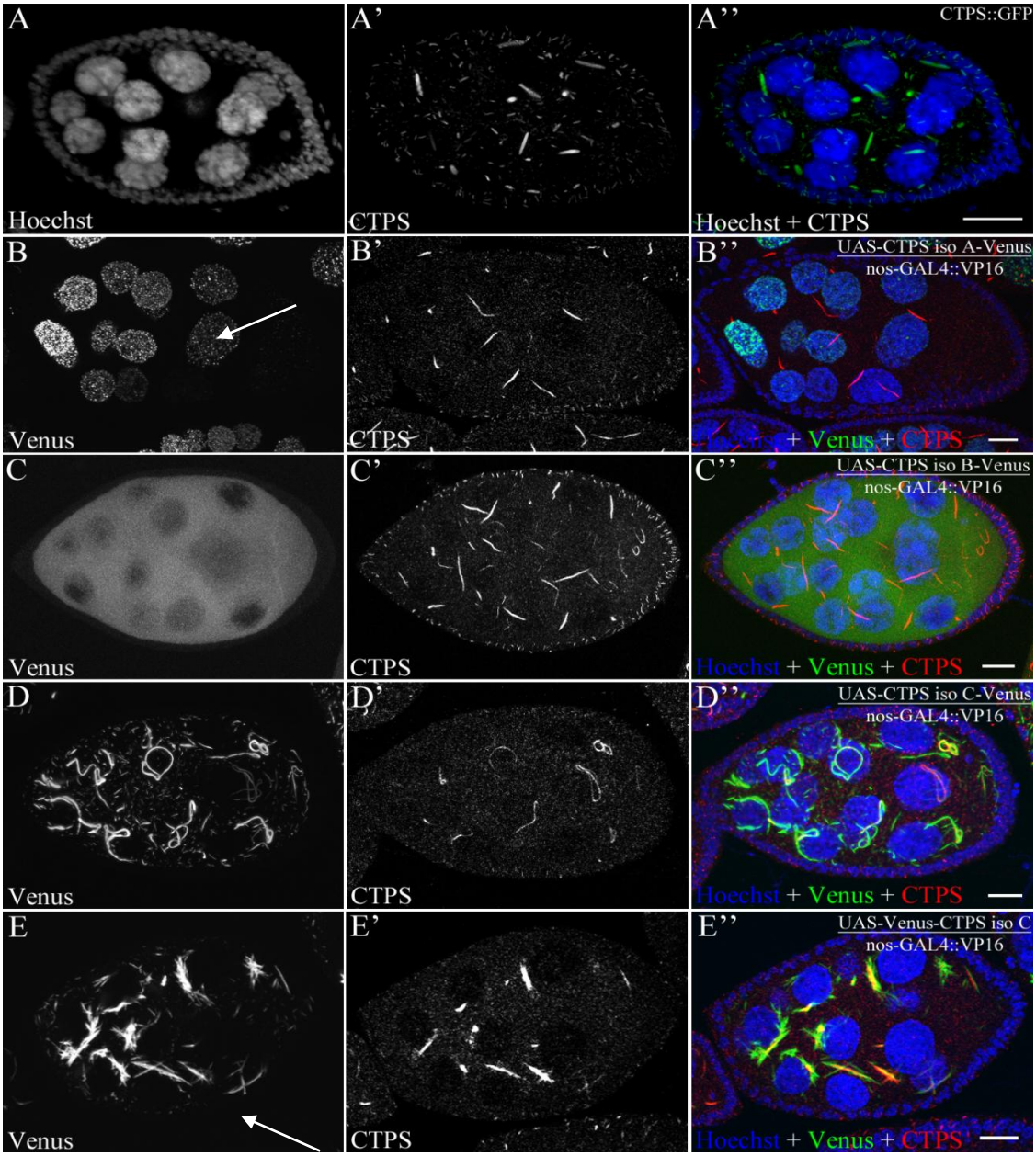


Figure 6.2. Different CTPS isoforms overexpression in the germline cells using nos-GAL4::VP16 driver. (A-A'') Endogenous cytoophidia in CTPS::GFP protein trap line egg chambers. (B-B'') CTPS iso A is localized in punctate structure in the nucleus (arrow) and does not affect endogenous cytoophidia. (C-C'') CTPS iso B is dispersedly localized in the cytoplasm of the egg chamber and does not affect the endogenous cytoophidia. (D-D'') C-terminal tagged CTPS iso C induced ectopic cytoophidia. The cytoophidia are also longer and more flexible. (E-E'') N-terminal tagged CTPS iso C disrupts cytoophidia morphology (arrow).

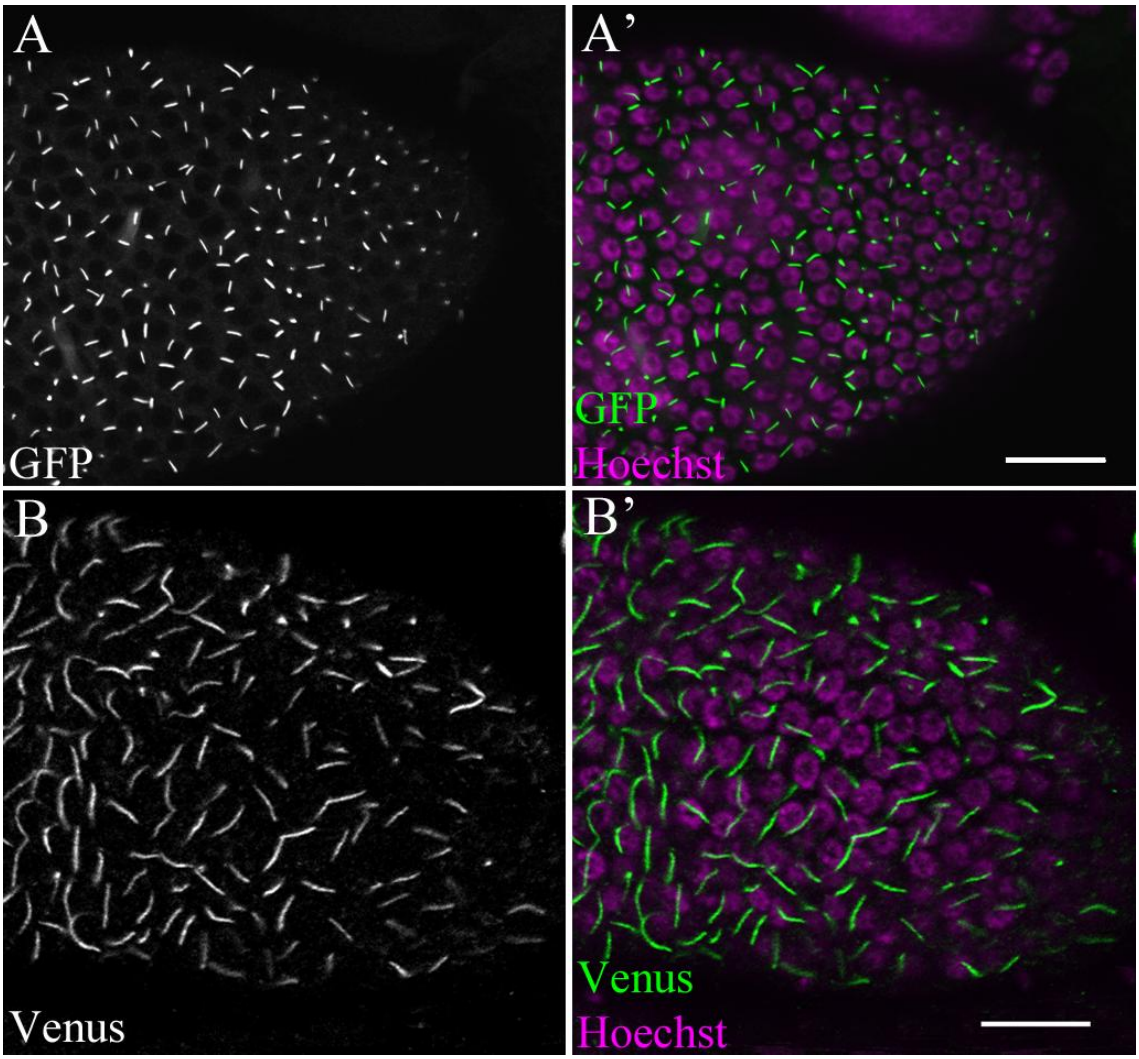


Figure 6.3. CTPS isoform C overexpression in follicle cells. (A) Endogenous cytoophidia formation in wild-type follicle cells. (B) Longer cytoophidia are seen in follicle cells overexpressing CTPS iso C under the Actin-GAL4 driver.

6.2.2.2. Testis

Since the CTPS isoform C is the only isoform to form cytoophidia, it would be interesting visualize the morphology of cytoophidia in other tissues. Endogenous cytoophidia are present in the testis, usually located in the proliferating region of the testis (Figure 6.3A-A'). The adult testis contains between five to nine GSCs which resides around twelve hubs cells at the posterior end of the testis. The GSCs will give rise to thousands of spermatids over the lifetime of the fly. GSCs will differentiate into a gonioblast which divides mitotically four times with incomplete cytokinesis, producing 16 cyst-cells connected by ring canals (de Cuevas and Matunis, 2011). Then, the 16 cyst-cells differentiate into spermatocytes which then undergo meiosis producing 64 mature spermatids (Terry et al., 2006).

When CTPS isoform C was overexpressed using the Act-GAL4 driver, more cytoophidia were seen in the testis and about 35% (n=22/63) of the testis looked significantly bigger (tumour-like) than wild-type testis (Figure 6.4B & D) and this fits the data that overexpressing CTPS does not cause sterility because the other 65% of the males have normal testes. The ectopic cytoophidia formation looked similar to testis of flies treated with DON (Chen et al., 2011). The size of the tumorous testis could be about three times (estimate) bigger than the wild-type testis. To understand this phenotype further, the testes were stained with HTS which labelled the ring canals, and coilin which brightly labels the spermatocytes (Liu et al., 2009) (Figure 6.3C-C''). Overexpressing CTPS isoform C increases the number of primary spermatocytes in the testis, generating the large tumour-like phenotype (Figure 6.3D-D''). These were further confirmed by the presence of large ring canals in the bright coilin labelled cells (Figure 6.3D'').

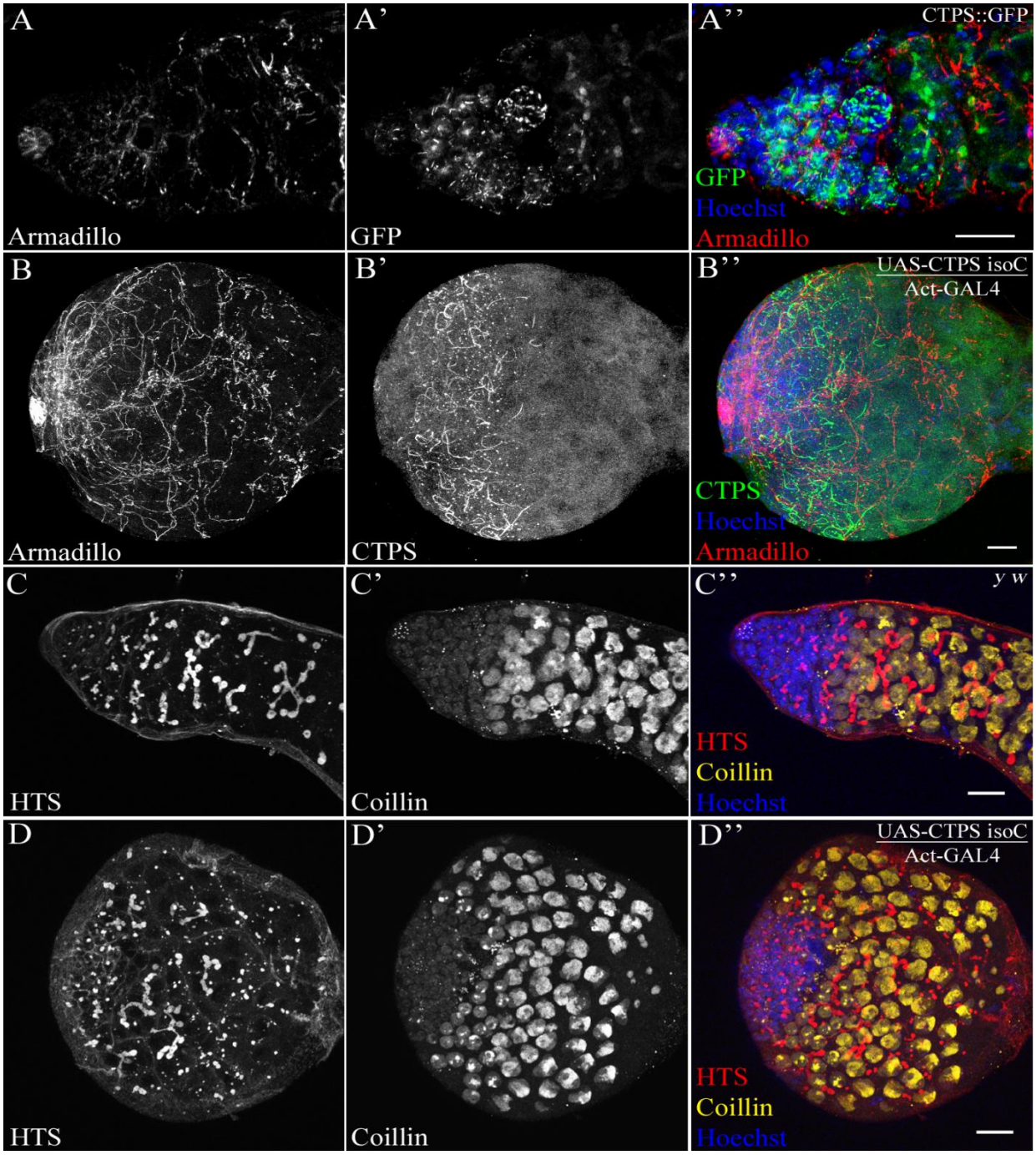


Figure 6.4. CTPS isoform C overexpression in testis. (A-A'') CTPS::GFP protein trap line showing endogenous cytoophidia formation. (B-B''') Overexpression of CTPS iso C using Act-GAL4 induces ectopic cytoophidia formation (B') and caused tumour-like phenotype in 35% of the males. (C-C'') y w testis showing wild-type expression of HTS (fusomes) and coilin (spermatocytes). (D-D'') Tumour-like phenotype in CTPS iso C overexpression testis is caused by an increased number of spermatocytes which are labelled by bright coilin staining.

6.2.2.3. Embryos

Not all tissues have obviously detectable cytoophidia (i.e. macro-cytoophidia). For example, embryos normally do not have detectable cytoophidia and the antibody staining against CTPS showed dispersed staining throughout embryogenesis (Figure 6.4A & C). This is also seen in the CTPS::GFP protein trap line (data not shown). Furthermore, without maternal contribution, CTPS mutants die during embryogenesis with severely disrupted embryos which means that CTPS is important for embryogenesis (further discussed in Chapter 7). So it would be interesting to see if overexpressing CTPS isoform C in the embryos would induce macro-cytoophidia formation.

As expected, embryos overexpressing CTPS isoform C promote cytoophidia formation throughout embryogenesis (Figure 6.4B, D & F). Even stage 1 embryos show a lot of cytoophidia formation. Stage 15 embryos (Figure 6.4F) have more cytoophidia compared to stage 12 embryos (Figure 6.4B). The morphology of the embryos does not seem to be affected by the ectopic CTPS isoform C and cytoophidia. These results strengthen the fact that overexpressing CTPS isoform C can induce cytoophidia formation even in tissues that do not have endogenous cytoophidia.

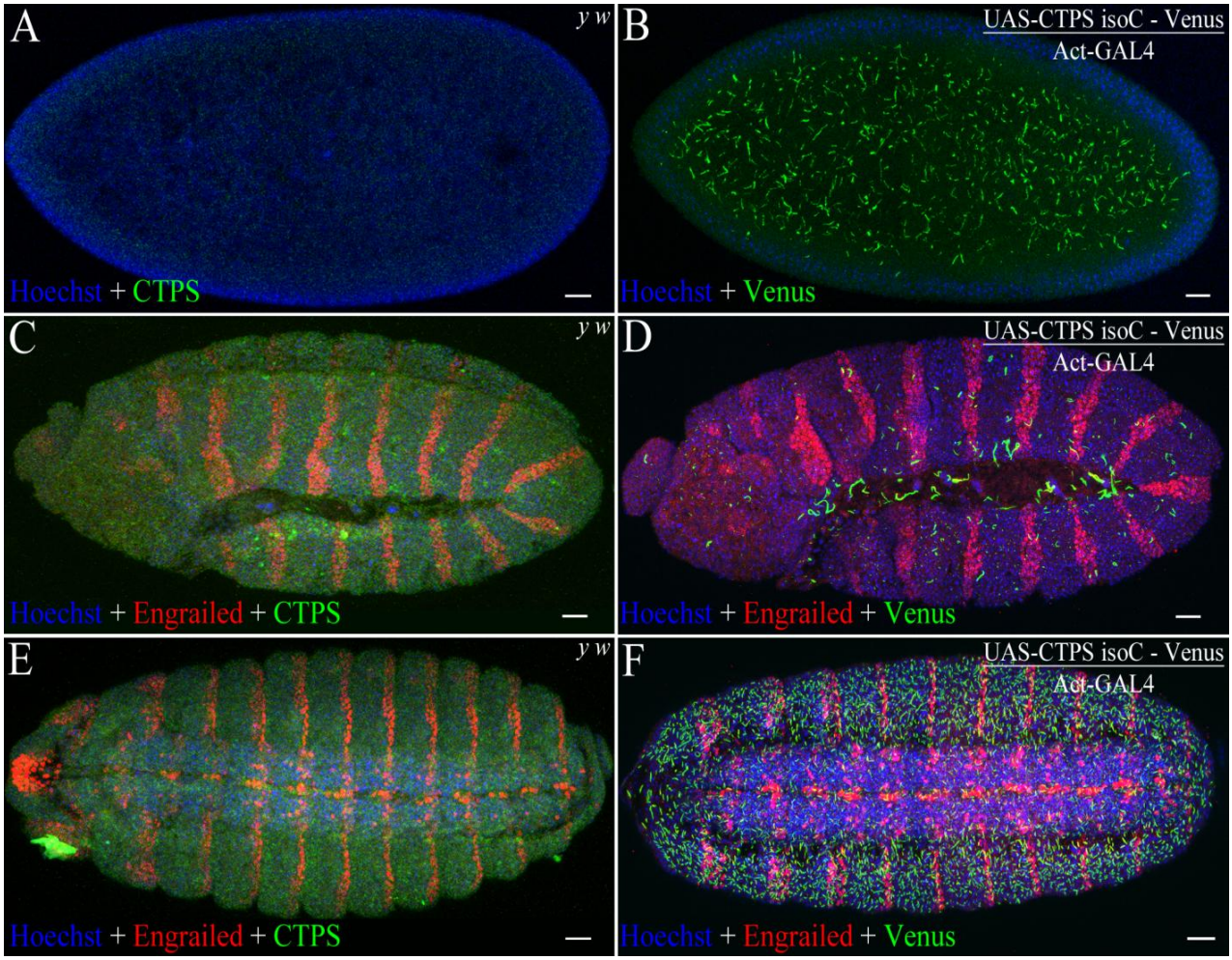


Figure 6.5. CTPS isoform C overexpression in *Drosophila* embryos. (A) Stage 1 *y w* embryos showing no cytoophidia formation. (B) Ectopic cytoophidia was seen in stage 1 embryos overexpressing CTPS isoC. (C) Stage 12 *y w* embryos showing disperse staining of CTPS with no cytoophidia formation. (D) Ectopic cytoophidia was seen in stage 12 embryos overexpressing CTPS isoC. (E) Stage 15 *y w* embryos showing disperse staining of CTPS with no cytoophidia formation. (F) Ectopic cytoophidia was seen in stage 15 embryos overexpressing CTPS isoC.

6.2.2.4. Adult brain and larval CNS

The *Drosophila* adult brain is another tissue which mostly does not have obvious macro-cytoophidia (Figure 6.6A). The expression of CTPS is dispersed in the cytoplasm with specific regions more enriched compared to other regions based on antibody staining and CTPS::GFP protein trap line. The region beside the optic lobe seems to have more CTPS (Figure 6.6A - Arrow). However, since most cells in the brain are mature neurons and with limited markers available, it is difficult to specify what those cells are.

The larval CNS also does not have macro-cytoophidia in most part except for the proliferating region in the optic lobe as described previously (Chen et al., 2011). Larval CNS has distinct cells which are well characterized. Multiple markers are also available to study the larval CNS which makes it a better system to study the distribution of cytoophidia than the adult brain. The expression of CTPS in the larval CNS shows that it is dispersed in the cytoplasm but that the neuroblasts have higher expression than other cells.

Analysing larvae overexpressing CTPS isoform C with an Act-GAL4 driver shows that cytoophidia were successfully induced in cells which do not have endogenous cytoophidia formation (Figure 6.6C-D’’’). Furthermore, the cytoophidia seems to be induced mostly in the neuroblast as marked by staining against Miranda, a marker for neuroblasts and not in other cells (Figure 6.6C-C’’’). Further analysis using the inducible GAL4 system confirms this observation where the GFP +ve neuroblasts which are overexpressing CTPS isoform C has cytoophidia, while the wild-type GFP –ve neuroblasts only have dispersed staining of CTPS (Figure 6.5D-D’’’). The progeny cells from the neuroblast do not seem to form cytoophidia even when CTPS isoform C was ectopically expressed. This could be due to the actin driver that does not drive as well in the progenies compared to the neuroblasts or the sensitivity of the confocal is not high enough to detect small cytoophidia.

The enriched disperse CTPS staining seen in the neuroblast has never been verified to be specifically CTPS. To verify that this dispersed staining in the neuroblast cytoplasm is specific to CTPS and not background staining, UAS-CTPS-RNAi transgene was induced using the inducible GAL4 system. The GFP +ve cells which are expressing the CTPS-RNAi knockdown CTPS and shows less enrichment in the neuroblast compared to GFP –ve wild-type neuroblasts (Figure 6.6E-E’’’). This experiment confirms that the neuroblasts have dispersed staining of CTPS.

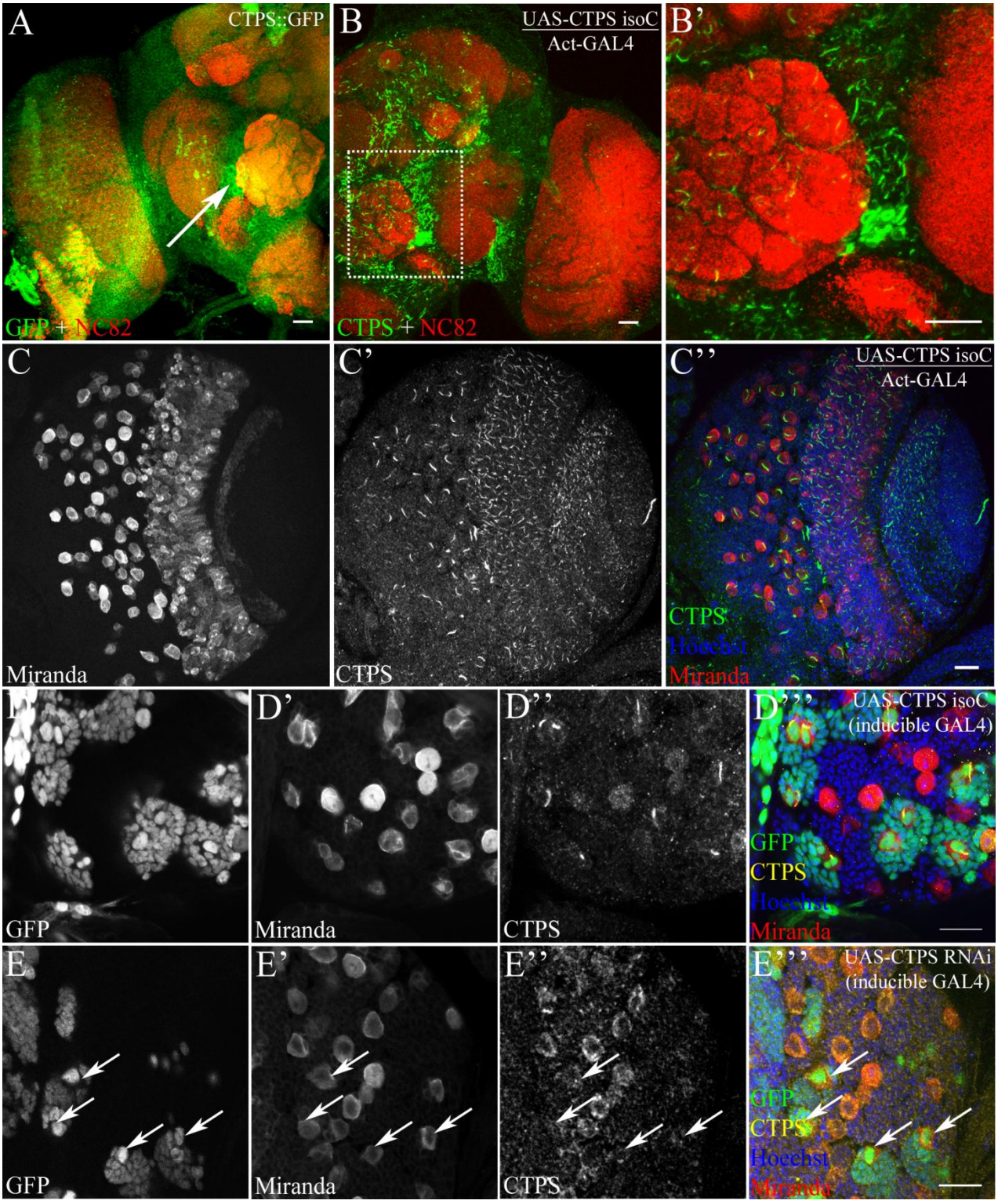

A
CTPS::GFP
GFP + NC82
B
UAS-CTPS isoC
Act-GAL4
CTPS + NC82
B'
C
Miranda
C'
CTPS
C''
UAS-CTPS isoC
Act-GAL4
CTPS
Hoechst
Miranda
D
GFP
D'
Miranda
D''
CTPS
D'''
UAS-CTPS isoC
(inducible GAL4)
GFP
CTPS
Hoechst
Miranda
E
GFP
E'
Miranda
E''
CTPS
E'''
UAS-CTPS RNAi
(inducible GAL4)
GFP
CTPS
Hoechst
Miranda

Figure 6.6. CTPS in the adult brain and larval CNS. (A) CTPS::GFP protein trap line adult brain showing a disperse expression of CTPS in the cytoplasm and no cytoophidia formation. Arrow showing cells beside the optic lobe which have higher CTPS expression. (B) Overexpression of CTPS isoC in the adult brain induces cytoophidia formation throughout the brain. (B') Zoomed in image of the cells that has higher CTPS expression. (C-C'') Overexpressing CTPS isoC in the larval brain induce cytoophidia formation in the neuroblast which is labelled by Miranda staining. (D-D''') Inducible GAL4 system showing only neuroblasts overexpressing CTPS isoC forms cytoophidia (GFP +ve) while wild-type neuroblasts have disperse CTPS staining (GFP –ve). (E-E''') Knocking down CTPS using CTPS RNAi reduces the disperse staining of CTPS in the neuroblast (arrow).

6.2.3. Identifying regions in CTPS that are important for cytoophidia formation

Since only CTPS isoform C forms cytoophidia and is able to induce cytoophidia formation, the focus then went into trying to understand why only CTPS isoform C localizes to cytoophidia and not the others. Using the free basic local alignment search tool for protein (BLASTp) from the National Centre for Biotechnology Information's (NCBI) website, the protein sequences of all three different isoforms were aligned to search for similarities. The alignment between CTPS isoform C and CTPS isoform A did not show many similarities between them and only about 4% of the sequences are able to align. This is also the same between CTPS isoform B and CTPS isoform A which only has 13% similarities. However, the similarity between CTPS isoform C and CTPS isoform B is 91% where only the first 56 amino acids of the CTPS isoform C and the first 53 amino acids from CTPS isoform B were different and the rest is completely identical (Figure 6.7). These differences in the N-terminal makes the CTPS isoform C forms cytoophidia while CTPS isoform B does not. Furthermore, this also shows that the 56 amino acids at the N-terminal of CTPS isoform C are important for cytoophidia formation. This correlates with the previous results where tagging Venus on the N-terminal of CTPS isoform C disrupts the cytoophidia (Figure 6.2E-E'').

Isoform C length=627, Isoform B length=623

Differences between Isoform C and Isoform B

```
Isoform C  1   MKYILVTGGV ISGVGKGVIA SSFGTLLKSC GLDVTSIKID PYINIDAGTF SPYEHG   56
Isoform B  1   MAPKKSTIVL NVEQFIHDIE ERPAIWNRNF HCNKAFLEQM WDELSGAHKL PS       52
```

Similarities between Isoform C and Isoform B

```
Score = 1183 bits (3060), Expect = 0.0, Method: Compositional matrix adjust.
Identities = 571/571 (100%), Positives = 571/571 (100%), Gaps = 0/571 (0%)

Isoform C  57   EVYVLDDGAEVDLDLGNYERFLDVTLHRDNNITTGKIYKLVIEKERTGEYLGKTVQVVPH  116
                EVYVLDDGAEVDLDLGNYERFLDVTLHRDNNITTGKIYKLVIEKERTGEYLGKTVQVVPH
Isoform B  53   EVYVLDDGAEVDLDLGNYERFLDVTLHRDNNITTGKIYKLVIEKERTGEYLGKTVQVVPH  112

Isoform C  117  ITDAIQEWVERVAQTPVQGSSKPQVCIVELGGTIGDIEGMPFVEAFRQFQFRVKRENFCL  176
                ITDAIQEWVERVAQTPVQGSSKPQVCIVELGGTIGDIEGMPFVEAFRQFQFRVKRENFCL
Isoform B  113  ITDAIQEWVERVAQTPVQGSSKPQVCIVELGGTIGDIEGMPFVEAFRQFQFRVKRENFCL  172

Isoform C  177  AHVSLVPLPKATGEPKTKPTQSSVRELRGCGLSPDLIVCRSEKPIGLEVKEKISNFCHVG  236
                AHVSLVPLPKATGEPKTKPTQSSVRELRGCGLSPDLIVCRSEKPIGLEVKEKISNFCHVG
Isoform B  173  AHVSLVPLPKATGEPKTKPTQSSVRELRGCGLSPDLIVCRSEKPIGLEVKEKISNFCHVG  232

Isoform C  237  PDQVICIHDLNSIYHVPLLMEQNGVIEYLNERLQLNIDMSKRTKCLQQWRDLARRTETVR  296
                PDQVICIHDLNSIYHVPLLMEQNGVIEYLNERLQLNIDMSKRTKCLQQWRDLARRTETVR
Isoform B  233  PDQVICIHDLNSIYHVPLLMEQNGVIEYLNERLQLNIDMSKRTKCLQQWRDLARRTETVR  292

Isoform C  297  REVCIAVVGKYTKFTDSYASVVKALQHAALAVNRKLELVFIESCLLEEETLHSEPSKYHK  356
                REVCIAVVGKYTKFTDSYASVVKALQHAALAVNRKLELVFIESCLLEEETLHSEPSKYHK
Isoform B  293  REVCIAVVGKYTKFTDSYASVVKALQHAALAVNRKLELVFIESCLLEEETLHSEPSKYHK  352

Isoform C  357  EWQKLCDSHGILVPGGFGSRGMEGKIRACQWARENQKPLLGICLGLQAAVIEFARNKLGL  416
                EWQKLCDSHGILVPGGFGSRGMEGKIRACQWARENQKPLLGICLGLQAAVIEFARNKLGL
Isoform B  353  EWQKLCDSHGILVPGGFGSRGMEGKIRACQWARENQKPLLGICLGLQAAVIEFARNKLGL  412

Isoform C  417  KDANTTEIDPNTANALVIDMPEHHTGQLGGTMRLGKRITVFSDGPSVIRQLYGNPKSVQE  476
                KDANTTEIDPNTANALVIDMPEHHTGQLGGTMRLGKRITVFSDGPSVIRQLYGNPKSVQE
Isoform B  413  KDANTTEIDPNTANALVIDMPEHHTGQLGGTMRLGKRITVFSDGPSVIRQLYGNPKSVQE  472

Isoform C  477  RHRHRYEVNPKYVHLLEEQGMRFVGTDVDKTRMEIIELSGHPYFVATQYHPEYLSRPLKP  536
                RHRHRYEVNPKYVHLLEEQGMRFVGTDVDKTRMEIIELSGHPYFVATQYHPEYLSRPLKP
Isoform B  473  RHRHRYEVNPKYVHLLEEQGMRFVGTDVDKTRMEIIELSGHPYFVATQYHPEYLSRPLKP  532

Isoform C  537  SPPFLGLILASVDRLNQYIQRGCRLSPRQLSDASSDEEDSVVGLAGATKSLSSLKIPITP  596
                SPPFLGLILASVDRLNQYIQRGCRLSPRQLSDASSDEEDSVVGLAGATKSLSSLKIPITP
Isoform B  533  SPPFLGLILASVDRLNQYIQRGCRLSPRQLSDASSDEEDSVVGLAGATKSLSSLKIPITP  592

Isoform C  597  TNGISKSCNGSISTSDSEGACGGVDPTNGHK  627
                TNGISKSCNGSISTSDSEGACGGVDPTNGHK
Isoform B  593  TNGISKSCNGSISTSDSEGACGGVDPTNGHK  623
```

Figure 6.7. BLASTp alignment of CTPS isoform C and CTPS isoform B showing the differences and similarities between the two isoforms.

Knowing that the N-terminal 56 amino acids in CTPS isoform C are important for cytoophidia, constructs were designed to verify that this is the case. Four Venus-tagged constructs were generated based on CTPS isoform C regions (Figure 6.7). The first construct is just the 56 amino acids from the N-terminal of CTPS isoform C (termed N-term). This construct is to see whether the 56 amino acids are able to form cytoophidia. The second construct is the truncated-CTPS isoform C (termed Trunc-IsoC) where 56 amino acids from the N-terminal of CTPS isoform C were removed. This is to verify and further confirm that the first 56 amino acids are required for cytoophidia localization. In theory, by removing these regions, the protein should be dispersed similar to CTPS isoform B. The third construct is the CTG domain (termed CTG). Even though 224 out of the 260 amino acids from this construct are present in the CTPS isoform B, it will be interesting to see if expressing this domain by itself is enough for the resulting protein to localize to cytoophidia. This is also to test if cytoophidia requires multiple binding sites. Finally, the fourth construct comprise of the GATase1 domain (termed GATase1) which is present in both CTPS isoform C and CTPS isoform B. This is going to be used as a control and also for future work when trying to rescue the mutants using specific domains. All of these constructs were made using the same Venus tagged vectors used previously.

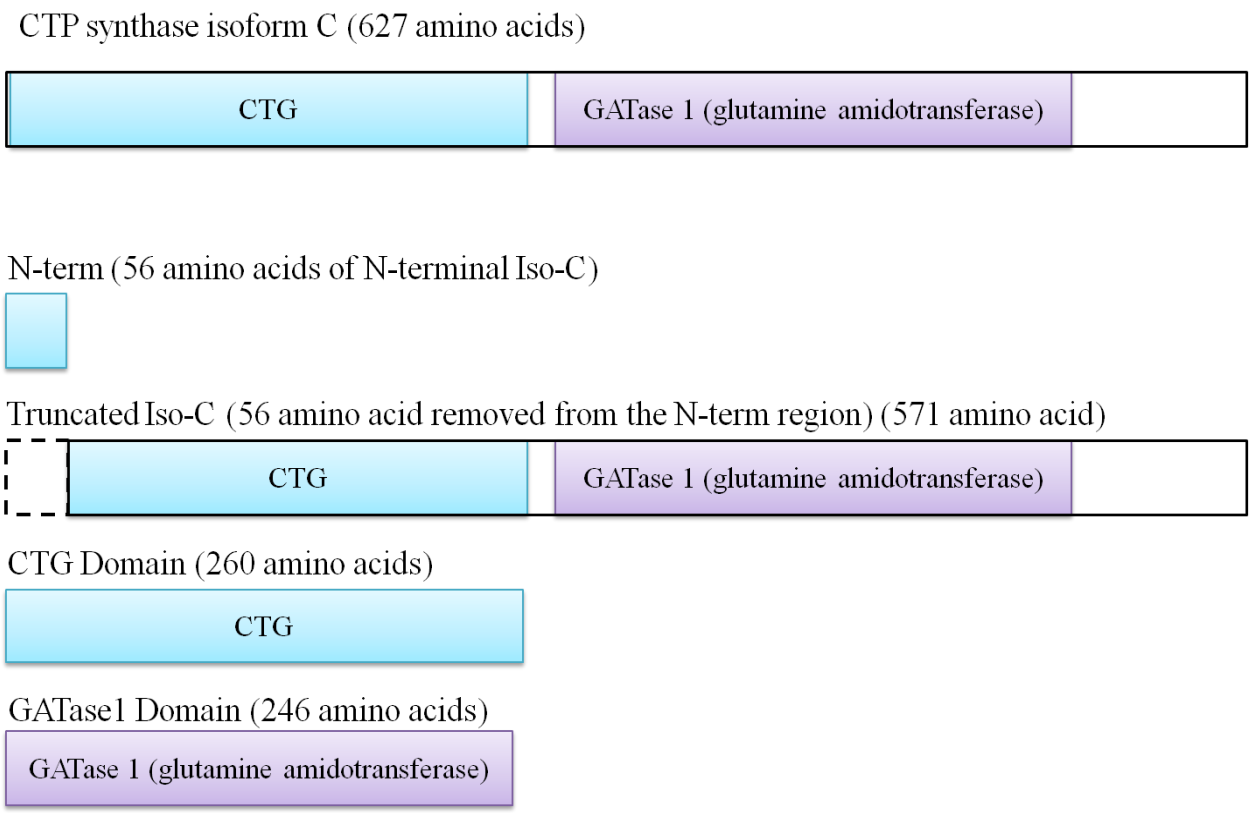


Figure 6.8. The domains of CTPS isoform C in which the transgenes were generated. Four transgenes, N-term, Truncated Iso-C, CTG domain and GATase1 domain were generated based on CTPS isoform C.

6.2.4. Analysing the transgenes in the egg chambers

To analyse the specific region transgene, the egg chambers were used. This is because it will be easier to pick up any changes in the cytoophidia as the egg chambers have the biggest cytoophidia. All of the transgenic flies were crossed to a maternal triple driver (MTD) line which consists of three GAL4 drivers; COG-GAL4:VP16, nos-GAL4.NGT and nos-GAL4:VP16 (Brennecke et al., 2007). COG-GAL4:VP16 was made in pCOG vector that contains a promoter from the out gene and the K10 3'UTR which drives expression from stage 1 egg chambers (Ni et al., 2008). Nos-GAL4:VP16 (Ni et al., 2008) has the 3' UTR from the nanos gene to get high expression for later stage (stage 6 and above) egg chambers and nos-GAL4.NGT contains 3'UTR from αTub84E which will deposit expression maternally (Ni et al., 2011). The MTD-GAL4 provides strong and robust expression throughout the germline and maternally deposit GAL4 to drive expression during embryogenesis.

First, the N-term construct which comprise of the first 56 amino acids from the N-terminus of CTPS isoform C were analysed. Interestingly, the construct expression did not localize to cytoophidia but it showed disperse expression. However, only the N-terminal tagged construct was available because the C-terminal tagged construct had a frame shift and could not be used. It was expected that this construct would still form cytoophidia or bind to endogenous cytoophidia but that was not the case. However, it is possible that since the Venus tag is 238 amino acids long, which is about four times bigger than the 56 amino acids region cloned, the tag could have interfered with the binding. A smaller Hemagglutinin (HA) tag which only consists of 9 amino acids might be a better choice.

Next, the UAS-Trun-IsoC-Venus transgene was analysed. By removing the 56 amino acids from CTPS isoform C, it was hypothesized that cytoophidia would not be able to form. Even though cytoophidia failed to form in the Trun-IsoC overexpression line, punctuate

structures were observed (Figure 6.9B-C''). The expression of Trun-IsoC is dispersed at earlier stage egg chambers but the punctuate structures are seen clearly at stage 8 egg chambers (Figure 6.8B) and are brighter at later stage egg chambers (Figure 6.8C). Staining against CTPS antibody showed that the endogenous cytoophidia is not affected by the punctuate structures (Figure 6.8B' and 6.8C'). In addition, the CTPS antibody staining also did not pick up the punctuate structure even though 64 out of the 88 peptides are still present in the Trun-IsoC transgene. However, the punctate structure was not visible in the C-terminal tagged construct (UAS-Venus-Trun IsoC) (Figure 6.9D-D''). The UAS-Venus-Trun IsoC construct showed dispersed cytoplasmic expression and also does not disrupt the endogenous cytoophidia formation.

The CTG domain is an important domain of CTPS because this region contains the active sites plus the 56 amino acids that are required to form cytoophidia. Overexpressing the UAS-CTG-Venus transgene in the egg chambers did not show cytoophidia formation, the transgene expression is dispersed in the cytoplasm (Figure 6.9E). Furthermore, staining against CTPS antibody did not pick up any cytoophidia formation in the germline but cytoophidia can still be seen in the follicle cells (Figure 6.9E'). This suggests that the endogenous cytoophidia disassociates when ectopic CTG domain is present. How and why this is happening remains elusive.

Finally, the GATase1 domain which is present in both CTPS isoform C and CTPS isoform B was overexpressed in the egg chambers. The expression of UAS-GATase1-Venus is identical to CTPS isoform B which is disperse in the cytoplasm (Figure 6.9F-F''). Also, the endogenous cytoophidia was also not affected as detected by CTPS antibody staining.

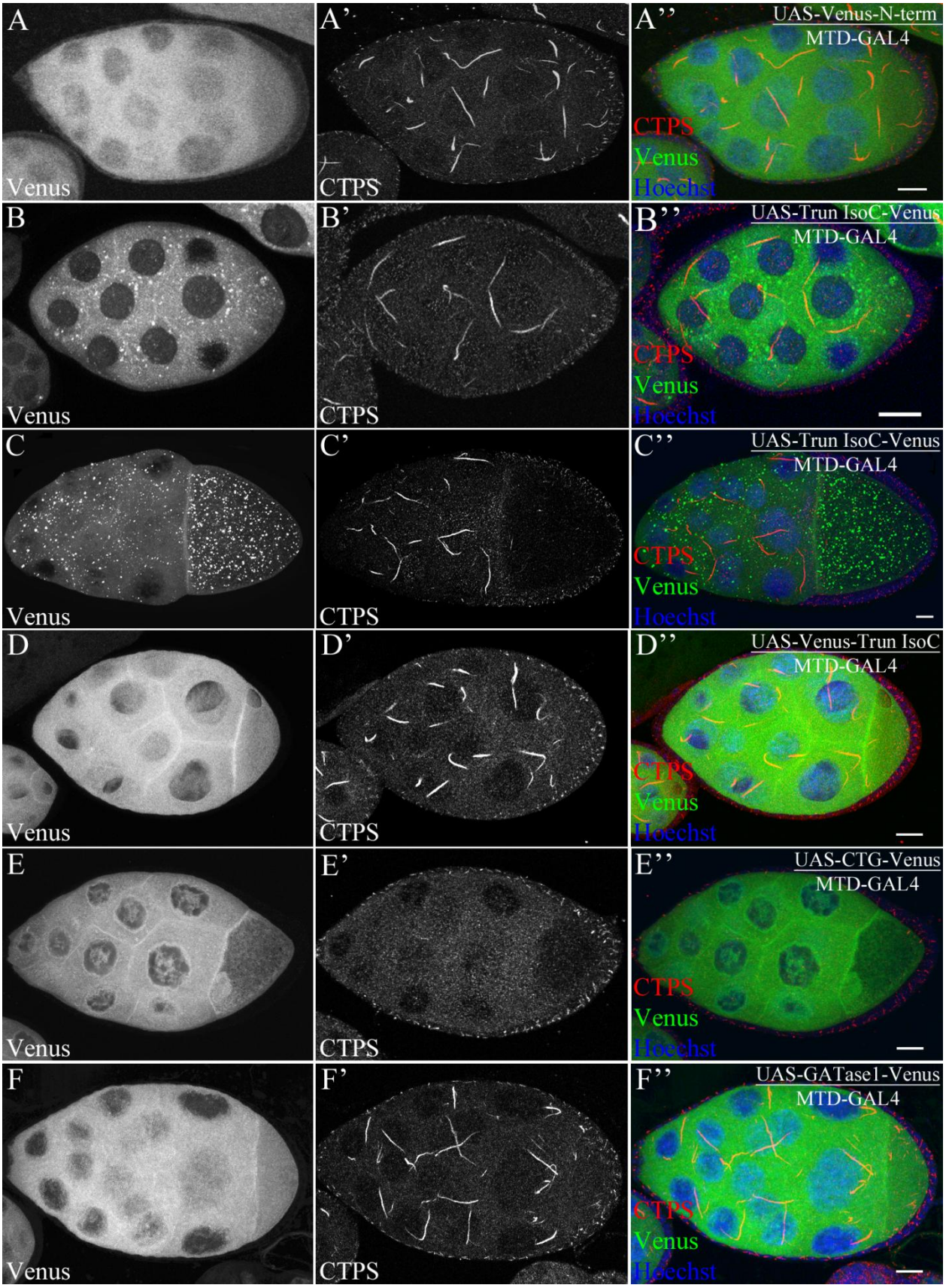

A
Venus
A'
CTPS
A''
UAS-Venus-N-term
MTD-GAL4
CTPS
Venus
Hoechst
B
Venus
B'
CTPS
B''
UAS-Trun IsoC-Venus
MTD-GAL4
CTPS
Venus
Hoechst
C
Venus
C'
CTPS
C''
UAS-Trun IsoC-Venus
MTD-GAL4
CTPS
Venus
Hoechst
D
Venus
D'
CTPS
D''
UAS-Venus-Trun IsoC
MTD-GAL4
CTPS
Venus
Hoechst
E
Venus
E'
CTPS
E''
UAS-CTG-Venus
MTD-GAL4
CTPS
Venus
Hoechst
F
Venus
F'
CTPS
F''
UAS-GATase1-Venus
MTD-GAL4
CTPS
Venus
Hoechst

Figure 6.9. Expression of the different transgenes in the egg chambers using MTD-GAL4. (A-A'') UAS-Venus-N-term which consists of the 56 amino acids showed dispersed cytoplasmic expression. (B-C'') UAS-Tunc isoC-Venus showed cytoplasmic expression and forms punctate structures. The punctate structures are more visible in later stage egg chambers (C). (D-D'') UAS-Venus-Trunc isoC does not show the punctate structure, only dispersed cytoplasmic expression. (E-E'') UAS-CTG-Venus showed disperse expressions and also disrupts endogenous cytoophidia formation. (F-F'') UAS-GATase1-Venus showed cytoplasmic expression.

Also, closer examination of all the transgene expressions reveal that the N-term and CTG transgenes have nuclear localization while Trunc IsoC and GATase1 transgenes does not (Figure 6.10A-E''). The N-term transgene did not show strong expression throughout oogenesis but the localization in the nucleus can be seen (Figure 6.10A-A''). The nuclear localization of the N-term is much lower than the expression in the cytoplasm. The CTG domain transgene showed very clear nuclear localization. However, it is not totally dispersed in the nucleus (Figure 6.10C). In addition, the expression in the nucleus is higher than the cytoplasm. Furthermore, the CTG domain transgene can also be seen in the germinal vesicle (GV) of the oocyte (Figure 6.10D-D''). These results show that there is a possibility that the 56 amino acids at the N-terminus of the CTPS isoform C have nuclear localization sequences as the other transgene that does not have the 56 amino acids did not have nuclear localization. However, the nuclear localization was not seen in CTPS isoform C overexpression.

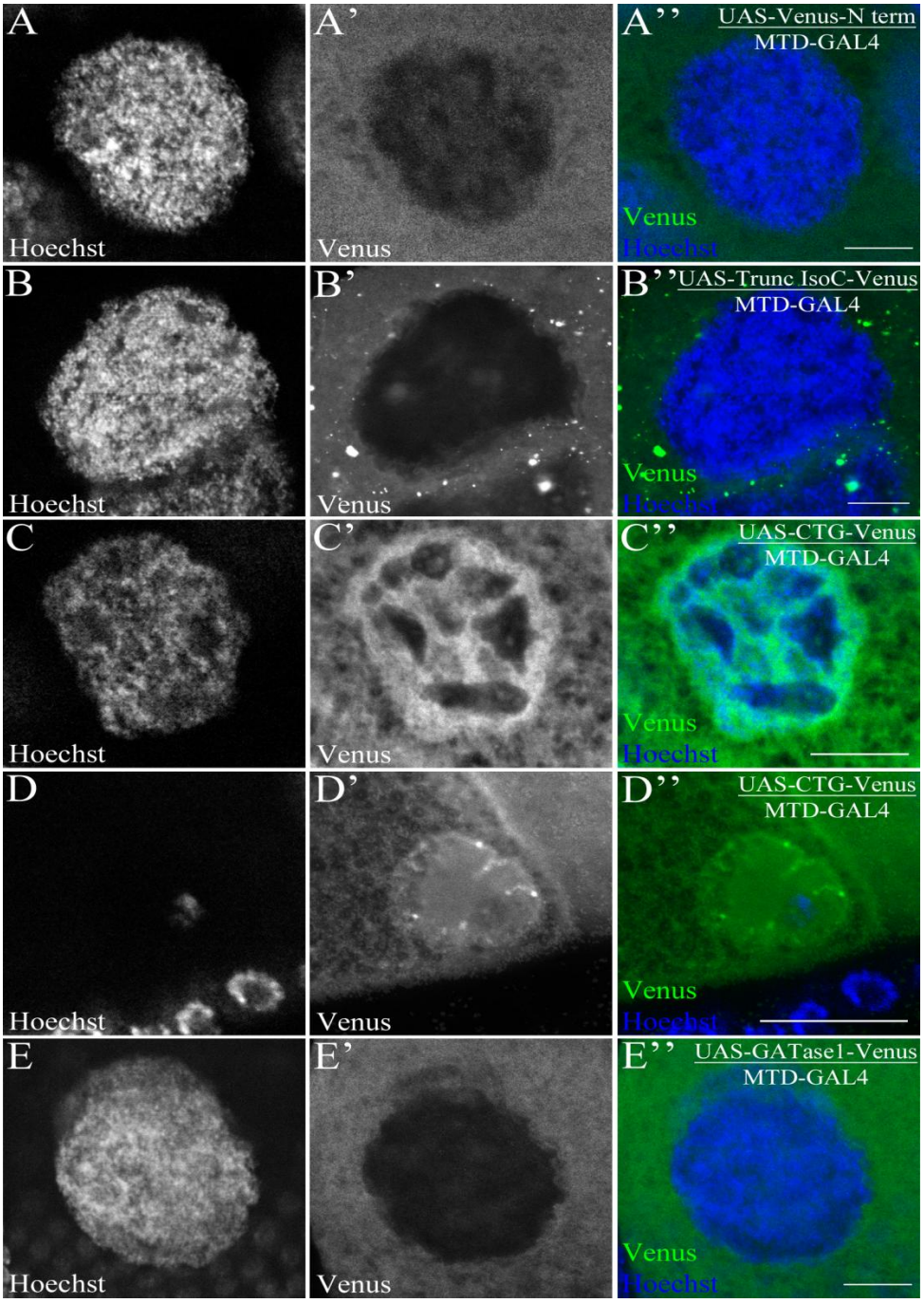


Figure 6.10. N-term and CTG transgenes have nuclear localization expression. (A-A'') UAS-Venus-N term has nuclear localization. (B-B'') UAS-Trunc IsoC-Venus does not have nuclear expression. (C-D'') UAS-CTG-Venus has bright nuclear expression (C') and it is also localized in the GV (D'). (E-E'') UAS-GATase1-Venus does not have nuclear expression.

6.3. Discussion

6.3.1. CTPS isoform C: the cytoophidia forming isoform

In this chapter, the expression of the three different CTPS isoforms were analysed and it was found that CTPS isoform A is expressed in punctate structure in the nucleus, CTPS isoform B is expressed dispersedly in the cytoplasm and only CTPS isoform C is localized in the cytoophidia. CTPS isoform A is very different from CTPS isoform B and CTPS isoform C as it shares very little sequences and region. Even CTPS genes from other species do not have similarities with the *Drosophila* CTPS isoform A. It also does not have the sites and region required for CTP synthesis. However, it contains an alcohol dehydrogenase transcription factor while the BESS region contains DNA binding domain which could explain its localization in the nucleus. Furthermore, the BESS region is a *Drosophila* specific region, which also explains why there are no similarities with other species' CTPS genes. There is also the possibility that CTPS isoform A is a totally different gene encoded in the same region as *Drosophila* CTPS.

It was surprising to see that only CTPS isoform C localizes to cytoophidia and CTPS isoform B, which has 91% similarity with CTPS isoform C, does not. It points to the fact that the 56 amino acids at the N-terminus region of CTPS isoform C are necessary for cytoophidia localization and the 53 amino acids in the N-terminus of isoform B, which has part of the MADF region, does not promote cytoophidia localization. However, the 56 amino acids tagged with Venus on its N-terminus did not show cytoophidia localization but that could be due to the large tag which makes it inconclusive. It is possible that the N-term transgene was not sufficient for cytoophidium localization, suggesting that distribution to the cytoophidium required additional domain(s) in the CTPS isoform C.

The CTPS isoform C transgene which localizes to cytoophidia can also promote cytoophidia formation in different tissues including those without obvious macro-cytoophidia formation. This raises the question as to whether the cytoophidia contains active (tetramer), inactive (dimer) or both forms of CTPS. The link between the active and inactive form of CTPS and cytoophidia is unclear at the moment as different results point to different directions. In the egg chamber which continuously producing RNA and proteins, large macro-cytoophidia and many micro-cytoophidia were seen which points to the idea that cytoophidia might contain active CTPS. However, cytoophidia disassociates as it becomes an embryo and endogenous cytoophidium is not present throughout embryogenesis. Embryogenesis requires a lot of cell division and a lot of transcription which occurs throughout embryogenesis. The endogenous cytoophidia comes back slowly during larval development as cytoophidia is detected in the lymph gland, salivary gland and certain parts of the CNS. High levels of dispersed CTPS were detected in the neuroblast. The neuroblast undergoes mitosis to form daughter cells which will differentiate into neurons and it is also actively transcribes the required genes for differentiation. There is also the possibility that a minimum threshold of CTPS is required for the formation of cytoophidia. The neuroblasts do have CTPS, however it might not be enough for macro-cytoophidia formation to occur.

6.3.2. Regions that are important for cytoophidia formation

It is still unclear why CTPS forms macro-cytoophidia in some tissues and not in others. The expression of the CTG domain might shed a bit of light on this. Overexpressing the CTG domain caused endogenous cytoophidia to disperse in the egg chambers. This is the first indication that there is more than one site/region required for cytoophidia formation. It is known from the experiments in this chapter that the 56 amino acids from the N-terminal of CTPS isoform C is one region required for cytoophidia formation but there must be at least

one more region that is required for cytoophidia formation. This is because when overexpressing the CTG domain, which only has one of the region required (the first 56 amino acids), it caused endogenous cytoophidia to disassociate. This is different from CTPS isoform C overexpression where longer cytoophidia was seen. The disassociation of cytoophidia could be due to the endogenous CTPS binds to the first region that is present in the CTG domain and since there is an abundance of the CTG domain present in the cell, the endogenous CTPS failed to form cytoophidia. It also shows that the 56 amino acids from the N-terminal of CTPS isoform C is the main region for cytoophidia formation but it is insufficient on its own.

Further evidence to supports the idea that cytoophidia formation requires more than one binding site is seen in the Trunc-IsoC transgene. It was thought that by removing the 56 amino acids from CTPS isoform C would disassociate cytoophidia and the transgene would be dispersedly expressed as CTPS isoform B expression. However, this is not the case as punctate structure were observed showing that the Trunc-IsoC transgene still have binding sites but it is not enough to form cytoophidia. Why the Trunc-IsoC transgene forms punctate structure while CTPS isoform B does not is still unknown. This might shed light onto the importance of the 53 amino acids that is present in the N-terminal of CTPS isoform B which are not present in CTPS isoform C or Trunc-IsoC transgene. The 53 amino acids of the C-terminal of CTPS isoform B could be important for the folding of the protein which protects it from forming cytoophidia or the punctate structure.

Although CTPS isoform C does not localize to the nucleus, the expression of the N-term and CTG domain transgenes have nuclear localization. Cytoophidia has never been seen in the nucleus as well in *Drosophila*. However, cytoophidia has been found in the nucleus in mammalian cells (Kemian Gou, personal communication).

One of the central questions raised in this chapter is what region is required for cytoophidia formation. Results from this chapter gave insights in understanding how cytoophidia forms and functions. The transgene study is very powerful but more work is required to further identify precisely which part is required for cytoophidia formation. Although overexpressing cytoophidia in the testis caused a tumour-like phenotype, the mechanisms and the role of cytoophidia in causing it is still unknown. Future work directed at understanding why cytoophidia forms will help identify its function whether it is tissue specific or globally.

Chapter 7
Identification of CTPS mutants

7.1. Introduction

7.1.1. Gene disruption

Other than gain of function study, gene disruption provides valuable information about the gene functions. There are two types of gene disruption. Knockouts are a classical method where the gene is disrupted by transposon insertion, mutagenesis or deletions. Sometimes a knockout will result in total gene disruption which is called 'null mutation' or it can result in a hypomorph where the gene product produces a reduced level of protein. The second type of gene disruption is gene knockdown which uses RNAi.

Transposable element insertion is an extremely powerful tool to disrupt gene function. Several systematic transposable element gene knockout projects have generated thousands of known individual insertions in the genome. The first such project is the P element Gene Disruption Project which is part of the Berkeley *Drosophila* Genome Project (BDGP) that uses the P-element insertion which mutates unique genomic open reading frames (Spradling et al., 1999). This first project isolated 1045 strains disrupting about 1000 different genes (25% of the whole genome). Since it was a success, the project continued to a second phase generating more lines but this time using the piggyBac transposon (Bellen et al., 2004). With the piggyBac transposon, the number of the BDGP gene disruption collection has increased to 7140 strains covering at least 5362 (~40%) annotated genes in 2004. Recently they completed the second phase providing access to at least 9440 genes with more than 14000 strains (Bellen et al., 2011). Several other large collections of insertion lines using the same principle were generated to further increase the potential of gene coverage (Kim et al., 2010; Thibault et al.,

2004). The most importing thing about these projects is that all of these insertions are publicly available.

CTPS mutants have not been generated in *Drosophila* but have been described previously in other organisms. Knocking out CTPS in Chinese hamster V79 cells causes the cells to stop DNA synthesis which is caused by the dramatic reduction of cytidine and consequently leads to arrested growth (Li et al., 1989). In addition, the cells were more sensitive to UV light compared to wild-type cells. CTPS mutants have also been characterized in *C. crecentus* (Ingerson-Mahar et al., 2010) where CTPS forms filaments which localizes to the inner curvature of the cell. Mutating CTPS caused the cells to grow very slowly due to the massive reduction of CTP and also represses the cell curvature.

7.1.2. Experimental description

In this chapter, CTPS gene disruption was pursued by analysing eight insertion lines that are located in the CTPS gene region. The insertion lines were analysed and recombined into a FRT site which will enables clonal studies to be carried out. CTPS mutants that disrupt cytoophidia formation were isolated and used for further analysis. CTPS mutants caused lethality in the larval stage. However, removal of the maternal contribution resulted in failure to complete embryogenesis. In addition, the preliminary search for other factors that regulate cytoophidia was also carried out.

7.2. Results

7.2.1. Isolating CTPS mutants

Isolation of CTPS mutants is crucial to understand the relationship between CTPS and cytoophidium. Analysing the CTPS gene (CG6854), three insertion lines were obtained from Bloomington stock centre and five insertion lines were obtained from the Harvard Exelixis collection (Thibault et al., 2004). The insertion lines are *e01207 (PBac{RB}), BG01116 (P{GT1}), d03622 (P{XP}), EY01546 (P{EPgy2}), DG16110 (P{wHy}), d07411 (P{XP}), d06966 (P{XP})* and *f01941 (PBac{WH})* (Figure 7.1A). All eight lines are homozygous lethal. One of the problems with the gene disruption project is the possibility of secondary mutations. This is also known as the 'hit-and-run' event which is reported to occur in ~30% in P element insertions and ~0.4% in the piggyBac transposon insertion (Salzberg et al., 1997; Thibault et al., 2004). In order to rule out these secondary site insertions, all eight lines were crossed with each other (complementary test). None of the trans-heterozygous flies were viable. Two deficiency lines *Df(3L)BSC837* and *Df(3L)BSC441* which have chromosomal deletions were then crossed to all eight lines. The *Df(3L)BSC837* line covers the whole CTPS gene while the *Df(3L)BSC441* covers the first half of the CTPS gene. Only two (*e01207* and *d06966*) out of the eight insertion lines are lethal in the complimentary test with the deficiency lines. This is very intriguing because all of the eight lines are lethal when crossed to each other but somehow only two lines are lethal when crossed with the deficiency lines. However, this could also mean that some of these lines are hypomorphic lines which somehow survive with the deficiency. Analysing the egg chamber of the six viable lines over deficiency shows that the cytoophidia is still present (data not shown).

Since all the eight lines are homozygous lethal, clonal analysis needs to be generated to study the effect on cytoophidia formation. A FRT site located at the 79D-F region (FRT2A) was recombined to all eight lines and clonal analyses were carried out. As expected, the two lines that were lethal over deficiencies, *d06966* and *e01207* egg chamber clones showed disruption in the formation of cytoophidia (Figure 7.1B and C). Surprisingly, another line, the *d07411* egg chamber clones also showed disruption on the formation of cytoophidia even though it was viable over the deficiencies (Figure 7.1D). The other five lines did not disrupt the formation of cytoophidia (data not shown). Finally, three lines; *CTPS[d06966]*, *CTPS[e01207]* and *CTPS[d07411]* were isolated from the eight insertion lines which disrupts the formation of cytoophidia. These three lines were further characterized.

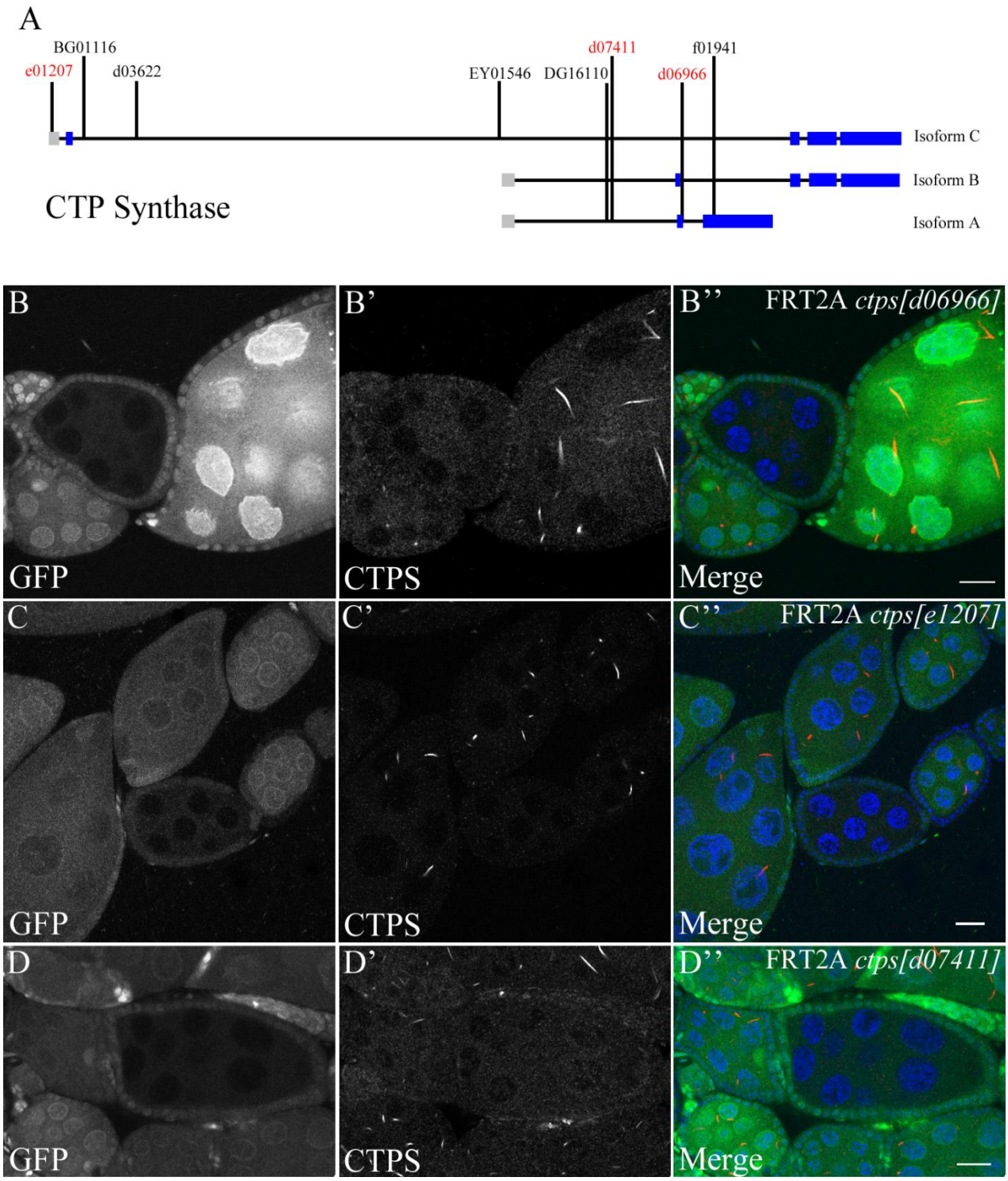


Figure 7.1. CTPS mutant lines. (A) Genetic map of CTPS and the insertion lines available. From the eight insertion lines available, three lines (labelled in red) caused disruption in cytoophidia formation. (B-D'') The three *ctps* mutants; *ctps[d06966]*, *ctps[e01207]* and *ctps[d07411]* clones (GFP –ve) showing no cytoophidia formation while the wild type egg chambers (GFP +ve) showing cytoophidia formation. Scale bars, 20 µm.

7.2.2. *ctps* mutants survives until the larval stage

The isolation of three CTPS mutants that disrupt cytoophidium formation is an important step in understanding the function of CTPS and cytoophidium. The next step is to characterize the mutants. Since the homozygous mutant did not survive until adulthood, finding out how long the mutants survive is crucial. To do this, all of the mutants were balanced with TM6B which carries the dominant recessive mutation Tubby (Tb) that makes the larvae and pupae have short bodies which are easily distinguishable (Craymer, 1980). Eggs from all three CTPS mutants were collected in an apple juice plates analysed every day from 3 days after egg deposition. From early on, all the mutant larvae were significantly smaller compared to wild-type control (Figure 7.2). Both $ctps^{d06966}$ (Figure 7.2A-E) and $ctps^{e01270}$ (Figure 7.2F-J) survive and continue to grow until 7 days after egg deposition. However, $ctps^{d07411}$ only survives until 5 days after egg deposition with very little growth (Figure 7.2K-M). Even at 5 days after egg deposition, the $ctps^{d07411}$ mutant larvae are still very small, making it the most severe mutant out of the three. Furthermore, all three CTPS mutants failed to go into the proper pupation stage. Sometime, they formed a pseudo-pupa. These phenotypes are also similar to *Dakt* mutant which is involved in the PI3K/Akt/TORC1 signalling cascade (Ghildiyal et al., 2010).

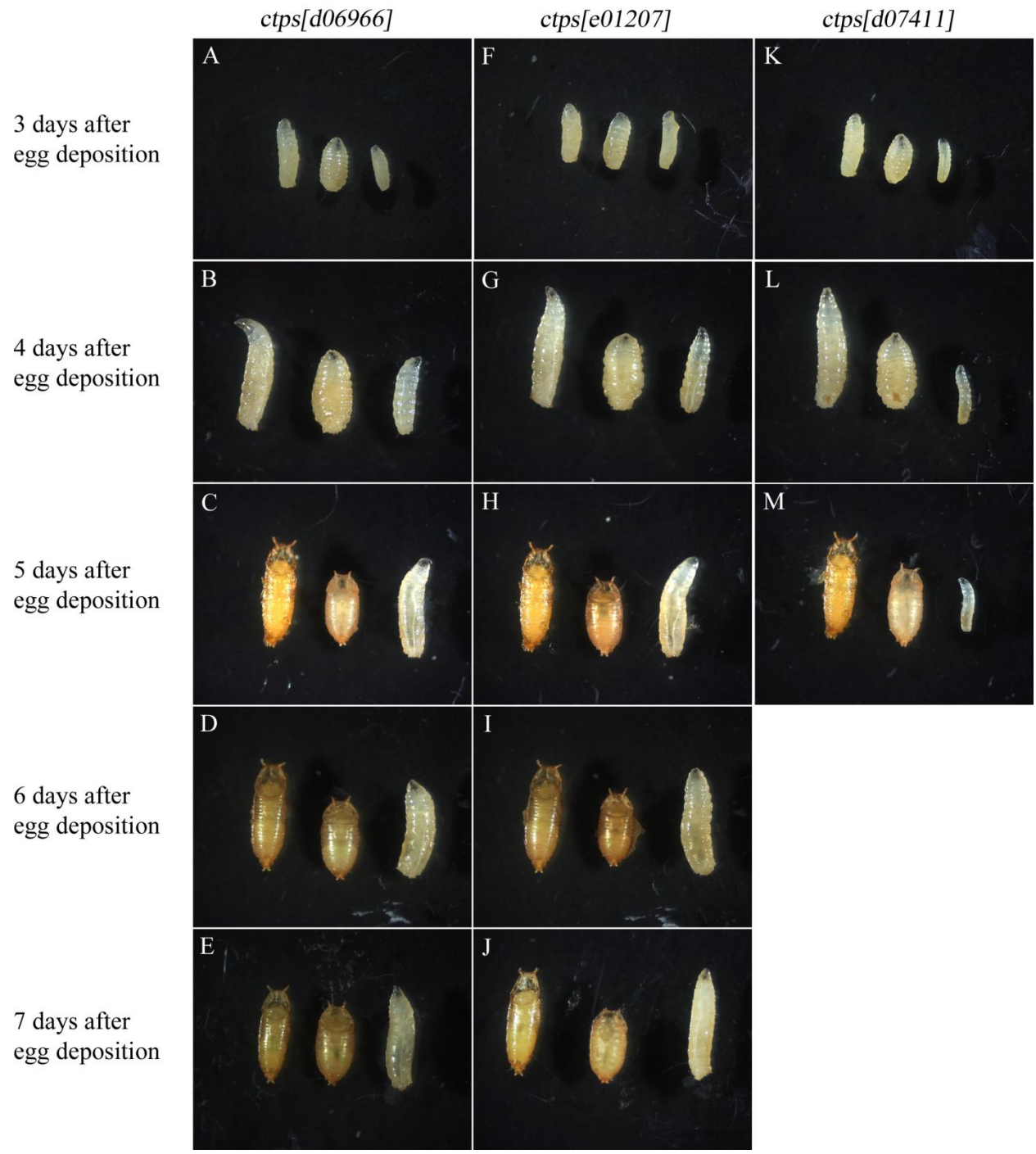


Figure 7.2. CTPS mutants survive until larvae stage. (A-M) From left, *y w*, heterozygous mutant balanced with TM6B Tb and homozygous mutants. (A-J) Homozygous *ctps[d06966]* and *ctps[e01207]* mutant larvae survive until 7 days after egg deposition with slower growth compared to wild-type. (L-M) Homozygous *ctps[e01207]* mutant larvae only survives until 5 days after egg deposition with very little growth.

7.2.3. CTPS is maternally inherited

Seeing that the homozygous mutants survive until the larvae stage, this could mean that CTPS is maternally inherited. This hypothesis is also backed by the fact that a lot of cytoophidia is seen in the egg chambers. To access and confirm this, the maternal contribution has to be removed meaning the egg chambers should be homozygous mutants as well. Mitotic clones are not very practical because the eggs laid are a mixture of homozygous and heterozygous mutants and sorting the egg chambers using GFP is very laborious. To tackle this problem, the germline clone technique using a dominant female sterile mutation *ovoD1* was used (Chapter 1 – 1.3.4.1). With this technique, all of the eggs laid are homozygous mutants as heterozygous mutant egg chambers degenerate after stage 4.

The germline clones were used on all three *ctps* mutants. Without the maternal contribution, none of the embryos from the three mutants hatched to form larvae. This supports the hypothesis that CTPS is maternally inherited and the maternally deposited CTPS protein is enough for the embryos to complete embryogenesis and hatch into larvae. Analysing the germline clone embryos shows that the mutant embryos have severe developmental defects compared to the wild-type (Figure 7.4A-F'). Staining against Engrailed shows that the *ctps* mutant embryos have segmental defects (Figure 7.4B). Engrailed is a homeodomain transcription factor that labels 14 bands (Figure 7.4A) along the embryos anterior-posterior axis (DiNardo and O'Farrell, 1987; Kornberg et al., 1985). Figure 7.4C shows that the formation of the embryos amnioserosa (as) is mislocalized at the posterior end as it should form at the dorsal part of the embryo as in Figure 7.4B. There are also embryos that have very little expression of engrailed (Figure 7.4D). Engrailed also stains the CNS of late stage embryos (Figure 7.4E). The embryos that manage to survive to late stage embryogenesis exhibit severe CNS formation defects (Figure 7.4F). These results show the importance of CTPS in the developing embryos.

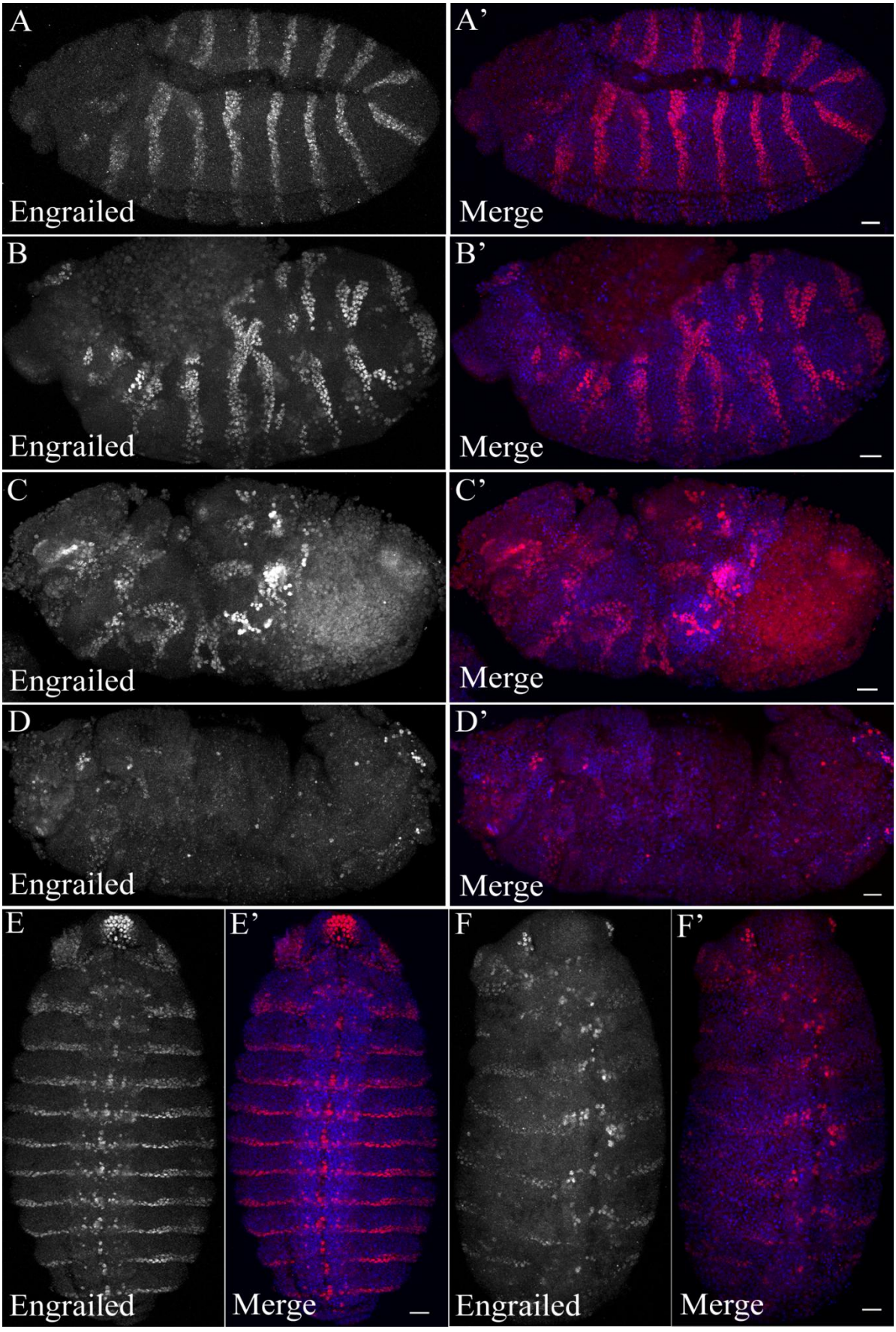

A
Engrailed
A'
Merge
B
Engrailed
B'
Merge
C
Engrailed
C'
Merge
D
Engrailed
D'
Merge
E
Engrailed
E'
Merge
F
Engrailed
F'
Merge

Figure 7.3. CTPS mutant failed to complete embryogenesis without maternal contribution. (A-A') Stage 11 *y w* embryos. (B-D") *ctps[d06966]* germline clone embryos showing severe developmental defects. (E-E') Stage 15 *y w* embryo. (F-F') Late stage *ctps[d06966]* germline clone embryo. In merge; Hoechst is blue and engrailed is red. Scale bars, 20 µm.

7.2.4. CTPS isoform C rescues mutant phenotype

With the isolation of CTPS mutants, it would be then reasonable to see if the mutants are able to be rescued by specific CTPS isoforms. Using the three CTPS isoforms transgenic line generated in previous chapter, the Actin-GAL4 driver was chosen for its stable ubiquitous expression. All three CTPS mutants were crossed so that the final progeny would be expressing specific UAS-CTPS isoform A, B or C (Table 2.2) under the Act-GAL4 driver on the second chromosome and the homozygous CTPS mutation on the third chromosome .

From all the crosses, only CTPS isoform C cDNA construct manages to rescue the lethal phenotype of all three CTPS mutants. However, the rescued adults were sterile. CTPS isoform A and B rescue crosses failed to produce viable adult progenies. This shows that CTPS isoform C is the main isoform of CTPS and its filament forming properties are important.

7.2.5. Characterizing CTP synthase mutant in the egg chamber

To understand the function of cytoophidia during development, the egg chamber germline cells were used as they have very clear and long cytoophidia. The hypothesis is that since there is a lot of cytoophidia in the egg chamber, it must have a function, whether its protein/RNA transport, storage or sensing. First, components of P body; Ago1 and Cup were screened using the *ctps*^{d06966} mutant. There was no clear indication of disruption of the P body components (Figure 7.4A-B''). Oskar and Orb were also stained in the egg chambers (Figure 7.4C-D''). The localization of Ago1, Orb and Cup in the developing oocyte was unchanged (Figure 7.4A-C). The localization of Cup in the P body is also visible meaning P bodies were not affected by cytoophidia (Figure 7.4B-C). The localization of Oskar at stage 9 egg chamber is also still visible (Figure 7.4D). Previously, it was reported that cytoophidia associates with Golgi bodies (Liu, 2010). However, staining the Golgi bodies using antibody against actin-binding protein 2 (ABP2) and Syntaxin 16 does not seem to change in the absence of cytoophidia suggesting that the interaction between Golgi bodies and cytoophidia is downstream of cytoophidium formation and cytoophidia is not required for Golgi distribution (Figure 7.4E-F).

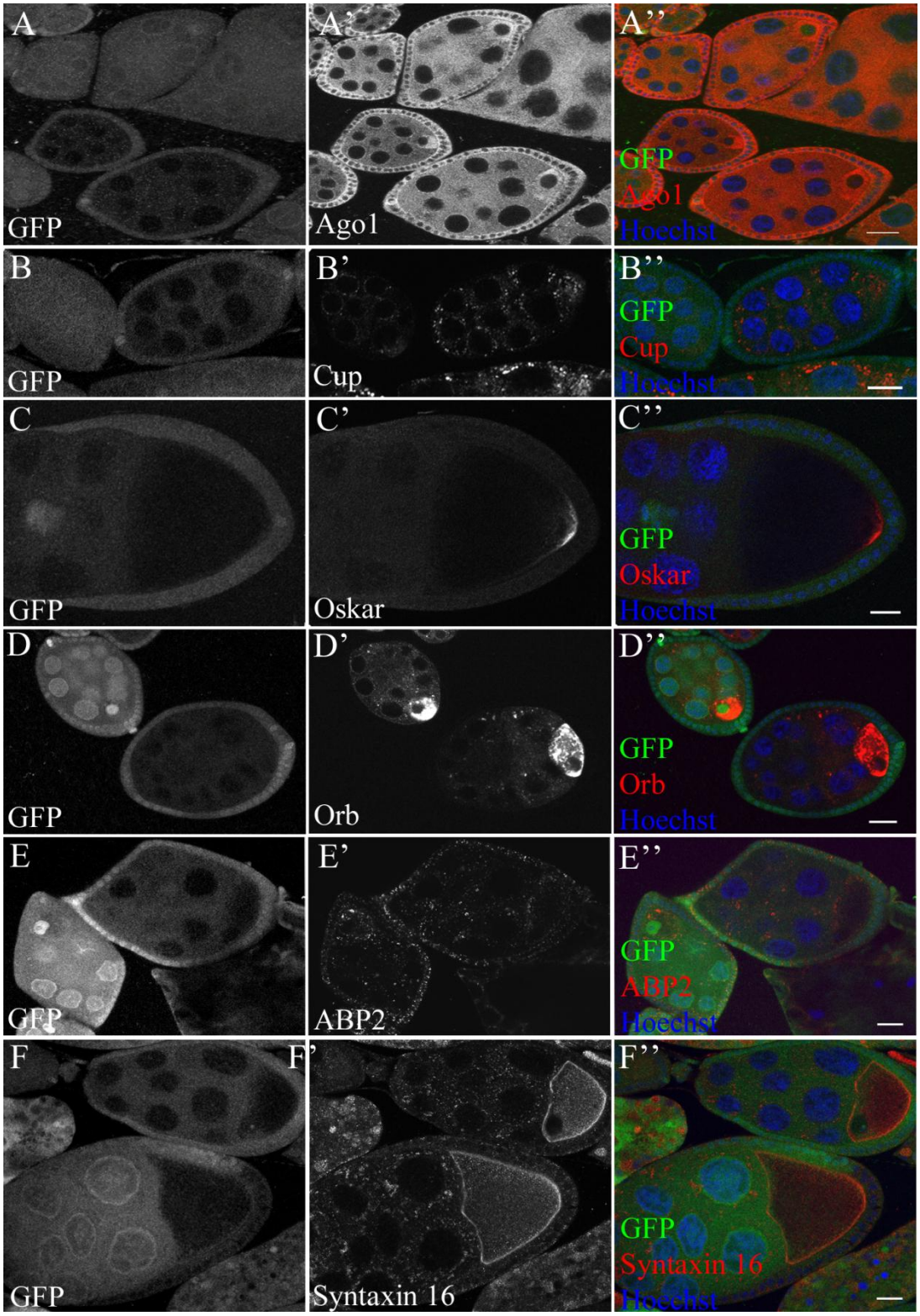


Figure 7.4. *ctps[d06966]* mutant egg chambers. (A-B'') P body components Ago1 and Cup are not affected in the mutant. (C-D'') Oskar and Orb protein localization are also not affected in the mutants. (E-F'') Golgi bodies also did not have any significant change as marked by ABP2 and Syntaxin16. Scale bars, 20 µm.

7.2.6. Reduction of String causes CTPS to be expressed in the nucleus

Based on previous analysis, it looks like macro-cytoophidia predominantly forms in non-dividing cells (e.g. egg chambers) and not in dividing cells (e.g. neuroblasts). Cell division is carefully controlled during development as it must be coupled with growth and proliferation. The cell cycle requires the activity of a cyclin-dependent kinase (CDK) at each G0/G1, G1/S and G2/M transition. The transition of G2/M requires CDC25 family proteins (Pines, 1998) and *Drosophila* has two *cdc25* homologs, *twine* and *string* (Alphey et al., 1992; Edgar and O'Farrell, 1989). String is expressed in the female germline and is known to cause cell division defects when overexpressed (Mata et al., 2000).

To find the relationship between cytoophidia formation and cell division, String was knocked down using RNAi in the follicle cells. Knocking down String caused the follicle cells and its nucleus to become significantly bigger (Figure 7.5A-B''). Furthermore, the CTPS staining not only stains cytoophidia but also the nucleus. Since the follicle cells undergo mitotic cell cycle from stage 1 to stage 6 egg chambers, the disruption in String could disrupt this process, resulting in bigger follicle cells. Overexpressing String caused the 8 cells phenotype and overexpressing its regulator, Tribbles caused the 32 cells phenotype in the egg chamber (Mata et al., 2000). However, the overexpression of String and Tribbles did not change the localization of CTPS (Figure 7.5C-D'').

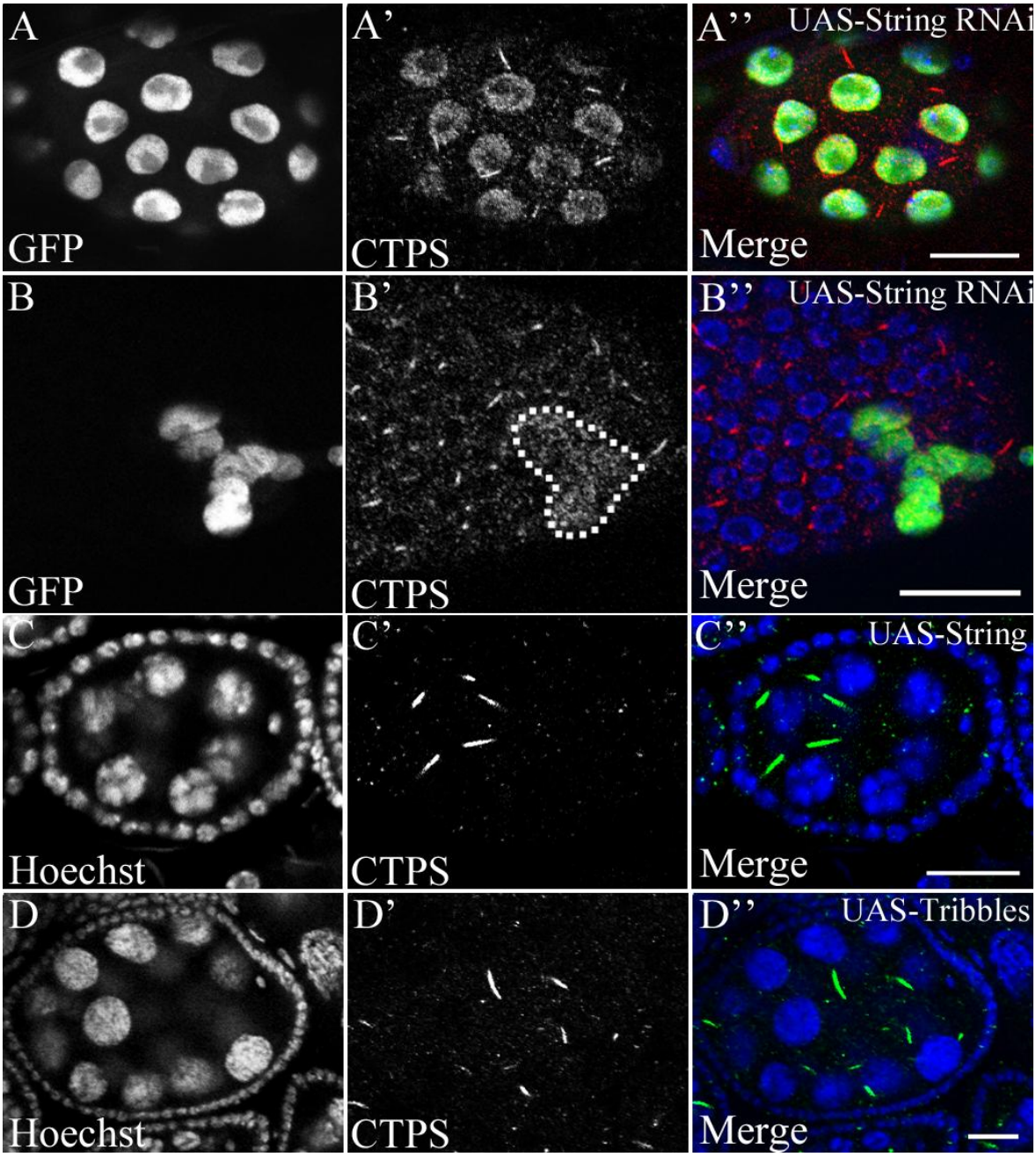


Figure 7.5. String affects CTPS localization. (A-B'') UAS-String-RNAi was induced using the inducible GAL4 system. (A) Clones were generated throughout the stage 5 egg chamber. (B) Small patch of cell clones at stage 8 egg chamber. Expression of CTPS was seen in the String knockdown cells. (C-D'') Overexpressing String and its regulator Tribbles did not affect the CTPS localization. Scale bars, 20 μm.

7.2.7. Cytoophidia and miRNAs

Since miRNAs have been thought to regulate about 60% of the genome, there is a chance that the components of cytoophidia (e.g. CTPS) might also be regulated by miRNAs. miRNA target prediction software like TargetScanFly 6.0 predicted that CTPS has four potential miRNA seed sites; miR-975, miR-997, miR-8, miR-932 and miR-987 while another target prediction algorithm PicTar predicts that CTPS has a miR-14 seed site. Although these target predictions are not accurate, they give a starting point.

Another way to test if cytoophidia is regulated by miRNAs is to analyse it in miRNA biogenesis protein overexpression and mutants. This will give experimental hints on whether cytoophidia is regulated by miRNAs. To test this, UAS-Ago1, UAS-Dicer-1 and UAS-Pasha were induced in the follicle cells (Figure 7.6A-C''). There is no significant change seen in the cytoophidia formation. In addition, UAS-miR-124 was also induced because miR-124 overexpression has been shown in previous chapter to be important for follicle cells and the egg chambers. However, overexpressing miR-124 also did not show significant changes in the morphology of cytoophidia (Figure 7.6D-D'').

Since overexpressing miRNAs did not have an effect on cytoophidia, mutants were then analysed to see if removing all miRNAs would have any effect on cytoophidia. Mitotic clones were generated for *ago1[k08121]* and *dicer-1[30D2]* and the GFP-ve clones still have cytoophidia (Figure 7.7A-B''). There is no clear morphology defect on the cytoophidia. To test if siRNAs affect cytoophidia, UAS-Dicer-2 RNAi was induced using the inducible GAL4. The knockdown of Dicer-2 did not affect cytoophidia (Figure 7.7).

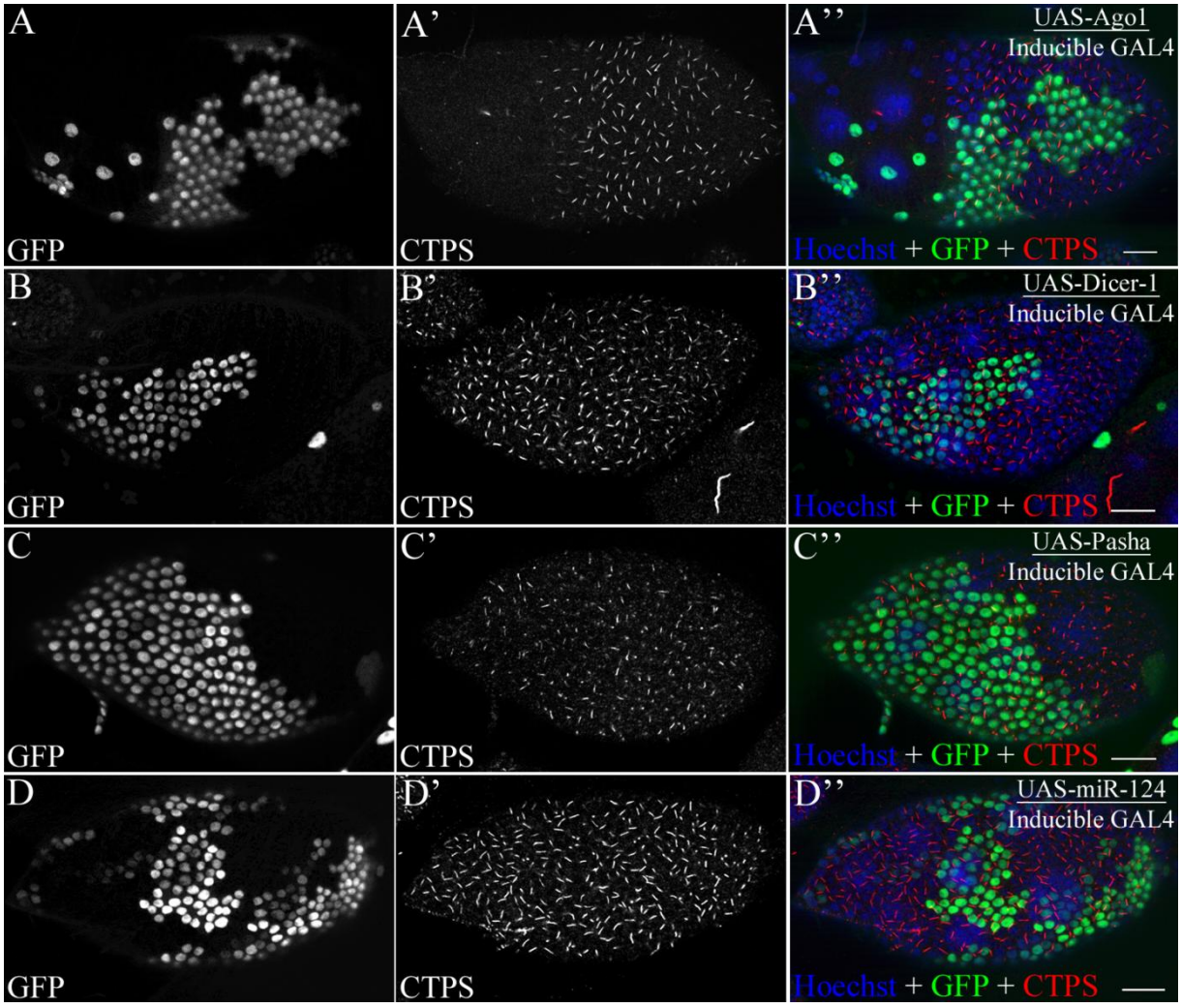


Figure 7.6. Overexpressing miRNA biogenesis proteins and miR-124 does not have any effect on cytoophidia. (A-C'') The formation of cytoophidia in the follicle cells did not change when cells are overexpressing Ago1, Dicer-1 or Pasha. (D-D'') Overexpressing miR-124 also did not affect cytoophidia. Scale bars, 20 μm.

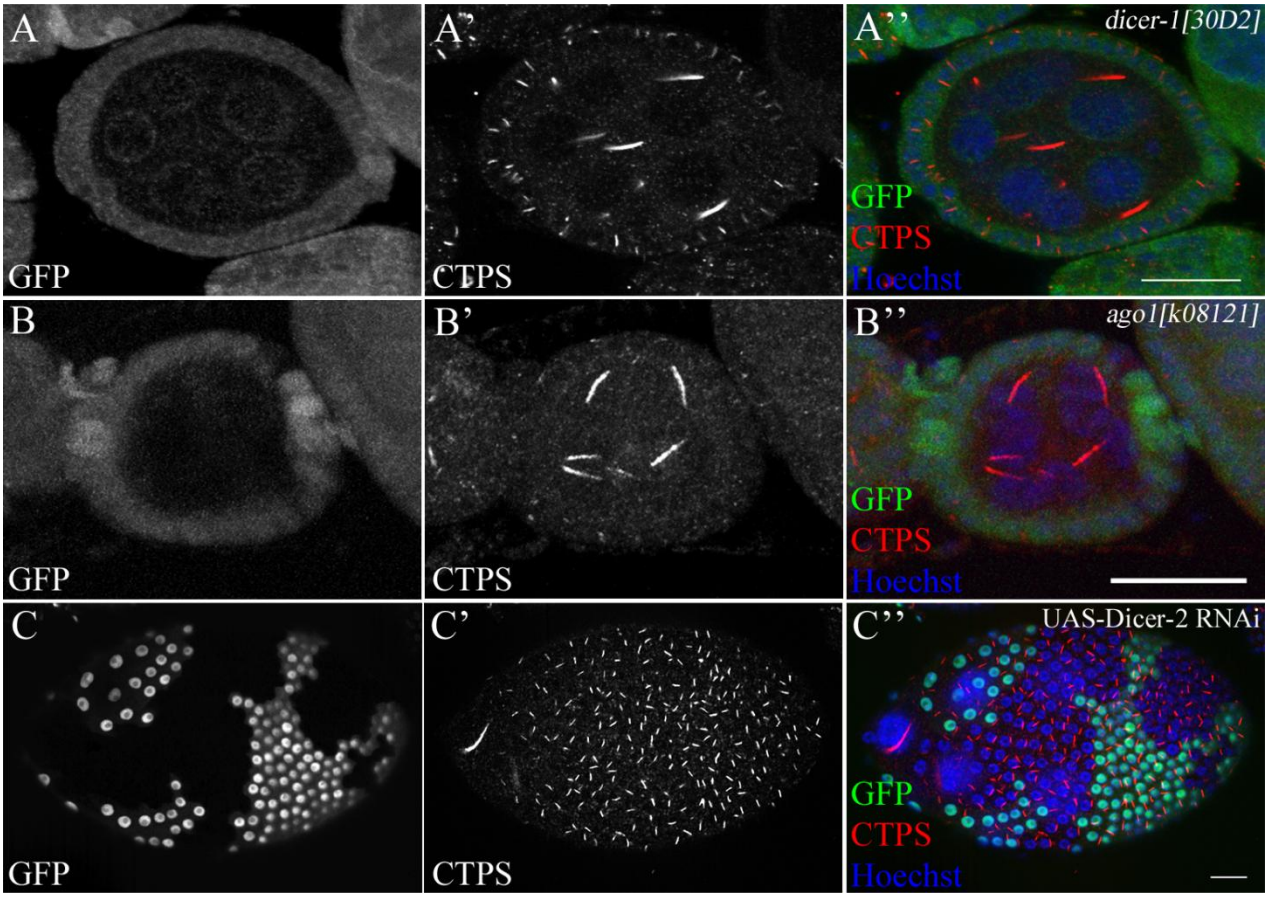


Figure 7.7. miRNAs and siRNAs biogenesis proteins do not affect cytoophidia. (A-B'') *dicer-1[30D2]* (A) and *ago1[k08121]* (B) mutant clones (GFP –ve) show no distinct effect on cytoophidia. (C-C'') Dicer-2 knockdown does not affect cytoophidia. Scale bars, 20 μm.

7.3. Discussion

7.3.1. CTPS is important for development

In this chapter, three CTPS mutants that disrupt cytoophidia formation were successfully isolated. These are very useful tools for studying CTPS and cytoophidia. In addition, the fundamental basics about CTPS can also be studied and understood before going deeper into understanding the cytoophidium structure. Here, the mutants were analysed and it was found that CTPS is maternally inherited. The maternal contribution of CTPS itself is enough for the mutant embryos to complete embryogenesis and survive to larvae stage as when maternal contribution was removed, the mutants do not complete embryogenesis. This result is in agreement with the fact that there were a lot of cytoophidia present in the egg chambers. On the other hand, macro-cytoophidia is rarely seen in mature eggs and is not present in embryos which could mean that this phenotype might not be related to the formation of cytoophidia. However, seeing that only the filament-forming isoform (CTPS isoform C) manages to rescue the mutants, the relationship between the phenotype of CTPS mutants, CTPS function and cytoophidia might be more complex. Looking at the cytoophidia point of view, the formation and disassociation of cytoophidia might have something to do with the level of CTPS in the cells. There could be a threshold of the level of CTPS needed in each cell to form cytoophidia and when the level drops below the threshold, cytoophidia disassociates. Also, since only CTPS is now known to be localized in cytoophidia, it is hard to determine whether cytoophidia disassociates or that CTPS disassociates from cytoophidia. If there are other markers found and confirm, then it would be interesting to see if the cytoophidia is still present or absent when CTPS is not present in tissues that cytoophidia is not detected in with CTPS. Isolating and separating the function of cytoophidia and CTPS would be important to fully characterize the properties of cytoophidia. However, it cannot be

ruled out that their functions might be related as only the filament forming isoform of CTPS manages to rescue the mutants.

Seeing that a lot cytoophidia is present in the egg chambers, and the importance of CTPS, it would seem that mutating CTPS would result have a severe effect on the development of egg chambers. The egg chambers are also actively transcribing RNA which would require CTP. However, after analysing the mutants, there were no clear defects found yet although a proper and thorough screen has not been carried out. P-bodies and Golgi bodies seemed not to be affected by the absence of CTPS and cytoophidia. Since this is a preliminary study, a lot more experiments are needed to fully characterize the mutants' egg chambers. Possible future experiments includes analysing the GSC, the number of clones generated by the mutant versus wild-type, and more importantly, using other cytoophidia markers (if present in the future), to see if cytoophidia disassociates.

7.3.2. CTPS interactions

Also, an interesting find is that CTPS antibody stains that nucleus of String knockdown follicle cells. This coincides with the result in Chapter 6 where the N-terminus of CTPS isoform C has nuclear localization sequences which were seen in the N-term and CTG domain transgenes. This means that CTPS can localize to the nucleus but it requires a certain condition. Forming cytoophidia might be one of the ways CTPS prevents itself to localize in the nucleus. Also the reason why knocked down of String results in CTPS localizing in the nucleus is still unknown. String is required for the transition between G2 to M phase. Follicle cells undergo mitotic cycle from stage 1 to stage 6 egg chambers and String must have played an important role in those stages. In addition, the knockdown of String resulted in bigger follicle cells which show its importance in maintaining the integrity of follicle cells. The

follicle cells might be stuck in the G2 phase with String is knockdown resulting in bigger follicle cells as the follicle cells cannot divide. CTPS also might be required in the division of follicle cells and might accumulate in the nucleus in small amounts which are undetected with antibody staining. However, if the cells are unable to divide, the nucleus continues to accumulate CTPS. These are all preliminary but important observations but more experiments are required to confirm this.

In the search to find a connection between miRNAs and cytoophidia formation, it was not clear if there is any as both overexpression and mutant study failed to show a link. There is also the possibility that there is no link and cytoophidia is not regulated by miRNAs. However, as discussed in previous chapters, overexpressing Ago1, Pasha or Dicer-1 itself might not be enough to dramatically increase the levels of total miRNAs. The mutants of Ago1, Dicer-1 and Pasha, which removes global level of miRNAs, might have a cancelling effect. Using these two methods is a quick way to determine whether cytoophidia is regulated by miRNAs or not but it might not tell the whole story. If one wants to pursue it further, then a miRNA screen might be a way to go.

Although this chapter consists of many preliminary data and observations, it is still important in the context of an attempt to understand the function of CTPS and cytoophidia during development. Many of the results presented here require more detailed experiments.

Chapter 8
Discussion and Conclusion

8.1. Mature miRNA levels mediate Ago1 driven germ line development

The miRNA field has gathered pace ever since it became apparent in the year 2000. However, this emerging field still has many questions unanswered. The work on this thesis starts with the spatial and temporal characterization of Ago1 using the Ago1::GFP protein trap line. Ago1 is enriched in the oocyte and clonal studies on multiple alleles show that Ago1, together with its miRNA biogenesis partners, Dicer-1, Drosha and Pasha are required for germ cell division and oocyte formation during oogenesis. The oocyte was determined, however, without miRNAs, it failed to maintain its state and reverted back to become a nurse cell. This is an interesting observation as the oocyte is the most important feature of the egg chamber because it will differentiate into a mature egg, without the oocyte, the egg chambers would serve no function. Somehow the egg chambers tries to determine an oocyte but failed to maintained it. Some egg chambers do manage to determine an oocyte (producing a 7 nurse cell, 1 oocyte egg chamber), however the number of escapers are really low. Furthermore, it is still unsure whether the oocyte determination defect is a direct cause of miRNAs or a secondary effect caused by misregulation of other oocyte determination genes. Genetic interaction study between Ago1 and other oocyte determination factor, for example Orb, might give some indication on how Ago1/miRNAs affect oocyte determination.

Furthermore, the role of Ago1, Dicer-1 and Drosha were further shown in the follicle cells. Ago1 and Pasha do not have as severe phenotypic defect as Dicer-1 and Drosha. Ago1 does show some phenotypic defects but none were detected in Pasha mutants or knockdowns. The possibility that Dicer-1 and Drosha might have other roles could not be ruled out. The discovery of mirtrons showed that several miRNAs could bypass Drosha and Pasha cleavage,

hence giving the possibility that there might be other types of miRNAs pathways that have yet to be discovered. Further experiments are required to dissect the mechanism of miRNA regulation in the follicle cells for example, the phenotype is prevalence in the later stage egg chamber but not so much in the earlier stage egg chamber which could mean that miRNAs are required for the transition from the mitotic cell cycle to endocycle stage. Also, since there seems to be a cell migration defects, the border cell is a fantastic tissue to study cell migration phenotype. This work also shows the co-localization of Ago1 and P body components *in vivo*. However, Ago1 is not required for the localization of P body components and Ago1 doesn't localize in P body in the nurse cells. There few cases where Ago1 can be seen in P bodies in the nurse cells and finding out what conditions (e.g. stress) facilitates Ago1 localization will be important as some predicted that degradation of miRNAs happens in P bodies as well.

In addition, the ectopic expression of miR-124a, which is a miRNA that is highly expressed in the brain, caused defects in the follicle cells, which are almost similar to the Dicer-1 and Drosha knockdowns. miR-124a could be constantly repressed in the follicle cells due to the gene(s) that it regulates which is important for follicle cell differentiation. Ectopic expression of miR-124 also caused the females to become sterile. Bioinformatics target predictions on miR-124a could bring up many genes that could potentially be its target. However, since the predictions are quite inaccurate, only by carrying out an experimental screening could the answers be found. Further experiments include carrying out a microarray or RNA-seq experiments on egg chambers that have miR-124 being overexpressed in the follicle cells. This will show genes that are downregulated when miR-124 is overexpressed. The list of genes could then be cross-checked with the bioinformatics target predictions of miR-124. Then, to test it further, the 3'UTR of the gene could be fused to a luciferase gene and carry out a luciferase assay in S2 cells. miR-124 is also needed to be expressed in the luciferase assay. It could be done by transfecting a miR-124 expression plasmid or the

sequence of pre-miR-124 could be inserted in the luciferase construct itself. As a control, a scrambled miR-124 and a scrambled miR-124 target site which will not have any knockdown occurring. With these experiments, the target of miR-124 could be identified and verified with experimental data which will be very important to show that miR-124 is not only a neuron-specific miRNA but a dynamic miRNA that have different functions in different tissues.

It is known that the Ago-bound miRNA complex is stable in the cell. However, there has not been a comprehensive study to determine the state of unloaded Ago proteins. The results from germline and somatic cells show that Ago1 levels decreased in the absence of mature miRNAs and it is independent of siRNAs. In addition, the ectopic expression of a single miRNA could further stabilize Ago1 resulting in increased levels of Ago1. The expression of mirtrons which bypass Pasha and Drosha cleavage itself could not rescue the degradation. Ago1 levels were not affected when Dicer-1 or Pasha was overexpressed. However, S2 cells seem to be shielded by these events and understanding the mechanism that is employed by S2 cells to protect Ago1 from being degraded requires further study. For start, the S2 cells miRNA biogenesis machinery needs to be re-examined. A miRNA-microarray on S2 cells which lacks Ago1, Dicer-1, Pasha and/or Drosha will show the miRNAs that is not downregulated. If by removing Dicer-1, Pasha or Drosha does not downregulate many miRNAs, then it is understandable why Ago1 is stable. There could be a different or modified machinery employed by S2 cells. Furthermore, the mechanism on how unloaded Ago1 is degraded *in vivo* also requires more experiments. Expressing a construct with Ago1 that can't load miRNAs tagged with GFP in S2 cells to monitor what happen to Ago1 when it is unloaded. Then, a stable S2 cells are generated with the mutated Ago1 and a normal Ago1 as a control. With these stable lines, a genome wide RNAi screening could be done to see what genes is involve in degrading unloaded Ago1. The genome wide RNAi screening service is offered by the *Drosophila* RNAi Screening Center (DRSC) in Harvard Medical School or the

Drosophila Sheffield RNAi Screening Facility (SRSF). The screening will be scored by genes that when it is knocked down, the level of GFP in the unloaded Ago1 increase. This list of genes effects the degradation of unloaded Ago1 which then can be further pursue to understand the mechanism. If these two studies are combined, it will be a significant contribution in understanding the fate of unloaded Ago1 and help to understand in more detail how Ago1 functions.

There is much evidence showing the importance of miRNAs during oogenesis. The miRNA regulation is required for the development of both germline cells and follicle cells. However, this regulation is very complex as seen in many studies. Some miRNAs if mutated could exhibit severe developmental defects but most of the time, mutating a single miRNA did not exhibit any defects. The complexity can also be seen when all miRNAs were removed which sometimes did not produce the same phenotype of mutating a single miRNA. This shows the ability of miRNAs to cancel out other miRNAs' effects. miRNAs are also known as master regulators as they tweak the expression of genes. Removing these miRNAs might not cause the cells to stop functioning, however, it could potentially cause the cell to not function in its optimum state. Although the miRNA field has evolved rapidly over the past decade, there are still many questions that are unanswered regarding miRNA regulation. In essence, this field is still young and will continue to evolve rapidly in the future. In conclusion, the results in Chapter 3 and Chapter 4 shows that miRNAs have a role in germ cell division, oocyte maintenance and follicle cell viability. Also, results in Chapter 5 shows that miRNAs are required for Ago1 stability. All these results have significantly contributed in understanding the basics of miRNA machinery. The field is still considered young and many more exciting discoveries will be made in the future which will help in translating miRNA research to generate therapeutics that uses miRNAs.

8.2. The assembly of cytoophidia is important for development

The identification of cytoophidia containing CTPS is just the beginning for this structure. In this thesis, CTPS was further analysed to understand how it forms cytoophidia. The CTPS isoform C was the only isoform of *Drosophila* CTPS to form cytoophidia. These findings lead to the dissection of CTPS isoform C in order to find regions which are important for cytoophidia assembly. One of the regions, which is the first 56 amino acid of the CTPS isoform C, was identified. Removing this region causes cytoophidia to disassemble and form punctate structure. This aggregation to form the punctate structure shows that a second region is present. In addition, it is now known that the N terminal is important as tagging in the N terminal region to full-length CTPS isoform C disrupts the cytoophidia morphology and tagging to N terminal of truncated isoform C (removal of the first 56 amino acid) disrupts the punctate structure formation. Furthermore, the addition of 53 amino acids in the CTPS isoform B also disrupts the aggregation. The importance of the cytoophidia formation is also shown in the ability to rescue the mutant lethality by only CTPS isoform C and not CTPS isoform B.

This is just the start of as many more experiments could be carried out based on these constructs. Identification of the other sites that is required for cytoophidia formation will help in understanding how cytoophidia forms. This can be done by generating constructs with systematically removing regions in isoform C to see which region disrupts cytoophidia formation. Then point mutations can be introduced to identify which amino acid is important. These experiments are important in understanding how cytoophidia is formed because previous study have shown that CTPS is present in two different forms; dimer and tetramer. However, seeing that CTPS can form filaments, it is thought that CTPS can actually form polymer. By knowing which part of the protein is required, predictions on how it forms the filament can be done and hopefully will help in understanding how CTPS forms cytoophidia.

Assessments of the mutants that disrupt cytoophidia formation unravel the importance of CTPS in development. Maternal contribution of CTPS is enough for the mutants to survive until they 3rd instar larvae but with a slower growth rate. The amount of cytoophidia present in the egg chambers could show a high amount of maternal contribution even though cytoophidia is usually not present in unfertilized egg and embryos. During oogenesis, CTPS might not be required for the development of the egg chamber as *ctps* mutants do not exhibit defective egg chambers. The axis of the egg chamber and the Golgi bodies which interact with cytoophidia were not affected in the *ctps* mutants. CTPS might be required more during zygotic transcription in embryogenesis which explains why, without maternal contribution, the embryos shows severe phenotypic defects in development. This also argues that the active form CTPS is not present in cytoophidia. However, it does not mean that cytoophidia only has the inactive form because during oogenesis, the egg chambers actively transcribe RNA and DNA which requires CTPS activity. There is also a possibility that since the egg chambers have a huge amount of CTPS, some is stored in cytoophidia. Cytoophidia was not affected when miRNAs were removed or overexpressed. Although it might have subtle changes, it cannot be detected by immunofluorescence.

To see if there is any miRNA that regulates CTPS, a miRNA-microarray could be done on the *ctps* mutants. This is a way to identify miRNA regulation because miRNAs are unstable when it has no target site. From the microarray data, miRNAs that are highly downregulated have the potential to be targeting CTPS. However, this have to be pursue cautiously because there are also the possibilities that an affect from CTPS or a secondary effect that could have caused the miRNAs to be downregulated. Further verification using the luciferase assay that has been mentioned above, will be able rule out any effect of CTPS and secondary effects that cause the particular miRNA to be degraded.

Characterization on the CTPS mutants that lack cytoophidia has just started. There are still many more tissues to analysed and questions to be answered. However, the main question of whether there are other components in cytoophidia is still un-answered. One way to identify other proteins that are present in cytoophidia is to do immunoprecipitation and then mass spectrometry. This will identify the proteins that bind to CTPS which can be used to check by either antibody staining or GFP tag to see if they also localize in cytoophidia. It will be very important to identify those proteins (if they are present) to better understand why they are localized to cytoophidia and most importantly, what is the function of cytoophidia.

The cytoophidia study is yet to grow, however it has the potential to be a field on its own. Its role in cancer could also be followed up as it is relevance to the study that found CTPS to be upregulated in cancer cells and also the present of more cytoophidia in apoptotic cells. If cytoophidia which contains CTPS is anything like mitochondria which contain ATP synthase, it will be a very important field in the future.

REFERENCES

Adams, M.D., Celniker, S.E., Holt, R.A., Evans, C.A., Gocayne, J.D., Amanatides, P.G., Scherer, S.E., Li, P.W., Hoskins, R.A., Galle, R.F., George, R.A., Lewis, S.E., Richards, S., Ashburner, M., Henderson, S.N., Sutton, G.G., Wortman, J.R., Yandell, M.D., Zhang, Q., Chen, L.X., Brandon, R.C., Rogers, Y.H., Blazej, R.G., Champe, M., Pfeiffer, B.D., Wan, K.H., Doyle, C., Baxter, E.G., Helt, G., Nelson, C.R., Gabor, G.L., Abril, J.F., Agbayani, A., An, H.J., Andrews-Pfannkoch, C., Baldwin, D., Ballew, R.M., Basu, A., Baxendale, J., Bayraktaroglu, L., Beasley, E.M., Beeson, K.Y., Benos, P.V., Berman, B.P., Bhandari, D., Bolshakov, S., Borkova, D., Botchan, M.R., Bouck, J., Brokstein, P., Brottier, P., Burtis, K.C., Busam, D.A., Butler, H., Cadieu, E., Center, A., Chandra, I., Cherry, J.M., Cawley, S., Dahlke, C., Davenport, L.B., Davies, P., de Pablos, B., Delcher, A., Deng, Z., Mays, A.D., Dew, I., Dietz, S.M., Dodson, K., Doup, L.E., Downes, M., Dugan-Rocha, S., Dunkov, B.C., Dunn, P., Durbin, K.J., Evangelista, C.C., Ferraz, C., Ferriera, S., Fleischmann, W., Fosler, C., Gabrielian, A.E., Garg, N.S., Gelbart, W.M., Glasser, K., Glodek, A., Gong, F., Gorrell, J.H., Gu, Z., Guan, P., Harris, M., Harris, N.L., Harvey, D., Heiman, T.J., Hernandez, J.R., Houck, J., Hostin, D., Houston, K.A., Howland, T.J., Wei, M.H., Ibegwam, C., Jalali, M., Kalush, F., Karpen, G.H., Ke, Z., Kennison, J.A., Ketchum, K.A., Kimmel, B.E., Kodira, C.D., Kraft, C., Kravitz, S., Kulp, D., Lai, Z., Lasko, P., Lei, Y., Levitsky, A.A., Li, J., Li, Z., Liang, Y., Lin, X., Liu, X., Mattei, B., McIntosh, T.C., McLeod, M.P., McPherson, D., Merkulov, G., Milshina, N.V., Mobarry, C., Morris, J., Moshrefi, A., Mount, S.M., Moy, M., Murphy, B., Murphy, L., Muzny, D.M., Nelson, D.L., Nelson, D.R., Nelson, K.A., Nixon, K., Nusskern, D.R., Pacleb, J.M., Palazzolo, M., Pittman, G.S., Pan, S., Pollard, J., Puri, V., Reese, M.G., Reinert, K., Remington, K., Saunders, R.D., Scheeler, F., Shen, H., Shue, B.C., Siden-Kiamos, I., Simpson, M., Skupski, M.P., Smith, T., Spier, E., Spradling, A.C., Stapleton, M., Strong, R., Sun, E., Svirskas, R., Tector, C., Turner, R., Venter, E., Wang, A.H., Wang, X., Wang, Z.Y., Wassarman, D.A., Weinstock, G.M., Weissenbach, J., Williams, S.M., WoodageT, Worley, K.C., Wu, D., Yang, S., Yao, Q.A., Ye, J., Yeh, R.F., Zaveri, J.S., Zhan, M., Zhang, G., Zhao, Q., Zheng, L., Zheng, X.H., Zhong, F.N., Zhong, W., Zhou, X., Zhu, S., Zhu, X., Smith, H.O., Gibbs, R.A., Myers, E.W., Rubin, G.M., Venter, J.C., 2000. The genome sequence of Drosophila melanogaster. Science 287, 2185-2195.

Alberts, B., Johnson, A., Lewis, J., Raff, M., Roberts, K., P., W., 2008. Molecular Biology of the Cell, 5th Edition. Garland Science, Taylor & Francis Group, New York/Abingdon.

Alphey, L., Jimenez, J., White-Cooper, H., Dawson, I., Nurse, P., Glover, D.M., 1992. twine, a cdc25 homolog that functions in the male and female germline of Drosophila. Cell 69, 977-988.

Ambros, V., 2004. The functions of animal microRNAs. Nature 431, 350-355.

Ameres, S.L., Hung, J.H., Xu, J., Weng, Z., Zamore, P.D., 2011. Target RNA-directed tailing and trimming purifies the sorting of endo-siRNAs between the two Drosophila Argonaute proteins. RNA 17, 54-63.

Anderson, P.M., 1983. CTP synthetase from Escherichia coli: an improved purification procedure and characterization of hysteretic and enzyme concentration effects on kinetic properties. Biochemistry 22, 3285-3292.

Aravin, A.A., Klenov, M.S., Vagin, V.V., Bantignies, F., Cavalli, G., Gvozdev, V.A., 2004. Dissection of a natural RNA silencing process in the Drosophila melanogaster germ line. Mol Cell Biol 24, 6742-6750.

Aravind, L., Iyer, L.M., Leipe, D.D., Koonin, E.V., 2004. A novel family of P-loop NTPases with an unusual phyletic distribution and transmembrane segments inserted within the NTPase domain. Genome Biol 5, R30.

Armknecht, S., Boutros, M., Kiger, A., Nybakken, K., Mathey-Prevot, B., Perrimon, N., 2005. High-throughput RNA interference screens in Drosophila tissue culture cells. Methods Enzymol 392, 55-73.

Aronow, B., Ullman, B., 1987. In situ regulation of mammalian CTP synthetase by allosteric inhibition. J Biol Chem 262, 5106-5112.

Azzam, G., Smibert, P., Lai, E.C., Liu, J.L., 2012. Drosophila Argonaute 1 and its miRNA biogenesis partners are required for oocyte formation and germline cell division. Dev Biol 365, 384-394.

Bartel, D.P., 2009. MicroRNAs: target recognition and regulatory functions. Cell 136, 215-233.

Baum, B., Li, W., Perrimon, N., 2000. A cyclase-associated protein regulates actin and cell polarity during Drosophila oogenesis and in yeast. Curr Biol 10, 964-973.

Bearne, S.L., Hekmat, O., Macdonnell, J.E., 2001. Inhibition of Escherichia coli CTP synthase by glutamate gamma-semialdehyde and the role of the allosteric effector GTP in glutamine hydrolysis. Biochem J 356, 223-232.

Behm-Ansmant, I., Rehwinkel, J., Doerks, T., Stark, A., Bork, P., Izaurralde, E., 2006. mRNA degradation by miRNAs and GW182 requires both CCR4:NOT deadenylase and DCP1:DCP2 decapping complexes. Genes Dev 20, 1885-1898.

Bejarano, F., Smibert, P., Lai, E.C., 2010. miR-9a prevents apoptosis during wing development by repressing Drosophila LIM-only. Dev Biol 338, 63-73.

Bellen, H.J., Levis, R.W., He, Y., Carlson, J.W., Evans-Holm, M., Bae, E., Kim, J., Metaxakis, A., Savakis, C., Schulze, K.L., Hoskins, R.A., Spradling, A.C., 2011. The Drosophila gene disruption project: progress using transposons with distinctive site specificities. Genetics 188, 731-743.

Bellen, H.J., Levis, R.W., Liao, G., He, Y., Carlson, J.W., Tsang, G., Evans-Holm, M., Hiesinger, P.R., Schulze, K.L., Rubin, G.M., Hoskins, R.A., Spradling, A.C., 2004. The BDGP gene disruption project: single transposon insertions associated with 40% of Drosophila genes. Genetics 167, 761-781.

Berdnik, D., Fan, A.P., Potter, C.J., Luo, L., 2008. MicroRNA processing pathway regulates olfactory neuron morphogenesis. Curr Biol 18, 1754-1759.

Bhaskar, V., Courey, A.J., 2002. The MADF-BESS domain factor Dip3 potentiates synergistic activation by Dorsal and Twist. Gene 299, 173-184.

Bischof, J., Maeda, R.K., Hediger, M., Karch, F., Basler, K., 2007. An optimized transgenesis system for Drosophila using germ-line-specific phiC31 integrases. Proc Natl Acad Sci U S A 104, 3312-3317.

Bohmert, K., Camus, I., Bellini, C., Bouchez, D., Caboche, M., Benning, C., 1998. AGO1 defines a novel locus of Arabidopsis controlling leaf development. Embo J 17, 170-180.

Bohnsack, M.T., Czaplinski, K., Gorlich, D., 2004. Exportin 5 is a RanGTP-dependent dsRNA-binding protein that mediates nuclear export of pre-miRNAs. Rna 10, 185-191.

Bolivar, J., Pearson, J., Lopez-Onieva, L., Gonzalez-Reyes, A., 2006. Genetic dissection of a stem cell niche: the case of the Drosophila ovary. Dev Dyn 235, 2969-2979.

Bortolamiol, D., Pazhouhandeh, M., Marrocco, K., Genschik, P., Ziegler-Graff, V., 2007. The Polerovirus F box protein P0 targets ARGONAUTE1 to suppress RNA silencing. Curr Biol 17, 1615-1621.

Bortolamiol, D., Pazhouhandeh, M., Ziegler-Graff, V., 2008. Viral suppression of RNA silencing by destabilisation of ARGONAUTE 1. Plant Signal Behav 3, 657-659.

Brand, A.H., Perrimon, N., 1993. Targeted gene expression as a means of altering cell fates and generating dominant phenotypes. Development 118, 401-415.

Bre, M.H., Pepperkok, R., Hill, A.M., Levilliers, N., Ansorge, W., Stelzer, E.H., Karsenti, E., 1990. Regulation of microtubule dynamics and nucleation during polarization in MDCK II cells. J Cell Biol 111, 3013-3021.

Brennecke, J., Aravin, A.A., Stark, A., Dus, M., Kellis, M., Sachidanandam, R., Hannon, G.J., 2007. Discrete small RNA-generating loci as master regulators of transposon activity in Drosophila. Cell 128, 1089-1103.

Buszczak, M., Paterno, S., Lighthouse, D., Bachman, J., Planck, J., Owen, S., Skora, A.D., Nystul, T.G., Ohlstein, B., Allen, A., Wilhelm, J.E., Murphy, T.D., Levis, R.W., Matunis, E., Srivali, N., Hoskins, R.A., Spradling, A.C., 2007. The carnegie protein trap library: a versatile tool for Drosophila developmental studies. Genetics 175, 1505-1531.

Carrington, J.C., Ambros, V., 2003. Role of microRNAs in plant and animal development. Science 301, 336-338.

Chakraborty, K.P., Hurlbert, R.B., 1961. Role of glutamine in the biosynthesis of cytidine nucleotides in Escherichia coli. Biochim Biophys Acta 47, 607-609.

Chatterjee, S., Grosshans, H., 2009. Active turnover modulates mature microRNA activity in Caenorhabditis elegans. Nature 461, 546-549.

Chekulaeva, M., Filipowicz, W., Parker, R., 2009. Multiple independent domains of dGW182 function in miRNA-mediated repression in Drosophila. Rna 15, 794-803.

Chen, C.Y., Zheng, D., Xia, Z., Shyu, A.B., 2009. Ago-TNRC6 triggers microRNA-mediated decay by promoting two deadenylation steps. Nat Struct Mol Biol 16, 1160-1166.

Chen, K., Zhang, J., Tastan, O.Y., Deussen, Z.A., Siswick, M.Y., Liu, J.L., 2011. Glutamine analogs promote cytoophidium assembly in human and Drosophila cells. J Genet Genomics 38, 391-402.

Chou, T.B., Noll, E., Perrimon, N., 1993. Autosomal P[ovoD1] dominant female-sterile insertions in Drosophila and their use in generating germ-line chimeras. Development 119, 1359-1369.

Chou, T.B., Perrimon, N., 1996. The autosomal FLP-DFS technique for generating germline mosaics in Drosophila melanogaster. Genetics 144, 1673-1679.

Christerson, L.B., Mckearin, D.M., 1994. Orb Is Required for Anteroposterior and Dorsoventral Patterning during Drosophila Oogenesis. Gene Dev 8, 614-628.

Clark, I.E., Jan, L.Y., Jan, Y.N., 1997. Reciprocal localization of Nod and kinesin fusion proteins indicates microtubule polarity in the Drosophila oocyte, epithelium, neuron and muscle. Development 124, 461-470.

Conaco, C., Otto, S., Han, J.J., Mandel, G., 2006. Reciprocal actions of REST and a microRNA promote neuronal identity. Proc Natl Acad Sci U S A 103, 2422-2427.

Cox, D.N., Lu, B., Sun, T.Q., Williams, L.T., Jan, Y.N., 2001. Drosophila par-1 is required for oocyte differentiation and microtubule organization. Curr Biol 11, 75-87.

Craymer, L., 1980. [New mutants report.]. Drosophila Information Service 55, 197-200.

Csorba, T., Lozsa, R., Hutvagner, G., Burgyan, J., 2010. Polerovirus protein P0 prevents the assembly of small RNA-containing RISC complexes and leads to degradation of ARGONAUTE1. Plant J 62, 463-472.

Czech, B., Zhou, R., Erlich, Y., Brennecke, J., Binari, R., Villalta, C., Gordon, A., Perrimon, N., Hannon, G.J., 2009. Hierarchical rules for Argonaute loading in Drosophila. Mol Cell 36, 445-456.

de Cuevas, M., Matunis, E.L., 2011. The stem cell niche: lessons from the Drosophila testis. Development 138, 2861-2869.

Deng, W.M., Althauser, C., Ruohola-Baker, H., 2001. Notch-Delta signaling induces a transition from mitotic cell cycle to endocycle in Drosophila follicle cells. Development 128, 4737-4746.

Deng, W.M., Bownes, M., 1998. Patterning and morphogenesis of the follicle cell epithelium during Drosophila oogenesis. Int J Dev Biol 42, 541-552.

Denli, A.M., Tops, B.B., Plasterk, R.H., Ketting, R.F., Hannon, G.J., 2004. Processing of primary microRNAs by the Microprocessor complex. Nature 432, 231-235.

Dietzl, G., Chen, D., Schnorrer, F., Su, K.C., Barinova, Y., Fellner, M., Gasser, B., Kinsey, K., Oppel, S., Scheiblauer, S., Couto, A., Marra, V., Keleman, K., Dickson, B.J., 2007. A genome-wide transgenic RNAi library for conditional gene inactivation in Drosophila. Nature 448, 151-156.

DiNardo, S., O'Farrell, P.H., 1987. Establishment and refinement of segmental pattern in the Drosophila embryo: spatial control of engrailed expression by pair-rule genes. Genes Dev 1, 1212-1225.

Djuranovic, S., Zinchenko, M.K., Hur, J.K., Nahvi, A., Brunelle, J.L., Rogers, E.J., Green, R., 2010. Allosteric regulation of Argonaute proteins by miRNAs. Nat Struct Mol Biol 17, 144-150.

Dobens, L.L., Raftery, L.A., 2000. Integration of epithelial patterning and morphogenesis in Drosophila ovarian follicle cells. Dev Dyn 218, 80-93.

Doerflinger, H., Benton, R., Shulman, J.M., St Johnston, D., 2003. The role of PAR-1 in regulating the polarised microtubule cytoskeleton in the Drosophila follicular epithelium. Development 130, 3965-3975.

Edgar, B.A., O'Farrell, P.H., 1989. Genetic control of cell division patterns in the Drosophila embryo. Cell 57, 177-187.

Endrizzi, J.A., Kim, H., Anderson, P.M., Baldwin, E.P., 2004. Crystal structure of Escherichia coli cytidine triphosphate synthetase, a nucleotide-regulated glutamine amidotransferase/ATP-dependent amidoligase fusion protein and homologue of anticancer and antiparasitic drug targets. Biochemistry 43, 6447-6463.

Endrizzi, J.A., Kim, H., Anderson, P.M., Baldwin, E.P., 2005. Mechanisms of product feedback regulation and drug resistance in cytidine triphosphate synthetases from the structure of a CTP-inhibited complex. Biochemistry 44, 13491-13499.

Eulalio, A., Huntzinger, E., Izaurralde, E., 2008. GW182 interaction with Argonaute is essential for miRNA-mediated translational repression and mRNA decay. Nat Struct Mol Biol 15, 346-353.

Eulalio, A., Huntzinger, E., Nishihara, T., Rehwinkel, J., Fauser, M., Izaurralde, E., 2009. Deadenylation is a widespread effect of miRNA regulation. Rna 15, 21-32.

Fabian, M.R., Mathonnet, G., Sundermeier, T., Mathys, H., Zipprich, J.T., Svitkin, Y.V., Rivas, F., Jinek, M., Wohlschlegel, J., Doudna, J.A., Chen, C.Y., Shyu, A.B., Yates, J.R., 3rd, Hannon, G.J., Filipowicz, W., Duchaine, T.F., Sonenberg, N., 2009. Mammalian miRNA RISC recruits CAF1 and PABP to affect PABP-dependent deadenylation. Mol Cell 35, 868-880.

Fire, A., Xu, S., Montgomery, M.K., Kostas, S.A., Driver, S.E., Mello, C.C., 1998. Potent and specific genetic interference by double-stranded RNA in Caenorhabditis elegans. Nature 391, 806-811.

Flynt, A.S., Lai, E.C., 2008. Biological principles of microRNA-mediated regulation: shared themes amid diversity. Nat Rev Genet 9, 831-842.

Forstemann, K., Horwich, M.D., Wee, L., Tomari, Y., Zamore, P.D., 2007. Drosophila microRNAs are sorted into functionally distinct argonaute complexes after production by dicer-1. Cell 130, 287-297.

Forstemann, K., Tomari, Y., Du, T., Vagin, V.V., Denli, A.M., Bratu, D.P., Klattenhoff, C., Theurkauf, W.E., Zamore, P.D., 2005. Normal microRNA maturation and germ-line stem cell maintenance requires Loquacious, a double-stranded RNA-binding domain protein. PLoS Biol 3, e236.

Garneau, N.L., Wilusz, J., Wilusz, C.J., 2007. The highways and byways of mRNA decay. Nat Rev Mol Cell Biol 8, 113-126.

Ghildiyal, M., Xu, J., Seitz, H., Weng, Z., Zamore, P.D., 2010. Sorting of Drosophila small silencing RNAs partitions microRNA* strands into the RNA interference pathway. RNA 16, 43-56.

Girard, A., Sachidanandam, R., Hannon, G.J., Carmell, M.A., 2006. A germline-specific class of small RNAs binds mammalian Piwi proteins. Nature 442, 199-202.

Golic, K.G., Lindquist, S., 1989. The FLP recombinase of yeast catalyzes site-specific recombination in the Drosophila genome. Cell 59, 499-509.

Goto, M., Omi, R., Nakagawa, N., Miyahara, I., Hirotsu, K., 2004. Crystal structures of CTP synthetase reveal ATP, UTP, and glutamine binding sites. Structure 12, 1413-1423.

Gregory, R.I., Yan, K.P., Amuthan, G., Chendrimada, T., Doratotaj, B., Cooch, N., Shiekhattar, R., 2004. The Microprocessor complex mediates the genesis of microRNAs. Nature 432, 235-240.

Grewal, S.S., 2009. Insulin/TOR signaling in growth and homeostasis: a view from the fly world. Int J Biochem Cell Biol 41, 1006-1010.

Guo, H., Ingolia, N.T., Weissman, J.S., Bartel, D.P., 2010. Mammalian microRNAs predominantly act to decrease target mRNA levels. Nature 466, 835-840.

Gutzeit, H.O., 1986. The role of microfilaments in cytoplasmic streaming in Drosophila follicles. J Cell Sci 80, 159-169.

Han, J., Lee, Y., Yeom, K.H., Kim, Y.K., Jin, H., Kim, V.N., 2004. The Drosha-DGCR8 complex in primary microRNA processing. Genes Dev 18, 3016-3027.

Han, J., Pedersen, J.S., Kwon, S.C., Belair, C.D., Kim, Y.K., Yeom, K.H., Yang, W.Y., Haussler, D., Blelloch, R., Kim, V.N., 2009. Posttranscriptional crossregulation between Drosha and DGCR8. Cell 136, 75-84.

Hatfield, S.D., Shcherbata, H.R., Fischer, K.A., Nakahara, K., Carthew, R.W., Ruohola-Baker, H., 2005. Stem cell division is regulated by the microRNA pathway. Nature 435, 974-978.

Hendrickson, D.G., Hogan, D.J., McCullough, H.L., Myers, J.W., Herschlag, D., Ferrell, J.E., Brown, P.O., 2009. Concordant regulation of translation and mRNA abundance for hundreds of targets of a human microRNA. PLoS Biol 7, e1000238.

Hong, A., Lee-Kong, S., Iida, T., Sugimura, I., Lilly, M.A., 2003. The p27cip/kip ortholog dacapo maintains the Drosophila oocyte in prophase of meiosis I. Development 130, 1235-1242.

Hutvagner, G., Simard, M.J., 2008. Argonaute proteins: key players in RNA silencing. Nat Rev Mol Cell Biol 9, 22-32.

Huynh, J.R., St Johnston, D., 2000. The role of BicD, Egl, Orb and the microtubules in the restriction of meiosis to the Drosophila oocyte. Development 127, 2785-2794.

Huynh, J.R., St Johnston, D., 2004. The origin of asymmetry: early polarisation of the Drosophila germline cyst and oocyte. Curr Biol 14, R438-449.

Ingerson-Mahar, M., Briegel, A., Werner, J.N., Jensen, G.J., Gitai, Z., 2010. The metabolic enzyme CTP synthase forms cytoskeletal filaments. Nat Cell Biol 12, 739-746.

Iovino, N., Pane, A., Gaul, U., 2009. miR-184 has multiple roles in Drosophila female germline development. Dev Cell 17, 123-133.

Ishizu, H., Nagao, A., Siomi, H., 2011. Gatekeepers for Piwi-piRNA complexes to enter the nucleus. Curr Opin Genet Dev 21, 484-490.

Iwasaki, S., Kawamata, T., Tomari, Y., 2009. Drosophila argonaute1 and argonaute2 employ distinct mechanisms for translational repression. Mol Cell 34, 58-67.

Iwasaki, S., Kobayashi, M., Yoda, M., Sakaguchi, Y., Katsuma, S., Suzuki, T., Tomari, Y., 2010. Hsc70/Hsp90 chaperone machinery mediates ATP-dependent RISC loading of small RNA duplexes. Mol Cell 39, 292-299.

Janowski, B.A., Huffman, K.E., Schwartz, J.C., Ram, R., Nordsell, R., Shames, D.S., Minna, J.D., Corey, D.R., 2006. Involvement of AGO1 and AGO2 in mammalian transcriptional silencing. Nat Struct Mol Biol 13, 787-792.

Jiang, F., Ye, X., Liu, X., Fincher, L., McKearin, D., Liu, Q., 2005. Dicer-1 and R3D1-L catalyze microRNA maturation in Drosophila. Genes Dev 19, 1674-1679.

Jin, Z., Xie, T., 2007. Dcr-1 maintains Drosophila ovarian stem cells. Curr Biol 17, 539-544.

Johnston, M., Geoffroy, M.C., Sobala, A., Hay, R., Hutvagner, G., 2010. HSP90 protein stabilizes unloaded argonaute complexes and microscopic P-bodies in human cells. Mol Biol Cell 21, 1462-1469.

Johnston, M., Hutvagner, G., 2011. Posttranslational modification of Argonautes and their role in small RNA-mediated gene regulation. Silence 2, 5.

Jones, C.I., Newbury, S.F., 2010. Functions of microRNAs in Drosophila development. Biochem Soc Trans 38, 1137-1143.

Kalidas, S., Sanders, C., Ye, X., Strauss, T., Kuhn, M., Liu, Q., Smith, D.P., 2008. Drosophila R2D2 mediates follicle formation in somatic tissues through interactions with Dicer-1. Mech Dev 125, 475-485.

Kammen, H.O., Hurlbert, R.B., 1959. The formation of cytidine nucleotides and RNA cytosine from orotic acid by the Novikoff tumor in vitro. Cancer Res 19, 654-663.

Kataoka, Y., Takeichi, M., Uemura, T., 2001. Developmental roles and molecular characterization of a Drosophila homologue of Arabidopsis Argonaute1, the founder of a novel gene superfamily. Genes Cells 6, 313-325.

Kawamata, T., Seitz, H., Tomari, Y., 2009. Structural determinants of miRNAs for RISC loading and slicer-independent unwinding. Nat Struct Mol Biol 16, 953-960.

Kawamata, T., Tomari, Y., 2010. Making RISC. Trends Biochem Sci 35, 368-376.

Keyes, L.N., Spradling, A.C., 1997. The Drosophila gene fs(2)cup interacts with otu to define a cytoplasmic pathway required for the structure and function of germ-line chromosomes. Development 124, 1419-1431.

Kim, D.H., Villeneuve, L.M., Morris, K.V., Rossi, J.J., 2006a. Argonaute-1 directs siRNA-mediated transcriptional gene silencing in human cells. Nat Struct Mol Biol 13, 793-797.

Kim, K., Lee, Y.S., Harris, D., Nakahara, K., Carthew, R.W., 2006b. The RNAi pathway initiated by Dicer-2 in Drosophila. Cold Spring Harb Symp Quant Biol 71, 39-44.

Kim, V.N., Nam, J.W., 2006. Genomics of microRNA. Trends Genet 22, 165-173.

Kim, Y.I., Ryu, T., Lee, J., Heo, Y.S., Ahnn, J., Lee, S.J., Yoo, O., 2010. A genetic screen for modifiers of Drosophila caspase Dcp-1 reveals caspase involvement in autophagy and novel caspase-related genes. BMC Cell Biol 11, 9.

Kiriakidou, M., Tan, G.S., Lamprinaki, S., De Planell-Saguer, M., Nelson, P.T., Mourelatos, Z., 2007. An mRNA m7G cap binding-like motif within human Ago2 represses translation. Cell 129, 1141-1151.

Kizaki, H., Ohsaka, F., Sakurada, T., 1985. CTP synthetase from Ehrlich ascites tumor cells. Subunit stoichiometry and regulation of activity. Biochim Biophys Acta 829, 34-43.

Kizaki, H., Williams, J.C., Morris, H.P., Weber, G., 1980. Increased cytidine 5'-triphosphate synthetase activity in rat and human tumors. Cancer Res 40, 3921-3927.

Klusza, S., Deng, W.M., 2011. At the crossroads of differentiation and proliferation: precise control of cell-cycle changes by multiple signaling pathways in Drosophila follicle cells. Bioessays 33, 124-134.

Kornberg, T., Siden, I., O'Farrell, P., Simon, M., 1985. The engrailed locus of Drosophila: in situ localization of transcripts reveals compartment-specific expression. Cell 40, 45-53.

Krichevsky, A.M., King, K.S., Donahue, C.P., Khrapko, K., Kosik, K.S., 2003. A microRNA array reveals extensive regulation of microRNAs during brain development. RNA 9, 1274-1281.

Lagos-Quintana, M., Rauhut, R., Yalcin, A., Meyer, J., Lendeckel, W., Tuschl, T., 2002. Identification of tissue-specific microRNAs from mouse. Curr Biol 12, 735-739.

Lai, E.C., 2002. Micro RNAs are complementary to 3' UTR sequence motifs that mediate negative post-transcriptional regulation. Nat Genet 30, 363-364.

Lantz, V., Chang, J.S., Horabin, J.I., Bopp, D., Schedl, P., 1994. The Drosophila orb RNA-binding protein is required for the formation of the egg chamber and establishment of polarity. Genes Dev 8, 598-613.

Lau, N.C., Robine, N., Martin, R., Chung, W.J., Niki, Y., Berezikov, E., Lai, E.C., 2009. Abundant primary piRNAs, endo-siRNAs, and microRNAs in a Drosophila ovary cell line. Genome Res 19, 1776-1785.

Lee, R.C., Feinbaum, R.L., Ambros, V., 1993. The C. elegans heterochronic gene lin-4 encodes small RNAs with antisense complementarity to lin-14. Cell 75, 843-854.

Lee, T., Luo, L., 2001. Mosaic analysis with a repressible cell marker (MARCM) for Drosophila neural development. Trends Neurosci 24, 251-254.

Lee, Y.S., Nakahara, K., Pham, J.W., Kim, K., He, Z., Sontheimer, E.J., Carthew, R.W., 2004. Distinct roles for Drosophila Dicer-1 and Dicer-2 in the siRNA/miRNA silencing pathways. Cell 117, 69-81.

Levitzki, A., Koshland, D.E., Jr., 1971. Cytidine triphosphate synthetase. Covalent intermediates and mechanisms of action. Biochemistry 10, 3365-3371.

Levitzki, A., Koshland, D.E., Jr., 1972a. Ligand-induced dimer-to-tetramer transformation in cytosine triphosphate synthetase. Biochemistry 11, 247-253.

Levitzki, A., Koshland, D.E., Jr., 1972b. Role of an allosteric effector. Guanosine triphosphate activation in cytosine triphosphate synthetase. Biochemistry 11, 241-246.

Lewis, B.P., Shih, I.H., Jones-Rhoades, M.W., Bartel, D.P., Burge, C.B., 2003. Prediction of mammalian microRNA targets. Cell 115, 787-798.

Li, I.C., Wu, C.L., Chu, E.H., 1989. Single-step selection of mammalian cell mutants deficient in CTP synthetase. Somat Cell Mol Genet 15, 85-91.

Lieberman, I., 1956. Enzymatic amination of uridine triphosphate to cytidine triphosphate. J Biol Chem 222, 765-775.

Lilly, M.A., Spradling, A.C., 1996. The Drosophila endocycle is controlled by Cyclin E and lacks a checkpoint ensuring S-phase completion. Genes Dev 10, 2514-2526.

Lim, L.P., Lau, N.C., Garrett-Engele, P., Grimson, A., Schelter, J.M., Castle, J., Bartel, D.P., Linsley, P.S., Johnson, J.M., 2005. Microarray analysis shows that some microRNAs downregulate large numbers of target mRNAs. Nature 433, 769-773.

Lipshitz, H.D., Smibert, C.A., 2000. Mechanisms of RNA localization and translational regulation. Curr Opin Genet Dev 10, 476-488.

Liu, J.-l., 2010. Intracellular compartmentation of CTP synthase in Drosophila. Journal of Genetics & Genomics 37.

Liu, J., Carmell, M.A., Rivas, F.V., Marsden, C.G., Thomson, J.M., Song, J.J., Hammond, S.M., Joshua-Tor, L., Hannon, G.J., 2004. Argonaute2 is the catalytic engine of mammalian RNAi. Science 305, 1437-1441.

Liu, J., Rivas, F.V., Wohlschlegel, J., Yates, J.R., 3rd, Parker, R., Hannon, G.J., 2005. A role for the P-body component GW182 in microRNA function. Nat Cell Biol 7, 1261-1266.

Liu, J.L., 2011. The enigmatic cytoophidium: compartmentation of CTP synthase via filament formation. Bioessays 33, 159-164.

Liu, J.L., Wu, Z., Nizami, Z., Deryusheva, S., Rajendra, T.K., Beumer, K.J., Gao, H., Matera, A.G., Carroll, D., Gall, J.G., 2009. Coilin is essential for Cajal body organization in Drosophila melanogaster. Mol Biol Cell 20, 1661-1670.

Liu, X., Park, J.K., Jiang, F., Liu, Y., McKearin, D., Liu, Q., 2007. Dicer-1, but not Loquacious, is critical for assembly of miRNA-induced silencing complexes. Rna 13, 2324-2329.

Long, C.W., Pardee, A.B., 1967. Cytidine triphosphate synthetase of Escherichia coli B. I. Purification and kinetics. J Biol Chem 242, 4715-4721.

Loya, C.M., Lu, C.S., Van Vactor, D., Fulga, T.A., 2009. Transgenic microRNA inhibition with spatiotemporal specificity in intact organisms. Nat Methods 6, 897-903.

Lund, E., Guttinger, S., Calado, A., Dahlberg, J.E., Kutay, U., 2004. Nuclear export of microRNA precursors. Science 303, 95-98.

Makeyev, E.V., Zhang, J., Carrasco, M.A., Maniatis, T., 2007. The MicroRNA miR-124 promotes neuronal differentiation by triggering brain-specific alternative pre-mRNA splicing. Mol Cell 27, 435-448.

Mallory, A., Vaucheret, H., 2010. Form, function, and regulation of ARGONAUTE proteins. Plant Cell 22, 3879-3889.

Margolis, J., Spradling, A., 1995. Identification and behavior of epithelial stem cells in the Drosophila ovary. Development 121, 3797-3807.

Martin, R., Smibert, P., Yalcin, A., Tyler, D.M., Schafer, U., Tuschl, T., Lai, E.C., 2009. A Drosophila pasha mutant distinguishes the canonical microRNA and mirtron pathways. Mol Cell Biol 29, 861-870.

Mata, J., Curado, S., Ephrussi, A., Rorth, P., 2000. Tribbles coordinates mitosis and morphogenesis in Drosophila by regulating string/CDC25 proteolysis. Cell 101, 511-522.

Mathonnet, G., Fabian, M.R., Svitkin, Y.V., Parsyan, A., Huck, L., Murata, T., Biffo, S., Merrick, W.C., Darzynkiewicz, E., Pillai, R.S., Filipowicz, W., Duchaine, T.F., Sonenberg, N., 2007. MicroRNA inhibition of translation initiation in vitro by targeting the cap-binding complex eIF4F. Science 317, 1764-1767.

Megosh, H.B., Cox, D.N., Campbell, C., Lin, H., 2006. The role of PIWI and the miRNA machinery in Drosophila germline determination. Curr Biol 16, 1884-1894.

Miyoshi, K., Tsukumo, H., Nagami, T., Siomi, H., Siomi, M.C., 2005. Slicer function of Drosophila Argonautes and its involvement in RISC formation. Genes Dev 19, 2837-2848.

Moazed, D., 2009. Small RNAs in transcriptional gene silencing and genome defence. Nature 457, 413-420.

Nagai, T., Ibata, K., Park, E.S., Kubota, M., Mikoshiba, K., Miyawaki, A., 2002. A variant of yellow fluorescent protein with fast and efficient maturation for cell-biological applications. Nat Biotechnol 20, 87-90.

Nakahara, K., Kim, K., Sciulli, C., Dowd, S.R., Minden, J.S., Carthew, R.W., 2005. Targets of microRNA regulation in the Drosophila oocyte proteome. Proc Natl Acad Sci U S A 102, 12023-12028.

Nakamura, A., Amikura, R., Hanyu, K., Kobayashi, S., 2001. Me31B silences translation of oocyte-localizing RNAs through the formation of cytoplasmic RNP complex during Drosophila oogenesis. Development 128, 3233-3242.

Neumuller, R.A., Betschinger, J., Fischer, A., Bushati, N., Poernbacher, I., Mechtler, K., Cohen, S.M., Knoblich, J.A., 2008. Mei-P26 regulates microRNAs and cell growth in the Drosophila ovarian stem cell lineage. Nature 454, 241-245.

Ni, J.Q., Markstein, M., Binari, R., Pfeiffer, B., Liu, L.P., Villalta, C., Booker, M., Perkins, L., Perrimon, N., 2008. Vector and parameters for targeted transgenic RNA interference in Drosophila melanogaster. Nat Methods 5, 49-51.

Ni, J.Q., Zhou, R., Czech, B., Liu, L.P., Holderbaum, L., Yang-Zhou, D., Shim, H.S., Tao, R., Handler, D., Karpowicz, P., Binari, R., Booker, M., Brennecke, J., Perkins, L.A., Hannon, G.J., Perrimon, N., 2011. A genome-scale shRNA resource for transgenic RNAi in Drosophila. Nat Methods 8, 405-407.

Niki, Y., Yamaguchi, T., Mahowald, A.P., 2006. Establishment of stable cell lines of Drosophila germ-line stem cells. Proc Natl Acad Sci U S A 103, 16325-16330.

Noree, C., Sato, B.K., Broyer, R.M., Wilhelm, J.E., 2010. Identification of novel filament-forming proteins in Saccharomyces cerevisiae and Drosophila melanogaster. J Cell Biol 190, 541-551.

Nottrott, S., Simard, M.J., Richter, J.D., 2006. Human let-7a miRNA blocks protein production on actively translating polyribosomes. Nat Struct Mol Biol 13, 1108-1114.

Nusslein-Volhard, C., Wieschaus, E., 1980. Mutations affecting segment number and polarity in Drosophila. Nature 287, 795-801.

Okamura, K., Chung, W.J., Ruby, J.G., Guo, H., Bartel, D.P., Lai, E.C., 2008. The Drosophila hairpin RNA pathway generates endogenous short interfering RNAs. Nature 453, 803-806.

Okamura, K., Hagen, J.W., Duan, H., Tyler, D.M., Lai, E.C., 2007. The mirtron pathway generates microRNA-class regulatory RNAs in Drosophila. Cell 130, 89-100.

Okamura, K., Ishizuka, A., Siomi, H., Siomi, M.C., 2004. Distinct roles for Argonaute proteins in small RNA-directed RNA cleavage pathways. Genes Dev 18, 1655-1666.

Okamura, K., Lai, E.C., 2008. Endogenous small interfering RNAs in animals. Nat Rev Mol Cell Biol 9, 673-678.

Okamura, K., Liu, N., Lai, E.C., 2009. Distinct mechanisms for microRNA strand selection by Drosophila Argonautes. Mol Cell 36, 431-444.

Okamura, K., Robine, N., Liu, Y., Liu, Q., Lai, E.C., 2011. R2D2 organizes small regulatory RNA pathways in Drosophila. Mol Cell Biol 31, 884-896.

Olsen, P.H., Ambros, V., 1999. The lin-4 regulatory RNA controls developmental timing in Caenorhabditis elegans by blocking LIN-14 protein synthesis after the initiation of translation. Dev Biol 216, 671-680.

Pappas, A., Yang, W.L., Park, T.S., Carman, G.M., 1998. Nucleotide-dependent tetramerization of CTP synthetase from Saccharomyces cerevisiae. J Biol Chem 273, 15954-15960.

Pare, J.M., Tahbaz, N., Lopez-Orozco, J., LaPointe, P., Lasko, P., Hobman, T.C., 2009. Hsp90 regulates the function of argonaute 2 and its recruitment to stress granules and P-bodies. Mol Biol Cell 20, 3273-3284.

Park, J.K., Liu, X., Strauss, T.J., McKearin, D.M., Liu, Q., 2007. The miRNA pathway intrinsically controls self-renewal of Drosophila germline stem cells. Curr Biol 17, 533-538.

Pek, J.W., Lim, A.K., Kai, T., 2009. Drosophila maelstrom ensures proper germline stem cell lineage differentiation by repressing microRNA-7. Dev Cell 17, 417-424.

Pepper, A.S., Beerman, R.W., Bhogal, B., Jongens, T.A., 2009. Argonaute2 suppresses Drosophila fragile X expression preventing neurogenesis and oogenesis defects. PLoS One 4, e7618.

Piccioni, F., Zappavigna, V., Verrotti, A.C., 2005. A cup full of functions. RNA Biol 2, 125-128.

Pillai, R.S., Bhattacharyya, S.N., Artus, C.G., Zoller, T., Cougot, N., Basyuk, E., Bertrand, E., Filipowicz, W., 2005. Inhibition of translational initiation by Let-7 MicroRNA in human cells. Science 309, 1573-1576.

Pines, J., 1998. Regulation of the G2 to M transition. Results Probl Cell Differ 22, 57-78.

Poulton, J.S., Huang, Y.C., Smith, L., Sun, J., Leake, N., Schleede, J., Stevens, L.M., Deng, W.M., 2011. The microRNA pathway regulates the temporal pattern of Notch signaling in Drosophila follicle cells. Development 138, 1737-1745.

Qi, H.H., Ongusaha, P.P., Myllyharju, J., Cheng, D., Pakkanen, O., Shi, Y., Lee, S.W., Peng, J., Shi, Y., 2008. Prolyl 4-hydroxylation regulates Argonaute 2 stability. Nature 455, 421-424.

Rand, T.A., Petersen, S., Du, F., Wang, X., 2005. Argonaute2 cleaves the anti-guide strand of siRNA during RISC activation. Cell 123, 621-629.

Raza, H., 2011. Dual localization of glutathione S-transferase in the cytosol and mitochondria: implications in oxidative stress, toxicity and disease. FEBS J 278, 4243-4251.

Reich, J., Snee, M.J., Macdonald, P.M., 2009. miRNA-dependent translational repression in the Drosophila ovary. PLoS One 4, e4669.

Reiter, L.T., Potocki, L., Chien, S., Gribskov, M., Bier, E., 2001. A systematic analysis of human disease-associated gene sequences in Drosophila melanogaster. Genome Res 11, 1114-1125.

Rhoades, M.W., Reinhart, B.J., Lim, L.P., Burge, C.B., Bartel, B., Bartel, D.P., 2002. Prediction of plant microRNA targets. Cell 110, 513-520.

Riddle, N.C., Leung, W., Haynes, K.A., Granok, H., Wuller, J., Elgin, S.C., 2008. An investigation of heterochromatin domains on the fourth chromosome of Drosophila melanogaster. Genetics 178, 1177-1191.

Rissland, O.S., Lai, E.C., 2011. RNA silencing in Monterey. Development 138, 3093-3102.

Robertson, J.G., 1995. Determination of subunit dissociation constants in native and inactivated CTP synthetase by sedimentation equilibrium. Biochemistry 34, 7533-7541.

Ruby, J.G., Jan, C.H., Bartel, D.P., 2007. Intronic microRNA precursors that bypass Drosha processing. Nature 448, 83-86.

Ruohola, H., Bremer, K.A., Baker, D., Swedlow, J.R., Jan, L.Y., Jan, Y.N., 1991. Role of neurogenic genes in establishment of follicle cell fate and oocyte polarity during oogenesis in Drosophila. Cell 66, 433-449.

Saito, K., Ishizuka, A., Siomi, H., Siomi, M.C., 2005. Processing of pre-microRNAs by the Dicer-1-Loquacious complex in Drosophila cells. PLoS Biol 3, e235.

Salzberg, A., Prokopenko, S.N., He, Y., Tsai, P., Pal, M., Maroy, P., Glover, D.M., Deak, P., Bellen, H.J., 1997. P-element insertion alleles of essential genes on the third chromosome of Drosophila melanogaster: mutations affecting embryonic PNS development. Genetics 147, 1723-1741.

Saraste, M., Sibbald, P.R., Wittinghofer, A., 1990. The P-loop--a common motif in ATP- and GTP-binding proteins. Trends Biochem Sci 15, 430-434.

Scheit, K.H., Linke, H.J., 1982. Substrate specificity of CTP synthetase from Escherichia coli. Eur J Biochem 126, 57-60.

Schneider, I., 1972. Cell lines derived from late embryonic stages of Drosophila melanogaster. J Embryol Exp Morphol 27, 353-365.

Schneider, M.D., Najand, N., Chaker, S., Pare, J.M., Haskins, J., Hughes, S.C., Hobman, T.C., Locke, J., Simmonds, A.J., 2006. Gawky is a component of cytoplasmic mRNA processing bodies required for early Drosophila development. J Cell Biol 174, 349-358.

Schuettler, J., Peng, Z., Zimmer, J., Sinn, P., von Hagens, C., Strowitzki, T., Vogt, P.H., 2011. Variable expression of the Fragile X Mental Retardation 1 (FMR1) gene in patients with premature ovarian failure syndrome is not dependent on number of (CGG)n triplets in exon 1. Hum Reprod 26, 1241-1251.

Seitz, H., Tushir, J.S., Zamore, P.D., 2011. A 5'-uridine amplifies miRNA/miRNA* asymmetry in Drosophila by promoting RNA-induced silencing complex formation. Silence 2, 4.

Sempere, L.F., Freemantle, S., Pitha-Rowe, I., Moss, E., Dmitrovsky, E., Ambros, V., 2004. Expression profiling of mammalian microRNAs uncovers a subset of brain-expressed microRNAs with possible roles in murine and human neuronal differentiation. Genome Biol 5, R13.

Senger, S., Csokmay, J., Akbar, T., Jones, T.I., Sengupta, P., Lilly, M.A., 2011. The nucleoporin Seh1 forms a complex with Mio and serves an essential tissue-specific function in Drosophila oogenesis. Development 138, 2133-2142.

Shcherbata, H.R., Althauser, C., Findley, S.D., Ruohola-Baker, H., 2004. The mitotic-to-endocycle switch in Drosophila follicle cells is executed by Notch-dependent regulation of G1/S, G2/M and M/G1 cell-cycle transitions. Development 131, 3169-3181.

Shcherbata, H.R., Ward, E.J., Fischer, K.A., Yu, J.Y., Reynolds, S.H., Chen, C.H., Xu, P., Hay, B.A., Ruohola-Baker, H., 2007. Stage-specific differences in the requirements for germline stem cell maintenance in the Drosophila ovary. Cell Stem Cell 1, 698-709.

Smibert, P., Bejarano, F., Wang, D., Garaulet, D.L., Yang, J.S., Martin, R., Bortolamiol-Becet, D., Robine, N., Hiesinger, P.R., Lai, E.C., 2011a. A Drosophila genetic screen yields allelic series of core microRNA biogenesis factors and reveals post-developmental roles for microRNAs. RNA.

Smibert, P., Bejarano, F., Wang, D., Garaulet, D.L., Yang, J.S., Martin, R., Bortolamiol-Becet, D., Robine, N., Hiesinger, P.R., Lai, E.C., 2011b. A Drosophila genetic screen yields allelic series of core microRNA biogenesis factors and reveals post-developmental roles for microRNAs. RNA 17, 1997-2010.

Song, J.J., Smith, S.K., Hannon, G.J., Joshua-Tor, L., 2004. Crystal structure of Argonaute and its implications for RISC slicer activity. Science 305, 1434-1437.

Spradling, A.C., 1993a. Developmental genetics of oogenesis. The development of Drosophila melanogaster 1, 1–70.

Spradling, A.C., 1993b. Developmental genetics of oogenesis. In: Martinez-Arias, editor. The development of *Drosophila melanogaster*. Cold Spring Harbor Laboratory Press, 1-70.

Spradling, A.C., Stern, D., Beaton, A., Rhem, E.J., Laverty, T., Mozden, N., Misra, S., Rubin, G.M., 1999. The Berkeley Drosophila Genome Project gene disruption project: Single P-element insertions mutating 25% of vital Drosophila genes. Genetics 153, 135-177.

Suzuki, Y., Minami, M., Suzuki, M., Abe, K., Zenno, S., Tsujimoto, M., Matsumoto, K., Minami, Y., 2009. The Hsp90 inhibitor geldanamycin abrogates colocalization of eIF4E and eIF4E-transporter into stress granules and association of eIF4E with eIF4G. J Biol Chem 284, 35597-35604.

Terry, N.A., Tulina, N., Matunis, E., DiNardo, S., 2006. Novel regulators revealed by profiling Drosophila testis stem cells within their niche. Dev Biol 294, 246-257.

Thibault, S.T., Singer, M.A., Miyazaki, W.Y., Milash, B., Dompe, N.A., Singh, C.M., Buchholz, R., Demsky, M., Fawcett, R., Francis-Lang, H.L., Ryner, L., Cheung, L.M., Chong, A., Erickson, C., Fisher, W.W., Greer, K., Hartouni, S.R., Howie, E., Jakkula, L., Joo, D., Killpack, K., Laufer, A., Mazzotta, J., Smith, R.D., Stevens, L.M., Stuber, C., Tan, L.R., Ventura, R., Woo, A., Zakrajsek, I., Zhao, L., Chen, F., Swimmer, C., Kopczynski, C., Duyk, G., Winberg, M.L., Margolis, J., 2004. A complementary transposon tool kit for Drosophila melanogaster using P and piggyBac. Nat Genet 36, 283-287.

Thomsen, S., Azzam, G., Kaschula, R., Williams, L.S., Alonso, C.R., 2010. Developmental RNA processing of 3'UTRs in Hox mRNAs as a context-dependent mechanism modulating visibility to microRNAs. Development 137, 2951-2960.

Tolia, N.H., Joshua-Tor, L., 2007. Slicer and the argonautes. Nat Chem Biol 3, 36-43.

Tomari, Y., Du, T., Zamore, P.D., 2007. Sorting of Drosophila small silencing RNAs. Cell 130, 299-308.

Tomari, Y., Matranga, C., Haley, B., Martinez, N., Zamore, P.D., 2004. A protein sensor for siRNA asymmetry. Science 306, 1377-1380.

Vaucheret, H., 2009. AGO1 homeostasis involves differential production of 21-nt and 22-nt miR168 species by MIR168a and MIR168b. PLoS One 4, e6442.

Vaucheret, H., Mallory, A.C., Bartel, D.P., 2006. AGO1 homeostasis entails coexpression of MIR168 and AGO1 and preferential stabilization of miR168 by AGO1. Mol Cell 22, 129-136.

Vetter, I.R., Wittinghofer, A., 1999. Nucleoside triphosphate-binding proteins: different scaffolds to achieve phosphoryl transfer. Q Rev Biophys 32, 1-56.

Wakiyama, M., Takimoto, K., Ohara, O., Yokoyama, S., 2007. Let-7 microRNA-mediated mRNA deadenylation and translational repression in a mammalian cell-free system. Genes Dev 21, 1857-1862.

Walker, J.E., Saraste, M., Runswick, M.J., Gay, N.J., 1982. Distantly related sequences in the alpha- and beta-subunits of ATP synthase, myosin, kinases and other ATP-requiring enzymes and a common nucleotide binding fold. EMBO J 1, 945-951.

Wang, Y., Juranek, S., Li, H., Sheng, G., Tuschl, T., Patel, D.J., 2008. Structure of an argonaute silencing complex with a seed-containing guide DNA and target RNA duplex. Nature 456, 921-926.

Weigmann, K., Klapper, R., Strasser, T., Rickert, C., Technau, G., Jackle, H., Janning, W., Klambt, C., 2003. FlyMove--a new way to look at development of Drosophila. Trends Genet 19, 310-311.

Weinmann, L., Hock, J., Ivacevic, T., Ohrt, T., Mutze, J., Schwille, P., Kremmer, E., Benes, V., Urlaub, H., Meister, G., 2009. Importin 8 is a gene silencing factor that targets argonaute proteins to distinct mRNAs. Cell 136, 496-507.

Weng, M.L., Zalkin, H., 1987. Structural role for a conserved region in the CTP synthetase glutamine amide transfer domain. J Bacteriol 169, 3023-3028.

Wolff, T., Ready, D.F., 1991. The beginning of pattern formation in the Drosophila compound eye: the morphogenetic furrow and the second mitotic wave. Development 113, 841-850.

Wu, J.S., Luo, L., 2006. A protocol for mosaic analysis with a repressible cell marker (MARCM) in Drosophila. Nat Protoc 1, 2583-2589.

Wu, X., Tanwar, P.S., Raftery, L.A., 2008. Drosophila follicle cells: morphogenesis in an eggshell. Semin Cell Dev Biol 19, 271-282.

Xie, T., Spradling, A.C., 2000. A niche maintaining germ line stem cells in the Drosophila ovary. Science 290, 328-330.

Xu, X.L., Li, Y., Wang, F., Gao, F.B., 2008. The steady-state level of the nervous-system-specific microRNA-124a is regulated by dFMR1 in Drosophila. J Neurosci 28, 11883-11889.

Yang, L., Chen, D., Duan, R., Xia, L., Wang, J., Qurashi, A., Jin, P., Chen, D., 2007. Argonaute 1 regulates the fate of germline stem cells in Drosophila. Development 134, 4265-4272.

Yang, W.L., Bruno, M.E., Carman, G.M., 1996. Regulation of yeast CTP synthetase activity by protein kinase C. J Biol Chem 271, 11113-11119.

Yang, W.L., McDonough, V.M., Ozier-Kalogeropoulos, O., Adeline, M.T., Flocco, M.T., Carman, G.M., 1994. Purification and characterization of CTP synthetase, the product of the URA7 gene in Saccharomyces cerevisiae. Biochemistry 33, 10785-10793.

Yi, R., Qin, Y., Macara, I.G., Cullen, B.R., 2003. Exportin-5 mediates the nuclear export of pre-microRNAs and short hairpin RNAs. Genes Dev 17, 3011-3016.

Yoda, M., Kawamata, T., Paroo, Z., Ye, X., Iwasaki, S., Liu, Q., Tomari, Y., 2010. ATP-dependent human RISC assembly pathways. Nat Struct Mol Biol 17, 17-23.

Yu, J.Y., Reynolds, S.H., Hatfield, S.D., Shcherbata, H.R., Fischer, K.A., Ward, E.J., Long, D., Ding, Y., Ruohola-Baker, H., 2009. Dicer-1-dependent Dacapo suppression acts downstream of Insulin receptor in regulating cell division of Drosophila germline stem cells. Development 136, 1497-1507.

Zappavigna, V., Piccioni, F., Villaescusa, J.C., Verrotti, A.C., 2004. Cup is a nucleocytoplasmic shuttling protein that interacts with the eukaryotic translation initiation factor 4E to modulate Drosophila ovary development. Proc Natl Acad Sci U S A 101, 14800-14805.

Zecca, M., Struhl, G., 2002. Subdivision of the Drosophila wing imaginal disc by EGFR-mediated signaling. Development 129, 1357-1368.

Zhang, X., Yuan, Y.R., Pei, Y., Lin, S.S., Tuschl, T., Patel, D.J., Chua, N.H., 2006. Cucumber mosaic virus-encoded 2b suppressor inhibits Arabidopsis Argonaute1 cleavage activity to counter plant defense. Genes Dev 20, 3255-3268.